

Characterization of the yeast adaptor protein
Ent3p and its interaction with the endosomal
SNAREs Vti1p, Pep12p and Syn8p

Dissertation

zur Erlangung des Doktorgrades der Naturwissenschaften
der Fakultät für Chemie der Universität Bielefeld

vorgelegt von
Jana Zimmermann
aus Siegen

Bielefeld 2010

Referent: Prof. Dr. Gabriele Fischer von Mollard

Korreferent: Prof. Dr. Thomas Dierks

Table of Contents

1 Introduction.....	1
1.1 Baker yeast as model organism	2
1.1.1 The yeast cell wall	3
1.1.2 Cell polarity of budding yeast cells.....	3
1.2 Protein transport in eukaryotic cells.....	4
1.3 Vesicle transport.....	6
1.3.1 Analysis of anterograde transport from TGN to vacuole.....	7
1.3.1.1 CPY transport.....	7
1.3.1.2 ALP transport.....	7
1.3.2 Retrograde transport from EE to TGN.....	8
1.3.2.1 A-ALP transport.....	8
1.3.2.2 Snc1p transport.....	9
1.4 SNAREs.....	9
1.4.1 The SNARE hypothesis.....	10
1.4.2 Molecular structure.....	11
1.4.3 SNAREs in membrane fusion.....	12
1.4.4 Yeast SNAREs.....	13
1.4.4.1 Pep12p.....	13
1.4.4.2 Vti1p.....	14
1.4.4.3 Syn8p.....	14
1.5 Adaptor proteins.....	15
1.5.1 ENTH-proteins.....	15
1.5.2 Structure and function of ENTH domain proteins.....	15
1.5.3 The yeast ENTH domain protein Ent3p.....	16
1.5.4 Interaction of Ent3p with endosomal SNAREs.....	17
1.6 Functions of Tvp23p.....	18
1.6.1 Yip4p and Yip5p.....	19
2 Aim of this Work.....	20
3 Material and Methods.....	21
3.1 Material.....	21
3.1.1 Lab Equipment.....	21
3.1.2 Chemicals.....	22
3.1.3 Proteaseinhibitors.....	23

3.1.4 Antibodies	23
3.1.5 Enzymes, Nucleotides and Standards.....	24
3.1.6 Kits for Isolation and Detection of DNA and Proteins.....	24
3.1.7 Bacteria Strains and Plasmids.....	25
3.1.8 Media for <i>S. cerevisiae</i> and <i>E. coli</i>	25
3.1.9 Stock Solutions and Buffers.....	27
3.1.10 Software.....	28
3.1.11 Internet services	28
3.2 Methods.....	29
3.2.1 Molecular Biology.....	29
3.2.1.1 Preparation of electrocompetent <i>E. coli</i> cells.....	29
3.2.1.2 Electroporation.....	29
3.2.1.3 DNA isolation from <i>E. coli</i>	29
3.2.1.4 Determination of DNA concentration.....	30
3.2.1.5 Cloning techniques.....	30
3.2.1.5.1 Polymerase chain reaction (PCR).....	30
3.2.1.5.2 Site directed mutagenesis by PCR.....	31
3.2.1.5.3 Colony PCR.....	32
3.2.1.5.4 Ethanol precipitation.....	32
3.2.1.5.5 Cloning of PCR-products with pGemT-easy.....	32
3.2.1.5.6 Digestion of DNA with restriction endonucleases.....	33
3.2.1.5.7 Agarose gel electrophoresis of DNA.....	33
3.2.1.5.8 Ligation of DNA inserts into plasmid vectors.....	34
3.2.1.6 Sequencing.....	34
3.2.1.7 DMSO-Stocks of <i>E. coli</i> and <i>S. cerevisiae</i>	34
3.2.2 Yeast Genetics.....	35
3.2.2.1 PLATE transformation.....	35
3.2.2.2 Lithium Acetate (LiAc) transformation.....	35
3.2.2.3 Isolation of yeast genomic DNA.....	36
3.2.2.4 Construction of yeast deletion mutants.....	36
3.2.2.5 Yeast two-hybrid assay.....	37
3.2.3 Biochemical Methods.....	39
3.2.3.1 Preparation of protein extract from yeast cells.....	39
3.2.3.2 Bradford assay for determination of protein concentration.....	39
3.2.3.3 SDS gel electrophoresis.....	39

3.2.3.4 Isoelectric focusing (IEF).....	41
3.2.3.4.1 Protein extract preparation.....	41
3.2.3.4.2 IEF-Electrophoresis.....	42
3.2.3.5 Coomassie blue staining.....	43
3.2.3.6 Western blot analysis.....	43
3.2.3.7 Preabsorption of antibodies.....	44
3.2.3.8 CPY Overlay-Assay.....	45
3.2.3.9 “Pulse-Chase” Immunoprecipitation (IP).....	45
3.2.3.9.1 CPY-IP.....	45
3.2.3.9.2 ALP-IP.....	47
3.2.3.9.3 Protein stability.....	48
3.2.3.10 Test for bacterial expression of recombinant His ₆ -tagged proteins.....	48
3.2.3.11 Purification of His ₆ tagged fusion proteins.....	49
3.2.3.12 Test for bacterial expression of recombinant Strep-tagged proteins.....	50
3.2.3.13 Purification of Strep-tag fusion proteins.....	51
3.2.3.14 Pulldown-Assay.....	52
3.2.4 Cell Biology.....	53
3.2.4.1 Growth test with cell wall perturbing agents	53
3.2.4.2 Subcellular fractionation.....	54
3.2.4.2.1 Differential centrifugation.....	54
3.2.4.2.2 by sucrose density gradient.....	55
3.2.4.3 Membrane binding assay.....	55
3.2.4.4 Indirect immunofluorescence.....	56
3.2.4.5 GFP fluorescence microscopy.....	58
3.2.4.6 Calcofluor staining.....	58
3.2.4.7 FM4-64 staining.....	59
3.2.4.8 Sedimentation-Assay	59
4 Results.....	60
4.1 Characterization of the interaction of Ent3p with Pep12p, Vti1p and Syn8p60	
4.1.1 Pep12p interacts with Ent3p via its FSD motif.....	60
4.1.1.1 Yeast-Two-Hybrid and Pull-down interactions.....	60
4.1.1.2 <i>In vivo</i> interactions of Ent3p with Pep12p FSD mutants.....	63

4.1.1.2.1	Localization of Pep12 mutants in immunofluorescence microscopy.....	63
4.1.1.2.2	Localization by sucrose density gradient.....	64
4.1.1.2.3	Pep12 stability is enhanced in Pep12p F20L.....	65
4.1.1.3	CPY transport.....	66
4.1.2	Characterization of the interaction surface of Ent3p with the endosomal SNAREs.....	67
4.1.2.1	Ent3p interaction with SNAREs is specific for the ENTH domain	67
4.1.2.2	Vti1p, Syn8p and Pep12p bind the same interaction surface of Ent3p but different amino acids	69
4.1.2.3	Interacting amino acids on Vti1p and Pep12p.....	71
4.1.2.4	Vti1p, Pep12p and Syn8p were sorted together.....	72
4.1.2.5	Location of Pep12p, Vti1p and Syn8p on vesicles or endosomes.....	76
4.1.2.6	Functions of Ent3p point mutants <i>in vivo</i>	78
4.1.3	The A-ALP transport is defective in ent3 Δ ent5 Δ double mutants.....	83
4.1.4	Recycling of GFP-Snc1p is blocked in ent3 Δ ent5 Δ cells.....	85
4.1.5	Yck2p is mislocalized in ent3 Δ ent5 Δ cells.....	87
4.2	Functions of the Ent3p domains.....	89
4.2.1	Functions of the Ent3p domains in the retrograde EE to TGN transport	89
4.2.2	For CPY transport the Ent3p C-terminus and the ENTH domain were necessary.....	92
4.2.3	Localization of the Ent3p domains via immunofluorescence microscopy	96
4.2.4	Function of Ent3p domains in cell wall assembly and budding and cell separation.....	97
4.2.4.1	The Ent3p domain mutants could not rescue the defect of the double mutant in a sedimentation assay.....	98
4.2.4.2	Budding patterns and cell separation.....	99
4.2.4.3	Cell wall assembly.....	104
4.2.5	Interactions of the Ent3p ENTH domain with its own C-terminus and the Ent5 ANTH domain.....	105
4.2.6	Ent3p phosphorylation assay by isoelectric focusing.....	106

4.3 Tvp23p has a role in retrograde transport from EE to TGN and interacts genetically with <i>VTI1</i>	108
4.3.1 Genetic interaction between <i>TVP23</i> and <i>VTI1</i>	109
4.4 Yip4p has a function in CPY and retrograde EE to TGN transport.....	111
4.4.1 Function of Yip4p and Yip5p in a CPY overlay assay.....	111
4.4.2 GFP-Snc1p transport in <i>yip4Δ</i> and <i>yip5Δ</i> deletion mutants	112
5 Discussion.....	114
5.1 Characterization of the Ent3p-SNARE interaction.....	114
5.1.1 Pep12p interacts with Ent3p via its FSD motif.....	115
5.1.2 Structural characterization of the Ent3p interaction surface.....	117
5.1.2.1 Both halves of the ENTH domain are specifically involved in the SNARE binding	117
5.1.2.2 Vti1p, Pep12p and Syn8p bind to the same surface on Ent3p but to different amino acids.....	119
5.1.3 Proof of interacting amino acids by charge-swap experiments.....	121
5.1.3.1 Interacting amino acids on Vti1p.....	121
5.1.3.2 Interacting amino acids on Pep12p.....	122
5.1.4 Vti1p, Pep12p and Syn8p were sorted as complex.....	123
5.1.5 Vti1p and Pep12p are t-SNAREs and Syn8p is a v-SNARE.....	124
5.1.6 <i>In vivo</i> functions of the Ent3p point mutants.....	126
5.1.6.1 The Y60D mutant has a severe growth defect.....	126
5.1.6.2 Rescuing abilities of the Ent3p F62D, E103W and R154E mutants.....	127
5.1.7 Ent3p and Ent5p have a function in retrograde transport to the TGN independently from SNARE binding.....	130
5.1.7.1 A-ALP transport from LE to the TGN.....	130
5.1.7.2 GFP-Snc1p.....	131
5.1.7.3 GFP-Yck2p.....	132
5.2 Functions of the Ent3p domains.....	133
5.2.1 The Ent3p C-terminus is sufficient for GFP-Snc1p and GFP-Yck2p recycling.....	133
5.2.1.1 Vacuole morphology of the Ent3p/Ent5p mutants	135
5.2.2 Both Ent3p domains were necessary for CPY sorting.....	136
5.2.3 Cell wall defects.....	137
5.2.4 Interactions of the ENTH domain with ANTH and itself.....	140

5.2.5 Ent3p phosphorylation.....	141
5.3 Tvp23p and Yip4p have a function in the retrograde EE to TGN transport	144
5.3.1 Vti1p and Tvp23p show genetic interactions in retrograde transport.	144
5.3.2 Yip4p has a function in retrograde EE to TGN and CPY transport.....	147
5.4 Outlook.....	149
6 Summary.....	150
7 Bibliography.....	152
Appendix.....	1
I Oligonucleotides.....	1
II Plasmids.....	5
III Yeast Strains.....	13
IV <i>Curriculum Vitae</i>	15
V Publications.....	16
Danksagung.....	17
Erklärung.....	19

Tables

Tab. 1: Antibodies.....	23
Tab. 2: β -galactosidase assay.....	62
Tab. 3: Summary of calcofluor staining experiments.	101
Tab. 4: Oligonucleotides.....	I
Tab. 5: Oligo categories.....	IV
Tab. 6: Plasmids.	V
Tab. 7: Yeast strains	XIII

Figures

Fig. 1.1: Protein transport routes in yeast cells.....	5
Fig. 1.2: Vesicle transport from its donor to the target membrane.....	6
Fig. 1.3: The yeast SNARE complexes.....	10
Fig. 1.4: SNARE complex formation.....	12
Fig. 1.5: The family of yeast ENTH domain proteins.....	16
Fig. 1.6: Crystal structure of the human epsinR-vti1b complex.....	18
Fig. 4.1: Pep12 interacts with Ent3p via its FSD	61
Fig. 4.2: In vitro pulldown assay of Ent3p with Pep12p FSD mutants.....	63
Fig. 4.3: Pep12 F20L and Δ FSD localization via IF microscopy.....	64
Fig. 4.4: Pep12p F20L is mislocalized in a sucrose density gradient.....	64
Fig. 4.5: Mutation of the Pep FSD motif causes an enhanced stability of Pep12p.	65
Fig. 4.6: CPY secretion of Pep12 mutants.....	66
Fig. 4.7: Construction of ENTH/ANTH chimera.....	68
Fig. 4.8: The specificity of the interaction of Ent3p with the endosomal SNAREs is determined by the first five helices of the ENTH domain.....	69
Fig. 4.9: Structure modeling and alignment of Ent3p and epsinR.....	70
Fig. 4.10: Endosomal SNAREs bind to the same surface of Ent3p but to different amino acids.....	71
Fig. 4.11: Charge-swap interactions between Vti1p, Pep12p and Ent3p.....	72
Fig. 4.12: Vti1p is mislocalized to denser fractions in the Ent3p R154E mutant....	73
Fig. 4.13: Vti1p localization in ent3 Δ ent5 Δ and syn8 Δ ent3 Δ ent5 Δ cells.....	74

Fig. 4.14: Pep12p was mislocalized in the Ent3p R154E point mutant.....	75
Fig. 4.15: Localization of 3xHA-Syn8p in a sucrose density gradient.....	76
Fig. 4.16: Localization of Vti1p, Pep12p and Syn8p in <i>tlg2Δ</i> cells.....	77
Fig. 4.17: Quantification of SNARE localization in <i>tlg2Δ</i> cells.....	78
Fig. 4.18: Ent3p point mutants do not rescue the <i>ent3Δent5Δ</i> CPY defects.....	79
Fig. 4.19: CPY pulse chase experiment with Ent3p point mutants.....	80
Fig. 4.20: Sedimentation assay with Ent3p point mutants.....	82
Fig. 4.21: Growth test with Ent3p point mutants.....	83
Fig. 4.22: A-ALP is slightly mislocalized in <i>ent3Δent5Δ</i> cells.....	84
Fig. 4.23: GFP-Snc1p localization was changed in <i>ent3Δent5Δ</i> cells.....	85
Fig. 4.24: Quantification of GFP-Snc1p transport and colocalization with FM4-64.	86
Fig. 4.25: GFP-Yck2p transport in <i>ent3Δent5Δ</i> cells and Ent3p point mutants	88
Fig. 4.26: The C-terminus of Ent3p is necessary for a correct GFP-Snc1p and GFP-Yck2p localization.....	91
Fig. 4.27: The Ent3p ENTH domain and the C-terminus were important for CPY sorting.....	93
Fig. 4.28: Expression test of the Ent3p domain mutants.....	94
Fig. 4.29: Membrane binding of Ent3p domains.....	95
Fig. 4.30: Localization of the ENTH domain and Ent3p -PI via IF microscopy.....	97
Fig. 4.31: Sedimentation assay Ent3p domains.....	98
Fig. 4.32: Analysis of haploid budding patterns in Ent3 domain mutants.....	99
Fig. 4.33: Multibudded cells and cells with calcofluor accumulations.....	100
Fig. 4.34: Calcofluor staining of <i>ent3Δent5Δ</i> diploid and haploid strains with and without pHO plasmid.....	103
Fig. 4.35: Complementation of <i>ent3Δent5Δ</i> cell wall defects by the Ent3p domains	104
Fig. 4.36: Interaction of the Ent3p ENTH domain with itself and the Ent5p ANTH domain.....	105
Fig. 4.37: Ent3p is phosphorylated in IEF.....	107
Fig. 4.38: GFP-Snc1p localization in <i>tvp23Δ</i> cells.....	109
Fig. 4.39: Synthetic defect in recycling of GFP-Snc1p to the late Golgi in <i>vti1-2</i> <i>tvp23Δ</i> cells.....	110
Fig. 4.40: The retrograde LE to TGN transport is not affected in <i>tvp23Δ</i> cells.....	111

Fig. 4.41: Yip4p has a function in the CPY transport.....	112
Fig. 4.42: YIP4 deletion caused a mislocalization of GFP-Snc1p.....	113
Fig. 5.1: The different alignments of Vti1p with human vti1b	121
Fig. 5.2: Functions of Ent3p in endosomal transport.....	143
Fig. 5.3: Interaction network of Tvp23p, Yip4p and Yip5p	147

Abbreviations

AA	Amino acid
AHT	Anhydrotetracycline
ALP	Alkaline phosphatase
ANTH	AP180 N-terminal homology
Amp	Ampicillin
APS	Ammonium peroxodisulphate
AP	Adaptor protein
ATP	Adenosine triphosphate
bp	Base pairs
BSA	Bovine Serum Albumin
cDNA	Complementary DNA
Cf	Calcofluor white
CIP	Calf intestinal phosphatase
CPY	Carboxypeptidase Y
$\Delta\Delta$	<i>ent3Δent5Δ</i> yeast strain
DAPI	4'-6-Diamino-2-phenylindol-dihydrochloride
ddH ₂ O	Double distilled water
DMSO	Dimethylsulfoxide
DNA	Desoxyribonucleic acid
dNTPs	Deoxynucleosidetriphosphates (dATP, dGTP, dCTP, dTTP)
<i>E. coli</i>	<i>Escherichia coli</i>
EDTA	Ethylenediamintetraacetate-disodium salt
EE	Early endosome
ENTH	Epsin N-terminal homology
ER	Endoplasmic Reticulum
EtOH	Ethanol
Fig.	Figure
GFP	Green fluorescent protein
h	hours
HA	Haemagglutinin
HEPES	N-2-Hydroxyethylpiperazin-N'-2-ethanesulfonic acid
His ₆	Hexa-histidine

HRP	Horseradish-Peroxidase
IF	Immunofluorescence microscopy
IgG	Immunoglobulin G
IP	Immunoprecipitation
IPTG	Isopropyl- α -D-thiogalactopyranoside
Kana	Kanamycin
kb	Kilobases
kDa	Kilodalton
L	Liter
LE	Late endosome
LB	Luria Bertani
μ	micro-
M	molar
mA	Milliampere
mg	Milligram
min	Minute
mL	Milliliter
mM	millimolar
MW	Molecular weight
nm	Nanometer
NSF	N-Ethylmaleimid-Sensitive-Factor
nt	Nucleotide
OD ₆₀₀	Optical density at 600 nm
PAGE	Poly-acrylamide gel electrophoresis
PCR	Polymerase chain reaction
<i>Pfu</i>	<i>Pyrococcus furiosus</i>
pH	Negative logarithm of hydrogen ion concentration
PI	Phosphatase inhibitor mix
PM	Plasma membrane
PMSF	Phenylmethylsulfonylfluoride
RNA	Ribonucleic acid
rpm	Rounds per minute
RT	Room temperature
SDS	Sodium dodecylsulfate

sec	Seconds
SNAP	Soluble-NSF-Attachment-Protein
SNARE	Soluble N-ethylmaleimide sensitive factor attachment protein receptor
ss	Single strand
Tab.	Table
TAE	Tris-acetate-EDTA-buffer
<i>Taq</i>	<i>Thermus aquaticus</i>
TE	Tris-EDTA-buffer
TEMED	N,N,N',N'-Tetramethylethylenediamine
TGN	<i>Trans</i> -Golgi network
T _m	Melting temperature
Tris	Tris-(hydroxymethyl)-aminomethane
ts	temperatursensitive
U	Unit
ON	Over night
UV	Ultraviolet
V	Volt
v/v	Volume/volume
w/v	Weight/volume
WT	Wildtype
Y2H	Yeast two-hybrid

1 Introduction

All living organisms can be divided into three groups: The eukaryotes (e.g. plants, animals and fungi) which are featured by internal enclosed membrane compartments (organelles) and two kinds of bacteria, the prokaryotes and the archae bacteria. Since eukaryotic cells are too large for delivering proteins exclusively by diffusion, there has to be a fast and efficient way of transporting proteins through the cell. To concentrate and deliver proteins with a high efficiency and specificity the proteins are packed into membrane spheres called vesicles. The vesicles are transported by diffusion or by motor proteins along cytoskeleton fibers to their destination which is determined by a specific lipid and protein composition of the vesicles membrane and target membranes (Behnia and Munro, 2005).

To study the molecular mechanisms of vesicle formation, loading of the vesicles with proteins, delivery to the target organelle and fusion with the target membrane, a common model organism is the baker yeast *Saccharomyces cerevisiae*. For example the yeast protein Ent3p is involved in specific cargo sorting when the vesicle is built. It sorts SNARE proteins which were destined for the late endosome into vesicles (Chidambaram *et al.*, 2004). The SNARE proteins mediate vesicle fusion when they reach their target membrane (Jahn and Scheller, 2006). Since sets of four different SNAREs function as “address sticker” for the vesicles the regulation and correct sorting of SNAREs is crucial so that the cargo vesicles reach their correct destination. Although the SNARE sorting is important for the function and survival of all eukaryotic cells there is not much known about this process.

1.1 Baker yeast as model organism

The beer and baker yeast *Saccharomyces cerevisiae* (also called budding yeast) is a unicellular eukaryote and belongs to the family of fungi. With its size of about 3-5 μm it is smaller than the most mammalian cells. It has a relatively simple genome with about 5800 genes on 16 chromosomes, which are completely sequenced. The yeast genes are easy to manipulate since the cells integrate transformed DNA fragments (with e.g. the lithium acetate method) with homologous regions into their genome. Genes can be deleted with this method or tags like the GFP-tag (green fluorescent protein) inserted. Single mutants can be easily obtained from the Euroscarf yeast strain collection. As for other model systems for yeast there also exist different strain backgrounds. In this study mainly the SEY (Robinson et al, 1988) and the BY (Euroscarf) backgrounds were used.

Haploid yeast cells proliferate by budding and exist in two mating types which are preset by the *MAT* locus on chromosome 3. There are *MAT α* and *MATa* cells which differ i.a. in their expressed pheromone receptor and the secreted pheromones (Nasmyth, 1982). The *MAT α* cells express the **a**-factor receptor (Ste3p) and secrete the α -factor and *vice versa* for *MATa* (Ste2p as α -factor receptor) cells. If a *MATa* cell gets in contact with a *MAT α* cell they fuse and form a single diploid cell. If diploid yeast cells were exposed to starvation conditions they build four haploid spores (together also called tetrad or ascus) which are surrounded and held together by the ascus wall. Diploid yeast cells can be used for analysis of gene defects since the phenotype abnormalities may be more severe in diploid homozygous mutants than in the haploid mutant cells. Another usage for mating is the construction of double or triple deletion mutants if the gene deletion by transforming deletion cassettes which were integrated does not work (for example if the resulting mutant is lethal which can be ascertained only by a mating approach). For inserting gene deletions by mating the appropriate haploid single or double mutants were mated, starved for spore building and the tetrads were dissected with a glass fiber aperture under a microscope. The separated spores were then analyzed for their mating and genotype.

1.1.1 The yeast cell wall

Yeast cells have a cell wall consisting mainly of glycans ($\beta(1-3)$ and a small amount of $\beta(1-6)$ glycan), chitin and mannoproteins. With 50% of the cell wall mass the $\beta(1-3)$ glycan is the backbone of the whole cell wall construction (Lipke and Ovalle, 1998). The Zymolyase mixture destroys the $\beta(1-3)$ linkages and so removes the cell wall. A yeast cell without cell wall is called spheroplast.

The chitin which contributes with 1-3% to the cell wall mass can be stained with the fluorescent dye calcofluor white (Pringle, 1991). Chitin is mainly localized at the bud scar (a scar of chitin which is left after separation of the daughter cell from the mother cell), the septum and in low amounts distributed in the cell wall. The $\beta(1\rightarrow4)$ linked chitin glycan is synthesized by three chitin synthases (Chs1-3p). The biggest portion of chitin is synthesized by Chs3p, a transmembrane protein which is transported from the TGN to the plasma membrane, where it synthesizes the chitin ring during budding, the chitosan of the ascus wall and the chitin distributed in the cell wall (Shaw *et al.*, 1991). Chs2p builds the primary septum during budding and Chs1p is supposed to have repair functions (Cabib *et al.*, 1992). The Chs3p can be endocytosed and recycles over a special early endosome species, the chitosome, back to the TGN (Valdivia and Schekman, 2002). Cells lacking Chs3p have defects in cell separation and maintaining the budding pattern (Shaw *et al.*, 1991).

1.1.2 Cell polarity of budding yeast cells

Haploid yeast cells build a new bud next to the bud scar of the previous one (axial budding pattern). After several budding cycles a chain of bud scars covers the cell wall of the mother cell which can be visualized under a microscope after calcofluor white staining (Pringle, 1991). Diploid cells are more oval shaped and build buds at both cell poles (bipolar budding pattern). Large scale mutagenesis screens obtained a lot of proteins which were involved in maintaining the bipolar budding pattern (e.g. Pruyne and Bretscher, 2000; Ni and Snyder, 2001). There involved are components of the cytoskeleton like actin (Act1p; Yang *et al.*, 1997) or

components of vesicular trafficking, lipid metabolism, protein modification machinery or proteins directly involved in bud-site selection and cell polarity such as Spa2p, Pea2p, Bni1p and Bud6p. These four proteins build the core of the polarisome complex which determines the yeast cell polarity (Sheu *et al.*, 1998).

Less proteins were known which change both, the haploid axial and the diploid bipolar budding pattern. There among are the GTP binding Ras-like protein Bud1p or the dolichyl-phosphatase Cwh8p (Ni and Snyder, 2001).

1.2 Protein transport in eukaryotic cells

After synthesis at the ribosomes proteins which are destined for secretion or organelles like the vacuole (lysosome in mammals) are translocated into the endoplasmic reticulum (ER) (Halic and Beckmann, 2005). Here starts the forward (anterograde) transport. Proteins dedicated for secretion, the lumen or the membrane of an organelle are further transported from the ER via the Golgi apparatus to the *trans*-Golgi network (TGN).

The TGN is a branching point for several transport routes. Secretory proteins and plasma membrane proteins (PM) like the yeast protein Snc1p, are packed into vesicles which can be directly transported to the plasma membrane (Lewis *et al.*, 2000) or reach the PM on a route via the early endosomes (EE).

Proteins with a function in the lysosome/vacuole were either routed to the vacuole in a direct manner, like the alkaline phosphatase ALP, or take a route via the endosomes like the soluble carboxypeptidase Y (CPY; Bowers and Stevens, 2005, fig. 1.1).

For the function of a cell it is essential that it can uptake proteins (e.g. nutrition and signal receptors) via the endocytotic transport way. These proteins are either recycled by recycling endosomes (RE) or transported through EE and late endosomes (LE; also referred to as multivesicular body, MVB) to the lysosome/vacuole for degradation (Toret *et al.*, 2008).

To sustain the intracellular homeostasis all these transport steps also have to proceed in the opposite direction (retrograde transport), so that all together the transport machinery of a cell consists of a complicated network of multiple transport steps. For the analysis of some trafficking routes marker proteins were established. For example the already mentioned soluble hydrolase CPY for the transport via the LE to the vacuole or the alkaline phosphatase (ALP) for the direct transport from TGN to the vacuole (Piper *et al.*, 1997).

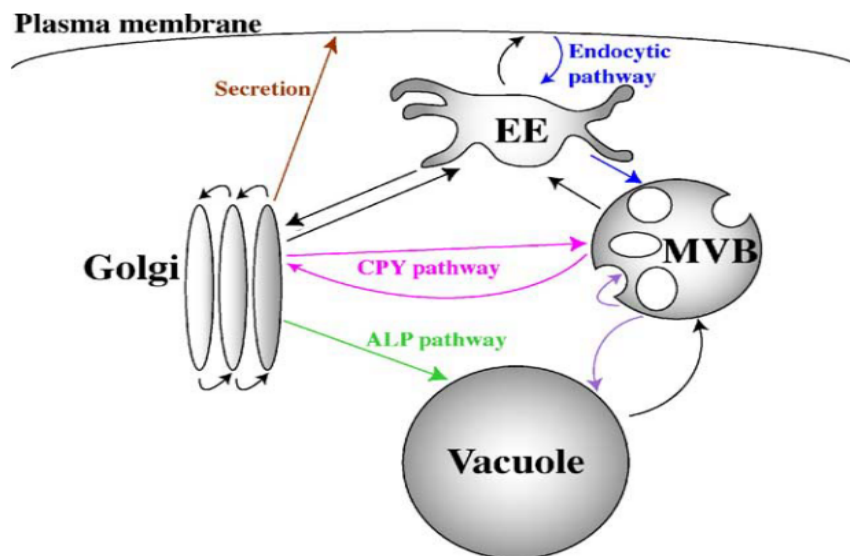


Fig. 1.1: **Protein transport routes in yeast cells.** Proteins, destined for the vacuole, can be routed over the multi vesicular bodies (MVB) to the vacuole like CPY or can be routed directly to the vacuole as ALP does. Proteins which have to be secreted can take a direct route or are transported to the early endosomes (EE) and then to the extracellular space. Proteins which take the endocytic pathway are endocytosed at the plasma membrane and sorted via the EE and MVB to the vacuole. Each forward transport step also occurs in a reverse, retrograde direction. (Bowers and Stevens, 2005, modified)

1.3 Vesicle transport

The vesicles are formed at their donor membrane (budding; fig. 1.2). During this process the membrane is bent and the coat molecules and sorting factors are concentrated at the budding vesicle. The vesicle coat consists of adaptor proteins which link cargo receptors and transmembrane cargo molecules to the clathrin triskelia which functions as vesicle scaffold. Integrated in the vesicle membrane are also factors which are important for the contact and fusion of the vesicle with the target membrane like tethering factors and SNAREs (N-methylmaleimide-sensitive-factor-attachment-protein-receptors). After the GTPase dependent scission (e.g. dynamin for clathrin coated vesicles; Vps1p in yeast) of the vesicle the coat is removed and the vesicle is transported via microfilaments, microtubules and motor proteins to its target membrane. The first contact is mediated by tethering factors on the target membrane and Rab proteins on the vesicle (tethering). The next step in vesicle fusion is the docking of the SNARE proteins. There are SNAREs on the vesicle (v-SNAREs) and on the target membrane (t-SNAREs). The complex built of four SNARE motifs yields the energy for vesicle fusion.

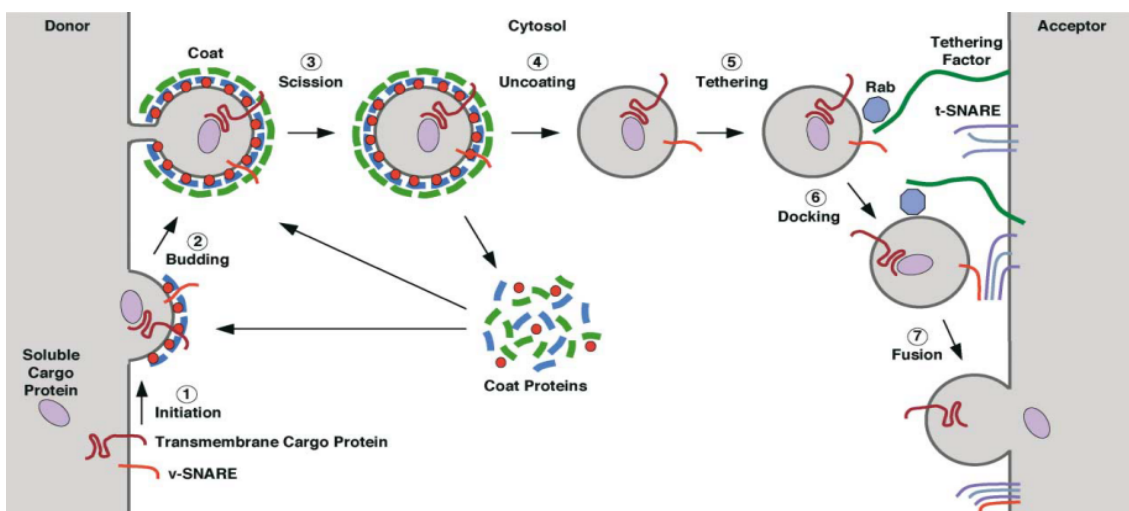


Fig. 1.2: **Vesicle transport from its donor to the target membrane.** In the initiation step (1) the cargo and coat molecules are concentrated at the side of vesicle budding (2). The budding process is induced by membrane curvature caused by the coat assembly and proteins like epsins. After dynamin dependent (in the case of clathrin coated vesicles) scission (3) the vesicle gets uncoated (4) and makes a first contact with the target membrane via Rab and tether proteins (tethering, 5). The SNAREs mediate the docking (6) process and drive the membrane fusion (7). (Bonifacino and Glick, 2004)

1.3.1 Analysis of anterograde transport from TGN to vacuole

One approach to analyse transport steps is to follow the trafficking of marker proteins. Well established markers for anterograde transport routes are the carboxypeptidase Y (CPY) for transport over late endosomes to the vacuole and the alkaline phosphatase for direct trafficking from TGN to the vacuole.

1.3.1.1 CPY transport

The soluble hydrolase Carboxipeptidase Y is an exopeptidase with a broad specificity which removes amino acids from the carboxy terminus of vacuolar proteins which are destined for degradation (Hayashi, 1976). It is synthesized as 111 aa preproCPY (ppCPY) including a 20 aa signal peptide which is cleaved after insertion into the ER. The resulting glycosylated 67 kDa CPY intermediate (p1CPY) is further processed to a higher glycosylated 69 kDa proCPY (p2CPY) in the Golgi. After transport over the LE to the vacuole the propeptide is removed by the proteinase Prb1p and the matured CPY (mCPY; 61 kDa) becomes active (Hasilik and Tanner, 1978). CPY is transported from the TGN to the late endosomes via the receptor Vps10p which cycles between the late Golgi and the late endosomes (Cooper and Stevens, 1996). If there is a block in the forward transport of CPY the p2 form is secreted. Due to its traffic dependent size differences CPY is a useful instrument to localize defects in specific transport steps (Rothman and Wieland, 1986).

1.3.1.2 ALP transport

In contrast to the CPY transport the alkaline phosphatase (ALP) bypasses the endosomes and is directly routed from the Golgi to the vacuole. ALP is a type II integral membrane protein with a short N-terminal cytoplasmic tail. At its C-terminus it contains a propeptide (pALP, 76 kDa) which keeps the enzyme inactive till cleavage in the vacuole by Pep4p (mALP; 72 kDa). Once activated it dephosphorylates phosphotyrosyl peptides (Klionsky and Emr, 1989). ALP is used

for the analysis of the endosome independent Golgi to vacuole trafficking. Therefore the kinetics of the propeptide removal give a good evidence for a forward transport defect of this route.

1.3.2 Retrograde transport from EE to TGN

For the retrograde transport steps there are some marker proteins known, too. The A-ALP construct can be used to analyze the LE to TGN transport whereas the GFP-Snc1p construct allows insights into the EE to TGN transport.

1.3.2.1 A-ALP transport

To analyze the transport kinetics in the retrograde late endosome to TGN transport ALP was further functionalized (Nothwehr *et al.*, 1993). Therefore a fusion protein (A-ALP) is used which consists of the transmembrane and luminal domains of ALP and the cytosolic domain of DPAP A which provides a sorting motif (Nothwehr and Hinds, 1997). The Dipeptidyl aminopeptidase A (DPAP A; also known as Ste13p) is a transmembrane protein located at the Golgi and it cleaves proteins at the carboxyl side of repeating X-Ala sequences. DPAP A is involved in the maturation of the alpha factor (Julius *et al.*, 1983) and is retained at the Golgi by a C-terminal signal motif based on aromatic amino acids (Phe-X-Phe-X-Asp; Nothwehr *et al.*, 1993).

The ALP part of the fusion protein can be easily detected or immunoprecipitated by established antibodies and gets processed during delivery. So the maturation of the A-ALP in the different organelles can be followed by a pulse chase approach.

With the DPAP A sorting motif A-ALP cycles between the TGN and the late endosome and the transport to the vacuole is very slow. If there is a block in the retrograde transport the A-ALP construct is faster delivered to the vacuole where it is proteolytically processed into its mature form (mA-ALP) and also degraded. The processing and degradation can be followed via a radioactive pulse chase approach where the A-ALP is labeled with ³⁵S-methionine/cysteine and immunoprecipitated after several chasing time points. The A-ALP forms are then

separated by SDS-PAGE. The main disadvantage of the method is, that the transport of A-ALP is not independent from the forward TGN to vacuole transport. If a mutant has several trafficking defects this may cause problems in the evaluation of the A-ALP experiment.

1.3.2.2 Snc1p transport

The GFP-Snc1p construct is a useful and established tool for the analysis of the retrograde early endosome to TGN transport (Lewis *et al.*, 2000). In contrast to the A-ALP construct GFP-Snc1p transport is not dependent on the forward TGN to endosome transport. Snc1p is sorted directly from the TGN to the plasma membrane and is then incorporated and routed through the EE back to the endosome. Its steady state distribution is mainly on the plasma membrane. Cells with a defect in the retrograde EE to TGN transport show an accumulation of GFP-Snc1p in the EE (Burston *et al.*, 2009).

1.4 SNAREs

Soluble N-methylmaleimide-sensitive-factor-attachment-protein-receptor (SNARE) proteins have an essential function in the membrane fusion process. SNAREs on vesicles (v-SNARES) and on the target membrane (t-SNARE) build a complex and by the resulting free energy, drive the fusion reaction. Up to date there are 25 SNAREs in yeast and over 40 SNAREs in mammals known (Jahn and Scheller, 2006). They all have a common motif of about 60-70 amino acids (aa) called the SNARE motif. Most of them have a C-terminal transmembrane domain and a N-terminus which provides a contact surface for regulating and sorting factors.

through proteins like Sec1p/Munc18 (SM) like proteins does also play an important role since e.g. on the early endosome several SNARE complexes are present: some to mediate fusion with the EE and some which are packed into vesicles and mediate fusion at their target organelles (Brandhorst *et al.*, 2006).

1.4.2 Molecular structure

If the SNAREs are not in a complex the 60-70 aa spanning SNARE-motif is relatively unstructured. Most of the SNAREs contain a C-terminal transmembrane domain and a short luminal C-Terminus (Jahn and Scheller, 2006). A few SNAREs are linked to the membrane via a palmitoyl-residue like SNAP-25 (Hess *et al.*, 1992) or a farnesyl-anchor like Ykt6p (Pylypenko *et al.*, 2008).

The SNARE complex can be structured into 15 hydrophobic layers and one hydrophilic layer exactly in the middle. The hydrophilic layer (0-layer) consists of one arginine (R) and three glutamines (Q) each contributed by one SNARE motif. This is the basis for the Q/R nomenclature of the SNAREs. The 3 Q SNAREs are further characterized by their -3 layer (Qa contributes a big hydrophobic residue, Qb/c SNAREs a small aa residue) and the similarity to the SNAP25 C- (Qc) or N- (Qb) terminal SNARE motif. Each SNARE complex consists of a combination of one R and one of each Q SNAREs (Qa, Qb, Qc).

There are different structures for the N-Termini of SNAREs known. R-SNAREs can be subdivided into “brevins” like synaptobrevin in mammalian synapses or the yeast Snc1p which contain a short variable N-terminus or the “longins” which contain conserved longin domains like yeast Ykt6p (Filippini *et al.*, 2001). Many of the Qa-SNAREs and some Qb or Qc-SNAREs have their N-terminus organized in an antiparallel three helices bundle. Since the C-Terminus of the SNARE is involved in the membrane fusion process, the N-terminus regulates in some cases the SNARE activity (Dulubova *et al.*, 1999) or is important for sorting the proteins to the appropriate organelle (Hirst *et al.*, 2004).

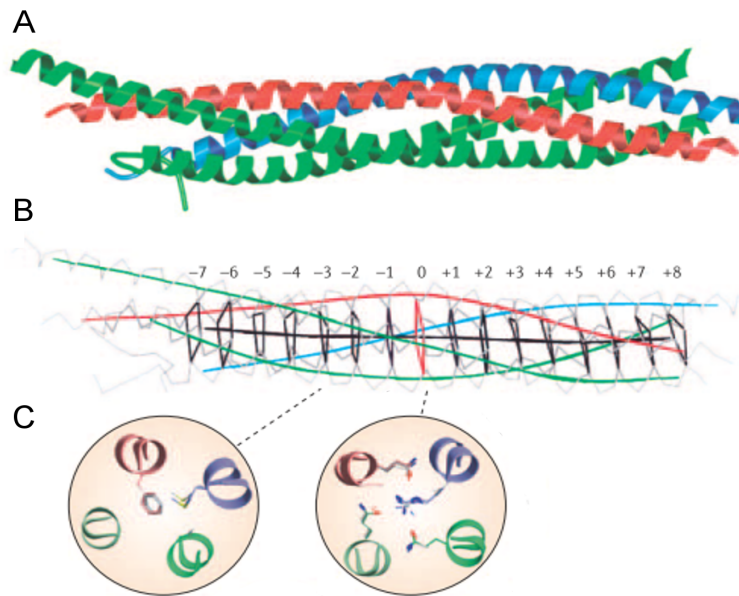


Fig. 1.4: **SNARE complex formation.** The SNARE complex is build of 4 alpha-helical SNARE motifs (Shown in **A** as ribbon structure). The R-SNARE is colored blue, the Qa SNARE red and the Qb and Qc SNAREs green. These motifs form a coiled-coil complex which can be characterized by 16 interacting layers (**B**, backbones where displayed as lines). Except of the middle 0-layer which is build of three glutamines (Q) and one arginine (R) (**C**, right circle), the layers are hydrophobic. The -3 layer (**C**, left circle) determines which SNARE is the Qa SNARE (large hydrophobic residue, red) and which are the Qb and Qc SNAREs (small residues, green). (Jahn and Scheller, 2006; modified)

1.4.3 SNAREs in membrane fusion

The first interaction of the vesicle with its target membrane is mediated by tethering and Rab proteins (tethering). These proteins also contribute to targeting specificity and the tethering process is GTP dependent since Rab proteins are small monomeric GTPases. The next step is the docking of the SNAREs from the target (t-SNAREs) and the vesicle (v-SNAREs) side. If the SNAREs find their right partners they form a SNARE complex and the resulting free energy overcomes the starting energy for membrane fusion. In the *trans*-SNARE complex at the beginning of the fusion process the t- and v- SNAREs are located on different membranes, when the fusion completes the SNAREs are located on the same membrane and the complex is called *cis*-SNARE complex. For disassembly in yeast the NSF (N-ethylmaleimide sensitive factor) ATPase Sec18p and a cofactor of the alpha-SNAP-family Sec17p are needed (Mayer *et al.*, 1996).

1.4.4 Yeast SNAREs

There are 25 SNAREs known in yeast. This work will focus mainly on the endosomal SNARE complex consisting of the Q SNAREs Pep12p, Vti1p, Syn8p and the R-SNARE Ykt6p.

1.4.4.1 *Pep12p*

Pep12p was first described in 1996 as a Qa SNARE which is involved in Golgi to endosome transport (Becherer *et al.*, 1996). It consists of 288 amino acids and is anchored in the membrane by a C-terminal transmembrane domain. Pep12p interacts with the other endosomal SNAREs Vti1p, Syn8p and Ykt6p and forms the SNARE complex for vesicle fusion at the late endosome (Dilcher *et al.*, 2001; Kweon *et al.*, 2003; Lewis and Pelham, 2002; Chidambaram *et al.*, 2004). Yeast cells which lack Pep12p show enlarged vacuolar compartments which were also referred as *vps* class D compartments (Raymond *et al.*, 1992). These compartments were typical for mutants which were defective in transport to the late endosome. Additionally it was shown that Pep12p is not only necessary for anterograde TGN to LE transport but also for the retrograde vacuole to LE and early endosome to late endosome pathway. This was shown by trafficking defects of CPY (TGN->vacuole), Ste3p (EE->vacuole) and RS-ALP (vacuole ->LE) in *pep12Δ* cells (Gerrard *et al.*, 2001).

Pep12p is sorted to the late endosomes in a Gga1/2p and Clathrin dependent manner. If the FSDSPEF motif close to the N-terminus of Pep12p is mutated or deleted it is mislocalized to the early endosomes but a direct interaction to the Gga proteins could not be shown (Black and Pelham, 2000). For the retrograde transport of Pep12p back to the Golgi the sorting nexin Grd19p and components of the retromer complex were required (Hetteema *et al.*, 2003).

1.4.4.2 Vti1p

The Vps10p interacting protein Vti1p is a 217 amino acids spanning Qb SNARE with a C-terminal transmembrane domain and a short (3 aa) luminal tail. Vps10p is the CPY sorting receptor which recycles between the TGN and endosomes. For identifying proteins involved in endosomal trafficking a yeast two-hybrid assay with the cytosolic tail of Vps10p was performed which yielded Vti1p as interactor (Fischer von Mollard *et al.* 1997). Up to now at least 4 different SNARE complexes were identified in which Vti1p plays a role. Together with Pep12p, Syn8p and Ykt6p Vti1p functions in the TGN to endosome transport (Fischer von Mollard *et al.*, 1997, Dilcher *et al.*, 2001; Lewis *et al.*, 2002), together with Sed5p, Sft1p and Ykt6p in retrograde Golgi trafficking (Fischer von Mollard *et al.*, 1997, Lupashin *et al.*, 1997), with Vam3p, Vam7p and Ykt6p/Nyv1p in transport to the vacuole and homotypic vacuole fusion (Ungermann *et al.*, 1999) and with Snc1/2p, Tlg1p and Tlg2p in retrograde EE to TGN transport (homotypic TGN fusion → Brickner *et al.*, 2001). Since the *vti1*Δ mutant is lethal temperature sensitive mutants of Vti1p were created for the analysis of its functions.

vti1-1, *vti1-11* and *vti1-2* (Fischer von Mollard and Stevens, 1999) have each two different amino acid exchanges in their SNARE motif. In the *vti1-1* mutant the TGN to late endosome transport is blocked and in the *vti1-11* mutant the TGN to LE, the LE to vacuole and the retrograde Golgi transport is blocked at restrictive temperature. For the *vti1-2* mutant defects in the TGN to LE, TGN to vacuole and LE to vacuole transport were shown.

1.4.4.3 Syn8p

Syn8p is a Qc SNARE which was discovered relatively late, since there was an error in the genome database which complicated the detection of the protein per similarity database search. Additionally *SYN8* deleted cells don't show any affected phenotype. So the first description came from the Pelham group in 2002 and still there is not much known about Syn8p besides it is involved in the endosomal SNARE complex, interacts with Ent3p (Chidambaram *et al.*, 2004), is possibly redundant with Tlg1p (Lewis *et al.*, 2002) and is additionally palmitoylated

for preventing protein degradation (Valdez-Taubas and Pelham, 2005).

1.5 Adaptor proteins

Two “classical” families of adaptor proteins in the transport of clathrin coated vesicles are the APs and the Ggas. Their function is to sort specific cargo proteins or cargo receptors into the nascent vesicles. Additionally they interact with other adaptor proteins and compounds of the vesicle coat like clathrin. In yeast cells there are three tetrameric APs (AP-1 to AP-3) and two monomeric Ggas (Gga1p and Gga2p) known. Beside Ggas and APs there are also more cargo specific adaptors like ENTH and ANTH domain proteins.

1.5.1 ENTH-proteins

Epsin-N-Terminal-homology (ENTH) proteins are a family of adaptor proteins which have the characteristic ENTH domain and an unstructured C-terminus in common. They function in clathrin dependent budding processes and, besides the cargo sorting function, have a role in inducing the membrane curvature (Legendre-Guillemain *et al.*, 2004).

1.5.2 Structure and function of ENTH domain proteins

The family of ENTH domain proteins consists of 4 members each in yeast (Ent1-4p) and mammals (epsin1-4). In Yeast cells Ent1p and Ent2p function in budding from the plasma membrane (PM; Wendland *et al.*, 1999) and Ent3p in endosomal and TGN budding (Duncan *et al.*, 2003). For Ent4p also a function in TGN to endosome transport is proposed (Deng *et al.*, 2009).

The ENTH domain has about 160 aa and is structured into 8 alpha-helices. ENTH proteins can bind specific phosphatidylinositols (PI) by the first about 30 aa of the protein. After binding the membrane an additional helix, called 0-helix forms and inserts into the membrane leaflet (Ford *et al.*, 2002). This contributes to membrane

curvature which is needed for the vesicle budding. Another feature of the ENTH domain is its binding capacity to SNARE proteins. For example Ent3p binds to Vti1p, Pep12p and Syn8p (Chidambaram *et al.*, 2004 and 2008) and the mammalian homologue epsinR (also called epsin-4, enthoprotin or CLINT) binds to vti1b, syntaxin7 and syntaxin8 (Chidambaram *et al.*, 2004 and 2008; Hirst *et al.* 2003). Several other protein interactions were mediated by the C-terminus. Ent1p and Ent2p have interaction sites for clathrin, ubiquitin (UIM), AP-1 and EH-domain proteins (NPF). Ent3p has no UIM and NPF but it has two binding sites for each the alpha-ear and the gamma ear of AP-1 and the gamma-adaptin ear homology domain (GAE) of Gga2p. Additionally it shows a weak binding capacity for clathrin (Duncan *et al.*, 2003).

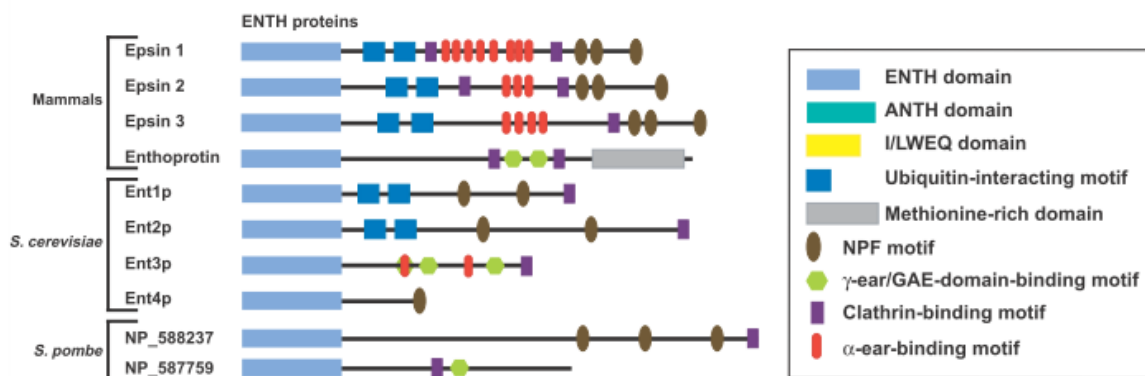


Fig. 1.5: **The family of yeast ENTH domain proteins.** There are four members known for mammals and yeast, respectively. Enthoprotin is also called epsinR, epsin-4 or CLINT. (Legendre-Guillemain *et al.*, 2004)

1.5.3 The yeast ENTH domain protein Ent3p

The mammalian homologue of Ent3p is epsinR which plays a role in the retrograde transport from endosomes to TGN and is supposed to be involved in the predisposition of human schizophrenia when a certain epsinR SNP (single nucleotide polymorphism) is present (Escamilla *et al.*, 2008; Pimm *et al.*, 2005).

Ent3p has a role together with Ent5p in the *trans*-Golgi network (TGN) to endosome transport. Ent3p can recruit cargo proteins such as the endosomal SNAREs Vti1p, Pep12p, Syn8p (Chidambaram *et al.* 2004 and 2008) and binds other coat proteins like Clathrin and Gga2p (Duncan *et al.*, 2003). Besides its

adaptor functions it is supposed that Ent3p can insert the 0-helix of its ENTH domain after phosphatidylinositol-3,5-bisphosphate (PI3,5P₂) binding in the membrane leaflet and may induce membrane curvature (Ford *et al.*, 2002) in the vesicle budding process. Ent3p shows some functional redundancies with the ANTH (AP180 N-terminal homology) family protein Ent5p. ANTH domain proteins are a functional related family of cargo specific adaptor proteins which also can bind clathrin, Gga and APs. The ANTH domain binds membranes also through interaction with PIs but in contrast to the ENTH domain it does not contain a 0-helix which inserts into the membrane leaflet (Stahelin *et al.*, 2003). Beside Ent5p three other ANTH domain proteins in yeast were found up to now (yAP1801, yAP1802 and Sla2p). There are also ANTH domain proteins in mammals and other organisms like in the *Schizosaccharomyces pombe* or *Arabidopsis thaliana*. Ent5p interacts with Vps27p at the late endosome and functions together with Ent3p in the sorting of proteins into the inner late endosomal vesicles (multivesicular bodies, MVB) (Eugster *et al.*, 2004). Both, Ent5p and Ent3p have functions in the TGN to endosome transport. The analysis of the Ent3p and Ent5p functions is complicated since cells with single deletions of *ENT5* or *ENT3* show no or only minor defects in transport steps between the TGN and the endosomes. Only the *ent3Δent5Δ* double mutant has severe defects in clathrin localization, α -factor maturation (Duncan *et al.*, 2003) and CPY transport (Chidambaram *et al.*, 2004). It is suggested that Ent3p cooperates more with Gga2p function and Ent5p is important for both Gga2p and AP-1 function (Costaguta *et al.*, 2006).

1.5.4 Interaction of Ent3p with endosomal SNAREs

Neither for the yeast Ent3p nor for the endosomal SNAREs Vti1p, Pep12p, and Syn8p crystal structures are available. Interaction studies were done so far using yeast two-hybrid or pull down assays (Chidambaram *et al.*, 2004 and 2008) or by studying genetic or functional interactions in the intact yeast cells. Immunoprecipitation experiments have shown to be difficult since cargo-adaptor interactions were very transient and weak. In 2007 the crystal structure of the mammalian complex of vti1b and epsinR was published by Miller *et al.*. The interaction motif proved to be a conformational motif and not a single stretch of

amino acids like the DPW motif for AP-2 interaction. Several interacting amino acids of different epsinR and vti1b helices were proven by pull-down assays after mutagenesis. For the interaction the regions between helix α 2-3, helices α 4-5 and the helix α 8 on epsinR were involved. The main interacting parts on vti1b were on the Ha helix and in the turn between helices Hb and Hc (Miller *et al.*, 2007).

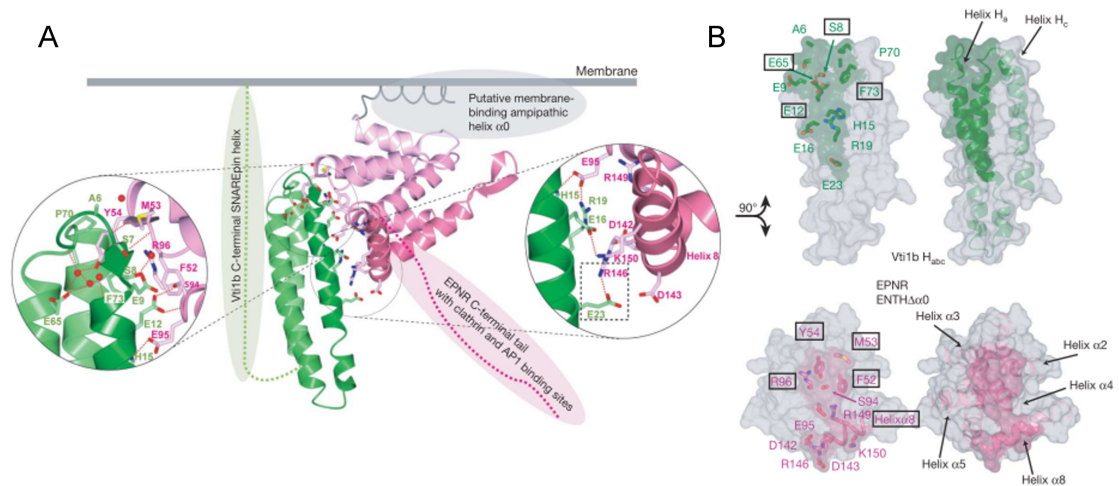


Fig. 1.6: **Crystal structure of the human epsinR-vti1b complex.** **A:** Ribbon structure of the interacting complex of vti1b (green) and epsinR (red). The interaction surface is shown enlarged in the circles. In **B** surface models were shown of vti1b (upper two panels) and epsinR (lower two panels). The amino acids mutated from Miller *et al.* are labeled and the amino acids which are necessary for interaction in a pull down assay additionally boxed (Miller *et al.*, 2007).

1.6 Functions of Tvp23p

The functions of SNAREs have to be tightly regulated. So there is a large network of interacting proteins based on each SNARE complex. To identify interaction partners for the essential SNARE Vti1p a suppressor screen with the *vti1-2* mutant was performed (Dilcher, 2002). One of the resulting suppressors of *vti1-2* temperature sensitive growth defect was identified as the Tlg2p compartment vesicle protein of 23 kDa (Tvp23p; Stein, 2007). This sparsely characterized membrane protein colocalizes with Tlg2p at the late Golgi (Inadome *et al.*, 2005), interacts with the Yip1-family proteins Yip4p and Yip5p and is supposed to have three transmembrane domains (Inadome *et al.*, 2007). Further interactions with the retromer subunit Vps35p were detected in a yeast two-hybrid screen by Vollert and Uetz (2004). *TVP23* is a non essential gene and its disruption causes no

defects in temperature tolerance, growth on high salt agar plates or the CPY, ALP and CPI (sorting into internal MVB vesicles) transport. But a strongly reduced growth at 35°C was detected when additionally the gene of the Ras-like GTPase Ypt6p was deleted (Inadome *et al.*, 2007). Ypt6p is necessary for the endosome derived fusion of vesicles at the late Golgi and the retrograde intra-Golgi transport (Luo and Gallwitz, 2003). All together this data gives a hint that Tvp23p may have a function in vesicle mediated transport at the Golgi apparatus.

1.6.1 Yip4p and Yip5p

An interaction of Tvp23p with Yip4p and Yip5p was shown by yeast two-hybrid assays and immunoprecipitation (Inadome *et al.*, 2007). Yip4p and Yip5p are Yip1p related membrane proteins which interact with several small Rab-GTPases e.g Ypt1p, Ypt10p, Ypt11p, Ypt6p, Sec4p and the other members of the Yip1-family (Calero *et al.* 2002). For Yip1p a function in the Golgi maintenance was shown in yeast (Shakoori *et al.*, 2003) and a similar function was proven for the human Yip1 homologues YIPF5 and YIF1A (Yoshida *et al.* 2008). For the mammalian yip3 a function as GDI (GTP dissociation inhibitor) displacement factor was suggested by Sivars *et al.* (2003). But neither for the single *YIP4/YIP5* deletion mutants nor for the double mutant any phenotype and therefore also no function was described in the literature.

2 Aim of this Work

The ENTH domain protein Ent3p functions together with Ent5p in the *trans*-Golgi network as cargo adaptor for endosomal SNAREs Vti1p, Pep12p and Syn8p. These SNAREs are necessary for vesicle fusion at the late endosome.

In a first project the structure and function of the interaction between Ent3p and the endosomal SNAREs Vti1p, Pep12p and Syn8p should be further characterized. Additionally it should be checked if Ent3p has also functions in the retrograde early endosome to TGN transport as it was shown for the mammalian homologue epsinR.

In a second project the functions of the separated Ent3p domains (ENTH domain, C-terminus and full length protein without phosphatidylinositide binding domain) in forward and retrograde endosomal transport should be analyzed. *ent3Δent5Δ* cells have cell wall and budding defects and it should be checked which Ent3p domains are necessary for a correct cell wall assembly and budding of the yeast cells.

In a third project a possible function of the uncharacterized protein Tvp23p and its interactors Yip4p and Yip5p in the endosomal transport should be checked since Tvp23p was a suppressor of the temperature sensitive *vti1-2* mutant.

3 Material and Methods

3.1 Material

3.1.1 Lab Equipment

Autoclave	Webeco	Bad Schwartau
Biofuge 13	Heraeus Instruments	Osterode
BioPhotometer	Eppendorf	Hamburg
Cover slips 24x50 mm u. 22x22 mm	Menzel-Glaser	Braunschweig
DPU-414 Thermal Printer	Seiko	Torrance, USA
Disposable cannulae 20Gx1, 27Gx3/4	Braun	Melsungen
Disposable syringes 10 mL	Braun	Melsungen
Ice machine	Ziegra B-100	Isernhagen
Freezer -20°C	Liebherr Premium	Ochsenhausen
Electroporator 2510	Eppendorf	Hamburg
Electrophoresis chambers DNA/protein	Mechanische Werkstatt Universität Bielefeld	Bielefeld
Electroporation cuvettes	Eppendorf	Hamburg
Disposal bags	Roth	Karlsruhe
Fluorescence lamp	Exfo X-Cite® 120PC	Quebec, Canada
Freezer -80°C	Heraeus Instruments	Osterode
French press "Aminco"	SLM Instruments	Bath, UK
Gel documentation system	Peqlab	Erlangen
Beaker 50, 100, 250 mL	Schott	Mainz
Glas pipettes 5/10/20 mL	Hirschmann EM	Eberstadt
Cryo tubes	Nunc	Wiesbaden
Fridge 4°C	Privileg	Fürth
LAS-Camera	Fujifilm LAS 3000	Düsseldorf
Liquid Scintillation counter Tricarb 2800 TR	Perkin Elmer	Waltham, USA
Magnetic stirrer	Heidolph	Nürnberg
Microscope	Leica DM5000 B	Solms
Microwave	LG Wavedom	Korea
Glass slides	Marienfeld Superior	Lauda-Königshofen
Parafilm® "M"	Pechiney	Chicago, USA

Peltier thermal cycler	MJ Research, Inc	Watertown, USA
Phosphoimager BAS-1800 II	Fuji photo film Co Ltd.	Japan
Pipetman 20, 200, 1000 µL	Gilson	Middleton, USA
Pipet tips	Sarstedt	Nümbrecht
Plastic tubes 10/15/50 mL	Sarstedt	Nümbrecht
Power Pack P25	Biometra	Göttingen
Protran® nitrocellulose membrane	Schleicher und Schüll	Dassel
Shaking incubator	New Brunswick Scientific	Edison, USA
Infinite 200 Fluorophotometer	Tecan Group	Männedorf, CH
Thermal shaker	Holten Lamin Air HVR 2448	Denmark
Tetrade dissection microscope	Nikon eclipse 50	Düsseldorf
Thermomixer 5436	Eppendorf	Hamburg
Thermoprinter	Mitsubishi P93	Ratingen
Ultracentrifuge	Beckman Optima™	Krefeld
Vortex Genie II	Scientific Industries	Kanada
Balance	Sartorius	Göttingen
Water treatment plant	Millipore Synergy UV	Billerica, USA
Water bath	Julabo Paratherm U4	Seelbach/Lahr
Westernblot chamber	Mechanische Werkstatt	Universität Bielefeld
Whatman GB002 paper	Schleicher and Schüll	Dassel
Centrifuge 5415C	Eppendorf	Hamburg
Centrifuge 5417R	Eppendorf	Hamburg

3.1.2 Chemicals

The chemicals used were obtained from the companies Roth (Karlsruhe), Sigma (Meckenheim) and Merck (Darmstadt) with the following exceptions:

Aminoacids	Biomol, Serva Siama. ICN	Hamburg, Heidelberg München Meckenheim
Bacto-Agar		Detroit, USA
Bacto-Pepton	DIFCO	Detroit, USA
Bacto-Trypton	DIFCO	Detroit, USA
BSA (Bovine Serum Albumin; Albumine bovine Fraction V)	Serva	Heidelberg
DMP (Dimethylpimelin- diimidatdihydrochlorid)	Fluka	Buchs
dNTPs	Amersham	Braunschweig

DSP (Dithiobis[succinimidyl-propionat])	Pierce	Rockford, USA
FM4-64	Molecular Probes™ (Invitrogen)	Karlsruhe
Yeast extract	DIFCO	Detroit, USA
Milk powder	Lasana	Herford
Phalloidin-TRITC (Tetramethyl-rhodamin-Isothiocyanat)	Sigma	Meckenheim
Phenol:Chloroform:Isoamylalcohol (25:24:1)	Fluka	Buchs
Ponceau S	Serva	Heidelberg
Protein-A-Sepharose	Pharmacia	Freiburg
Yeast-Nitrogen-Base	DIFCO	Detroit, USA

3.1.3 Proteaseinhibitors

Leupeptin	Biomol, Hamburg
Pepstatin A	Biomol, Hamburg
Phenylmethylsulfonylfluorid (PMSF)	Serva, Heidelberg

100 μ L 100x Proteaseinhibitor-Mix:
 50 μ L 100 mM PMSF (17,4 mg/mL in ethanol)
 10 μ L Pepstatin
 39 μ L Methanol
 1 μ L Leupeptin (10 mg/mL in H₂O)

3.1.4 Antibodies

Tab. 1: Antibodies

Antibody	Molecular weight / kDa	species	Dilution for Western blot	Dilution for immunofluorescence	Source
Pep12p	33	Rabbit	1:1000		FvMollard
Pep12p	33	Mouse		1:100	Eugene
Ent3p	48	Rabbit	1:500	1:100	FvMollard
CPY	69	Mouse	1:100		T. Stevens
CPY	69	Rabbit			T. Stevens

Antibody	Molecular weight / kDa	species	Dilution for Western blot	Dilution for immunofluorescence	Source
ALP	72	Mouse	1:100		T. Stevens
ALP	72	Rabbit			T. Stevens
HA		Mouse	1:1000	1:200	Covance
HA		Mouse	1:50		T. Stevens
Use1p	35	Rabbit	1:1000		M. Dilcher
Vti1p	27	Rabbit	1:3000	1:300 (AP)	T. Stevens
Vph1p	100	Mouse	1:100		T. Stevens
Cy2		anti mouse		1:400	Dianova
Cy3		anti mouse		1:400	Dianova
Goat-anti-mouse horseradish peroxidase			1:10000		Sigma
Goat-anti-rabbit horseradish peroxidase			1:10000		Sigma

3.1.5 Enzymes, Nucleotides and Standards

1 kb-DNA-ladder	Gibco BRL, Eggenstein
Prestained protein standard	BioRad, München
Restriction endonucleases	New England Biolabs, Frankfurt a. M.
T4-Ligase	Fermentas, St. Leon-Rot
<i>Taq</i> -DNA-polymerase	Clontech, Bioline
AccuPrime™ <i>Taq</i> -DNA Polymerase system	Invitrogen, Karlsbad
<i>Pfu</i> -polymerase	Stratagene, Heidelberg
Ultrapure dNTP set	Pharmacia, Freiburg
Zymolyase®-20T	Seikagaku, Tokyo (Japan)

3.1.6 Kits for Isolation and Detection of DNA and Proteins

QIAEX®II agarose gel extraction Kit	Qiagen, Hilden
QIAprep Spin miniprep Kit	Qiagen, Hilden
SuperSignal® West Pico Chemilumineszenz Substrat	PIERCE, Rockford (USA)
Bradford reagent	Roth, Karlsruhe

3.1.7 Bacteria Strains and Plasmids

Strains:

XL1-Blue

Genotype: *recA1, endA1, gyrA96, thi-1, hsdR17, supE44, relA1, lac[F', proAB, lacI^qZΔM15, Tn10(Tet^r)^f*; reference: Stratagene, Heidelberg

DH5-α

genotype: *supE44, thi-1, recA1, relA1, hsdR17(rK⁻mK⁺), thi-1, ΔlacU169 (Φ80 lacZΔM15), endA1, gyrA (Nal^r)*; reference: Gibco BRL, Eggenstein

BL21-CP

genotype: *ompT hsdS(r_S⁻ m_S⁻) dcm⁺ Tet^r gal λ(DE3) endA Hte [argU proL Cam^r] [argU ileY leuW Strep/Spec^r]*; reference: Stratagene, Heidelberg

Tables with used and constructed **plasmids** and **yeast strains** as well as the **oligonucleotides** used for plasmid construction, sequencing and gene deletions can be found in the appendix.

3.1.8 Media for *S. cerevisiae* and *E. coli*

Synthetic Deficiency (SD)-medium

6.7 g Yeast nitrogen base without aminoacids
were dissolved in 860 mL of ddH₂O and autoclaved. After cooling

40 mL	50% Glucose (2% final conc.)
100 mL	10x Amino acid mix were added

The 10 x amino acid mix was prepared using the following table.

Supplements	Concentration (g/L)
Adenine	0.20
L-Tyrosine	0.30
L-Phenylalanine	0.50
L-Arginine	0.20
L-Lysine	0.60
L-Threonine	2.00
Uracil	0.20
L-Leucine	1.20
L-Tryptophan	0.20
L-Histidine	0.20

For the desired SD medium the appropriate amino acids were left out and the 10x mix was autoclaved.

YEPD (1L)

20 g Peptone
 10 g Yeast extract
 were dissolved in 960 mL ddH₂O, autoclaved and
 40 mL 50% Glucose (2% final conc.)
 were added.

For preparing YEPD or SD plates 1.5% (YEPD) or 2% (SD) agar were added before autoclaving and the medium was poured into Ø 10 cm Petri dishes.

Luria Bertani (LB)

1 g Glucose
 5 g Bacto-yeast extract
 5 g NaCl
 10 g Bacto-Tryptone

The medium was autoclaved and for bacteria selection 100 µg/mL Ampicillin or 50 µg/mL Kanamycin were added.

For preparation of LB-plates 1.5% Agar was added before autoclaving.

For blue-white screen 100 μ L 105 mM IPTG (in water) and 50 μ L 50 mg/mL X-Gal (in DMF) were mixed and streaked evenly on the plate.

3.1.9 Stock Solutions and Buffers

10 x PBS (1 L)

1.5	M	NaCl	(87,70 g)
160	mM	Na ₂ HPO ₄	(28,48 g)
40	mM	NaH ₂ PO ₄	(5,52 g)

dissolved in ddH₂O and adjusted to pH 7.4 with NaOH.

50 x TAE (1 L)

2	M	Tris	(242 g)
0.1	mM	Na ₂ EDTA (Titriplex III)	(37 g)
57	mL	acetic acid	

filled up to 1 L with ddH₂O.

TE (100 mL)

10	mM	Tris-HCl, pH 7.5	(1 mL 1 M stock solution)
50	mM	0.5 M EDTA	(200 μ L)

filled up to 100 mL with ddH₂O.

TE β (10 mL)

10	mM	Tris-HCl, pH 8.0	(1 mL 1 M stock solution)
50	mM	EDTA	(200 μ L 0.5 M stock solution)
1	%	β -Mercaptoethanol	(50 μ L)

filled up to 10 mL with ddH₂O.

Spheroplast-buffer (10 mL)

1.2	M	Sorbitol	(6 mL 2 M stock solution)
50	mM	KPO ₄ , pH 7,3	(3.5 mL 1 M stock solution)
1	mM	MgCl ₂	(100 μ L 0.1 M stock solution)

filled up to 10 mL with ddH₂O.

10% SDS

10 g sodium dodecylsulfate in 100 mL ddH₂O

0.5 M EDTA

14.61 g ethylenediaminetetraacetate (Titriplex III) were dissolved in 100 mL ddH₂O and adjusted to pH 8.0 with 10 N NaOH.

1 M Tris-HCl

12.11 g Tris were dissolved in 80 mL ddH₂O, adjusted to the desired pH with concentrated HCl and filled up to 100 mL with ddH₂O.

3.1.10 Software

E-Capt 12.7	Organization of pictures taken on the UV-transillumination system
Aida 4.06.117	Program for picture processing and quantification of western blots
Leica FW4000	Controlling software for the Leica DM5000 microscope
GIMP 2.6.1	Image processing software
ImageJ 1.40	Image processing software especially for microscopy pictures
OpenOffice 3.0	Software for text and spreadsheet processing
Pymol 0.99	Visualization and modeling of three dimensional protein structures
Citavi 2.5	Organization of literature

3.1.11 Internet services

BLAST	Sequence alignment
NEBcutter	displays restriction sites for endonucleases
PubMed	literature search
ExPASy	protein database and link collection/proteomic Server
SGD	<i>Saccharomyces</i> genome database
PDB	database for protein structures
ClustalW	multiple sequence alignments
3D-jigsaw	template based protein modeling

3.2 Methods

3.2.1 Molecular Biology

3.2.1.1 Preparation of electrocompetent *E. coli* cells

For an efficient transformation of *E. coli* cells with plasmid DNA via electroporation the cells have to be prepared as follows. 10 mL over night culture were diluted in 1 L LB-medium and cultivated at 37°C till an OD₆₀₀ 0.3-0.35. The cells were cooled down on ice, pelleted at 4°C and washed with 1 L cold water. After resuspension in 0.5 L cold water, the cells were centrifuged two times more and resuspended in 20 mL and 2 mL cold and sterile 10% glycerol, respectively. 40 µL and 80 µL aliquots were frozen at -80°C.

3.2.1.2 Electroporation

To transform DNA into the cells, the electrocompetent *E. coli* were thawed on ice and 2 µL Plasmid DNA was added. The mixture was given into a precooled electroporation cuvette and electroporated with 2000 V. Shortly after the pulse 500 µL SOC-medium were added and the cells were incubated 20-40 min at 37°C. The cells were streaked on an appropriate LB selection plate containing either 100 µg/mL Ampicillin or 50 µg/mL Kanamycin.

3.2.1.3 DNA isolation from *E. coli*

To isolate plasmid-DNA from *E. coli* cells a kit provided by Qiagen or Promega was used or the following procedure (for yielding high amounts of DNA from XL1-blue) was performed:

To extract DNA by phenole/chloroform extraction 1.5 mL bacteria culture were pelleted, resuspended in 100 µL lysozyme solution and incubated for 5 min at RT. For cell lysis 200 µL 0.2 M NaOH/ 1% SDS were added, mixed by inverting and incubated for further 5 min at RT. The cell suspension was supplemented with

150 µL 3 M sodium acetate (pH 5.2), inverted, incubated for 5 min at RT and centrifuged for 10 min at 13.000 rpm (13.000 g). The supernatant was mixed with 1 mL ice cold 100% ethanol and the precipitated DNA was pelleted by centrifugation for 15 min at 4°C and 13.000 rpm. The pellet was washed with 750 µL ice cold 70% ethanol and air dried. The purified DNA was resuspended in 20 µL TE with 100 µg/mL RNase A and stored at 4°C or -20°C.

Lysozyme solution

50 mM glucose
10 mM EDTA
25 mM Tris-HCl pH 8.0
in ddH₂O, stored at 4°C

3.2.1.4 Determination of DNA concentration

For Determination of DNA concentration the Nanodrop[®]-Spectrophotometer (Peqlab) was used as described in the user manual.

3.2.1.5 Cloning techniques

3.2.1.5.1 Polymerase chain reaction (PCR)

An indispensable method for cloning DNA fragments is amplifying DNA via polymerase chain reaction (PCR). It is used for generation of the desired DNA fragment from a library or plasmid template as well as for scanning the cloned plasmids on the desired product.

The PCR consists of an initial denaturation step, three cycling amplifying steps and a final extension step. During the amplification process the DNA is heated up to 95°C for denaturation, then cooled down to the primer annealing temperature and heated up again till the Polymerase optimum working temperature for extension of the primer fragments. The protocol varies depending on the used polymerase and preparation size.

For a standard PCR reaction the following mixture was used:

Taq-Polymerase (Roche):

H ₂ O	82.5	μL
10xBuffer	10	μL
dNTPs 10 mM each	1	μL
3' primer (100 pm/μL)	2.5	μL
5' primer (100 pm/μL)	2.5	μL
DNA	1	μL
Taq-polymerase (1:10 <i>Pfu</i> -polymerase)	1	μL

Program:

1. 94°C 2 min
 2. 94°C 40 sec (denaturation)
 3. x°C 40 sec (annealing, primer T_m, see tab. 4 in the appendix)
 4. 72°C 40 sec (extension, depends on fragment length, 1 kb~1 min)
 5. 72°C 3 min (*final extension*)
- steps 2.-4. were repeated 30-35 times.

For large fragments which were difficult to amplify the AccuPrime Taq was used:

AccuPrime™

H ₂ O	85.5	μL
10xbuffer II (dNTPs incl.)	10	μL
3' primer (100 pm/μL)	2.5	μL
5' primer (100 pm/μL)	2.5	μL
DNA	1	μL
AccuPrime™ polymerase	1	μL

Program:

1. 94°C 2 min
 2. 94°C 30 sec
 3. e.g. 53°C 30 sec
 4. 68°C e.g. 2 min
 5. 68°C 3 min
- steps 2.-4. were repeated 30-35 times.

3.2.1.5.2 Site directed mutagenesis by PCR

To induce specific nucleotide exchanges special primers were designed which contain the exchanged nucleotides and about 20 nucleotides complementary to the 3' sequence of template next to the mutation. The 5' sequences of the primers were constructed to overlap. The overlapping sequence should have a T_m in a sensible range. These forward and reverse mutagenesis primers were combined in two separate PCR reactions with Primers binding either to the desired start or stop sequences. The overlapping two PCR fragments were amplified in a second PCR to achieve the complete fragment including the mutation. Therefore the fragments were mixed in an equimolar concentration (about 10-20 nmol) and amplified with Taq/Pfu mix to yield a DNA construct which can be cloned into pGEM-T-easy®.

3.2.1.5.3 Colony PCR

A very quick method to check transformed *E. coli* colonies on the presence of the desired plasmid is to use raw cell material in the PCR mix.

A very small amount of cells was taken from the agar plate with a tooth pick and for backup one streak was made on a fresh LB-plate. Without taking new cells the tooth pick was rotated in the complete PCR mix.

Colony-PCR (*E. coli*)

H ₂ O	21	μL
10xbuffer	2.5	μL
dNTPs 10 mM each	0.25	μL
3' primer (100 pm/μL)	0.5	μL
5' primer (100 pm/μL)	0.5	μL
<i>Taq</i> -polymerase	0.25	μL

The PCR run was conducted as described before.

3.2.1.5.4 Ethanol precipitation

For concentration and purification of PCR-product an ethanol precipitation was carried out. To 100 μL PCR product 1/10 volume 3 M sodium acetate pH 5,2 and 250 μL ice cold 100% ethanol were added. The mixture was vortexed and kept on dry ice for 10 min. The precipitated DNA was pelleted down for 10 min at 13.000 rpm and 4°C in a microcentrifuge. The pellet was washed with 70% ethanol, centrifuged for one minute and air dried. The dry pellet was resuspended in 50 μL TE or water.

3.2.1.5.5 Cloning of PCR-products with pGEM® T-easy

Some restriction endonucleases may not cut properly at the end of PCR products. This causes problems when the digested PCR product should be ligated directly into a plasmid vector. To overcome this difficulty cloning via the pGEM® T-easy vector kit is an easy and fast method. The system takes advantage of the feature of the *Taq* polymerase which adds overhanging adenosine bases to the PCR products. The pGEM® T-easy vector is linearized and contains overhanging

thymidine bases so that PCR products can be ligated directly into the vector without using restriction enzymes. From the ligated construct the insert can be subcloned into the designated vector.

For the ligation the following mixture was compounded:

0.5 μ L	pGEM [®] T-easy vector
3.5 μ	Insert (ethanol precipitated PCR product solved in 10 μ L ddH ₂ O)
1.5 μ L	ligase buffer
1 μ L	T4-ligase

The ligation mixture was incubated at 4°C over night and transformed into *E. coli* via electroporation (1.2.1.2).

3.2.1.5.6 Digestion of DNA with restriction endonucleases

For specific digestion of DNA fragments restriction endonucleases were used. These enzymes recognize short, mostly palindromic, nucleotide sequences and cut them, resulting in ends with overhanging nucleotides (“sticky”-ends) or without overhang (“blunt” ends).

The following mixtures were prepared:

<u>Preparative (100 μL):</u>			<u>analytic (10 μL):</u>		
25	μ L	DNA	1	μ L	DNA
10	μ L	10 x reaction buffer	1	μ L	10 x reaction buffer
10	μ L	10 x BSA (if required)	1	μ L	10 x BSA (if required)
2	μ L	each enzyme	0.2	μ L	each enzyme
53	μ L	ddH ₂ O	6.6	μ L	ddH ₂ O

The reaction batches were incubated over night (PCR-product) or for 2 h (plasmid DNA) at 37°C and analyzed by agarose gel electrophoresis.

3.2.1.5.7 Agarose gel electrophoresis of DNA

To control DNA fragments from PCR or endonuclease treatment the ability of DNA to move through an agarose gel to which an electric field is applied is utilized. The negatively charged DNA moves towards the plus terminal and the velocity of the movement (of linear DNA) depends on the number of nucleotides. For fragments between 0.5 and 1 kb an 1% agarose gel in TAE containing about 0,005%

ethidiumbromide was used. To the DNA samples 6x loading buffer was added and the samples were loaded on the gel. Depending on the gel size 60-100 mA were applied. Through the DNA intercalating ethidiumbromide the DNA could be visualized on an UV-transilluminator.

6x loading buffer

0.15 % (w/v) Bromphenolblue (marker line for about 400 bp)
0.15 % Xylenecyanol FF (marker line for about 4 kb)
40 % Saccharose in 1x TAE
in ddH₂O

3.2.1.5.8 Ligation of DNA inserts into plasmid vectors

When digested vector and insert DNA were obtained in adequate concentration and purity the ligation was executed with the help of the enzyme T4 DNA-Ligase. The ligase links the 3' hydroxy end of one with the 5' phosphate end of another DNA fragment under ATP consumption. The ligation was carried out as followed:

1.5 μL 10x Ligase buffer
1 μL T4 Ligase (Fermentas)
1 μL linearized vector DNA
insert DNA in a molar ratio 10:1 with the vector

The batch was filled up to 15 μL with ddH₂O and incubated over night at 16°C.

3.2.1.6 Sequencing

Samples for sequencing were delivered to the sequencing core facility (SCF) of the University Bielefeld. The samples were diluted to 250 ng/μL in 10 μL ddH₂O.

<https://scf.cebitec.uni-bielefeld.de/>

3.2.1.7 DMSO-Stocks of *E. coli* and *S. cerevisiae*

For cryo-conservation bacteria and yeast cells were streaked on appropriate agar plates and cultivated over night at 37°C or 30°C, respectively. The cells were taken from the plate, resuspended in a 7% DMSO solution and directly frozen at -80°C.

3.2.2 Yeast Genetics

3.2.2.1 PLATE transformation

For protein expression in yeast cells an easy method is to shuttle the desired gene into the cells via an expression plasmid. The PLATE method is a very simple and quick method and yields a sufficient efficiency for plasmid transformations. Yeast cells were taken from a fresh grown agar plate and resuspended in PLATE solution. After addition of 2 μL plasmid DNA the cells were heat shocked for 30 min at 42°C. Afterward the cells were pelleted, resuspended in SOS medium and regenerated for 20-30 min in a 30°C water bath. To select the transformed yeast clones the cells were streaked on appropriate selection plates and incubated for 3-5 days at 30°C.

3.2.2.2 Lithium Acetate (LiAc) transformation

One method to transform especially linear DNA fragments for genomic integration is the LiAc-transformation. After over night incubation 50 mL yeast culture with an OD_{600} of 0.5-0.8 were pelleted, washed with sterile water, resuspended in 12.5 mL Lisorb and incubated for 30 min at 30°C. The cells were centrifuged again, resuspended in 150 μL Lisorb and directly used for transformation as followed.

150 μL cells, 110 μL DNA-Mix (100 μL PCR product + 10 μL single strand salmon sperm DNA) were mixed well and 900 μL 40% PEG3350 in LiAc/TE were added. The mixture was incubated at 30°C for 30 min and heat shocked for 15 min in a 42°C water bath.

After pelleting, the transformed cells were resuspended in 300 μL sterile SOS medium, incubated for 1 h at 30°C and streaked on an appropriate SD-agar plate.

<u>LiSorb 100 mL</u>			final conc.
18.2	g	sorbitol	1 M
1	mL	1M Tris-HCl pH 8.0	10 mM
10	mL	1M lithium acetate	100 mM
200	μL	0.5 M EDTA	1 mM
Filled up to 100 mL with ddH ₂ O and autoclaved before use			

<u>40% PEG in LiAc/TE 50 mL</u>			final conc.
20	g	Polyethyleneglycol MW 3359	40%
5	mL	1 M Lithium-Acetate	100 mM
0.5	mL	1M Tris-HCl pH 8.0	10 mM
100	µL	0.5 M EDTA	1 mM

Filled up to 50 mL with ddH₂O and autoclaved before use

SOS

500	µL	YEPD
500	µL	2M Sorbitol
6.5	µL	1M CaCl ₂

Prepared freshly directly before the experiment

3.2.2.3 Isolation of yeast genomic DNA

A yeast cell culture was grown over night to at least 0.7 OD. From this culture 1.5 mL were pelleted, resuspended in 250 µL lysis buffer and shaken over night at 55°C. Then the culture was supplemented with 20 µL 25 mM MgCl₂, mixed and boiled at 95°C for 5 min. The cell debris was removed by centrifugation for 10 min at 13.000 rpm (13.000 g) and the supernatant was taken for PCR.

Lysis buffer

200	mM	NaCl
2	mM	Tris pH8.0
0.5	mM	EDTA

directly before use proteinase K was added to a final concentration of 2 mg/mL .

3.2.2.4 Construction of yeast deletion mutants

One method for deleting genes of the yeast genome is the one-step-gene-disruption via homologous recombination. In contrast to the work with mammalian cells the yeast genome is very easy and fast to manipulate. Deletion mutants are a common tool for analyzing the function of genes and their products.

For the one-step-gene-disruption special primers were needed. The primers were constructed with a complementary sequence of about 40 nucleotides to the gene at the 5' end and 20 nucleotides complementary sequence to a marker gene (e.g. a *LEU2*-cassette) at the 3' end. With these primers the marker gene is amplified from a plasmid or genomic DNA via PCR. The amplified DNA was transformed into yeast cells by lithium acetate transformation and selected on appropriate SD-agar

plates.

The genomic DNA from the achieved yeast clones was isolated (3.2.2.3) and a PCR was done for control of the correct insertion of the marker cassette.

3.2.2.5 Yeast two-hybrid assay

A powerful tool to screen and analyze protein-protein interactions is the yeast two-hybrid (Y2H) assay. For checking specific interactions the two proteins of interest were fused to the disconnected DNA-binding domain (bait) and the transcription activating domain (prey) of a transcription factor, respectively.

We used the LexA/VP16 Y2H System (Brent *et al.*, 1985) where the bait protein is fused to the DNA binding bacterial repressor LexA (pLexN) and the prey protein to the transactivation domain VP16 (pVP16-3) from the Herpes simplex virus.

This two plasmid constructs were transformed (see 1.2.2.1) into the L40 yeast strain containing reporter genes for *lacZ* and the *HIS3* Gene. The fusion proteins were translated and transported to the nucleus. If an interaction takes place, the two domains of the transcription factor (TF) come close enough to restore the TF-function and the chromosomal reporter gene(s) were transcribed.

on agar plates

If the *HIS3*-gene was activated, the cells were able to grow on His-deficiency SD plates. For suppression of background expression of *HIS3* 3-aminotriazole, an inhibitor of the *HIS3* gene product His3p, was titrated (1-10 mM) into the agar-medium.

Liquid culture β -Galactosidase assay (Yeast Protocols Handbook, Clontech)

For quantifying the relative strength of an interaction the liquid culture β -X-Gal assay can be used. The cells were grown over night in 5 mL SD-medium. 2 mL of this culture were transferred into 8 mL YEPD medium and further incubated for 3-5 h at 30°C with shaking. The optical density at 600 nm (OD_{600}) was recorded. 1.5 mL cell culture were pelleted by centrifugation (10.000 g for 30 s) and the

pellet was washed once with 1.5 mL Z-buffer. The cells were centrifuged again and the pellet was resuspended in 300 μ L Z-buffer. From the cell solution 100 μ L were transferred to a fresh reaction tube and the cells were lysed by three cycles of freezing in liquid nitrogen and thawing in a 37°C water bath (each for about 0.5-1 min). For a blank measurement 100 μ L Z-buffer was filled in an additional reaction tube and treated like the samples. To the blank and sample tubes 0.7 mL Z-buffer + β -mercaptoethanol (0.27 mL β -mercaptoethanol in 100 mL Z-buffer) were added. For starting the reaction 160 μ L ONPG (*o*-nitrophenyl β -*D*-galactopyranoside; 4 mg/mL in Z-buffer, adjusted to pH 7.0) were filled into the reaction tubes and the preparation was incubated at 30°C till a yellow color occurred in the positive control. The reaction was stopped by adding 0.4 mL 1 M Na₂CO₃ and the elapsed time (t) for the reaction was listed. The reaction mix was centrifuged for 1 min at 10.000 g and the supernatant was transferred into cuvettes. The absorption was measured at 420 nm and the β -galactosidase units (U) were calculated with the following equation:

$$U = 1.000 \times OD_{420} / (t \times 5 \times OD_{600})$$

One U of β -galactosidase is defined as the amount which hydrolyzes 1 μ L ONPG into *o*-nitrophenol and *D*-galactose per min and per cell.

Z-Buffer

Na₂HPO₄ • 7H₂O 16.1 g/L

NaH₂PO₄ • H₂O 5.50 g/L

KCl 0.75 g/L

MgSO₄ • 7H₂O 0.246 g/L

adjusted to pH 7.0 and autoclaved. Can be stored at room temperature for up to 1 year.

3.2.3 Biochemical Methods

3.2.3.1 *Preparation of protein extract from yeast cells*

Thorner extraction

10 mL of yeast cell culture were grown into the logarithmic phase and at least 3 OD were harvested by centrifugation. The pellet was washed with 1 mL ddH₂O and after discarding the supernatant, about 50 μ L glass beads were added.

For 1 OD cells 40 μ L preheated (70°C) Thorner buffer with 5% mercaptoethanol and protease inhibitors were added and the mixture was vortexed well for 10 min at 70°C. After additional vortexing for 2 min at RT the extract was centrifuged for 5 min at 4°C and 13.000 rpm. The supernatant was stored at -20°C or directly loaded on a SDS-gel (10 μ L extract + 5 μ L 3x stop, boiled 5 min at 95°C).

3.2.3.2 *Bradford assay for determination of protein concentration*

For determination of DNA concentration the Bradford Kit from BioRad was used in combination with the Tecan-Plate reader for evaluation. To determine the protein concentration 100 μ L sample, 700 μ L buffer and 200 μ L undiluted Bradford reagent were mixed and shaken for 10 min at RT. For a standard curve BSA dilutions from 0-16 μ g in 800 μ L Z-buffer plus 200 μ L undiluted Bradford reagent were used. The absorption of the sample was measured in the Tecan reader at 595 nm.

3.2.3.3 *SDS gel electrophoresis*

To analyze specific proteins it is necessary to separate them from the many other proteins in the cell extract. For dividing proteins by their mass and size a sodium dodecylsulfate (SDS) gel electrophoresis can be done. The charges of the proteins were masked by SDS which additionally unfolds the protein. Disulfide bridges were reduced by thioles like β -mercaptoethanol (β -ME) or dithiothreitol (DTT) so

that in an electric field the migration velocity of the protein through a gel with defined pore size mainly depends on the size of the protein.

The gel consists of an acrylamide / N,N-methylenbisacrylamide mixture which is cross linked in a radical polymerization reaction where ammonium persulfate (APS) is used as radical starter and N, N, N', N'-tetramethylethylenediamine (TEMED) as the catalyst of the reaction.

Before loading on the gel the samples were cooked for 5 min in 3x stop buffer, centrifuged for 30 s at 13.000 rpm and loaded into the pockets of the stacking gel. For assignment of the protein sizes a protein ladder mix was loaded into one pocket.

3 x Stop-buffer (45 mL)

1 spatula bromphenolblue
15 g sucrose
4.5 g SDS
18.8 mL 1 M Tris-HCl, pH 6.8
26.2 mL ddH₂O

before use 900 µL 3x stop-buffer and 100 µL β-mercaptoethanol were mixed.

10 x running buffer

10 g/L SDS
30.2 g/L Tris
144 g/L glycine
in ddH₂O

Ammonium Persulfat (APS)

10 % (w/v) ammonium persulfate in ddH₂O

resolving gel (15 mL):

acrylamide-concentration	8% gel	11% gel
1.5 M Tris-HCl, pH 8.8	3.75 mL	3.75 mL
30% acrylamide/ 0,8% bis-acrylamide	5.5 mL	6.25 mL
ddH ₂ O	5.45 mL	4.65 mL
10 % (w/v) SDS	150 µL	150 µL
10 % (w/v) APS	150 µL	150 µL
TEMED	7.5 µL	7.5 µL

stacking gel (7,5 mL):

5,6% gel
(pH 6.8) 936 µL
1.39 mL
4.95 mL
75 µL
150 µL
7.5 µL

3.2.3.4 Isoelectric focusing (IEF)

Additionally to segregating proteins according to their size polypeptides can also be separated in dependency of their charge. If proteins were loaded on a pH gradient gel without SDS the protein will move in an electric field through the gel till it reaches its isoelectric point. The isoelectric point is dependent from the charged amino acids of a protein and the posttranslational modifications. In this work the IEF was used to prove the phosphorylation of a protein. This procedure is carried out in a capillary tube and the range of the gradient is adjusted by the concentration of small zwitterionic peptides, so called ampholines. After separation for charge the gel stick from the capillary tube is placed on a SDS gel and the proteins were segregated for size.

3.2.3.4.1 Protein extract preparation

For each sample 15 OD cells were cultured over night, pelleted and washed with 2.5 mL cold lysis buffer 1. Then the cells were pelleted again and resuspended either in lysis buffer 1 (for CIP treatment) or lysis buffer 2 (for treatment with phosphatase inhibitors (PI)).

The cell suspensions were filled in glass tubes with 0.8 g glass beads and were alternately vortexed forcefully for 30 s and put for 30 s on ice five times.

The lysed cell components were transferred to an 1.5 mL reaction tube and the sample in lysis buffer 1 was treated with calf intestinal phosphatase (CIP).

Therefore 0.5 μ L CIP (Roche, 1 U/ μ L) were added to the samples and one preparation was incubated for 5 min and one for 15 min at 37°C. The PI samples were incubated 5 min at 37°C.

All samples were centrifuged for 5 min at 2000 rpm (4°C) and the supernatant was prepared further for loading on the IEF capillary tubes.

Lysis buffer 1

50	mM	Tris-HCl pH 7.5
0.2	M	Sorbitol
1	mM	EDTA

Lysis buffer 2

as lysis buffer 1 with additionally		
100	mM	NaF
8	mM	NaVO ₃

3.2.3.4.2 IEF-Electrophoresis

The cell lysate was mixed at least 1:1 with lysis solution (10-15 µg overall protein), shaken for 5 min at RT and centrifuged 5 min at 13.000 rpm.

The acrylamide gel for the capillary tubes with 1.2 mm inner diameter and 6 cm length was prepared as followed:

The IEF acrylamide solution was thawed and per mL solution 1 µL TEMED and 1 µL APS were added. One side of the tube was closed with Parafilm and 100 µl of the gel-solution were filled in and were covered with a layer of water. After polymerization the water was changed to lysis solution and the tubes were stored over night at room temperature.

Before use the lysis solution was removed and the tubes were fixed in the IEF-chamber. The cell lysates were applied to the tubes and carefully covered with 0.02 M NaOH. The upper tank of the chamber was also filled with 0.02 M NaOH, the lower tank with 0.01 M phosphoric acid.

The following currency scheme was chosen:

1. 30 min 100 V
2. 150 min 200 V
3. 15 min 400 V

After the run the tubes were frozen at -20°C.

To separate the proteins for size the gel from the tubes was applied on a SDS-acrylamide gel.

IEF acrylamide solution

15.1-17.1 g Urea (8-8.2 M) in

3	mL	ampholine mixture (e.g. 2 mL pH3.5-10 + 1 mL pH 5-8)
4	mL	acrylamide mixture (28.8% (w/v) acrylamide + 1.6% (w/v) bis-acrylamide)
6	mL	10% (v/v) NP40 in H ₂ O
4.6	mL	ddH ₂ O

The mixture was portioned and frozen at -80°C

Lysis solution

14.3	g	Urea in
0.5	mL	ampholine mixture
1.25	mL	β-mercaptoethanol
5	mL	10% (v/v) NP 40 in H ₂ O
10	mL	dd H ₂ O

The mixture was portioned and frozen at -80°C

3.2.3.5 Coomassie blue staining

For staining proteins in a SDS-gel a Coomassie-blue staining was performed. The dye Coomassie G-250 from Serva absorbs light at 595 nm after protein binding. Since the absorption is directly proportional to the protein concentration in the gel this assay can be used for quantification. The SDS gel was stained with the Coomassie solution at RT till the desired bands were visible (1-2 h). Then the gel was destained (in 50 % (v/v) Methanol, 10 % (v/v) Acetic acid, 40 % (v/v) ddH₂O) till the background staining was gone. The gel was washed several times in ddH₂O and dried in a gel drier.

Coomassie-blue solution

0.1	% (w/v)	Serva blue R (Coomassie brilliant blue R-250)
25	% (v/v)	Isopropanol
10	% (v/v)	Acetic acid
65	% (v/v)	ddH ₂ O

3.2.3.6 Western blot analysis

To detect specific proteins which were separated by SDS-Gel electrophoresis a Western blot analysis was performed. The SDS masked proteins from the gel were transferred to a nitrocellulose membrane via an electric field. Semi-dry-blot-buffer soaked Whatman papers and nitrocellulose membrane were stacked on the blot apparatus together with the gel as followed: 3x Whatman paper, nitrocellulose membrane, gel, 3x Whatman paper.

The blot was performed for one hour with an amperage depending on the size of

the membrane. For one cm² of membrane one mA current was applied. After transfer, the membrane was washed once with water and incubated for about 2 min in Ponceau red solution to stain the proteins on the membrane. For antibody treatment the membrane was blocked with 2% milk powder in PBST for 30 min. Then the first antibody was applied in appropriate dilution (in 2% milk powder/PBST) for 1 h. After three washing steps (each 5 min) with PBST the second antibody directed against the Fc part of the first antibody and linked to a horseradish peroxidase (HRP) was added for 1 hour. The second antibody was washed off with 5 PBST washing steps (each 5 min) and the Tween was removed from the membrane by washing at least 5 min with PBS. For detection of the protein bands the membrane was incubated with ECL solution (Pierce Western blotting substrate 1+2) for 5 min.

The ECL solution contains Luminol which is enzymatically oxidized by HRP in a peroxidase buffer. The oxidized excited state product emits light as it decays to its ground state. The light is detected by a CCD camera (Fuji Film LAS 3000).

10x semi-dry-buffer

5.80 g Tris
2.92 g glycine
3.7 mL 10 % (w/v) SDS
Filled up to 1 liter with ddH₂O, adjusted with NaOH to pH 9.2

200 mL/L methanol (add directly before use)

PBS-T

0,1 % (w/v) Tween-20[®] in PBS

3.2.3.7 Preabsorption of antibodies

For some antibodies it is necessary to enhance the specificity with a preabsorption using yeast acetone powder. For the preabsorption a yeast strain is used which does not contain the antigen of the antibody. About 200 OD₆₀₀ cells were cultured over night and harvested at 1-2 OD₆₀₀/mL. The cells were pelleted, resuspended in PBS (10-30 OD₆₀₀/mL) and 1 mg/100 OD₆₀₀ Zymolyase was added. After 15 min spheroplasting at 30°C the cells they were cooled down for 5 min on ice. 4

volumes cold acetone were added and the mixture was put on ice for 30 min. The cells were pelleted, washed with cold acetone and the pellet was dried in a mortar. The powder was grind to a very fine consistence and used for preabsorption at a concentration of 10 mg/mL in the antibody serum. The preabsorption was performed for 4 h at room temperature or over night at 4°C. To remove the powder the antibody solution was spun hard for 10 min. The supernatant was used as preabsorbed serum.

3.2.3.8 CPY Overlay-Assay

Cells were grown till log-phase and diluted to 0.05 OD. 10 µL of the cell dilution were dropped on a YEPD plate and incubated for 24 h at 30°C. A nitrocellulose membrane was placed on the agar and the plate was again incubated for 24 h at 30°C. The nitrocellulose membrane was washed with water and treated with mouse-anti-CPY antibody as described in 3.2.3.6.

3.2.3.9 “Pulse-Chase” Immunoprecipitation (IP)

3.2.3.9.1 CPY-IP

The vacuolar soluble hydrolase CPY is processed from a p1-form in the ER (67 kDa) to a glycosylated p2-form (69 kDa) in the TGN and late endosomes to a mature form (mCPY, 61 kDa) in the vacuole where a signal peptide is cleaved. If there is a defect in one of the transport steps from the ER to the vacuole the preforms were enriched in the cell or secreted into the medium. This features of CPY allow its usage as sensor for transport steps in this pathway. To receive a result which is highly sensitive and can be quantified a radioactive pulse-chase immuno-precipitation is a useful method.

The cells were grown for two days to a logarithmic stage in SD medium. 0.5 OD cells were resuspended in SD-met + 50 mM KPO₄ pH5.7 + 2 mg/mL BSA and preincubated for 15 min at 30°C.

7 µL ³⁵S-methionine/cysteine (70 µCi; Express-protein-labeling mix [³⁵S], NEN, Perkin Elmer) were added and the cell suspension was further incubated at 30°C

for exactly 10 min (pulse). The pulse was stopped by adding 50 μ L Met+Cys (equal volumes of 10 mg/mL methionine and cysteine) and the cell suspension was incubated for 30 min at 30°C (chase). The protein expression of the cells was stopped by transferring the cells into reaction tubes containing 5 μ L 1 M NaN_3 . The cells were pelleted and the supernatant was transferred to reaction tubes with 10 μ L protease inhibitor mix (external fraction). The pellet (internal fraction) was resuspended in 1 mL 50 mM Tris pH 9.5, 10 mM DTT, 10 mM NaN_3 (DTT-mix) and incubated for 5 min at 30°C. For spheroplasting, the DTT mix was removed by centrifugation and the cells were resuspended and incubated for 30-45 min at 30°C in spheroplast mix containing 250 μ g/mL Zymolyase. To lyse the yeast cells they were pelleted and resuspended in 100 μ L 10xIP-buffer + 10 μ L 100x protease inhibitor mix and 670 μ L water. To the external fraction 100 μ L 10xIP-buffer and 150 μ L water were added. Internal and external fractions were boiled for 5 min at 95°C. After the fractions were cooled down 50 μ L washed Pansorbin (washed three times with 20 mM Tris pH 7.5, 100 mM NaCl, centrifugation for 30 sec at 11000 rpm) in 220 μ L water were added for preabsorption (at least 15 min on ice). The Pansorbin beads were separated by 5 min centrifugation at 11000 rpm and the supernatant was transferred into reaction tubes containing 2 μ L anti-CPY serum. 5 μ L of the supernatant from the internal fractions were counted in a scintillator. In 1 h 30 min incubation on ice the binding of the CPY to the antibody proceeded. For the precipitation 50 μ L washed Pansorbin were added and the mixture was again incubated for 1 h 30 min.

The beads with bound CPY were washed twice with wash buffer (5 min with 1 mL wash buffer and centrifugation at 12000 rpm for 30 sec), resuspended in 40 μ L 2xstop buffer and stored at -20°C.

For SDS-gel electrophoresis the samples were heated for 5 min at 95°C, cooled down, centrifuged 2 min and 20 μ L were loaded on an 8% SDS-gel. The electrophoresis was performed with low current for 5-6 h.

The gel was fixed (50% (v/v) Methanol, 10% (v/v) Acetic acid, 40% (v/v) ddH₂O) washed several minutes in water and dried in a gel drier.

The exposition of the gel was done with a phosphorimager plate (Fujifilm BAS-MS 2325) for 2 days and developed in a phosphorimager.

10x IP buffer

90 mL	1 Tris-HCl pH8.0
1 g	SDS
4 mL	25% Triton X-100
4 mL	0.5 M EDTA
2 mL	ddH ₂ O

Wash buffer

0.9 M	500 µL	1 M Tris pH 8.0	10 mM
1%	500 µL	10% SDS	0.1%
1%	200 µL	25% Triton X-100	0.1%
20 mM	200 µL	0.5 M EDTA	2 mM
filled up to 50 mL with ddH ₂ O			

Spheroplast-mix

30 mL	2 M Sorbitol	1.2 M
2.5 mL	1 M KPO ₄ pH 7.3	50 mM
0.5 mL	1 M NaN ₃	10 mM
17 mL	ddH ₂ O	

3.2.3.9.2 ALP-IP

The alkaline phosphatase (ALP) is a transmembrane protein which is transported as a 76 kDa precursor form (pALP) from the ER to the TGN and from there directly to the vacuole. There it is cleaved in a Pep4p dependent way to an enzymatically active 72 kDa mature form (mALP). Defects in this transport step can be detected by following the pALP stability after several time points.

To analyze the cycling of proteins between late endosomes and TGN the model protein A-ALP can be used. It consists of the transmembrane and luminal domain of ALP and the cytosolic domain of Ste13p which provides a trafficking signal from TGN to endosomes and the retrieval back (Nothwehr *et al.*, 1993). There is a defect in the retrograde trafficking from LE to TGN the A-ALP is transported more efficiently to the vacuole and there is less pA-ALP detectable in the cells.

The cells were prepared as described for CPY IP (0.5 OD cells per time point). After 15 min preincubation at 37°C the cells were pulsed with 10 µL ³⁵S-Met/Cys per time point for exactly 10 min at 37°C. The chase was performed by adding 50 µL Met+Cys (equal volumes each 10 mg/mL) per time point for 10 min, 60 min and 120 min at 37°C.

After each time point 500 µL cell suspension were transferred into a 1.5 mL reaction tube with 5 µL NaN₃ and kept on ice. The cells were centrifuged for 20 s and the supernatant was discarded. Spheroplasting was done as described before

(3.2.3.9.1). The cells were lysed in 50 μ L 1% SDS, 8 M Urea with 100x protease inhibitors for 5 min at 95°C. After cooling down a mixture with 100 μ L 10xIP without SDS, 850 μ L H₂O, 10 μ L protease inhibitors and 50 μ L washed Pansorbin (washing Pansorbin described in 3.2.3.9.1) was added and incubated at least 15 min on ice (preabsorption). The Pansorbin was removed by centrifuging for 5 min and from the cell fractions 5 μ L were counted in the scintillator. The supernatants were transferred to 1.5 mL reaction tubes containing 2 μ L ALP sera. Incubation, washing and further processing was done as for the CPY-IP (3.2.3.9.1).

10xIP without SDS		final conc.
90 mL	Tris-HCl pH 8.0	0.9 M
4 mL	25% Triton X-100	1%
4 mL	0.5 M EDTA	20 mM
2 mL	H ₂ O	

3.2.3.9.3 Protein stability

Proteins with sorting defects can have a prolonged or shortened lifetime due to a slower or faster transport to the vacuole where many proteins are degraded. Therefore the samples were prepared as described for the ALP-IP (3.2.3.9.2) except for the chase times. To monitor the whole lifetime of a protein the chase was performed for 10 min, 3 h and 5 h.

3.2.3.10 Test for bacterial expression of recombinant His₆-tagged proteins

To purify specific proteins the polypeptides can be linked to a tag. With tags which specifically bind to a column the proteins can be purified by affinity chromatography.

Agarose linked chelating nitriloacetate (NTA) molecules each bind up to 4 coordination sites of a Ni²⁺ ion. The two remaining coordination sites of the Ni²⁺ can be bound by imidazole rings of histidine residues. Therefore the hexa-histidine tag (His₆) can be used for purification of proteins. To elute the bound protein a solution with imidazole in excess under acidic conditions can be used.

For testing the best conditions for the bacterial expression of recombinant fusion proteins as proteins with Strep- or His-tags different temperatures and production times were tested.

2.5 mL over night culture were added to 25 mL 2xYT medium (including antibiotics) and incubated for 1.5 h at 37°C. For the 0-value (uninduced) 3 mL cell culture were centrifuged, resuspended in 500 µL PBS and frozen.

The induction was performed by adding 0.2 mM IPTG. The culture was split up into three parts. The first 7 mL culture were further incubated at 24°C, the second at 30°C and the third at 37°C. After 3 and 5 h 3 mL cell culture were pelleted, resuspended in 500 µL PBS and frozen. For lysis the cells were thawed, supplemented with 5 µL PMSF and sonicated three times for 30 s at maximum power. The cell debris was separated by centrifuging for 10 min at 13.000 rpm (4°C) and the pellet was resuspended in 500 µL PBS.

10 µL of the supernatant and pellet fractions with 10 µL 2x stop buffer were boiled for 5 min and loaded on a SDS gel. The proteins were visualized by a Coomassie blue staining.

3.2.3.11 Purification of His₆ tagged fusion proteins

The bacterial cells were inoculated in 25 mL 2xYT medium with antibiotics (100 µg/mL ampicillin or 50 µg/mL kanamycin) and grown over night. This culture was added to 475 mL 2xYT (incl. Amp or Kana) and grown till an OD₆₀₀ of circa 0.9. The induction was performed as determined in the expression test (see 3.2.3.10). After the expression time the cell culture was pelleted (15 min, 5000 rpm, 4°C, SLA1500 rotor), resuspended in 20 mL binding buffer and frozen.

The lysis of the cells was performed with the French press. Directly before lysis protease inhibitors were added and the the culture was pressed two times with 20.000 psi through the French press. The cell debris was separated by centrifugation (10 min, 12000 rpm, 4°C, SS34 rotor) and to the supernatant the Ni-NTA (1 mL Ni-NTA gel washed three times with binding buffer) was added. The pellet was resuspended in binding buffer and stored for loading on the SDS gel.

The protein-Ni-NTA mix was incubated for at least 1 h at 4°C and loaded on a

column. Unbound proteins were collected for the SDS gel and the gel matrix was washed with 10 mL wash buffer. For the elution 1 mL fractions were collected in 1.5 mL reaction tubes. Following elution solutions were added:

- 2 mL wash buffer with 50 mM (pH 6.0),
- 2 mL wash buffer with 100 mM (pH 6.0),
- 2 mL wash buffer with 250 mM imidazole (pH 6.0),
- 2 mL wash buffer with 500 mM imidazole (pH6.0).

From the elution fractions 2 μ L were loaded on the SDS gel, from other fractions 5 μ L were loaded.

The column was washed with wash buffer and stored in binding buffer at 4°C

binding buffer

50 mM NaPO₄ pH 8.0
300 mM NaCl
1 mM EDTA
in ddH₂O

wash buffer

50 mM NaPO₄ pH 8.0
300 mM NaCl
in ddH₂O

3.2.3.12 Test for bacterial expression of recombinant Strep-tagged proteins

Another established method is the purification of proteins by Streptactin affinity chromatography. Streptactin is a version of bacterial streptavidin protein modified by IBA which binds with very high affinity to the vitamin biotin.

The Strep-tag is an artificial short amino acid sequence which shows a high affinity to Streptactin and can be eluted by the natural ligand biotin.

For testing the expression of Strep tagged proteins in bacteria the cells were cultured and lysed as described for His-tagged proteins. For induction of the expression the following terms were tested:

	1:20 diluted AHT	final concentration	Time	Temperature
1	0		2 h	30°C
2	1.5 µL	50 µg/L	2 h	30°C
3	1.5 µL		4 h	30°C
4	1.5 µL		2 h	24°C
5	1.5 µL		4 h	24°C
6	3 µL	100 µg/L	2 h	30°C
7	3 µL		4 h	30°C

AHT (anhydrotetracycline) induces the expression of the Strep-fusion protein. For the SDS gel 16 µL sample with 8 µL 3x stop buffer were boiled for 5 min at 95°C and 15 µL were loaded.

3.2.3.13 Purification of Strep-tag fusion proteins

For purification of Strep-tagged proteins 10 mL bacteria culture were grown over night in 2xYT medium with antibiotics. The over night culture was added to 250 mL 2xYT (with antibiotics) and cultured further about 1 h at 37°C and 1 h at 30°C till an OD₆₀₀ of 0.5. The induction of protein expression was done using the conditions determined by the expression test (3.2.3.12). The bacteria cells were pelleted for 10 min at 10.000 rpm (SLA1500 rotor) and 4°C, resuspended in buffer W and frozen. To lyse the cells 40 µL protease inhibitors were added directly before treatment with the French press (2x20.000 psi at medium). The cell fragments were pelleted for 10 min at 13.000 rpm (*g*) at 4°C. The supernatant (contains soluble proteins) was filtrated through a 0.2 µm filter. 2 µL of the pellet and the filter fraction were stored for SDS gel.

For purification an IBA-Streptactin Superflow column was used. To equilibrate the column it was flushed two times with 4 mL buffer W till the column material turned yellow. The supernatant with the extracted proteins was loaded on the column and 2 µL of the flow through were collected for the SDS gel. The bound proteins were washed 5 times with 1 mL buffer W and eluted with 5 times 0.5 mL buffer E (buffer W with 2.5 mM desthiobiotin). The collected 0.5 mL fractions were aliquoted and

2 μL of each fraction were loaded on a SDS gel with following Coomassie blue staining.

To regenerate the column it was washed 3 times with 5 μL buffer R (buffer W + 1 mM HABA) and stored in buffer R or W.

buffer W

100 mM	Tris pH 8.0
150 mM	NaCl
1 mM	EDTA
in ddH ₂ O	

3.2.3.14 Pulldown-Assay

To verify results from a yeast two-hybrid assay the interaction can be checked in an *in vitro* pull down assay. The interaction partners were expressed in *E. coli* cells, purified and their concentration was determined by a Bradford protein assay. One interaction partner was expressed with a His₆-tag for binding to the Ni-NTA column.

In 100 μL pull down buffer the proteins were diluted in concentrations from 0.5 μM -2 μM dependent on the experiment and proteins used. The buffer contained 1% Triton, 10-20 mM imidazole in PBS and in the case of strong unspecific reactions 250 mM NaCl.

After mixing the interaction partners the solution was incubated for 30 min at 4°C, centrifuged 1 min at 13000 rpm (4°C) and the supernatant was transferred to a fresh 1.5 mL reaction tube.

For purification of the protein complexes 10 μL 50% Ni-NTA slurry were added and the suspension was incubated for 30 min at 4°C. To minimize unspecific binding the Ni-NTA can be preincubated with 1%BSA/PBS for 30 min at 4°C. After two washing steps with PBS the Ni-NTA was filled up to the start volume with PBS.

The Ni-NTA protein complex mixture was washed two times with PBS 1%Triton (10 mM imidazole if necessary) and resuspended in 50 μL 1xStop with β -mercaptoethanol for the SDS gel (10 μL were loaded). After the SDS-gel run the proteins were transferred to a nitrocellulose membrane and treated with antibodies as described in 3.2.3.6 or for detection of Strep-tagged proteins treated as followed:

The blot was incubated for 1 h at RT with PBS 0.5% Tween 1% BSA, for 1 h with streptactin-HRP (1:4000 in PBS 0.5% Tween 1% BSA), washed twice 1 min with PBST, once for 1 min with PBS and incubated for 5 min with ECL solution.

3.2.4 Cell Biology

3.2.4.1 Growth test with cell wall perturbing agents

To check whether cells have cell wall defects they can be grown on agar plates complemented with cell wall perturbing agents like SDS, calcofluor, sorbitol and NaCl. The detergent SDS destroys the cell membrane especially when it can access the membrane easily because of a defective cell wall. Calcofluor binds chitin and inhibits the cell wall assembly. Cells with chitin accumulations at the cell wall are Calcofluor sensitive, cells with a defect in chitin transport or integration are Calcofluor resistant. Sorbitol and NaCl cause osmotic stress. Cells with defective cell wall are more sensitive to this agents.

The cells were grown over night into logarithmic stage and diluted to 0.01, 0.005 and 0.001 OD₆₀₀/mL in ddH₂O. 10 µL of the cell suspensions were dropped on the agar plates and pictures were taken for the following 1-5 days. The plates were prepared with:

- 1.2 M and 2 M sorbitol,
- 0.5, 1 M and 1.4 M NaCl,
- 25 and 50 µg/mL calcofluor,
- 0.01 and 0.005% SDS,
- and YEPD as positive control.

3.2.4.2 Subcellular fractionation

For a biochemical analysis of the localization of specific proteins it is necessary to separate the organelles of a cell. There are two common methods to achieve a organelle separation. With differential centrifugation the organelles are separated by their size and sedimentation velocity and with a sucrose density gradient the organelles can be separated by their density.

3.2.4.2.1 Differential centrifugation

To obtain the cell lysates for the differential centrifugation 20 OD cell culture in a logarithmic stage were pelleted, resuspended in 2 mL TE β , incubated for 10 min at 30°C and pelleted again. The cells were spheroplasted by incubation for 1 h at 30°C in 2 mL spheroplast buffer containing 60 μ L 10 mg/mL Zymolyase. The cells were washed three times with spheroplast buffer and lysed in 1 mL lysis buffer (containing protease inhibitors) with a glass potter (tight, 5 times). The cell debris was removed by 5 min centrifugation at 2000 rpm (500 g, 4°C). From the supernatant about 400 μ L were collected for the SDS-gel (fraction H) and 500 μ L were centrifuged for 10 min at 4°C and 13.000 rpm (13.000 g). From the supernatant 450 μ L were further centrifuged at 50.000 rpm (200.000 g, 4°C) and the pellet was resuspended in 500 μ L lysis buffer (fraction P13). The pellet and supernatant of the 200.000 g centrifugation step were separated and stored as S200 (supernatant) or P200 (pellet in 450 μ L lysis buffer with protease inhibitors).

From all fractions (H, P13, P200, S200) 20 μ L were mixed with 10 μ L 3xstop buffer and 20 μ L were loaded on a SDS gel. The proteins were blotted from the gel onto a nitrocellulose membrane and treated with antibiotics and ECL solution as described in 3.2.3.6.

spheroplast buffer

1.2 M Sorbitol
50 mM KPO₄ buffer pH 7.3
1 mM MgCl₂
in ddH₂O

lysis buffer

50 mM Tris pH7.5
0.2 M Sorbitol
1 mM EDTA
in ddH₂O

3.2.4.2.2 Sucrose density gradient

The preparation of the cell lysates was performed as described for the differential centrifugation (3.2.5.2.1) aside from a cell volume of 30 OD and resuspension in 1.5 mL lysis buffer. After removal of the cell debris the supernatant was transferred on the following sucrose gradient:

- 0.5 mL 55% sucrose w/w in 10 mM HEPES NaOH pH7.6
- 1.0 mL 37% “ “
- 1.5 mL 34% “ “
- 2.0 mL 32% “ “
- 2.0 mL 29% “ “
- 1.0 mL 27% “ “
- 1.5 mL 22% “ “

The gradient tubes were filled to the brim with lysis buffer and tared. The gradients were centrifuged for 16 h over night at 4°C (27.000 rpm, about 100.000 *g*). After 16 h the organelles should have moved to the position in the gradient which equates to their own density. After stopping the centrifugation (without brake) 1 mL fractions of the gradient were removed from top to bottom and their density was measured with a refractometer.

From each fraction 30 µL were mixed with 15 mL 3xstop buffer and 40 µl were loaded on a SDS gel. The proteins were blotted from the SDS-gel onto a nitrocellulose membrane and treated with antibiotics and ECL solution as described in 3.2.3.6.

3.2.4.3 Membrane binding assay

The association of Ent3p with intracellular membranes was checked by a subcellular fractionation approach. The cells were grown into logarithmic stage and washed with ice cold lysis buffer (20 mM HEPES pH 6.8, 150 mM potassium acetate, 10 mM magnesium chloride and 250 mM sorbitol). After washing the cells were resuspended in ice cold lysis buffer (supplemented with protease inhibitors) filled in a glass tube containing glass beads and lysed by alternating strong

vortexing and cooling on ice for 30 sec, respectively. The cell debris was removed by 5 min centrifugation at 500 g. The supernatant was subsequently centrifuged for 10 min at 13.000 g and for 20 min at 200,000 g. The pellet fractions (P13 and P200) and supernatant after 200,000 g (S200) were loaded together with a homogenate fraction (H) on a SDS gel. The proteins were detected by western blotting as described in 3.2.3.6. The band intensities were quantified with the AIDA software.

3.2.4.4 Indirect immunofluorescence

If an antibody for an specific protein is available it is possible to localize the protein in the cell via immunofluorescence microscopy. This technique has the advantage that no tag which maybe constricts the function of the protein has to be attached. A disadvantage is the unspecific reaction of some antibodies and that the staining has to be done with fixed cells. The fixed state of the cells may not resemble a native condition.

Fixation:

To prepare the cells for fixation 2.5 OD cells were pelleted, resuspended in 10 mL YEPD and grown for 3-4 h at 30°C. 1 mL 37% formaldehyde was added and the suspension was incubated for 30 min at 30°C. For the final fixation the cells were centrifuged, the pellet was resuspended in 2 mL fixative and incubated over night on a rocker.

Permeabilization of the cells:

The cells were pelleted and resuspended in 1 mL TE β , incubated for 10 min at RT, pelleted again and the resuspended in 900 μ L spheroplast buffer and 100 μ L Zymolyase/Glusulase mix. The spheroplasting was performed for 30 min at 30°C. After the cell wall was removed by spheroplasting the cells were washed with sorbitol-azide and resuspended in 500 μ L 1.2 M sorbitol (1.2 M sorbitol in ddH₂O). For permeabelizing 500 μ L 2% SDS-sorbitol were added quickly to the cells and incubated for exactly 2 min. Then the cells were washed twice with 1.2 M sorbitol and resuspended in 300-500 μ L 1.2 M Sorbitol

Preabsorption of antibodies:

To reduce unspecific binding of the antibodies they can be preabsorbed with yeast cells which don't contain the antigen of the antibody (cells treated as described above).

The volume of antibody solution which is needed for the whole experiment was determined and the respective amount of fixed yeast cell culture without the antigen was centrifuged and resuspended in the same amount of PBS-BSA.

The antibody was added to its final concentration to the yeast suspension and incubated for 1 h at RT. The cells were removed by centrifugation for 30 sec at 13.000 rpm and the supernatant was used as antibody-dilution on the microscopy slides.

Antibody treatment:

From the cell suspension in 1.2 M sorbitol 40 μ L were filled in each well of the microscope slide (each well treated before with 20 μ L 1 mg/mL poly-L-lysine, washed 6 times with ddH₂O and dried for at least 10 min). After 10 min the not attached cells were aspirated and the cells in the wells were washed three times with PBS-BSA and left with the last PBS-BSA for 15 min at RT in a humid chamber. The washing solution was aspirated and 20 μ L of the (preabsorbed) antibody dilution per well were added for 1 h at room temperature in the wet chamber. The cells were washed 6 times with PBS-BSA and 20 μ L of the secondary antibody per well (Cy2 od Cy3 linked goat-anti-rabbit/mouse antibody) were applied. After 1 h incubation in a dark, humid chamber the cells were washed 9 times with PBS-BSA and mounted in circa 8 μ L mounting medium. The cover slip was attached and fixated with nail polish. The slides were stored at -20°C and viewed under a fluorescence microscope.

<u>Fixative</u>			<u>Zymolyase/Glusulase</u>	
1	g	para-formaldehyde	1.5	mg/mL Zymolyase
25	mL	H ₂ O	250	μ L/mL Glusulase
187.5	μ L	6 N NaOH	in spheroplast buffer	
0.34	g	KH ₂ PO ₄		
adjusted to pH 6.5 and stored at -20°C				

Sorbitol-azide

1.2 M sorbitol
5 mM NaN₃
in ddH₂O

PBS-BSA

5 mg/mL BSA
5 mM NaN₃
in 1x PBS

Sorbitol 2% SDS

1.2 M sorbitol
5 mM NaN₃
2 % SDS
in ddH₂O

Mounting medium

50 mg p-phenyldiamine in
5 mL 1x PBS
45 mL 100% glycerol
2-3 μL DAPI
were mixed, aliquoted and stored at -80°C

3.2.4.5 GFP fluorescence microscopy

If there are no antibodies available against a special protein an alternative is to attach the 26 kDa green fluorescent protein (GFP) via cloning techniques at the C or N-terminus of the protein. Originally isolated from the jellyfish *Aequorea victoria* a lot of modifications were done to yield better spectral characteristics (e.g. e(enhanced)GFP) or different emission peaks (e.g. YFP (yellow), CFP (cyan) etc.). The Yeast cells expressing the eGFP fusion protein were grown till early logarithmic phase (Snc1-GFP) or logarithmic phase (GFP-Yck2), pelleted and resuspended in PBS. The cell suspension was dropped on a slide and directly viewed under a fluorescence microscope with an mayor excitation peak at 488 nm and emission at 509 nm.

3.2.4.6 Calcofluor staining

The yeast cell wall is mainly built of glucanes, mannoproteins and chitin. Especially during budding the chitin has an important role for maintaining cell wall integrity. Chitin is transported and linked to the glucanes via three main transporters to the plasma membrane (Chs1-3p). With the staining of the chitin on the cell wall transport defects of the transporters and/or defects in the budding behavior can be analyzed. Therefore 20 mL yeast cell culture were grown over night into logarithmic phase and fixated by incubation with 2 mL 37% formaldehyde for 30 min at 30°C. Then the cells were pelleted, resuspended in 2 mL 4% formaldehyde in PBS and incubated again for 30 min at room

temperature. The fixed cells were washed with PBS and resuspended in 500 μL PBS. For each time point 15 μL 1 mg/mL Calcofluor (in ddH₂O) were added to 100 μL cell suspension. The incubation was carried out for 5 min and for 1 h in the dark. The cells were washed three times with PBS and resuspended in 10 μL mounting medium.

3.2.4.7 FM4-64 staining

FM4-64 is a lipophilic dye which integrates into the cell membrane and is endocytosed via the early endosomes to the vacuole. After five minutes it can be found in the early endosomes, after 15min in the late endosomes and after 30 min in the vacuole. By staining the yeast cells with FM4-64 transport defects can be observed or the morphology of endosomes and vacuole can be visualized.

0.7 OD₆₀₀ of a yeast over night culture were centrifuged, resuspended in 120 μL YEPD and supplemented with 1 μL 16 mM FM4-64 (in DMSO). The cells were incubated for 5 min, 15 min or 30 min at room temperature in the dark, washed with YEPD and resuspended in 20 μL YEPD. For microscopy 3 μL of the cell suspension were dropped onto a slide and directly viewed under a fluorescence microscope (Texas red filter).

3.2.4.8 Sedimentation-Assay

If yeast cells have defects in their cell wall assembly they may build cell aggregates. This aggregates settle faster in a cuvette than non-aggregating cells. The Sedimentation can be followed by spectroscopy at 600 nm.

The cells were grown till log-phase, pelleted and resuspended in 1 mL ddH₂O. The cell suspension was transferred into a cuvette and the OD₆₀₀ was measured every 10 min. The relative OD was calculated ($\text{OD}_{\text{measured}}/\text{OD}_{\text{Start}}$) and plotted against the elapsed time.

4 Results

4.1 Characterization of the interaction of Ent3p with Pep12p, Vti1p and Syn8p

The yeast ENTH protein Ent3p binds the endosomal SNAREs Vti1p, Pep12p and Syn8p in a yeast two-hybrid and an *in vitro* pulldown assay and shows genetic interactions with this SNAREs (Chidambaram *et al.*, 2008). ENTH proteins are cargo adaptors which bind beside their cargo molecules also clathrin and other cargo adaptors like APs and Ggas. One aim of my work was to study the cargo-adaptor interaction between Ent3p and the SNAREs in detail. First I checked if the FSD motif on Pep12p is crucial for the Ent3p binding.

4.1.1 Pep12p interacts with Ent3p via its FSD motif

The localization of Pep12p at the late endosome is dependent on its **FSDSPEF** motif in a Gga1/2p dependent manner (Black and Pelham, 2000). But a direct interaction between Pep12p and the cargo adaptor protein Gga1/2p could not be proved. In a previous work the Qa SNARE Pep12p was found to be an interaction partner of Ent3p (Chidambaram *et al.*, 2004). Since Ent3p also interacts with the gamma-ear like domains of Gga2p (Duncan *et al.*, 2003) Ent3p could function as additional cargo sorter linking Gga2p and Pep12p.

4.1.1.1 Yeast-Two-Hybrid and Pull-down interactions

To prove the FSD motif as interacting region of Pep12p with the Ent3-ENTH domain, yeast two-hybrid (Y2H) constructs were generated containing Pep12p with deleted FSD motif (Δ FSD, aa 19-26 deleted) or the amino acid exchange F20L in the bait vector pLexN. The assay was performed with Ent3p ENTH domain in pVP16-3 as prey vector and empty pVP16-3 as negative control. When the bait and prey fusion proteins interact the function of an artificial transcription factor (VP16+LexA) is restored. Then the *HIS3* gene product is expressed and allows the cells to grow on histidine deficient medium like the THULL medium.

The constructs were transformed into L40 yeast cells and the assay was performed on THULL plates containing 5 mM 3-aminotriazole to reduce the background expression. After three days a picture of the agar plate was taken and displayed in figure 4.1.A.

The mutation of the Pep12-FSD motif completely abolished the interaction with Ent3p in the two hybrid assay.

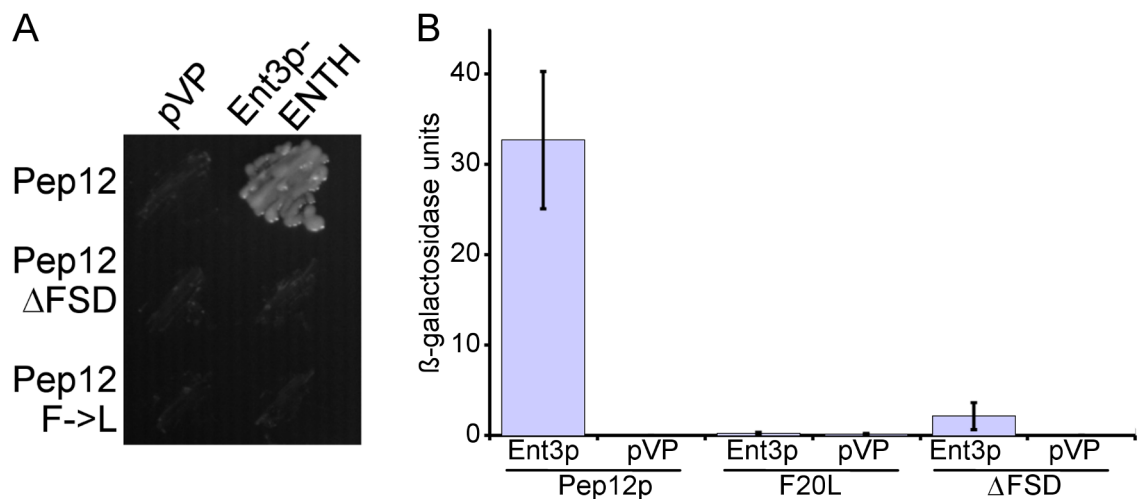


Fig. 4.1: Pep12 interacts with Ent3p via its FSD motif. **A:** Yeast two-hybrid assay for analysis of the interaction between the N-terminal domain of Pep12p (AA 1-200, pBK171) or Pep12p mutants with aa 19-26 deleted (Δ FSD, pJZ10) or F20L aa exchange (pJZ9) and Ent3p-ENTH (aa 1-172, pKW3). Pep12p and Ent3p constructs were cloned into yeast two hybrid vectors pLexN and pVP16-3, respectively. As negative control the empty pVP16-3 was used. For the assay the constructs were transformed into L40 yeast strain and the cells were grown for three days on THULL plates containing 5 mM 3-AT. A complete loss of interaction between Ent3p-ENTH and the Pep12p mutants was observed. **B:** Liquid β -galactosidase assay with Pep12p FSD mutants. The L40 cells containing the yeast two-hybrid plasmids were lysed and incubated with ONPG as substrate for the reporter gene product β -galactosidase. The absorption at 420 nm was measured and the β -Gal units calculated (see next to table 2). The interaction of Ent3-ENTH (pKW3) was almost completely lost in FSD mutants. The experiment was done 2-4 times and standard deviations were included in the diagram as error bars.

To prove this result a liquid β -galactosidase assay was done. The yeast strains from the yeast two-hybrid assay were grown into logarithmic phase and lysed by freeze and thaw cycles in liquid nitrogen and a 37°C water bath, respectively. As substrate for the β -galactosidase which is encoded on a reporter gene for Y2H interaction, ONPG (*o*-nitrophenyl- β -D-galactopyranosid) was used. The cells were incubated with the substrate at 30°C till a yellow color caused by the cleaved substrate occurred in the positive control and the reaction was stopped by adding

Na₂CO₃. The absorption was measured in a spectrophotometer at 420 nm and the β-galactosidase units (U) were calculated (see below). The galactosidase assay confirmed the result from the Y2H assay (fig. 4.1.B and table 2). The F20L mutation of Pep12p inhibited the interaction with Ent3p ENTH domain completely. The ΔFSD mutant showed a very weak interaction with Ent3p-ENTH (2.1 U, SD of three independent experiments = 1.5 U). In the strain containing the Pep12p N-terminus and the Ent3p ENTH domain 32 U (SD 7.6, n=4) were measured. In the control strains with empty prey vector (pVP) and in the Pep12p F20L with Ent3p-ENTH strain no significant signal over the background was obtained.

Tab. 2: β-galactosidase assay

	U	SD
Pep12+ Ent3	32.68	7.59
Pep12+ pVP	0.00	0.01
F20L+ Ent3	0.20	0.14
F20L+ pVP	0.15	0.07
ΔFSD+ Ent3	2.13	1.50
ΔFSD+ pVP	0.00	0.00

Equation for β-Gal Units:

$$U = \frac{1000 \cdot OD_{420}}{t \cdot V \cdot OD_{600}}$$

t = elapsed time in min of incubation

V = 0.1 mL x concentration factor (cell culture volume/resuspension vol. of Z-buffer: 1.5 mL culture / 300 μL Z-Buffer = 5)

OD₆₀₀ = Optical density at 600 nm of 1 mL cell culture

To further prove the FSD motif as crucial for the Ent3p interaction an *in vitro* pulldown assay was done with bacterially expressed and purified Strep-tagged Ent3p-ENTH and His₆-Pep12p N-terminus. His₆-Tlg1p was used as a negative control. The Pep12p ΔFSD and F20L constructs were cloned into the His₆-fusion vector pET28b and purified via Nickel-NTA columns (Qiagen). The purification of Ent3p-ENTH-Strep was performed with the Strep-Tactin Superflow column from IBA. For the pull down 0.75 μmol/200 μL protein of each SNARE and the Ent3-ENTH were used, precipitated with Ni-NTA agarose and the resulting samples were loaded on a 15% SDS Gel. Immunoblotting was done with anti-Pep12 antibody (52t) and anti-Ent3p antibody (YWOPt). On the blot significantly less Ent3p was detected after pulldown with the FSD mutant strains (fig. 4.2). For quantification the amount of WT Ent3p-ENTH bound to Pep12p was set as 1. The

amount of bound Ent3p to Pep12p F20L was reduced to about 10% (0.1) and with Δ FSD to about 30% (0.3). This shows that indeed the FSD motif is important for the binding of Pep12p to Ent3p.

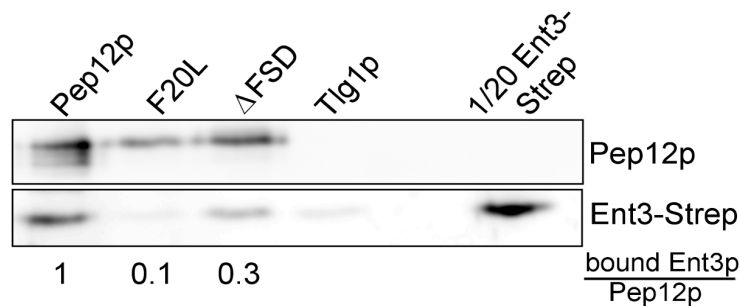


Fig. 4.2: ***In vitro* pulldown assay of Ent3p with Pep12p FSD mutants.** Ent3p-ENTH fused to a Strep-tag with His₆-fused Pep12p. Bacterially expressed fusion proteins were purified with appropriate purification columns and 0.75 μ mol of each SNARE and the Ent3-ENTH were incubated and precipitated with anti-Pep12p antibody. The proteins were loaded on a 15% SDS SDS gel and the immunoblotting was done with antibodies directed against Pep12p (upper panel) or Ent3p (lower panel). Ent3-Strep (aa 1-172, C-terminal fusion, pKW5) showed binding to His₆-Pep12p (aa 1-268, WT control, N-terminal fusion, pFvM135) and only a weak binding to His₆-Tlg1 (aa 1-135, negative control, pFN3). The interaction with Pep12 F20L (pSK3) and Pep12 Δ FSD (aa 19-26 deleted, pSK4) was strongly reduced (to 10% for F20L and 30% Δ FSD).

4.1.1.2 *In vivo* interactions of Ent3p with Pep12p FSD mutants

4.1.1.2.1 Localization of Pep12 mutants in immunofluorescence microscopy

In *ent3 Δ ent5 Δ* cells the localization of Pep12p was altered to a more dispersed distribution in the double mutants (Chidambaram *et al.*, 2008). In cells containing Pep12p with the F20L mutation or deleted FSD motif no mislocalization could be observed (fig. 4.3). The defect of WT Pep12p in *ent3 Δ ent5 Δ* cells was not very strong and the Pep12p antibody showed some unspecific reactions so the immunofluorescence could not support the *in vitro* data and the Pep12p stability assay.

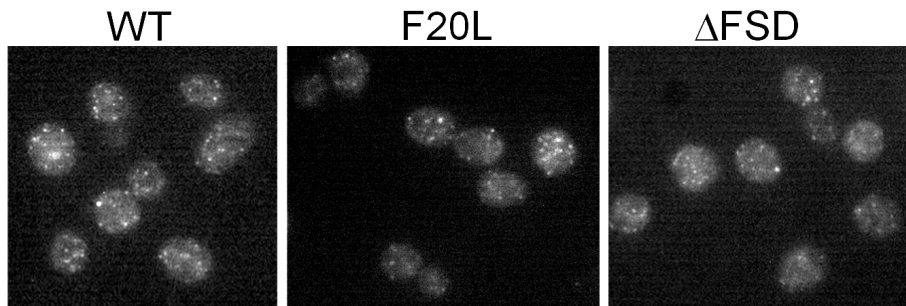


Fig. 4.3: **Pep12 F20L and Δ FSD localization via immunofluorescence microscopy.** WT (SEY6210) and *pep12 Δ* (SCY27) cells containing mutated Pep12p F20L (pJZ11) or Δ FSD (pCP4) were fixed and treated with preabsorbed antibody against Pep12p. No difference between the localization of the WT and the mutant Pep12p was detectable.

4.1.1.2.2 Localization by sucrose density gradient

A more sensitive assay to analyze the Pep12p localization is the sucrose density gradient centrifugation. Here the cell organelles were separated by their density and the distributions of specific proteins can be analyzed by immunoblotting.

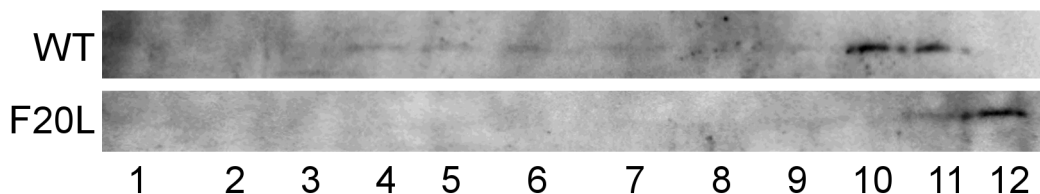


Fig. 4.4: **Pep12p F20L is mislocalized in a sucrose density gradient.** WT (SEY) and mutant (SCY27 with pJZ11) were lysed and fractionated by a sucrose density gradient from 22-55% sucrose, loaded on a 11% SDS gel and treated with antibodies against Pep12p.

In earlier studies we saw a strong defect in Pep12p localization in the *ent3 Δ ent5 Δ* mutants in a sucrose density gradient. In WT cells Pep12p is broadly distributed from fractions 4 to 11 with an increasing trend to denser fractions. In the F20L mutant no Pep12p was detected in fractions 4-9 (fig. 4.4). Instead the Pep12p amount in fraction 12 was enhanced. This fits to the observation that Pep12p is shifted to denser fractions in the *ent3 Δ ent5 Δ* double mutant. The experiment was

only performed once but since it is consistent with the data from Black and Pelham (2000) it was not repeated.

4.1.1.2.3 Pep12p stability is enhanced in Pep12p F20L

To check the consequence of the Pep12p mutation *in vivo* the Pep12p stability was analyzed by a pulse chase approach. For *ent3Δ* previous experiments have shown that Pep12p is more stable in this mutant due to a defect in the transport to the vacuole where Pep12p is degraded (Chidambaram, 2005). When the Pep12p-Ent3p interaction (and therewith the Pep2p transport) depends on the FSD motif mutation also the Pep12p FSD mutants should be more stable.

The cells were pulsed with radioactively (^{35}S) labeled methionine/cysteine for 25 min and chased for 10 min, 3h and 5h at 37°C. Then they were spheroplasted, lysed and CPY was immunoprecipitated by adding rabbit-anti-CPY antibody and Pansorbin. The CPY/Pansorbin suspension was loaded on an 8% SDS gel which was dried after run and applied to a phosphorimager plate for exposing. The CPY bands on the phosphorimager plate were detected with a phospholuminescence detector (phosphorimager).

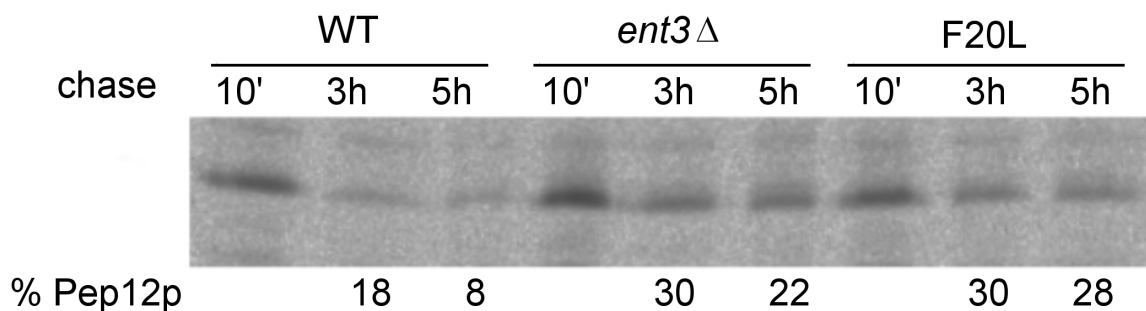


Fig. 4.5: **Mutation of the Pep FSD motif causes an enhanced stability of Pep12p.** Pulse chase immunoprecipitation of Pep12p in WT (SEY6210), *ent3Δ* (SCY2) and Pep12p F20L (*CEN* Pep12-F20L (pJZ11) in *pep12Δ* (SCY27, SEY6210 background)). Cells were labeled with [^{35}S]met/cys for 25 minutes and chased for 10 min, 3h and 5h at 37°C. Pep12p from the cellular extracts was immunoprecipitated with anti-Pep12p antibody and the amounts of Pep12p were quantified. The F20L mutant was more stable than the WT. The defect was comparable to the defect in the *ent3Δ* mutant. The indicated values were obtained by quantifying the bands of this exemplary blot with AIDA software.

Similar as in the *ENT3* deficient cells, where 27% Pep12p were still detectable after 5 h (SD 6%), the stability of the F20L mutant Pep12p is enhanced (26% after 5 h, SD 3%) to the threefold of WT Pep12p (9% protein after 5 h, SD 3%). The values are means from three independent experiments. In fig. 4.5 one exemplary blot is shown.

4.1.1.3 CPY transport

The soluble hydrolase carboxypeptidase Y (CPY) is routed via its receptor Vps10p from the TGN to the late endosome and from there to the vacuole where it is cleaved into an active form (mCPY). A block in the CPY transport as described for *pep12Δ* cells (Becherer *et al.*, 1996) results in an enhanced secretion of the CPY pro-forms (pCPY). To see whether the Pep12p F20L mutants were still functional a pulse chase experiment with radioactive labeled cys/met (^{35}S) was performed. WT cells (SEY) and *pep12Δ* (SCY27) cells containing the Pep12p F20L (pJZ17) or Pep12p Δ FSD (pCP4) plasmid were grown into logarithmic phase at 30°C, pulsed for 10 min by adding radioactive [^{35}S]-Met/Cys and then chased for 30 min at 30°C. After IP with anti CPY antibody, gel run and drying the samples were exposed on a phosphoimager plate.

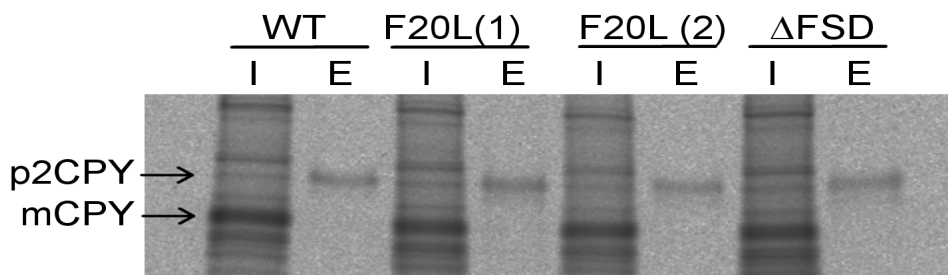


Fig. 4.6: **CPY secretion of Pep12 mutants.** WT (SEY) and Pep12p F20L (SCY27 pJZ11) and Δ FSD (SCY27 pCP4) mutant cells were pulsed for 10 min and chased for 30 min at 30°C. The IP was done with a fresh aliquot of rabbit anti-CPY antibody. To compare the results with the old antibody aliquot the F20L mutant was tested with new (1) and old (2) antibodies. There was no difference detectable in CPY secretion between WT and mutants. I = internal fraction; E = external fraction.

No significant difference could be detected between WT and mutant cells (fig. 4.6). Since there was a high unspecific reaction of the antibody in the internal fraction a freshly thawed CPY antibody aliquot was used and for comparison the F20L mutant was also precipitated with antibody from the old aliquot (fig. 4.6, F20L (2)). No difference between the aliquots and therefore no improvement could be obtained. From this experiment the F20L and the Δ FSD mutants are functional enough to sustain the CPY transport to the vacuole.

4.1.2 Characterization of the interaction surface of Ent3p with the endosomal SNAREs

In mammals the interaction of epsinR with Vti1b was characterized by solving the crystal structure of the interaction complex (Miller *et al.*, 2007). But if this interaction is conserved from the yeast Vti1p and Ent3p to the mammalian system and how the interaction of Ent3p with the other two interacting SNAREs works in detail was not yet studied. One aim of this work was to further characterize these interactions by yeast two hybrid approaches and *in vivo* studies in yeast cells.

4.1.2.1 Ent3p interaction with SNAREs is specific for the ENTH domain

To analyze the specificity of Ent3p-SNARE interaction chimera were constructed each consisting of one half of the Ent3p-ENTH and one half of Ent5p-ANTH or epsinR-ENTH domain (fig. 4.7). These constructs were cloned into the yeast two-hybrid prey vector pVP16-3 and transformed together with the endosomal SNARE N-termini (in pLexN) into L40 yeast cells. For the interaction screen the cells were streaked on THULL (for Vti1p) plates with 1 mM 3-aminotriazole (3-AT; for vti1b, Pep12p and Syn8p) and pictures were made after 2-4 days incubation at 30°C.

ChimA	Ent3 1-S112	Ent5 I112-172
ChimB	Ent5 1-V111	Ent3 I113-172
ChimC	Ent3 1-S112	epsinR I105-162
ChimD	epsinR1-H104	Ent3 I113-172

Fig. 4.7: **Construction of ENTH/ANTH chimera.** Parts of Ent3p-ENTH, Ent5p-ANTH and epsinR-ENTH were amplified and fused by PCR with bridging oligos. Constructs were cloned into the yeast two-hybrid vector pVP16-3.

In constructs where one half of Ent3p-ENTH was exchanged to the accordant half of Ent5p-ANTH the interaction with the SNAREs Vti1p, Pep12p and Syn8p was completely lost (fig. 4.8.A). This indicates that for the interaction both halves of the ENTH domain were needed and that this interaction is specific for the ENTH domain and cannot partially be substituted by Ent5p-ANTH. To prove that the interacting motif is not in the region where the domains were divided additional chimera ChimE and ChimF were constructed. ChimE consists of Ent3p aa 1-126 fused to Ent5p aa 130-172 and ChimF of Ent5p aa 1-82 fused to Ent3p aa 83-172. Again in this constructs no Y2H interaction could be observed (fig. 4.8.B).

If parts of the ENTH domain were exchanged to parts of the mammalian epsinR-ENTH domain the interaction remains if the first five helices of the Ent3p (with yeast SNAREs) and epsinR (with vti1b) were present (fig. 4.8.B). This was in particular true for the mammalian system (epsinR-Ent3 + vti1b, ChimD). The interactions of the Ent3p-epsinR (ChimC) with the yeast SNAREs was very weak but well reproducible for Vti1p but hard to reproduce for Pep12p and Syn8p. This was due to a high background expression of the reporter gene for those constructs and therefore a high growth of the Pep12p and Syn8p constructs together with the empty pVP vector.

Together this experiments showed that the interactions in the mammalian system were transferable to the yeast system and even parts can be exchanged between Ent3p and epsinR without a complete loss of interaction. The motif is like in the mammalian system no single stretch of amino acids, at least two regions on both halves of the ENTH domain were necessary for the interaction. The first five

helices were crucial for the specificity of the interaction and were less conserved from yeast to mammals than the last three helices of the ENTH domain.

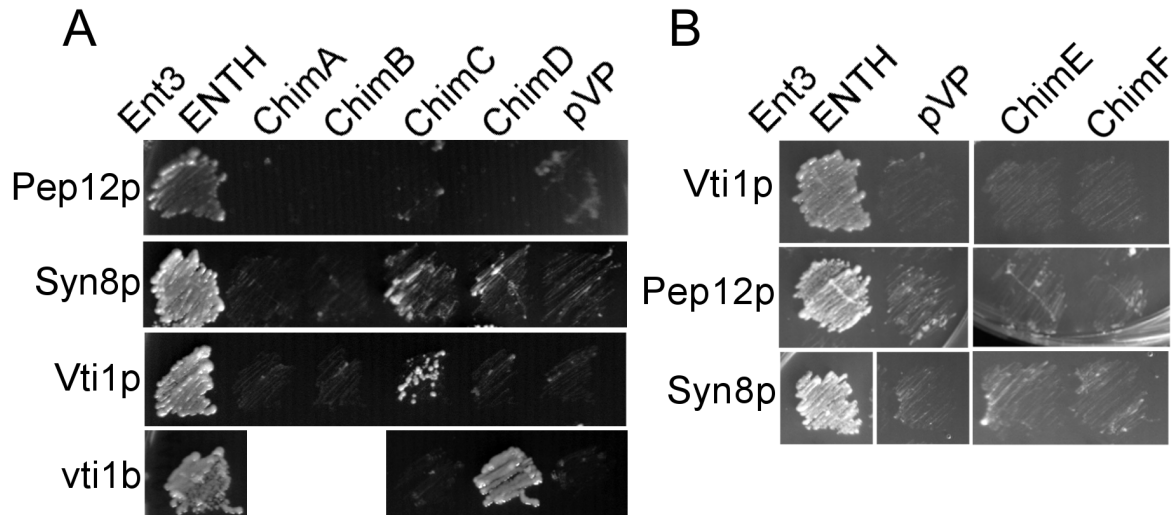


Fig. 4.8: **The specificity of the interaction of Ent3p with the endosomal SNAREs is determined by the first five helices of the ENTH domain.** Chimera constructs (ChimA=pCW5, ChimB=pCW6, ChimC=pCW7, ChimD=pCW8, ChimE=pCW11, ChimF=pCW12) and SNAREs (Vti1p=pBK118, vti1b=pBK111, Pep12p=pBK171, Syn8p=pBK165) were transformed into L40 cells and the yeast two hybrid assay was performed by streaking the cells on THULL agar plates without (Vti1p) or with 1 mM 3-AT (vti1b, Pep12p, Syn8p). The positive control for vti1b (first column) was the combination with epsinR in pVP16-3 (pBK130), for the yeast SNAREs Ent3p-ENTH in pVP16-3 (pKW3) was used. Pictures were taken after 2-4 days incubation at 30°C. **A:** Interactions were detected between ChimC and Vti1p and with less clarity also Syn8p and Pep12p. Vti1b interacted with ChimD. **B:** With the alternative Ent3/Ent5 constructs ChimE and ChimF no reproducible interaction could be obtained.

4.1.2.2 Vti1p, Syn8p and Pep12p bind the same interaction surface of Ent3p but different amino acids

To analyze the interaction surface in more detail Ent3p point mutants were constructed by site directed mutagenesis. In mammals the mutation of F52D, M53S/Y54D and R96S resulted in a loss of interaction with vti1b (Miller *et al.*, 2007). The exchange E95W had no influence on the interaction. Crystal structures of yeast Ent3p or the endosomal SNAREs were not available so via sequence alignment (Blast) and structure modeling (3D-jigsaw) the appropriate amino acid exchanges Y60D, F62D, R154E and E103W in yeast Ent3p were determined (fig. 4.9.A-C). The mutations were inserted by PCR based site directed mutagenesis. The Ent3p ENTH constructs (aa 1-172) were cloned into the yeast two-hybrid

vector pVP16-3 and full length proteins under endogenous promoter in the yeast *CEN* expression vector pRS316.

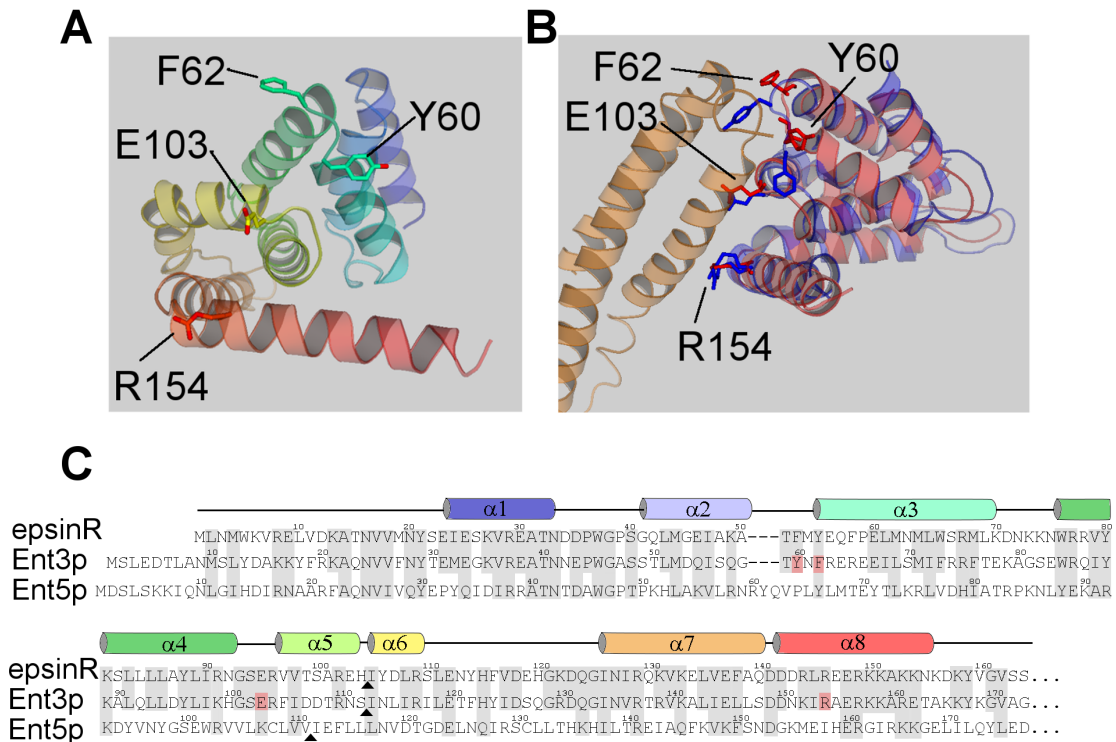


Fig. 4.9: **Structure modeling and alignment of Ent3p and epsinR.** **A:** Ent3p amino acid sequence was aligned with 3D-Jigsaw to human epsinR crystal structure (2V8S). Amino acids which were mutated for the yeast two-hybrid assay were marked as ball-and-stick view and labeled. **B:** The modeled Ent3p (3D-jigsaw; illustrated with Pymol) structure (red) was aligned to human epsinR (blue) in complex with human vti1b (orange, complex structure: 2QY7A). **C:** Sequence alignment of human epsinR with yeast Ent3p and Ent5p. Conserved residues were boxed in gray, mutated amino acids in red. The point where the domains were separated for constructing the chimera (A-D) were marked with a triangle. The illustrated helices above the sequences were colored analogous to the structure model in A.

Like in the mammalian system the amino acid exchanges of Y60D (F52D in epsinR), F62D (Y54D) and R154E (R146E) resulted in a loss of interaction with Vti1p (fig. 4.10). Additionally the E103W mutation had no impact on the interaction so that the interaction surface showed a very similar profile in yeast and in mammals. For the interaction with Pep12p and Syn8p it could be shown that the interaction surface is identical but the interacting amino acids were partially different. For the interaction with Pep12p all four checked amino acids were necessary, for Syn8p just E103 and R154. With this set of mutants it is possible to block the interactions with two of the three SNARE partners (Y60D, F62D did not

interact with Vti1p and Pep12p, E103W did not interact with Pep12p and Syn8p) or with all Q-SNAREs of the complex (R143E). Through a mutation inserted probably via the PCR reaction a fifth mutant was obtained. This F62D G58R double mutant was able to interact with Pep12p and Syn8p. The interaction with Pep12p was surprising since the F62D mutation alone abolished the interaction with Pep12p.

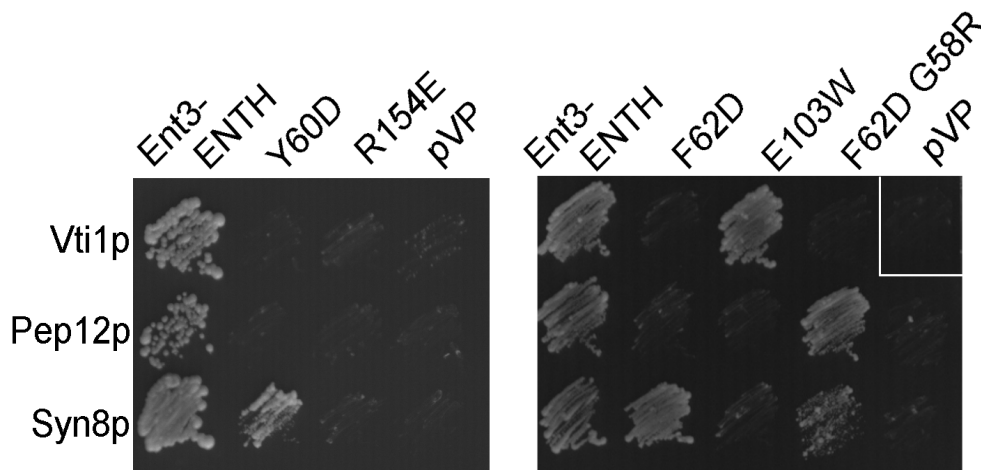


Fig. 4.10: **Endosomal SNAREs bind to the same surface of Ent3p but to different amino acids.** Ent3p ENTH (pKW3) and the ENTH point mutants F62D (pAN4), E103W (pAN5), Y60D (pJZ19), F62D G58R (pAN6) were transformed together with the N-termini of the yeast SNAREs Vti1p (pBK118), Pep12p (pBK171) and Syn8p (pBK165) into L40 cells. The cells were streaked onto THULL agar plates containing 2 mM 3-AT and pictures were made after 2 days incubation at 30°C. The F62D and Y60D mutants still interacted with Syn8p and E103W with Vti1p. The R154E mutant could not bind any of the three SNAREs. The double mutant F62D G58R interacted with Pep12p and Syn8p. As negative control the empty pVP16-3 vector together with the SNAREs was used.

4.1.2.3 Interacting amino acids on Vti1p and Pep12p

I could show that the amino acids R154, Y60, F62 and E103 of Ent3p were necessary for the interaction with the SNAREs Vti1p, Pep12p and Syn8p. To find the interacting amino acid (aa) on Vti1p and Pep12p for the charge swap mutant aa Ent3p R154E, potential interacting acidic aa on Vti1p and Pep12p were mutated into basic amino acids to restore the interaction. The mutants checked were Vti1p E9R and E17R and Pep12p E12R. The mutant constructs were transformed into the L40 yeast two-hybrid strain and the cells were streaked on THULL agar plates containing 1mM 3-AT. In the former assay (fig. 4.10) The interaction of Vti1p and Pep12p was abolished for R154E, Y60D and F62D. Vti1p still interacted with E103W, Pep12p did not.

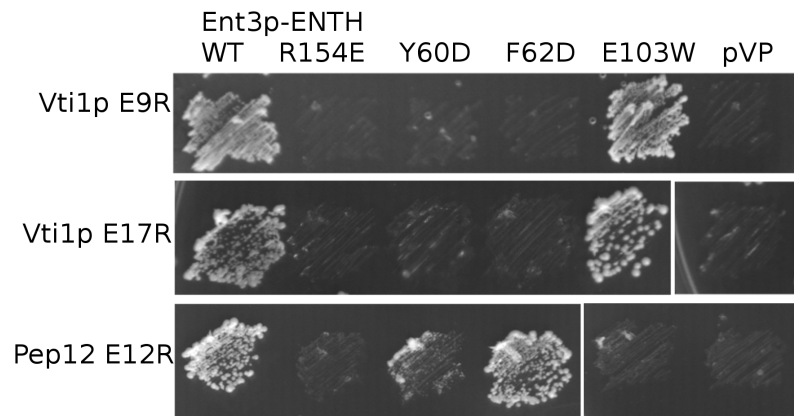


Fig. 4.11: **Charge-swap interactions between Vti1p, Pep12p and Ent3p.** The SNARE mutant constructs Vti1p E9R (pCP33), E17R (pJAL7) and Pep12p E12R (pCP34) were transformed into L40 cells and streaked onto THULL plates containing 1mM 3-AT. Pictures were made after three days incubation at 30°C. For Vti1p no charge-swap interaction was obtained. For Pep12p E12R an interaction with Ent3p F62D and weakly with Y60D was restored.

For Vti1p no interacting amino acid could be confirmed (fig. 4.11). The E9R and the E17R mutants did not restore the interaction with Ent3p R154E or Y60D/F62D. The interaction with wild type Ent3p and E103W was still intact. Interestingly the Pep12p E12R mutant restored an interaction with Ent3p F62D and less pronounced with Y60D. The interaction with WT Ent3p was not affected for this mutant. So the amino acid E12 is not crucial for the ENTH binding but must be located in the complex in the neighborhood of F62 and Y60 on Ent3p.

4.1.2.4 *Vti1p, Pep12p and Syn8p were sorted together*

The set of point mutants was used to investigate the sorting of the SNARE complex. In *ent3Δent5Δ* cells Pep12p and Vti1p were mislocalized in a sucrose density gradient (Chidambaram *et al.*, 2008). For Pep12p a mislocalization was also shown in an immunofluorescence approach (Chidambaram *et al.*, 2008). A 3xHA-Syn8p fusion was constructed and a mislocalization in *ent3Δent5Δ* was also true for Syn8p (fig 4.15). For the point mutants in the *ent3Δent5Δ* background the sucrose density gradient experiment was repeated and the fractions checked for Vti1p, Pep12p and HA-Syn8p localization.

Vti1p

Vti1p is distributed over several organelles in the cells. So its allocation in the sucrose density gradient is broadly from fraction 4 to 12 with a peak at fraction 5 and a shoulder from fractions 8-10 in WT or *ent5* Δ cells (fig. 4.12.A).

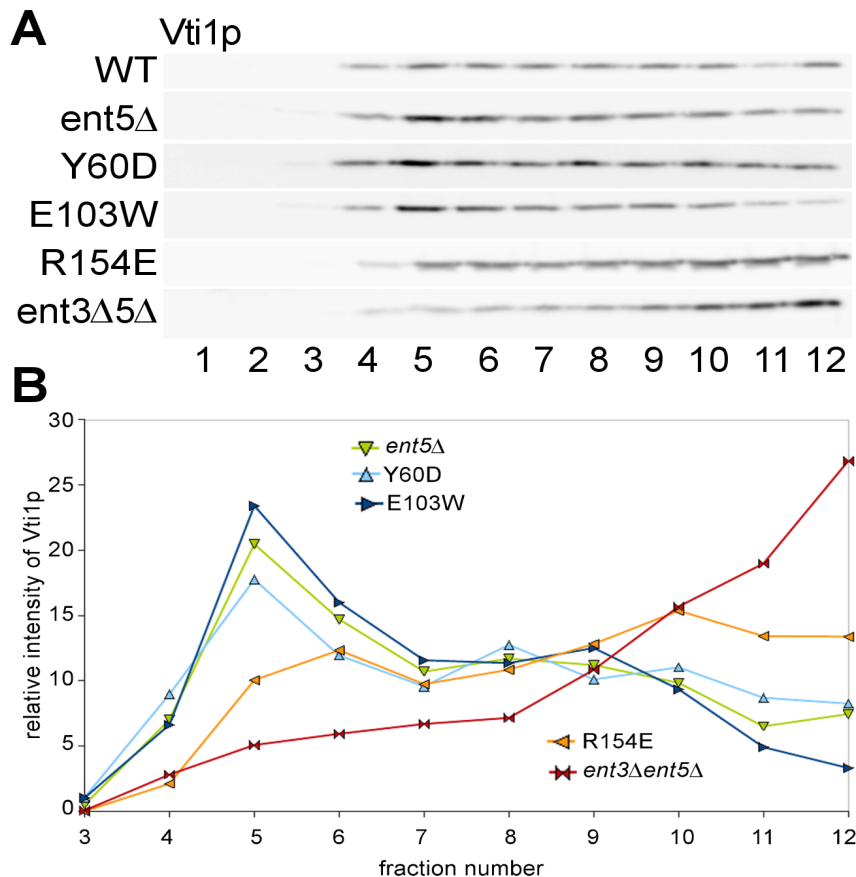


Fig. 4.12: Vti1p is mislocalized to denser fractions in the Ent3p R154E mutant.

A: Localization analysis of Vti1p in a sucrose density gradient (22-55% sucrose in HEPES pH 7.6). WT (BY4742), *ent5* Δ , *ent3* Δ *ent5* Δ (BKY13), and *ent3* Δ *ent5* Δ cells containing Ent3p point mutants (Y60D = pJZ17, E103W = pCP13, R154E = pJZ18) were grown into logarithmic phase, osmotically and mechanically lysed and loaded on a sucrose gradient which was centrifuged for 16 h at 100.000 g. From the 1 mL fractions 40 μ L (from a 30 μ L + 15 μ L 3xStop mix) were loaded on a 11% SDS-gel and the proteins were visualized by immunoblotting (rabbit-anti-Vti1p and goat-anti-rabbit HRP antibodies). **B:** The band intensities of the blot (A) were quantified with AIDA software and the relative intensities were determined by the equation $I_{rel} = 100/\Sigma_i * I$ where Σ_i is the sum of all intensities and I the single band intensity.

In the blot another peak for the WT cells in fraction 12 was detected which was due to an incomplete removal of cell debris in the first 500 g centrifugation step. Therefore the WT data was not included in the diagram fig. 4.12.B. For *ent3Δent5Δ* double mutants the band intensities continuously ascended, particularly from fractions 8-12.

The E103W and the Y60D point mutants could completely rescue the defect of the double mutant. The R154E mutant showed some rescue ability but had a significant shift of the Vti1p localization to denser fractions.

With immunofluorescence microscopy with anti-Vti1p antibody there was only a very weak defect in *ent3Δent5Δ* cells which was hard to reproduce (fig. 4.13). In wild type cells Vti1p is distributed in differently sized spots throughout the cell. In *ent3Δent5Δ* cells the distribution seems to be more dispersed and less dot-like like it was observed for Pep12p in the double mutant but less pronounced. A bit stronger was the defect in the *syn8Δent3Δent5Δ* mutants but still a defect was hard to reproduce.

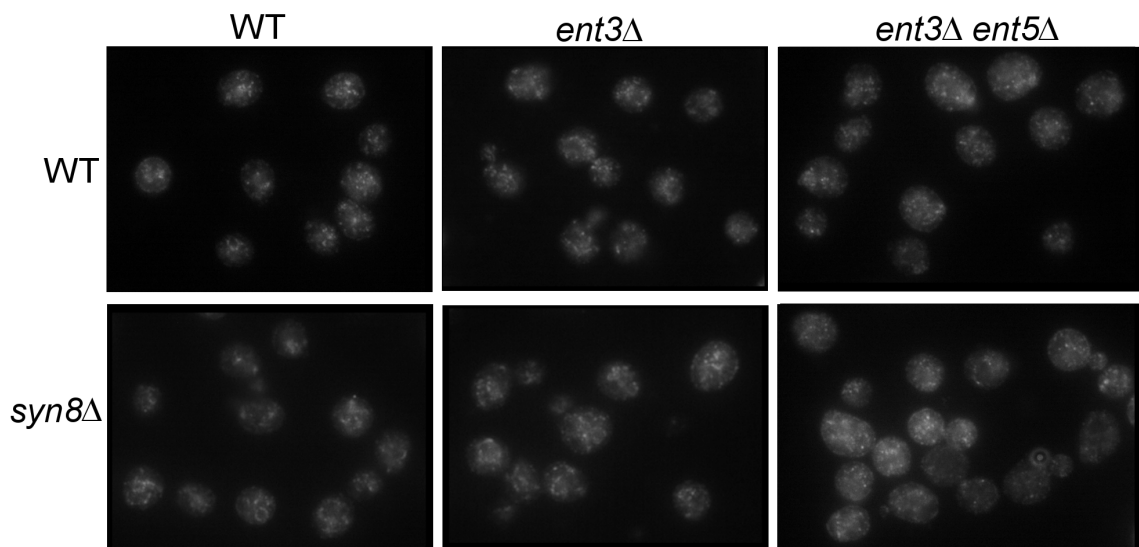


Fig. 4.13: **Vti1p localization in *ent3Δent5Δ* and *syn8Δent3Δent5Δ* cells.** Cells were grown into logarithmic stage, fixed, spheroplasted and stained with affinity purified rabbit-anti-Vti1p and Cy2 labeled secondary antibody. Vti1p is localized in punctual structures in all tested strains (WT = BY4742, *ent3Δ* = BY *ent3Δ*, *ent3Δent5Δ* = BKY13, *syn8Δ* = BY *syn8Δ*, *syn8Δent3Δ* = JZY1, *syn8Δent3Δent5Δ* = JZY2).

Pep12p

For Pep12p, which also was mislocalized in IF, the localization in the sucrose gradient in *ent3Δent5Δ* cells was clearly shifted to denser fractions (fractions 10-12; fig. 4.14). In WT cells it is mainly localized at late endosomes and shows a distribution in the sucrose density gradient from fractions 3-12 with a peak from 8-10. As for Vti1p, the E103W and Y60D mutants rescued the localization defect. The R154E mutant showed even less rescuing ability for Pep12p than for Vti1p.

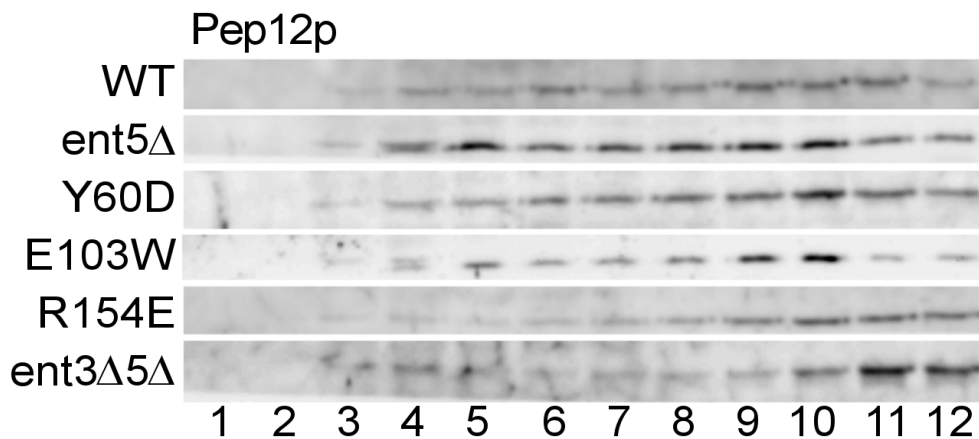


Fig. 4.14: **Pep12p was mislocalized in the Ent3p R154E point mutant.** Localization analysis of Pep12p in a sucrose density gradient (22-55% sucrose in HEPES pH 7.6). WT (BY4742), *ent5Δ*, *ent3Δent5Δ* (BKY13), and *ent3Δent5Δ* cells containing Ent3p point mutants (Y60D = pJZ17, E103W = pCP13, R154E = pJZ18) were grown into logarithmic phase, osmotically and mechanically lysed and loaded on a sucrose gradient which was centrifuged for 16 h at 100.000 g. Of each fraction 40 μ L (from a 30 μ L + 15 μ L 3xStop mix) were loaded on a 11% SDS-gel and the proteins were visualized by immunoblotting (rabbit-anti-Pep12p and goat-anti-rabbit HRP antibodies).

Syn8p

For Syn8p detection a 3xHA-tagged Syn8p (pSC19) was subcloned into a *CEN* vector with *HIS3* marker (pRS313) and transformed in the WT (BY4742), BY *ent5Δ*, BY *ent3Δent5Δ* (BKY13) and the double mutant strains containing the Ent3p point mutants. After the sucrose density gradient fractionation, separation of the proteins by SDS-PAGE and transfer to a nitrocellulose membrane the blots were treated with mouse-anti-HA antibody (Covance, HA.11 Clone 16B12). Even

though the antibody was monoclonal and specific in mammalian cells (Covance provider manual) in yeast cells it showed some unspecific binding and only a weak reaction with its epitope, the HA tag.

Syn8p was found in the sucrose density gradient from fractions 4-10 in WT, *ent5Δ*, E103W, Y60D and also in the R154E mutant (fig. 4.15). In the *ent3Δent5Δ* double mutant it was clearly shifted to denser fractions. So it seems that in all three tested point mutants Syn8p was able to keep a proper localization although in the Y2H assay the interaction of Ent3p with all three SNAREs was abolished.

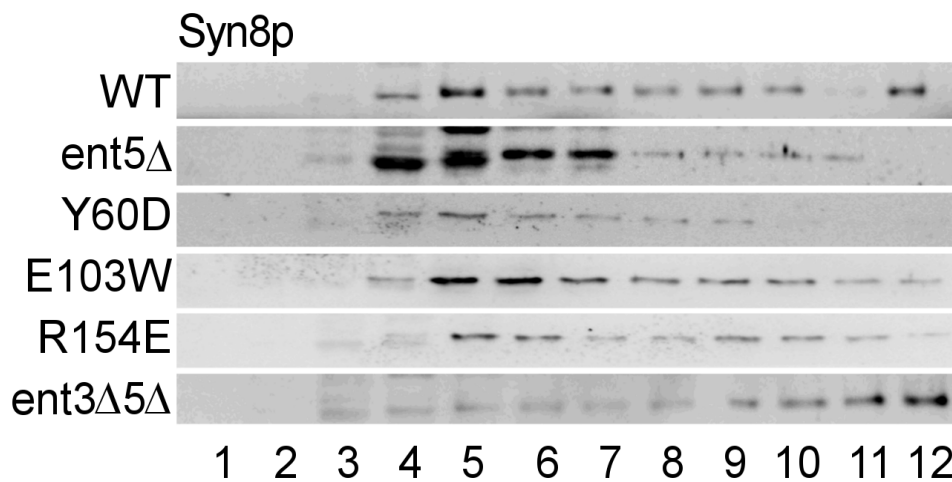


Fig. 4.15: **Localization of 3xHA-Syn8p in a sucrose density gradient** (22-55% sucrose in HEPES pH 7.6). WT (BY4742), *ent5Δ*, *ent3Δent5Δ* (BKY13), and *ent3Δent5Δ* cells containing Ent3p point mutants (Y60D = pJZ17, E103W = pCP13, R154E = pJZ18) were grown into logarithmic phase, osmotically and mechanically lysed and loaded on a sucrose gradient which was centrifuged for 16 h at 100.000 g. Of the fractions 40 μ L (from a 30 μ L + 15 μ L 3xStop mix) were loaded on a 11% SDS-gel and Syn8p was visualized by immunoblotting (mouse-anti-HA (Covance) and goat-anti-mouse HRP antibodies). The localization of 3xHA Syn8p was dependent on Ent3p and Ent5p as it is mislocalized in the *ent3Δent5Δ* double mutant. In the point mutants the Syn8p distribution was not significantly changed.

4.1.2.5 Location of Pep12p, Vti1p and Syn8p on vesicles or endosomes

Syn8p is sorted somehow differently than the other two SNAREs. One possibility is that Pep12p and Vti1p are t-SNAREs and permanently located at the endosomes and Syn8p is a v-SNARE which cycles between endosomes and TGN. To prove this hypothesis the localization of the SNAREs was analyzed by a sucrose density gradient in *tlg2Δ* cells. Tlg2p is a SNARE which is involved in retrograde fusion at the TGN. Lack of this SNARE results in a block of retrograde

endosome to TGN transport (see also chapter 4.3, fig. 4.38). This block should affect the localization of a v-SNARE whose localization is dependent of cycling but leave the t-SNAREs unaffected. The *tlg2Δ* and BY4742 WT cells were transformed with the HA-Syn8p construct and the samples from the sucrose gradient were loaded on a SDS-Gel, transferred to a nitrocellulose membrane and the SNAREs were detected by immunoblotting.

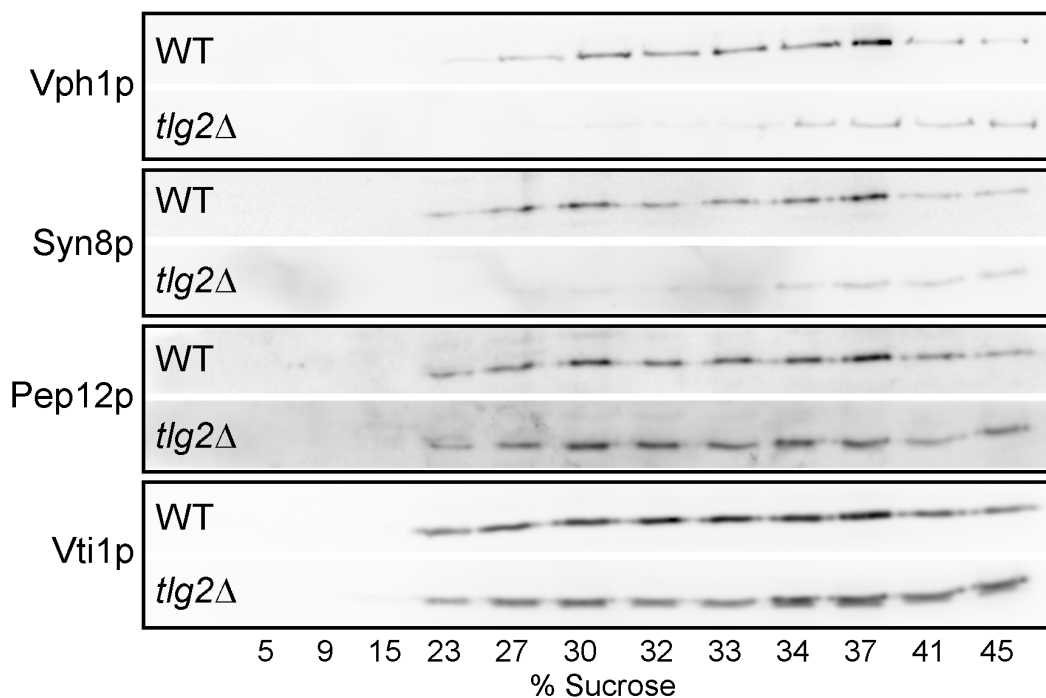


Fig. 4.16: **Localization of Vti1p, Pep12p and Syn8p in *tlg2Δ* cells.** BY4742 and BY *tlg2Δ* cells were transformed with HA-Syn8 (pJZ21), lysed and loaded on a sucrose gradient. After SDS-PAGE and blotting the proteins were detected via immunoblotting with antibodies against Vti1p, Pep12p and HA (Syn8p). As control the vacuolar ATPase subunit Vph1p was used. Syn8p, but not Pep12p or Vti1p, was shifted to denser fractions in *tlg2Δ* cells.

A clear shift of HA-Syn8p could be observed in the *tlg2Δ* cells (fig. 4.16). Pep12p had a WT distribution and Vti1p showed just a marginal shift. The control protein Vph1p which is located in the vacuole membrane showed also a shift to denser fraction which could be due to fragmented vacuoles of the *tlg2Δ* mutant. This could also explain the small shift of Vti1p in *tlg2Δ* cells. The experiment was conducted twice with a good accordance. For quantification the bands of one exemplary blot were quantified with the AIDA software and plotted against the fraction number (fig. 4.17). In WT cells Pep12p is localized in two peaks at fractions 6 and 10. This

distribution is not significantly changed in *tlg2Δ* cells. Vti1p showed a more broad distribution which is shifted in a low extend to denser fractions. Syn8p had a single peak in WT cells at fraction 5 which was shifted mainly to fraction 10. This result points to a localization of Syn8p on vesicles and Pep12p and Vti1p on the endosomes.

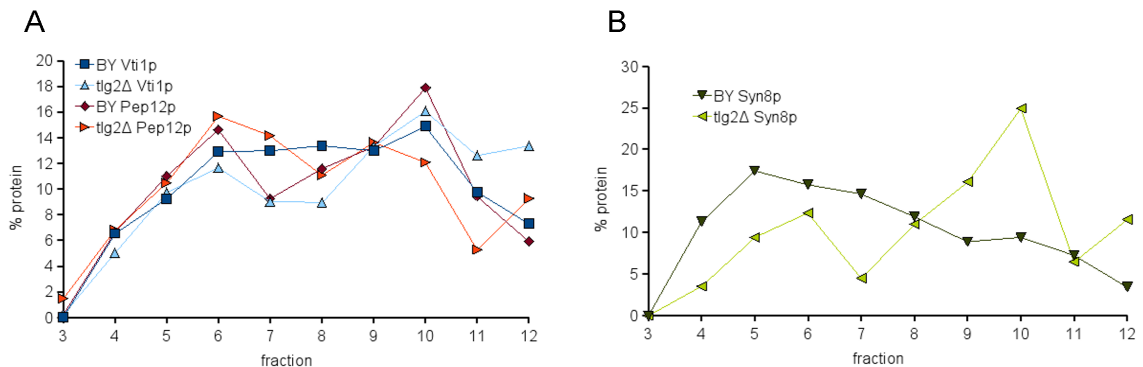


Fig. 4.17: Quantification of SNARE localization in *tlg2Δ* cells. The bands from fig 4.16 were quantified with AIDA and plotted. Thereto the percentage of each band intensity in relation to the sum of all intensities was determined and plotted against the fraction number. Pep12p localized equally in WT and *tlg2Δ* cells, Vti1p showed a slight shift (**A**) and Syn8p was markedly mislocalized to denser fractions (**B**).

4.1.2.6 Functions of *Ent3p* point mutants *in vivo*

So in three of the *Ent3p* point mutants the interaction with two SNAREs was abolished and the R154E mutant could not interact with any of the SNAREs. To analyze the influence of the lacking SNARE binding *in vivo* the point mutants were cloned under endogenous promotor into a *CEN* expression vector and the CPY transport, cell wall assembly and trafficking of GFP-Snc1p and GFP-Yck2p was analyzed. Therefore the constructed plasmids were transformed in an *ent3Δent5Δ* strain. It was necessary to use the double mutant since single *ent3Δ* mutants did not show a severe phenotype. *ent3Δ* had a low CPY secretion defect which can be detected in a CPY overlay assay but barely in a pulse chase experiment (Chidambaram *et al.*, 2008).

CPY transport

pep12Δ mutants have a strong CPY secretion defect (Becherer *et al.*, 1996). In *ent3Δent5Δ* mutants the defect was weaker and even less pronounced in *ent3Δ* cells but still strong enough to see significant amounts of secreted CPY in the relative sensitive overlay assay. To see if the Ent3p point mutants can rescue the CPY defect of the double mutant liquid yeast cell cultures were spotted onto YEPD agar plates, covered for 24 h with a nitrocellulose membrane and this was treated with anti-CPY antibody.

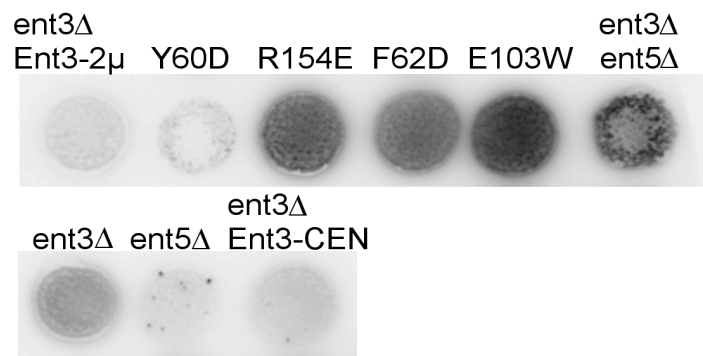


Fig. 4.18: **Ent3p point mutants do not rescue the *ent3Δent5Δ* CPY defects.** For the CPY overlay assay 0.05 OD cells in logarithmic phase were spotted onto YEPD agar plates, incubated 24 h at 30°C without and adjacent 24 h with nitrocellulose membrane. The membrane was washed, incubated with mouse-anti-CPY and goat anti-mouse-HRP antibodies and the chemoluminescence was detected using ECL substrate and a LAS camera.

As expected the *ent5Δ* and *ent3Δ* yeast cells transformed with *ENT3* on a 2 μ or *CEN* plasmid had no CPY secretion defect. *ent3Δ* cells had a weak, *ent3Δent5Δ* cells a stronger defect. The mutants R154E, E103W and F62D could not rescue the defect of the double mutant (fig. 4.18). The Y60D point mutant had a very strong growth defect at all temperatures and therefore no analysis was possible (see also Fig. 4.21).

The Ent3p point mutants could not rescue the CPY defect of the *ent3Δent5Δ* mutant in the overlay assay. To quantify this defect a CPY-pulse chase experiment with radioactively labeled CPY was performed.

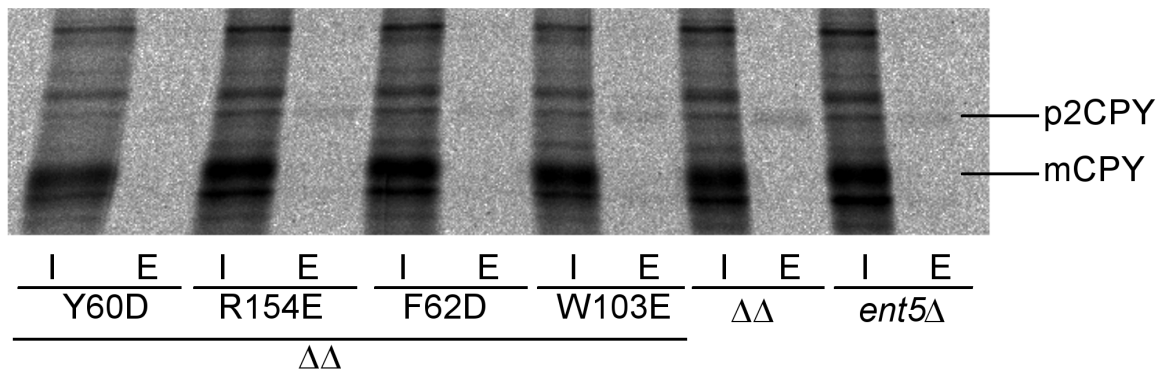


Fig. 4.19: **CPY pulse chase experiment with Ent3p point mutants.** *ent3Δent5Δ* ($\Delta\Delta$), *ent5Δ* and $\Delta\Delta$ cells containing the point mutant constructs were cultured and pulsed for 10 min with [^{35}S]cys/met and chased for 30 min, all at 30°C. The CPY was immunoprecipitated with rabbit-anti CPY serum and loaded on an 8% SDS gel. The radioactive labeled CPY was visualized with a phosphoimager after exposing the gel on a phosphoimager plate. No defect could be detected in the point mutants.

The cells were grown into logarithmic phase at 30°C, pulsed for 10 min by adding radioactive [^{35}S]-Met/Cys and then chased for 30 min at 30°C. After lysis and IP with Pansorbin coupled anti-CPY antibody the extracts were loaded on an 8% SDS gel which was dried and the CPY bands were detected with a phosphoimager.

A weak p2CPY secretion was detectable for the *ent3Δent5Δ* double mutant. The *ent5Δ* control secreted less p2CPY. The secretion of the point mutants was more comparable to *ent5Δ* than to the double mutant (fig. 4.19). The evaluation of this experiment (three times repeated) was difficult because of the high unspecific reaction of the CPY antibody. A new antibody aliquot (from the same rabbit) and fresh Pansorbin were tested but no improvement could be achieved.

The result seems to be contradicting the overlay assay but maybe the pulse chase experiment was just not sensitive enough to detect the small amount of secreted CPY in the point mutants.

Cell wall assembly

To check whether the Ent3p point mutants exhibit defects in cell wall assembly a sedimentation assay and a growth test on agar plates with cell wall disturbing agents were performed.

In earlier studies we observed an aggregated phenotype of the *ent3Δent5Δ* mutant cells (Zimmermann, 2006). The double mutants have defects in their cell wall assembly and tended to produce more than one bud at a time. This probably causes cell aggregates in contrast to the dispersed phenotype of WT cells. The cell aggregation can be quantified by a sedimentation assay. The more and the bigger the aggregates in the culture are, the shorter is the sedimentation half-life time.

In the sedimentation assay the Y60D and R154E mutants could not rescue the phenotype to a level of the BY WT or the *ent3Δ* strains. While WT and *ent3Δ* cells had sedimentation half life times ($t_{1/2}$) of 166 min and 160 min (SD 8.5 min), respectively, the point mutants Y60D and R154E had $t_{1/2}$ of 140 min (SD 0.7 min) and 125 min (SD 5.7 min; fig. 4.20). Especially the R154E mutant could not rescue the defect of the double mutant where half of the cells were sedimented after 122 min (SD 14.9 min). The standard deviations were obtained from two independent experiments except of BY WT for which only one experiment was performed. The values for the controls were consistent with the data I obtained from my diploma work ($t_{1/2}$: BY = 168 min SD 10 min; *ent3Δ* 179 min, SD 22 min; *ent3Δent5Δ* 126 min, SD 6 min; Zimmermann, 2006).

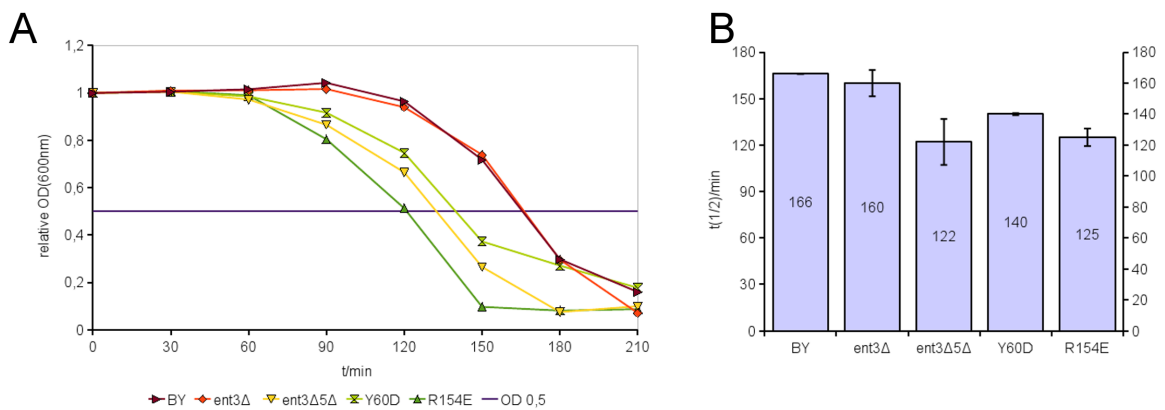


Fig. 4.20: Sedimentation assay with Ent3p point mutants. **A:** Yeast cells were grown into logarithmic stage and 1 OD was pelleted and resuspended in 1 mL ddH₂O. The OD₆₀₀ was measured every 30 min, relativized to time point 0 = 1 and plotted against time (t). The plot is shown for one exemplary experiment. **B:** The sedimentation half life time ($t_{1/2}$) of two independent experiments (BY = one experiment) was calculated, averaged and a standard deviation (SD) was determined. For BY and *ent3Δ* cells $t_{1/2}$ was 166 min and 160 min (SD=8.5 min), respectively. For the *ent3Δent5Δ* double mutant the $t_{1/2}$ was significantly reduced (122 min, SD=14.9 min). The Ent3p point mutants could not completely rescue the defects of the double mutants (Y60D [BKY13 pJZ17] $t_{1/2}$ =140 min, SD=0.7 min; R154E [BKY13 pJZ18] $t_{1/2}$ =125 min, SD=5.7 min). The R154E mutant had a stronger defect than the Y60D mutant.

Cells with defects in their cell wall assembly often show a sensitivity or resistance to cell wall perturbing agents. So were cells with chitin depositions on the cell wall sensitive to calcofluor white or cells in which the overall cell wall integrity is disturbed are sensitive to osmotic stress. Osmotic stress can be induced with high concentrations of NaCl or sorbitol. When in the case of cell wall defects the plasma membrane is more accessible the cells are sensitive to the detergent sodium-dodecylsulfate (SDS).

The Y60D mutant had a strong growth defect at 30°C on regular YEPD plates (fig. 4.21). The cells even grow worse than the *ent3Δent5Δ* double mutant and this defect was not due to the expression level (see Fig. 4.28). The F62D, E103W and R154E mutants showed a complete rescue of the double mutants defects on agar plates with SDS, NaCl or sorbitol (fig. 4.21). In contrast they were not able to rescue the defects on the CF plates completely. With 25 μg/mL calcofluor they showed a partial complementation ability which was lost with addition of 50 μg/mL calcofluor.

However, there was no difference between the single mutants and the difference between the phenotypes of wild type and double mutant was quite small so that a less severe defect would be difficult to detect with this assay.

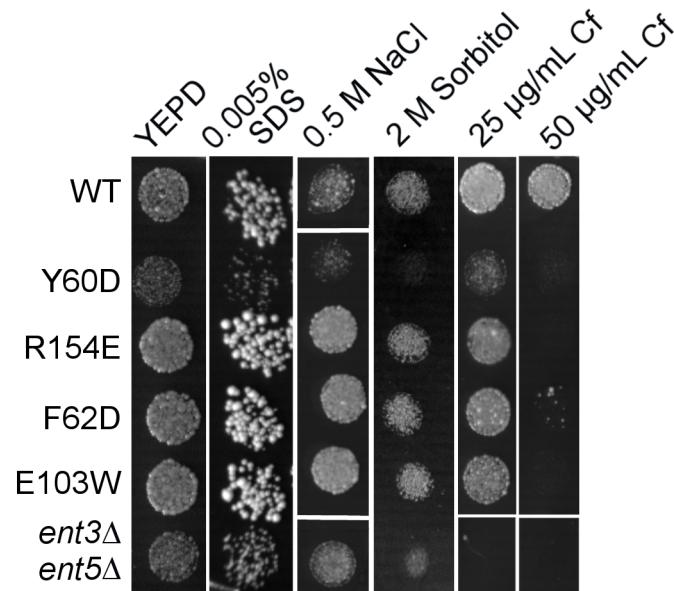


Fig. 4.21: **Growth test with Ent3p point mutants.** Controls (WT = BY4742, *ent3Δent5Δ* = BKY13) and *ent3Δent5Δ* cells (BKY13) transformed with plasmids containing Ent3p point mutants (Y60D = pJZ17, F62D = pCP11, E103W = pCP13, R154E = pJZ18) were spotted onto YEPD agar plates supplemented with 0.005% SDS, 0.5 M NaCl, 2 M sorbitol, 25 µg/mL or 50 µg/mL calcofluor (Cf). The plates were incubated at 30°C and pictures were taken after 2-3 days. The Y60D mutant had a strong growth defect even on YEPD plates. The other mutants could rescue the defect of the double mutant on SDS, NaCl and sorbitol but only partially on calcofluor plates.

4.1.3 The A-ALP transport is defective in *ent3Δent5Δ* double mutants

The A-ALP construct consists of of the cytosolic domain of DPAP A (dipeptidyl aminopeptidase A) fused with the transmembrane and luminal parts of the alkaline phosphatase (ALP). Because of the DPAP A trafficking signal the A-ALP recycles from the LE to the TGN where it its mainly localized. A defect or block in this transport results in a faster transport to the vacuole and therefore a faster maturation and degradation of the A-ALP. The vacuolar mature A-ALP (mA-ALP) can be separated from the pro-form (pA-ALP) in a SDS gel. WT (SNY18) and *ent3Δent5Δ* cells which lack the native ALP (*PHO8* gene) were transformed with

an A-ALP plasmid (pSN246) and cultured over night at 30°C. The cells were pulsed with radioactively labeled [³⁵S]-cys/met for 10 min 37°C. The pulse was stopped by adding non-radioactive cys/met and the chase was performed for 10 min, 60 min and 120 min at 37°C. The cells were lysed and an IP was done with rabbit anti-ALP antibody. The IP fractions were loaded on an 8% SDS gel and the detection of the bands was done by exposing a phosphorimager plate on the gel and detecting the radioactivity with a phosphorimager.

The experiment was done three times and in all three experiments a slightly reduced pA-ALP amount was detected in the *ent3Δent5Δ* mutant. As seen in the standard deviations the variations of the band intensities were relatively high. The defect is most significant in the 120 min values. There 46% (SD 25%) of the pulsed A-ALP amount remained in the WT cells and 23% (SD 8%) in the double mutant (fig. 4.22).

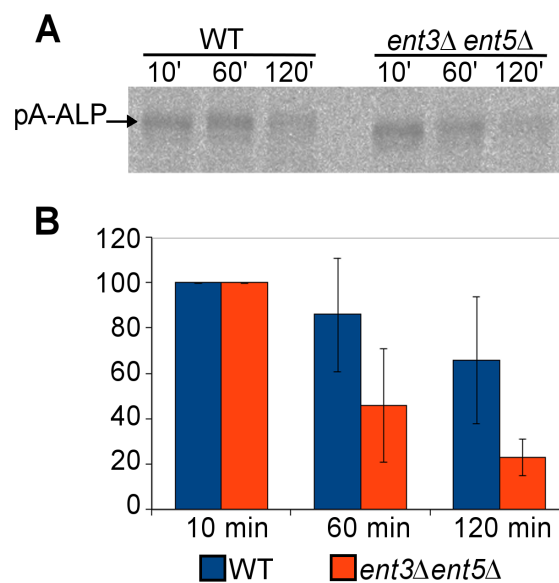


Fig. 4.22: **A-ALP is slightly mislocalized in *ent3Δent5Δ* cells.** **A:** WT (SNY18) and *ent3Δent5Δ* (CPY1) cells transformed with an A-ALP plasmid (pSN246) were pulsed for 10 min with [³⁵S]met/cys and chased for 10 min, 60 min and 120 min at 37°C. A-ALP was precipitated from the cell lysates with anti-ALP antibody and the radioactively labeled protein was detected on a SDS gel with a phosphorimager. **B:** The band intensities of pA-ALP from three independent experiments were quantified and the 10 min values set to 100%. After 60 min 86% (SD 25%) pA-ALP in the WT and 26% (26%) in the *ent3Δent5Δ* mutant were detected and after 120 min 46% (25%) in WT and 23% (8%) in the double mutant of A-ALP was left in the cells.

4.1.4 Recycling of GFP-Snc1p is blocked in *ent3Δent5Δ* cells

The CPY secretion defect was due to a partial block in the anterograde TGN to late endosome transport. To analyze the retrograde transport in Ent3p mutants the GFP-Snc1p construct was used. The transport of Snc1p is independent of the forward TGN to endosome transport since the protein travels from TGN directly to the plasma membrane and recycles then via the early endosomes back to the TGN. Is the recycling step blocked the GFP-Snc1p construct accumulates in internal structures whereas its native localization is mainly on the plasma membrane (Lewis *et al.*, 2000). Via this assay a defect in the retrograde transport for *ent3Δent5Δ* could be detected. In the double mutants the PM localization of GFP-Snc1p was almost completely lost (fig. 4.23). The single mutants showed under the microscope no significant difference in GFP-Snc1p localization.

To check whether the SNARE binding ability of Ent3p has an influence on the retrograde EE to TGN transport the GFP-Snc1p construct was co-transformed with the point mutants in *ent3Δent5Δ* cells (BKY13) and the localization of the GFP-constructs was analyzed.

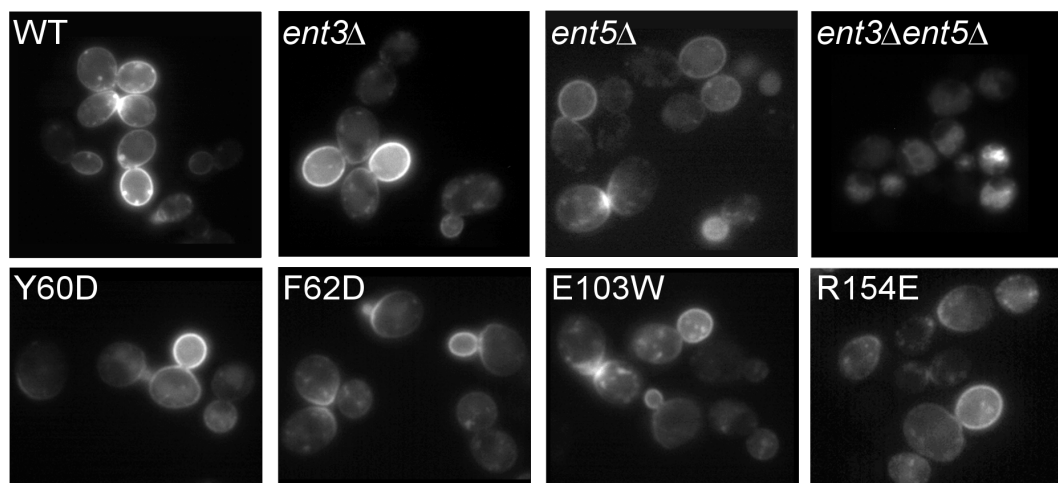


Fig. 4.23: **GFP-Snc1p localization was changed in *ent3Δent5Δ* cells.** WT (BY4742) *ent3Δ*, *ent5Δ* and *ent3Δent5Δ* cells were transformed with a GFP-Snc1p plasmid (pGS416; *CEN*, *URA3*). A clear shift to internal structures was visible for the double mutant. *ent3Δent5Δ* cells which were transformed with plasmids containing Ent3p point mutants (Y60D = pJZ17, F62D = pCP11, E103W = pCP13, R154E = pJZ18) were transformed with the GFP-Snc1p plasmid with *HIS* marker (pCP25; *CEN*, *HIS3*). The point mutants did not show significant changes in GFP-Snc1p localization.

For the localization of GFP-Snc1p no significant differences between the point mutants and the WT could be observed. To analyze the GFP-Snc1p localization in detail the cells with PM staining were counted and the values plotted in fig. 1.24. In the WT cell culture 83% of the cells had a plasma membrane staining (SD 5%) and in *ent3Δent5Δ* cells 4% (SD 3%). In the quantification also a small but significant defect was visible in the *ent3Δ* and *ent5Δ* single mutants (64%, SD 9% and 68%, SD 6%, respectively). Standard deviations were calculated from the data of three independent experiments with together at least 800 counted cells per cell line. The point mutants rescued the defect of the double mutant to a level comparable to the single mutants (F62D = 62%, SD 14%; E103W 53% SD 9%; R143E 59%, SD 11%; 3 independent experiments). Just the Y60D mutant had a lower rescuing ability (45% PM staining with SD 2%; two experiments) but there is not clear whether this defect depends on SNARE binding because this mutant had also a strong growth defect.

So indeed the SNARE binding of Ent3p seems not to be important for its function in the transport step from the early endosome to the TGN.

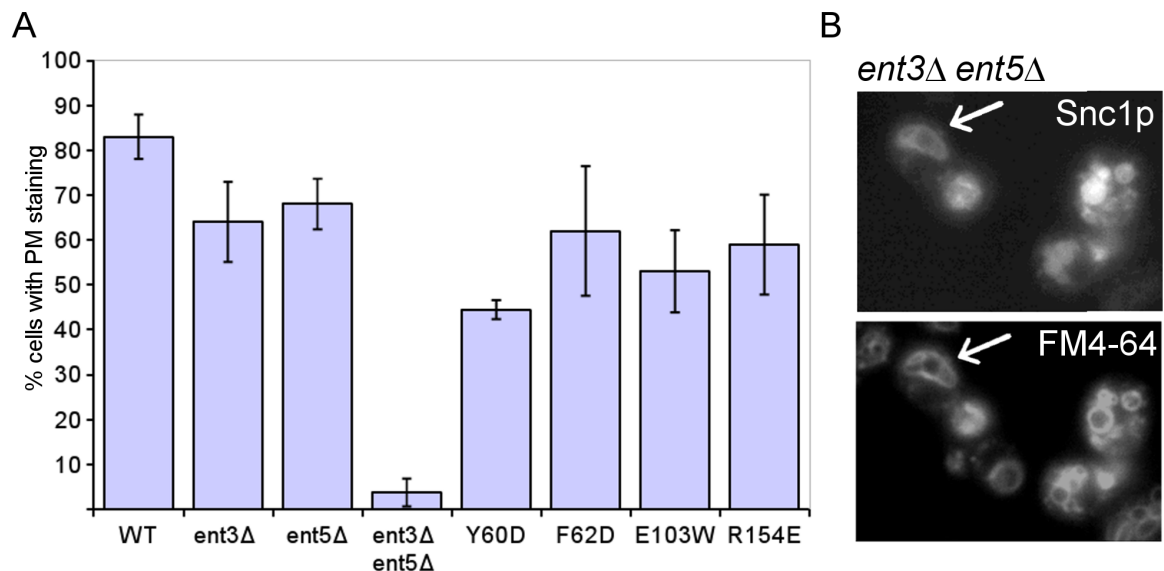


Fig. 4.24: Quantification of GFP-Snc1p transport and colocalization with FM4-64. A: Cells were prepared as described in fig. 4.23. The cells with a visible plasma membrane staining were counted as positive. WT: 83% (SD 5%), *ent3Δ*: 64% (SD 9%), *ent5Δ*: 68% (SD 6%) and the double mutant: 4% PM staining (SD 3%). **B:** FM4-64 staining of vacuolar membranes and colocalization with GFP-Snc1p in *ent3Δent5Δ* (BKY13) cells. The cells were incubated for 30 min with FM4-64, washed and viewed under a fluorescence microscope. There was a good colocalization of the FM4-64 and the GFP-Snc1p signals.

As it seems that the GFP-Snc1p is partially mislocalized to the vacuole in *ent3Δent5Δ* cells a co-localization of GFP-Snc1p with the fluorescent, lipophilic dye FM4-64 was performed. FM4-64 integrates into the plasma membrane, gets endocytosed and transported over the early endosomes (5 min after endocytosis) and late endosomes (after 15 min) to the vacuole (after 30 min). For vacuolar staining the cells were incubated 30 min with FM4-64 at 30°C, washed and viewed under the fluorescence microscope. The FM4-64 staining colocalized nicely with the GFP-Snc1p staining. That means that the Snc1p is missorted to vacuole and indicates that the block is in fact in the retrograde step between EE and TGN and not a block in the exocytosis from the TGN.

4.1.5 Yck2p is mislocalized in *ent3Δent5Δ* cells

To check the transport of another protein which functions at the plasma membrane and is recycled via endosomes, the localization of GFP-Yck2p was analyzed. The cell lines were transformed with a GFP-Yck2p plasmid (pPB2) and viewed under a fluorescence microscope. The *ent3Δent5Δ* mutant showed a clear staining of the vacuole membranes which was not visible in WT or *ent3Δ/ent5Δ* single mutants. Like in the GFP-Snc1p analysis the point mutations on Ent3p had no influence on the GFP-Yck2p transport. No mislocalization of GFP-Yck2p could be observed (fig. 4.25).

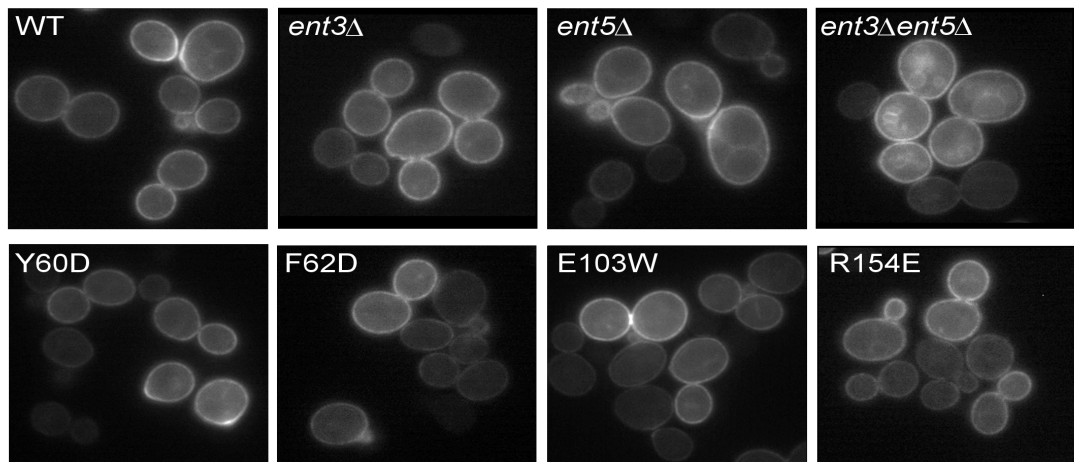


Fig. 4.25: **GFP-Yck2p transport in *ent3Δent5Δ* cells and Ent3p point mutants.** For GFP-Yck2p transport analysis WT (BY4742), *ent3Δ*, *ent5Δ* and *ent3Δent5Δ* (BKY13) cells were transformed with a GFP-Yck2p plasmid (pPB2; *CEN*, *URA3*). The double mutant showed a partial mislocalization to vacuolar structures. *ent3Δent5Δ* cells which were transformed with *CEN* plasmids containing Ent3p point mutants (Y60D = pJZ17, F62D = pCP11, E103W = pCP13, R154E = pJZ18) were cotransformed with a GFP-Yck2p plasmid with *HIS3* marker (pCP29). For the point mutants no significant changes in GFP-Yck2p localization could be detected.

4.2 Functions of the Ent3p domains

Ent3p contains besides its ENTH domain an unstructured C-terminus which provides a contact surface for other vesicle coat proteins like Gga2p or clathrin. The ENTH domain interacts with the endosomal SNAREs, binds via the first 28 amino acids to PI3,5P₂ and supposedly contributes to membrane curvature during vesicle budding. If the Ent3p C-terminus has some other functions than just binding cargo molecules and proteins of the clathrin coat is not known yet.

To characterize the role of the Ent3p domains in vesicle budding and cargo sorting the two domains of Ent3p were cloned separately into *CEN* expression vectors under *TPI* promoter and were transformed into a BY *ent3Δent5Δ* strain (BKY13). Additionally a plasmid was constructed containing both Ent3p domains but lacking the first PI binding 28 amino acids.

4.2.1 Functions of the Ent3p domains in the retrograde EE to TGN transport

To check if the separated Ent3p domains can rescue the defect of the double mutant in GFP-Snc1p transport the *ent3Δent5Δ* cells (BKY13) were co-transformed with the GFP-Snc1p and the Ent3p domain constructs. The cells were cultured over night till an early logarithmic stage, resuspended in PBS and viewed under a fluorescence microscope (fig. 4.26.A). The ENTH domain alone could not rescue the localization defect completely and most of the cells showed an intracellular staining of the GFP construct (14% cells with PM staining (SD 3%) in contrast to WT: 83% (SD 5%), *ent3Δ*: 64% (SD 9%) and *ent5Δ*: 68% (SD 6%)). The double mutant had 4% PM staining (SD 3%, fig. 4.26.C and chapter 4.1.4).

The C-terminus alone and the -PI mutant could restore the function of the recycling steps to a level comparable to the single mutants (-PI: 52% (SD 3%), C-term.: 50% (SD 14%)).

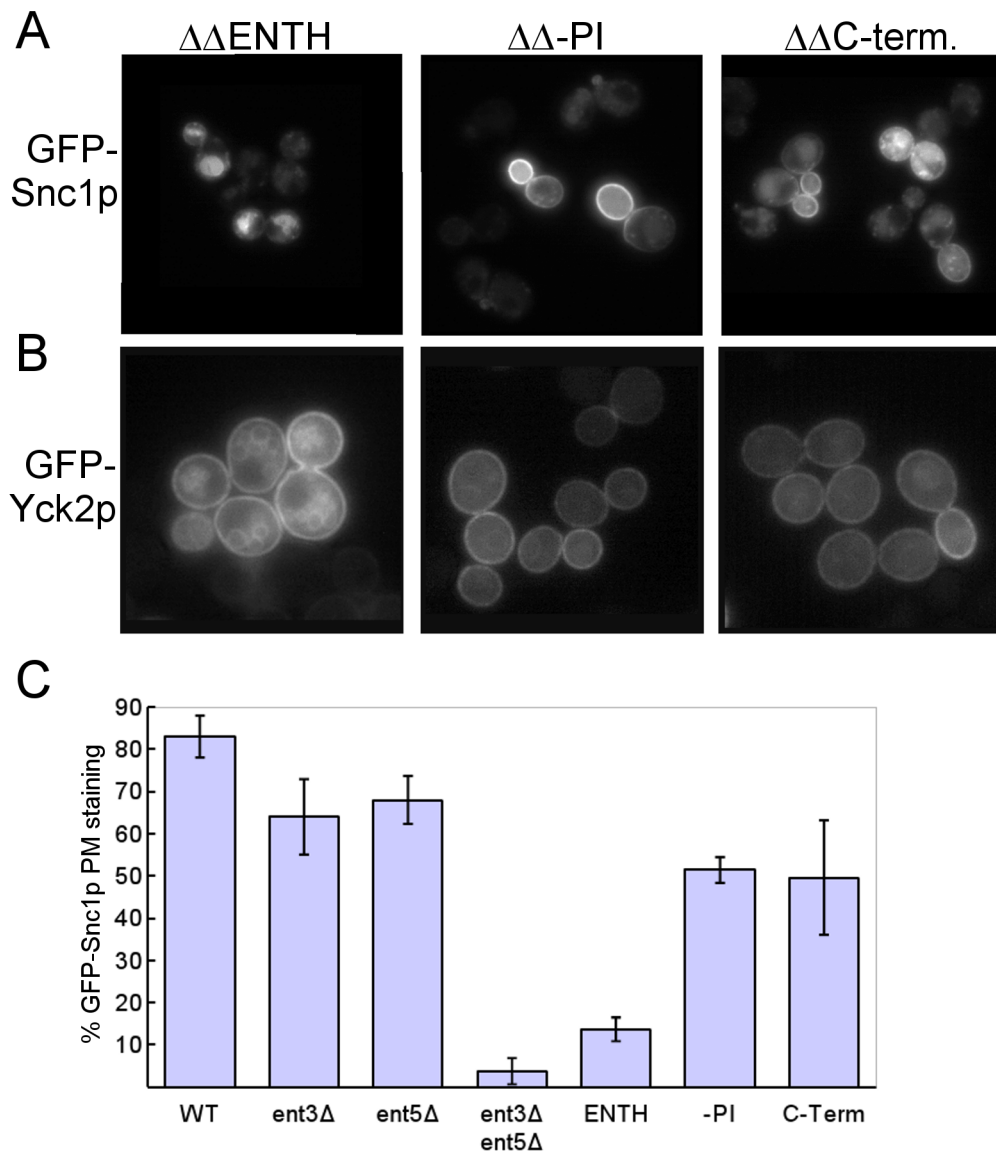


Fig. 4.26: **The C-terminus of Ent3p is necessary for a correct GFP-Snc1p and GFP-Yck2p localization.** *ent3 Δ ent5 Δ* cells were transformed with *CEN* plasmids under *TPI* promoter containing the Ent3p ENTH domain (pCP7; $\Delta\Delta$ ENTH), the C-terminus (pCP9; $\Delta\Delta$ C-term.) and Entp3 without PI binding domain (pCP8; $\Delta\Delta$ -PI). Additionally in these cell lines a GFP-Snc1p plasmid (pCP25 (*CEN*, *HIS3*)) or a GFP-Yck2p plasmid (pCP29 (*CEN*, *HIS3*)) was transformed. The cells were grown into an early logarithmic stage (GFP-Snc1p) or into a logarithmic stage (GFP-Yck2p), resuspended in PBS and directly viewed under a fluorescence microscope. In the $\Delta\Delta$ ENTH cells the localization of GFP-Snc1p (**A**) and GFP-Yck2p (**B**) was shifted to internal structures. The two other mutants had a WT distribution of the GFP-tagged proteins (see also fig. 4.23 and 4.25). **C**: Quantification of GFP-Snc1p plasma membrane staining. Cells with visible PM staining were counted as positive. The standard deviations were obtained from 3-5 independent experiments. For each strain at least 800 cells were counted.

Yck2p trafficking

In the GFP-Yck2p trafficking assay the -PI and C-term mutants which were in an *ent3Δent5Δ* background could rescue the defect of the *ent3Δent5Δ* double mutant (fig. 4.26.B). Only a very weak vacuolar staining was observed. The ENTH domain mutant was not able to rescue the defect of the double mutant. Here also the GFP-Snc1p was partially mislocalized to the vacuolar membranes (fig. 4.26.A). Additionally a similar fragmented vacuole phenotype as in the *ent3Δent5Δ* strain could be observed for the ENTH mutant but not for the -PI and C-term mutants. An additional FM4-64 staining for the domain mutants should be done to prove the vacuole phenotype defect.

4.2.2 For CPY transport the Ent3p C-terminus and the ENTH domain were necessary

To check if the Ent3p domains can rescue the CPY transport defect of the *ent3Δent5Δ* cells a CPY overlay assay was performed. The cells in logarithmic stage were spotted onto YEPD agar plates and grown for 24 h at 30°C. Then a nitrocellulose membrane was applied to the yeast spots and in a further 24 h incubation step at 30°C the secreted CPY was bound by the membrane. The detection of the CPY was performed by immunoblotting with anti-CPY antibody which detects all CPY forms. As a WT control the *ent3Δ* cells were transformed with full length *ENT3* on a 2μ plasmid (pSC4).

WT and *ent5Δ* cells had no CPY secretion defect. A defect could be detected as expected for *ent3Δ* and in a higher amount for *ent3Δent5Δ*. Both domains of Ent3p separately could not rescue the defect of the double mutant (fig. 4.27). The strength of defect of the C-term. and ENTH domain was comparable. In some experiments the ENTH domain alone (pCP7) in *ent3Δent5Δ* showed a slight growth defect.

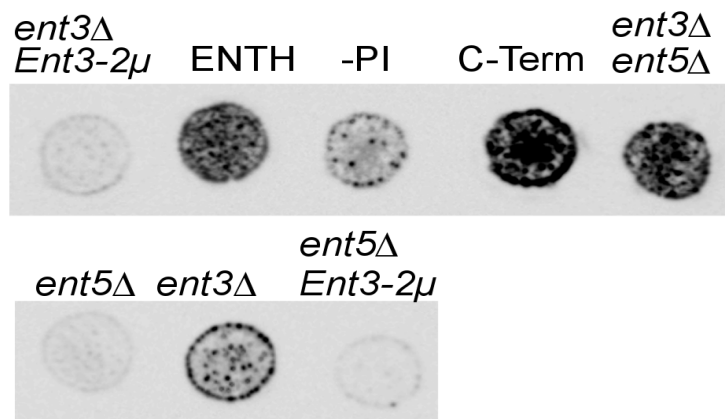


Fig. 4.27: **The Ent3p ENTH domain and the C-terminus were important for CPY sorting.** For the CPY overlay assay *ent3Δent5Δ* cells were transformed with *CEN* plasmids under *TPI* promotor containing either the Ent3p ENTH domain (pCP7), Ent3p without PI binding domain (-PI, pCP8) or the Ent3p C-terminus (pCP9). For positive control *ent3Δ* and *ent5Δ* cells were transformed with WT *ENT3* on 2μ plasmids (pSC4). The *ent3Δent5Δ* strain without plasmid was used as positive control. The cells were grown 24 h without and the 24 h covered with nitrocellulose membrane on a YEPD agar plate. The membrane was treated with mouse-anti CPY and goat-anti-mouse antibodies. The ENTH and C-term constructs could not rescue the defect of the double mutant. The defect of the -PI mutant was comparable to the *ent3Δ* mutant.

To be sure that the lower CPY secretion of the -PI mutant was not due to a lower expression of the mutant the expression was checked by preparing Thorner protein extracts which were loaded on a SDS gel. The Ent3p -PI and ENTH domain mutants could be detected with an anti-Ent3p antibody (YWOPt). The amount of Ent3p -PI in the protein extract was even higher than in the ENTH mutant (fig. 4.28). It showed a higher expression than the native WT Ent3p which was expected because the mutants were expressed under a strong *TPI* promotor.

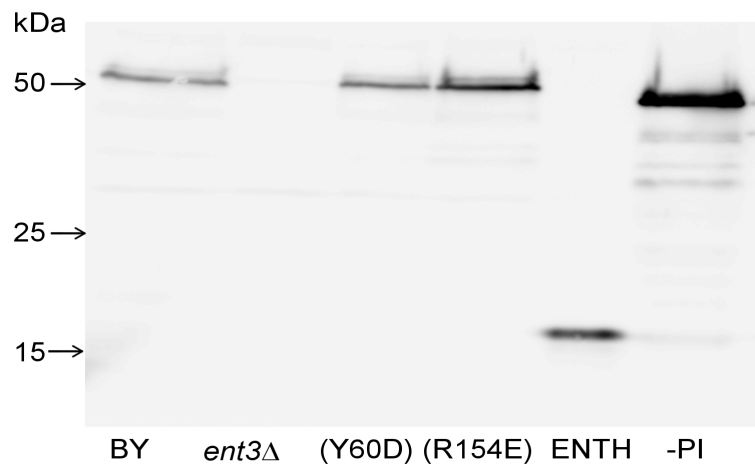


Fig. 4.28: **Expression test of the Ent3p domain mutants.** Thorner extracts were prepared from over night yeast cell culture and same amounts were loaded on a SDS polyacrylamide gel. The proteins were transferred onto a nitrocellulose membrane which was then treated with rabbit anti-Ent3p and goat anti-rabbit-HRP antibodies. The BY WT strain was used as positive control, the BY *ent3Δ* strain as negative control. The ENTH domain (BKY13 pCP7) was detected at about 17 kDa and the -PI mutant (BKY13 pCP8) at about 48 kDa. Also on this blot the expression of the Ent3p point mutants (see chapter 4.1.2.6) was tested. Y60D = BKY13 pJZ17, R154E = BKY13 pJZ18.

Membrane binding of Ent3p constructs

The -PI construct was able to rescue the CPY defect to a level comparable to the *ent3Δ* strain. The deleted amino acids in this construct bind to PI(3,5)P₂ and therefore contribute to membrane binding. To connect the functionality of Ent3p to its membrane binding capacity a subcellular fractionation by differential centrifugation was performed where the amount of membrane bound Ent3p was determined. After an initial centrifugation step at 500 g to remove the cell debris a part of the lysate was stored as homogenate fraction (H) and the rest was sequentially centrifuged at 13.000 g and 200.000 g. The resulting pellet fractions were named P13 and P200 and the supernatant after the 200.000 g centrifugation S200. The protein samples were loaded on SDS gels and transferred to a nitrocellulose membrane. To detect the Ent3p C-terminus a 3xHA tag, for which commercial antibodies (Covance HA.11 clone 16B12) were available, was fused to the construct (pLS1).

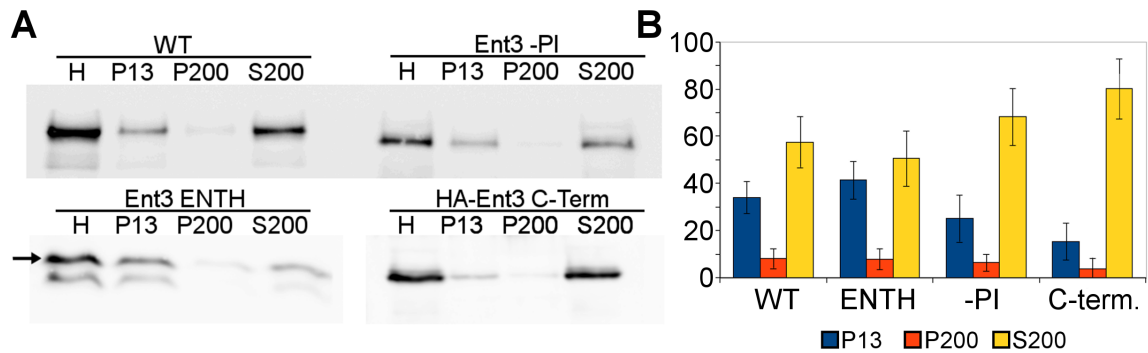


Fig. 4.29: Membrane binding of Ent3p domains. **A:** Yeast cell extracts were successively centrifuged at 13.000 *g* and 200.000 *g* and pellet fractions (P13 and P200) as well as the homogenate fraction and the 200.000 *g* supernatant (S200) were loaded on a SDS gel and immunoblotted with anti-Ent3p or anti-HA (C-term.) antibodies. **B:** The band intensities were quantified and the percentage of fractions determined on the basis of the sum of P13, P200 and S200 intensities. The standard deviation (SD) was obtained from four or three (C-term.) independent experiments. In WT (BY *ent3Δ* pSC4) cells 42% (SD 11%) and in cells containing the ENTH domain 49% (*ent3Δent5Δ* pCP7, SD 12%) of Ent3p were membrane bound. The amount of Ent3p in membrane fractions was reduced in cells with the -PI construct to 32% (SD 12%, pCP8) and 20% (SD 13%) in the cells with the HA-tagged C-terminus (pLS1).

In WT (*ent3Δ* pSC4) cells 42% of Ent3p was membrane bound (SD 13%). This amount was reduced in the -PI mutant to 32% (SD 12%) and the construct lacking the complete ENTH domain to 20% (SD 13%; fig. 4.29). The ENTH domain without the C-terminus but containing the PI-binding domain bound to 49% (SD 12%) to the P13 and P200 membranes. The standard deviations were obtained from four or three (C-term.) independent experiments. The fraction of Ent3p on P200 membranes which contains parts of the Golgi apparatus and vesicles was not significantly changed in all four samples. The differences were observed in the ratio between the P13 fraction which contains ER, vacuole and Golgi membranes and the fraction of the soluble proteins S200.

Especially the Ent3p C-terminus showed a reduced ability of membrane binding. An enhanced membrane binding of the ENTH domain as observed in the *Dictyostelium discoideum* Epsin (Brady *et al.*, 2008) was not observed. The difference of 7% between WT and ENTH domain was within the standard deviation. From the membrane assay the result of the rescuing defect of the -PI mutant maybe correlated to the slight loss of membrane binding ability.

4.2.3 Localization of the Ent3p domains via immunofluorescence microscopy

Because the membrane association of Ent3p is very transient and dynamic it is mainly dispersed in the cells. The membrane association was not significantly changed for the ENTH domain in the differential centrifugation approach. To further prove that the localization of the ENTH domain and the -PI mutant were not altered the yeast strains were analyzed via immunofluorescence microscopy. As a control the *ent3Δent5Δ* mutant was also treated with anti-Ent3p antibody.

Even with preabsorbtion of the Ent3p antibody a slight dot-like background staining of the *ent3Δent5Δ* cells was visible (fig. 4.30). The staining of the WT Ent3p was much stronger so that the staining could be assumed to be specific. No significant change in the localization of the Ent3p mutants could be detected. The ENTH domain had a more dot-like and less dispersed staining but this result was difficult to reproduce. The staining of the ENTH mutant was slightly weaker compared with the WT and the -PI strains. The expression rate of the ENTH mutants was not reduced in comparison with the WT (fig. 4.28).

Additionally an immunofluorescence microscopy with an HA-tagged Ent3p C-terminus was performed but due to very high unspecific reactions of the HA antibody the staining could not be evaluated.

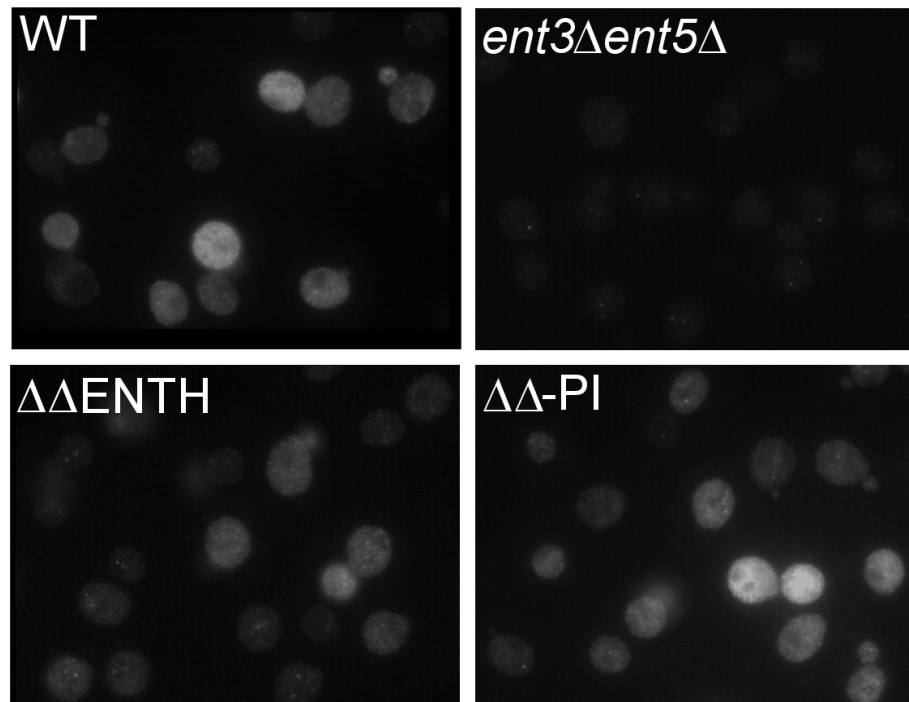


Fig. 4.30: **Localization of the ENTH domain and Ent3p -PI via immunofluorescence microscopy.** WT (BY4742), *ent3Δent5Δ* (BKY13) and *ent3Δent5Δ* cells with ENTH domain (BKY13 pCP7) or the Ent3p without PI binding domain (BKY13 pCP8) were fixed and treated with preabsorbed anti-Ent3p antibody. The cells were viewed under a fluorescence microscope. Ent3p is mainly dispersed in the WT cells. In the *ENT3* depleted double mutant some punctuated background staining was visible. The Ent3p domain mutants showed no significant difference in the localization of Ent3p.

4.2.4 Function of Ent3p domains in cell wall assembly and budding and cell separation

In earlier studies the *ent3Δent5Δ* double mutants showed defects in the cell wall assembly, budding polarity and cell separation (Zimmermann, 2006 and Chidambaram, 2005). To find out which of the Ent3p domains were necessary for maintaining the function in these processes again the domain constructs transformed in *ent3Δent5Δ* cells were used and compared with WT cells and the *ent3Δ/ent5Δ* single and double mutants.

4.2.4.1 The Ent3p domain mutants could not rescue the defect of the double mutant in a sedimentation assay

To check whether the Ent3p domains can complement the aggregated phenotype of *ent3Δent5Δ* cells a sedimentation assay was performed. The wild type (BY4742) cells had a sedimentation half-life time ($t_{1/2}$) of 166 min (one experiment). The *ent3Δ* cells showed a sedimentation behavior comparable to the WT ($t_{1/2}$ =160 min, SD 9 min in two independent experiments (n); fig. 4.31). The Ent3p domain mutants could not rescue the defect of the double mutant (BKY13, $t_{1/2}$ =122 min, SD 15 min, n=2).

The ENTH domain mutant (BKY13 pCP7) had a $t_{1/2}$ of 117 min (SD 10 min, n=2), the C-term (BKY13 pCP9) of 126 min and the -PI mutant 126 min (pCP8, one experiment).

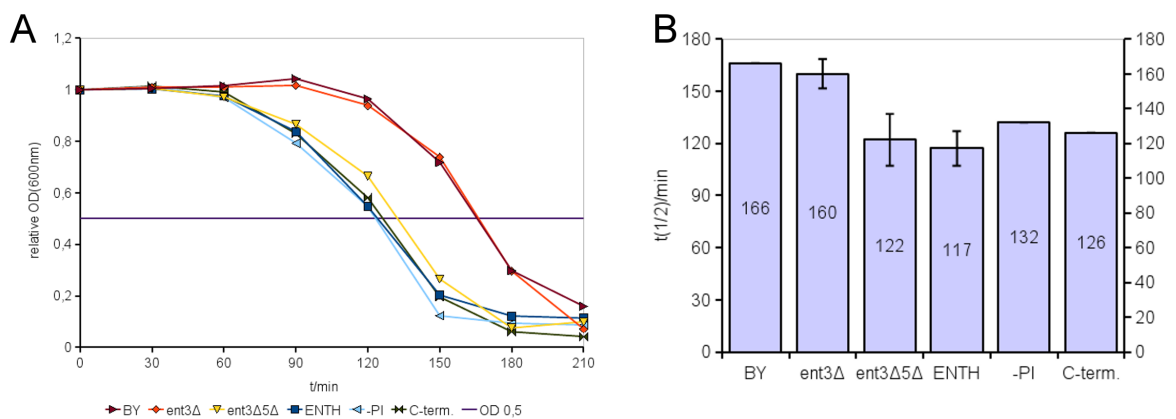


Fig. 4.31: Sedimentation assay Ent3p domains. **A:** BY WT, *ent3Δ*, *ent3Δent5Δ* (BKY13) and *ent3Δent5Δ* with Ent3p ENTH domain (BKY13 pCP7), C-terminus (BKY13 pCP8) or Ent3p -PI (BKY13 pCP9) were cultured into a logarithmic stage and 1 OD cell culture was resuspended in 1 mL H₂O and transferred into a cuvette. The OD_{600nm} was measured every 30 min. The start OD₆₀₀ was set as 1.0 and the relative ODs were calculated and plotted against the time. The half-value time was determined from the relative OD at 0.5 (purple line). **B:** The half-value times ($t_{1/2}$) were displayed as bars and the values in minutes were shown in the center of the bars. For *ent3Δ*, *ent3Δent5Δ* and the ENTH domain 2 independent experiments were performed and the SD is depicted as error bars in the diagram. For the other strains one experiment was done. All three mutants were not able to complement the defect completely. The ENTH mutant had an even shorter half-value time than the double mutant.

4.2.4.2 Budding patterns and cell separation

In earlier studies it was observed that *ent3Δent5Δ* cells had defects in maintaining the cell polarity and in cell separation during budding. The *ent3Δent5Δ* cells transformed with the Ent3p domains were stained with calcofluor white and analyzed under the fluorescence microscope. Pictures were made from three slices of the same microscope field and for analysis of the budding pattern haploid cells with two or more bud scars were counted. Cells with an axial budding pattern were classified as WT and cells with bipolar or random budding pattern as defect.

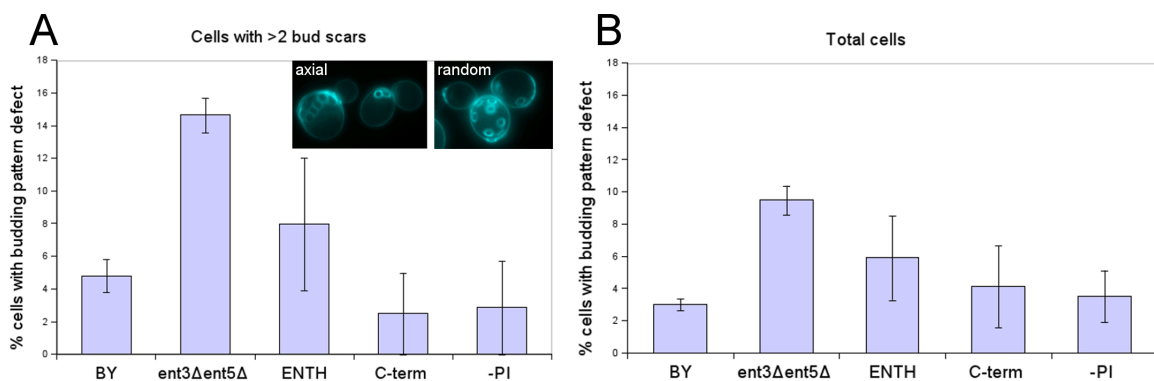


Fig. 4.32: Analysis of haploid budding patterns in Ent3 domain mutants. Yeast cells in logarithmic stage were fixed with formaldehyde and stained 5 min with calcofluor white. The cells were examined under the fluorescence microscope and three layers of one microscope field were photographed and evaluated. Cells with 2 bud scars and more than 2 bud scars (**A**) were counted separately as defect if they had a non-axial budding pattern. For the total cells data (**B**) these values were summed. Additionally microscope pictures of example cells for axial (*ent5Δ* cells) and random (*ent3Δent5Δ* cells) budding pattern were shown in A. The Standard error of mean (SEM) was determined from three (BY, *ent3Δent5Δ* and ENTH) or two (C-term. and PI) independent experiments. *ent3Δent5Δ* cells had budding pattern defects which were rescued by the -PI and C-term. constructs. The ENTH construct had a lower rescuing ability. Used strains and plasmids: BY (WT) = BY4742, *ent3Δent5Δ* = BKY13, ENTH = BKY13 pCP7, C-term. = BKY13 pCP9, -PI = BKY13 pCP9).

For cells with more than two bud scars (fig. 4.32.A) 4.8% (standard error of mean (SEM) 1.0%) of WT cells and 14.6% (SEM 1.1%) of *ent3Δent5Δ* cells showed an abnormal budding pattern (three independent experiments, about 100 cells counted). Since the defect of the double mutant was less clear in cells with just two bud scars the total amount of defect cells was smaller (3.0 for BY WT

(SEM 0.4%), 9.5% for *ent3Δent5Δ* (SEM 0.9%); Fig. 4.32.B). The evaluation of the Ent3p domains was difficult since there was a high variability in the percentages of defect cells. The values and error bars of the Ent3p domains implicate that there is a rescuing effect of all three constructs. However, from the tendency of the experiments the ENTH domain alone showed the least rescuing ability (8.0% defect cells with SEM 4.1% for >2 bud scars and 5.9% defect with SEM 2.6% for total cells; three independent experiments analyzed). The budding pattern phenotype of the C-term and the mutant without -PI domain was indistinguishable from the WT strain. (C-Term: >2 bs 2.5% (SEM 2.5%) and total 4.1% (SEM 2.6%); -PI: >2 bs 2.9% (SEM 2.9%) and total 3.5% (SEM 1.6%); two independent experiments).

A similar but less clear picture was obtained from the analysis of the cell separation and the occurrence of calcofluor (cf) accumulations. Cells with more than one bud were counted as defect or multibudded (fig.4.33.A). The standard error of mean (SEM) was determined from five experiments for the *ent3Δent5Δ* strain, four for the BY WT, three for the ENTH domain and two for the C-term and the -PI mutants.

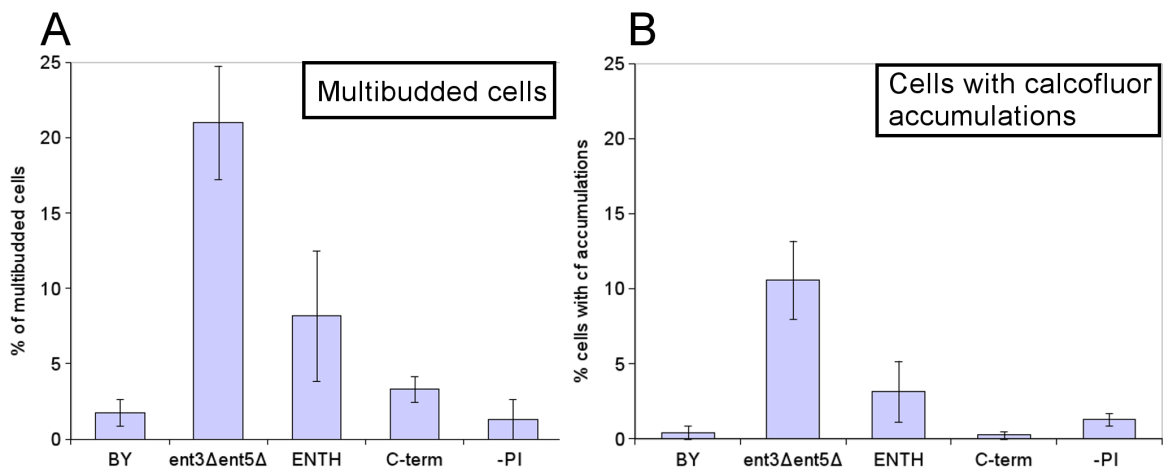


Fig. 4.33: Multibudded cells and cells with calcofluor accumulations. Cells were treated as described in fig. 4.32 (same pictures were evaluated) and cells with more than one bud (multibudded; **A**) or calcofluor depositions/accumulations (**B**) were counted as defect. In both cases the *ent3Δent5Δ* mutant displayed defects and the ENTH construct could not rescue the defect completely. For the multibudded analysis the SEM was determined from 5 (*ent3Δent5Δ*), 4 (BY WT), 3 (ENTH) or 2 (-PI and C-term.) experiments. For the calcofluor deposition analysis the SEM was determined from 3 (WT, *ent3Δent5Δ*, ENTH) or two (-PI, C-term.) experiments.

In the analysis of the cell separation and chitin distribution (which is visualized by calcofluor white staining) again the ENTH domain alone showed not a complete rescuing ability (8.2% multibudded (SEM 4.3%) and 3.2% with cf accumulations (SEM 2.0%). Although there was a high variability in the experiments the tendencies within the experiments were constant.

However for all three experiments both the C-terminus and the ENTH domain showed rescuing ability. The C-terminus seems to be more important than the ENTH domain. The haploid *ent3Δent5Δ* cells as well as the Ent3p domain expressing cells did not show significant amounts of misshaped cells although it was reported before (Chidambaram, 2005, see also the experiments with pHO plasmid below). All evaluated data is summarized in table 3.

Tab. 3: **Summary of calcofluor staining experiments.** bs = bud scars, SEM = standard error of mean, exp = number of independent experiments, CF = calcofluor

	Buding pattern >2bs			Buding pattern total		
	% defect	SEM	Cells/(exp)	% defect	SEM	Cells/(exp)
BY	4.8	1.0	137 (3)	3.0	0.4	234 (3)
<i>ent3Δent5Δ</i>	14.6	1.1	75 (3)	9.5	0.9	181 (3)
ENTH	8.0	4.1	63 (3)	5.9	2.6	130 (3)
C-term	2.5	2.5	46 (2)	4.1	2.6	109 (2)
-PI	2.9	2.9	66 (2)	3.5	1.6	130 (2)

	Multibudded			CF accumulations		
	% defect	SEM	Cells/(exp)	% defect	SEM	Cells/(exp)
BY	1.8	0.9	389 (4)	0.4	0.4	586 (3)
<i>ent3Δent5Δ</i>	21.0	3.8	452 (5)	10.6	2.6	435 (3)
ENTH	8.2	4.3	260 (3)	3.2	2.0	345 (3)
C-term	3.3	0.8	153 (2)	0.3	0.3	338 (2)
-PI	1.3	1.3	198 (2)	1.3	0.4	234 (2)

Calcofluor staining of diploid cells with and without pHO plasmid

The budding pattern and cell separation defect was much more severe in diploid *ent3Δent5Δ* cells (Chidambaram, 2005 and Zimmermann, 2006). So I wanted to check if the rescuing abilities of the mutants were more pronounced in the diploid cells. I used a BY *ent3Δent5Δ* diploid strain which was constructed by mating type switch of BKY13 (resulting in SCY34) and mating (BKY13 x SCY34 = SCY35). The mating type switch was performed by transforming a pHO-plasmid containing an endonuclease which cuts in the primary mating type (MAT) locus and activates the alternative MAT locus with the opposite mating type. The selection marker on the pHO plasmid was the same as for the Ent3p mutant construct so the pHO plasmid was removed by replica plating. For an initial test the *ent3Δent5Δ* cells with and without pHO plasmid were directly stained 5 min with calcofluor white, washed three times with PBS and viewed under a fluorescence microscope.

From this experiment it seems that the pHO plasmid itself has an influence on the budding and cell separation behavior (fig. 4.34). The cells with plasmid were enlarged, misshaped and have completely lost their bipolar budding pattern. The diploid cells where the plasmid was removed showed a haploid WT like axial budding pattern. So since it is not sure which effects came from the pHO plasmid new *ent3Δent5Δ* diploid cells without mating type switch should be constructed. The homozygous *ent3Δ* and *ent5Δ* single deletion diploid cells showed no significant differences in their budding and cell separation behavior.

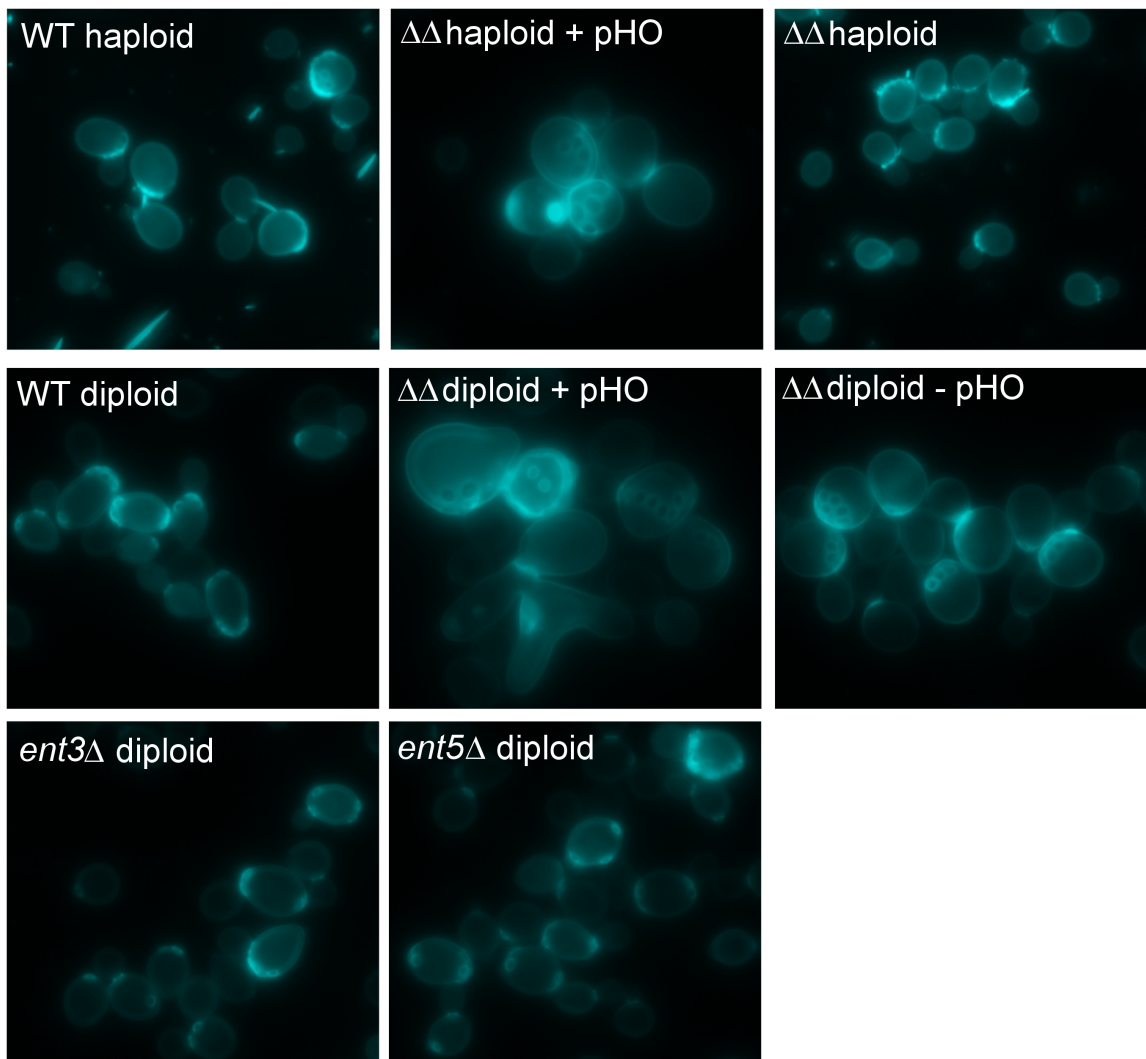


Fig. 4.34: **Calcofluor staining of *ent3Δent5Δ* diploid and haploid strains with and without pHO plasmid.** Cells were grown over night in YEPD, stained for 5 min at RT with calcofluor white, washed three times with PBS and viewed under a fluorescence microscope. Pictures from three slices of one microscopy field were taken and merged for the displayed figure. The pHO plasmid induces morphological defects. $\Delta\Delta$ = *ent3Δent5Δ*. The pictures were scaled equally. Used strains: WT = *ent3Δ* pSC5 (*ENT3* under endogenous promotor), $\Delta\Delta$ haploid+pHO = SCY34, $\Delta\Delta$ haploid = BKY13, WT diploid = pJZ9, $\Delta\Delta$ diploid + pHO = SCY35, $\Delta\Delta$ diploid – pHO = SCY36, *ent3Δ* and *ent5Δ* diploids were obtained from Euroscarf.

4.2.4.3 Cell wall assembly

The integrity of cell wall assembly can be analyzed by growing the yeast cells on agar plates containing cell wall disturbing agents. The *ent3Δent5Δ* mutant showed a sensitivity to SDS, NaCl, sorbitol and calcofluor. If the Ent3p domains alone were sufficient for maintaining the cell wall integrity the respective domain mutant should complement this defects. Plates with 0.01% SDS, 0.5 M NaCl, 2 M sorbitol and 25 μg/mL calcofluor white were used.

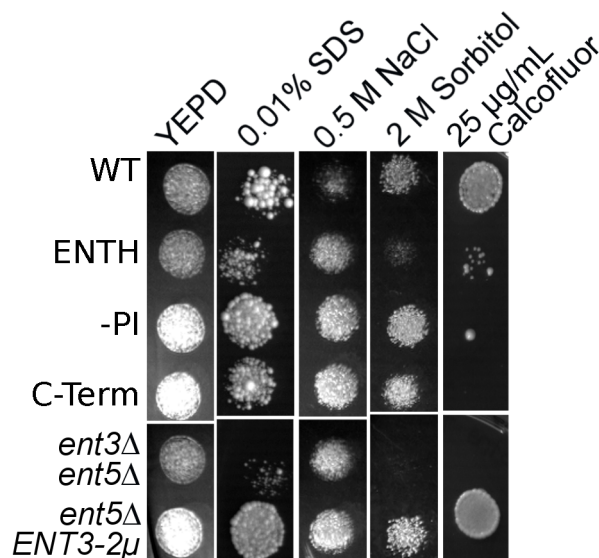


Fig. 4.35: **Complementation of *ent3Δent5Δ* cell wall defects by the Ent3p domains.** Growth test on agar plates containing cell wall perturbing agents. WT (BY4742) and *ent5Δ ENT3-2μ* (pSC4), as well as *ent3Δent5Δ* (BKY13) cells and *ent3Δent5Δ* cells containing the ENTH domain (pCP7), the C-terminus (pCP9) and Ent3p without PI binding domain (pCP8) were spotted onto YEPD agar plates containing 0.01% SDS, 0.5 M NaCl, 2 M Sorbitol and 25 μg/mL calcofluor. The plates were incubated at 30°C and pictures were taken after 1-6 days. The C-term. and -PI constructs complemented the defects of the *ent3Δent5Δ* double mutant except for the growth on calcofluor plates. The ENTH domain showed a lower ability for complementation on SDS, NaCl and SDS but not on Calcofluor plates.

The lowest rescuing ability on SDS, NaCl and sorbitol plates had the ENTH construct (fig. 4.35). The experiment was repeated several times and the growth of the yeast strains was very variable. However, all of the constructs were able to rescue the *ent3Δent5Δ* defects to some extent. But the slightly less pronounced ability for complementing of the ENTH domain indicated some functions for the C-terminus but possibly not for the ENTH domain in the cell wall assembly and

maintaining processes. In contrast at the calcofluor plates the ENTH domain showed the highest rescuing ability although all three mutants complemented the defect of the double mutant very weakly.

4.2.5 Interactions of the Ent3p ENTH domain with its own C-terminus and the Ent5 ANTH domain

Another point which may be important for the regulation of Ent3p is if it undergoes auto interaction. To check this the interaction of the Ent3p C-terminus with the ENTH domain and additionally with Ent5p was tested in a yeast two-hybrid assay. Since the Ent3p C-terminus in the pLexN vector (combined with empty pVP vector) induced too much background expression of the *HIS3* reporter gene, the C-terminus was subcloned into the pVP vector (pCP26) and the Ent3p ENTH domain into the pLexN vector (pCP27). For the ENTH/ANTH interaction the ENTH domain in pLexN and full length Ent5p (pFW5) or its ANTH domain (pBK160) both in pVP16 were used.

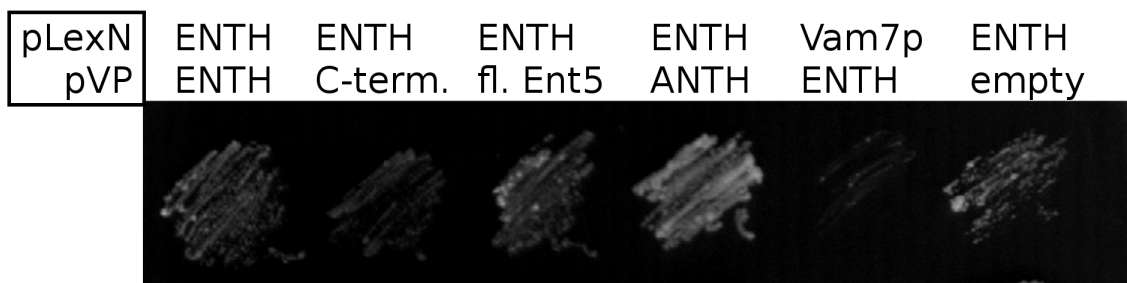


Fig. 4.36: **Interaction of the Ent3p ENTH domain with itself and the Ent5p ANTH domain.** The ENTH and ANTH constructs were cloned into pVP16-3 and pLexN and transformed into L40 cells. The strains were streaked on THULL plates containing 15 mM 3-AT and the picture was taken after three days incubation at 30°C. Used plasmids: ENTH pLexN=pCP27, ENTH in pVP=pKW3, Ent3p C-term. In pVP = pCP26, full length (fl.) Ent5p in pVP=pFW5, Ent5p ANTH in pVP= pBK160, Vam7p N-term. in pLexN (as further negative control)=pJZ6, empty = pVP16-3. The Ent3p ENTH domain interacted with the Ent5p ANTH domain and weaker with full length Ent5p but not with its own C-terminus.

The combinations with the Ent3p C-term in the pVP vector gave also a high background expression, which was not reduced until addition of 15 mM 3-AT. With addition of 20 mM 3-AT the background expression was lost but the signal for the positive control, too. In three independent experiments there was clearly no

interaction between the ENTH domain of Ent3p and its own C-terminus. Surprisingly a reproducible interaction of Ent3p ENTH with the Ent5p ANTH domain and weaker with the full length Ent5p was detected.

4.2.6 Ent3p phosphorylation assay by isoelectric focusing

A lot of proteins in the cell are regulated by phosphorylation. In a large scale phosphorylation screen Ent3p was identified as substrate of the protein kinases Hrr25p and Mek1p (Ptacek *et al.*, 2005). In another large scale screen five potential phosphorylation sites in the C-terminus and none in the ENTH domain of Ent3p were obtained (S203, S294, S320, S365, S407). The modification of serine 203 was received in two independent screens (Li *et al.*, 2007, Albuquerque *et al.*, 2008). Additionally the neighboring amino acid D202 is important for some Ent3p functions (Friant *et al.*, 2003, *ent3-1*). To prove the phosphorylation of Ent3p in an independent specific assay an isoelectric focusing (IEF) was performed. Every phosphorylation introduces three additional charges into the protein. This difference in charge has an influence on the isoelectric point of the protein and can be visualized by the IEF experiment. The dephosphorylation of Ent3p during the cell lysis was inhibited by adding the phosphatase inhibitors NaVO₃ and NaF. For control the cell extracts were also incubated for 5 or 30 Min with calf intestinal phosphatase (CIP). If there is a phosphorylation of Ent3p the IEF dot should shift to a more basic region in the CIP treated samples.

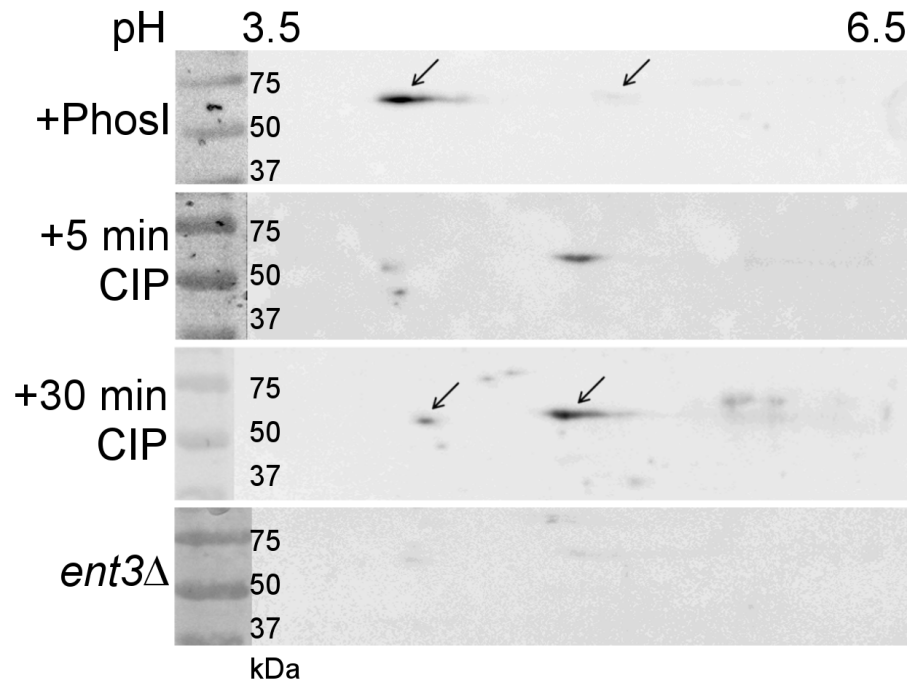


Fig. 4.37: **Ent3p is phosphorylated in IEF.** Cell lysates of WT (BY4742) cells were treated with phosphatase inhibitors (PhosI) or with calf intestinal phosphatase (CIP) for 5 or 30 min. 10 μ g protein were loaded on an IEF gel and the immunoblotting was performed with anti-Ent3p antibody (1:500). The experiment was repeated several times and the result was reproducible in three experiments. Phosphorylated (left side) and unphosphorylated (right side) Ent3p dots are marked with an arrow.

In the cell lysates treated with phosphatase inhibitors (PhosI) Ent3p occurred at a more acidic area of the dot plot. This localization was shifted to a more basic area when the proteins were treated with CIP. From this result a phosphorylation of Ent3p is very likely although the experiment was hard to reproduce. A final prove of the phosphorylation e.g. via mutagenesis of potential phosphorylation sites should be done.

4.3 Tvp23p has a role in retrograde transport from EE to TGN and interacts genetically with VTI1

The SNARE Vti1p is involved in several transport steps. The deletion of the *VTI1* gene is lethal. So for the analysis of Vti1p functions temperature sensitive mutants were generated. In suppressor screens for *vti1-2* a library of over-expressed yeast proteins was screened by Dilcher (2002) and Tvp23p was identified as rescuing protein of the growth defect of *vti1-2* (Stein, 2007). Tvp23 is a protein of unknown function. It is supposed that it may have a function in vesicle transport since it interacts with Yip4p and Yip5p (Inadome *et al.*, 2007). The Yip1p family proteins Yip4p and Yip5p in turn interact with a variety of small Rab GTPases like Ypt10p, Ypt11p, Ypt31p, Ypt32p, Sec4p (Calero *et al.*, 2002).

To find a concrete function of the *vti1-2* suppressor Tvp23p the *tvp23Δ* mutant cell line was transformed with a GFP-Snc1p plasmid (pGS416) and imaged via the fluorescence microscope. GFP-Snc1p travels from the TGN directly to the plasma membrane and is recycled back via early endosomes to the TGN. If there is a defect in retrograde transport the GFP-Snc1p gets trapped in the early endosomes and localization is shifted from the PM to intracellular dot like structures.

In *tvp23Δ* cells a small shift of the localization to intracellular structures could be observed (fig. 4.38). In WT (SEY6210) cell culture 74% of the cells had a plasma membrane (PM) staining, *tvp23Δ* cells showed 68% PM staining. Although the difference was small it is significant as calculated by a student's t-test (P=0.043). As a control the *tlg2Δ* strain was also tested. The SNARE Tlg2p is involved in the retrograde transport from early endosomes to the TGN. The GFP-Snc1p localization in this strain was completely shifted to internal structures which implicated a complete block of this transport. In the *tvp23Δ* mutant the transport is slightly affected but not completely blocked.

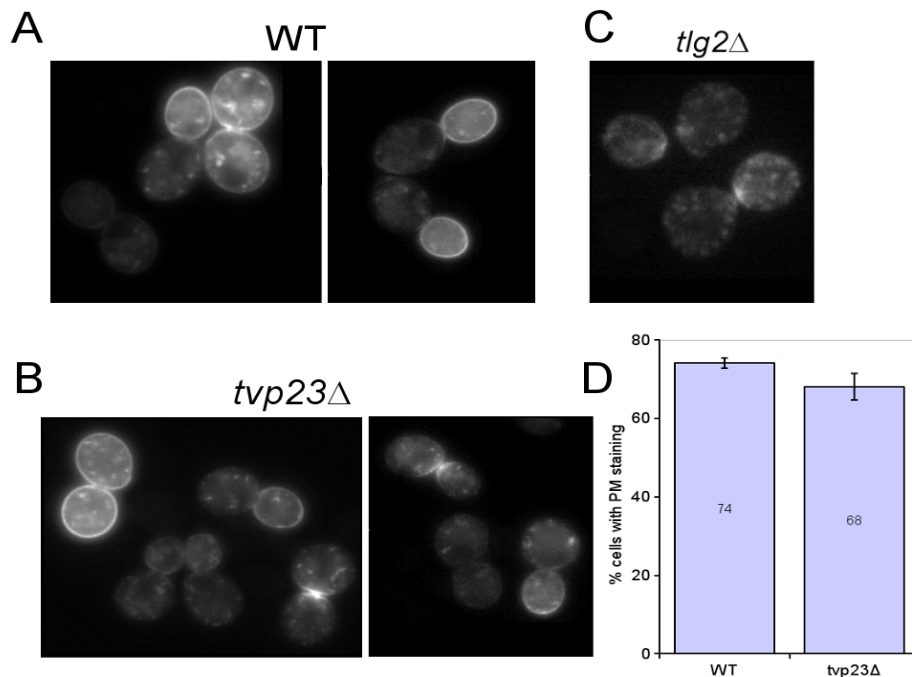


Fig. 4.38: **GFP-Snc1p localization in *tvp23Δ* cells.** WT (SEY6210, **A**) and *tvp23Δ* (ISY5, SEY background, **B**) cells were transformed with GFP-Snc1p plasmid (pGS416) and viewed in logarithmic phase under a fluorescence microscope. As control *tlg2Δ* cells were used which mislocalize the GFP-Snc1p construct completely into intracellular structures (**C**). Cells with PM staining were counted and quantified (**D**). 74% of the WT cells had a PM staining (SD 1.3 in 3 independent experiments with 738 cells counted) and 68% of the *tvp23Δ* mutant (SD 3.4%, 4 experiments, 795 cells).

4.3.1 Genetic interaction between *TVP23* and *VTI1*

Since *TVP23* is a suppressor of *vti1-2* it was then checked if the *tvp23Δvti1-2* double mutant shows additional defects. Already the temperature sensitive mutant *vti1-2* showed a significant reduction in PM localization of GFP-Snc1p (fig. 4.39). In 46% of the *vti1-2* cells at 24°C a PM staining could be observed (SD 2.0%). In the *tvp23Δvti1-2* double mutant the PM staining was further reduced to 35% (SD 1.2%) The data was obtained from three independent experiments with at least 700 counted cells per strain.

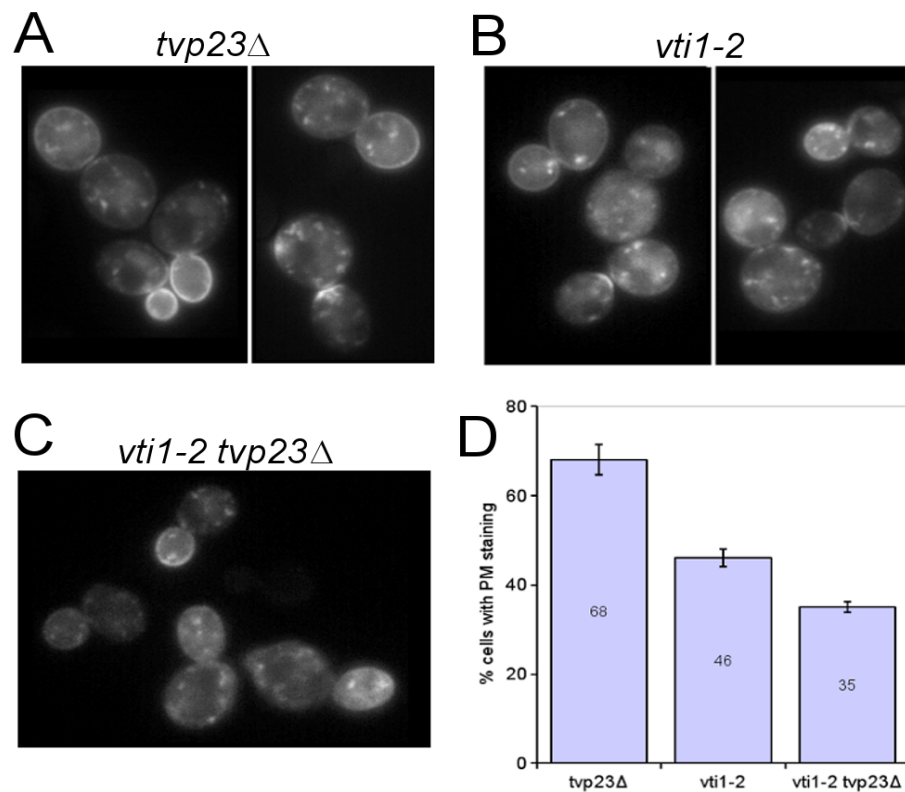


Fig. 4.39: **Synthetic defect in recycling of GFP-Snc1p to the late Golgi in *vti1-2 tvp23Δ* cells.** *tvp23Δ* (ISY5, **A**), *vti1-2* (FvMY24, **B**) and *vti1-2 tvp23Δ* cells (ISY6, **C**) expressing GFP-Snc1p were grown at 24°C and analyzed by fluorescence microscopy. (**D**) Quantification of cells with a GFP-Snc1p plasma membrane (PM) localization: 35% of *vti1-2 tvp23Δ* cells had PM staining (909 cells 3 experiments, SD 1.2) compared with 46% of *vti1-2* cells (726 cells in 3 experiments, SD 2.0). The differences between *vti1-2* and *tvp23Δ vti1-2* were statistically significant in 3 independent experiments ($P = 0.0012$, Student's *t* test).

The GFP-Snc1p construct is a tool to analyze the EE to TGN transport. To check whether Tvp23p has also an influence on the LE to TGN retrograde trafficking an A-ALP pulse chase experiment was performed. A defect in retrograde LE to TGN trafficking would result in a faster processing and therewith a reduced stability of pA-ALP. As shown in fig. 4.40 no defect for the *tvp23Δ* mutant could be observed. For *vps5Δ* but not for *tvp23Δ* an acceleration of the A-ALP processing as determined from the ratio between pA-ALP and vacuolar mA-ALP was observed. The *vps5Δ* strain was used as positive control, since there was a defect in this mutant already described (Nothwehr and Hinds, 1997). The result indicates that *tvp23Δ* has a function together with Vti1p specifically in the retrograde EE to TGN transport but not in the retrograde trafficking from the LE.

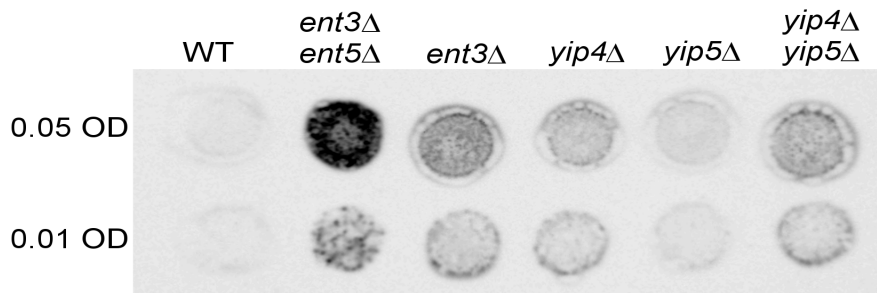


Fig. 4.41: **Yip4p has a function in the CPY transport.** Overlay assay with BY WT (BY4742) *ent3Δ*, *yip4Δ*, *yip5Δ* and *yip4Δyip5Δ* (CPY2) strains. 0.05 and 0.01 OD cells were spotted on YEPD agar plates and incubated 24 h with and without nitrocellulose membrane at 30°C. The membrane was treated with mouse-anti CPY (1:100) and goat-anti-mouse-HRP (1:10.000) antibodies. The defect of the *yip4Δ* strain was comparable to the *ent3Δ* strain and not significantly enhanced in the *yip4Δyip5Δ* double mutant. The experiment was reproduced three times.

With the CPY overlay assay a first function of Yip4p in yeast cells is discovered (fig. 4.41). The *yip4Δ* strain had a CPY secretion defect (comparable to *ent3Δ*). This defect is not increased in the *yip4Δyip5Δ* double mutant. The defects detected were not strong but well reproducible. This result implicates a function for Yip4p but not for Yip5p in the transport of CPY which leads from the TGN to the late endosome.

4.4.2 GFP-Snc1p transport in *yip4Δ* and *yip5Δ* deletion mutants

To analyze a second transport route for a potential function of Yip4p and Yip5p the plasmamembrane localization of GFP-Snc1p was checked. GFP-Snc1 is transported from the TGN to the PM and recycles back via the EE. A block in the retrograde PM to TGN transport results in a mislocalization of Snc1p to internal structures, possibly early endosomes.

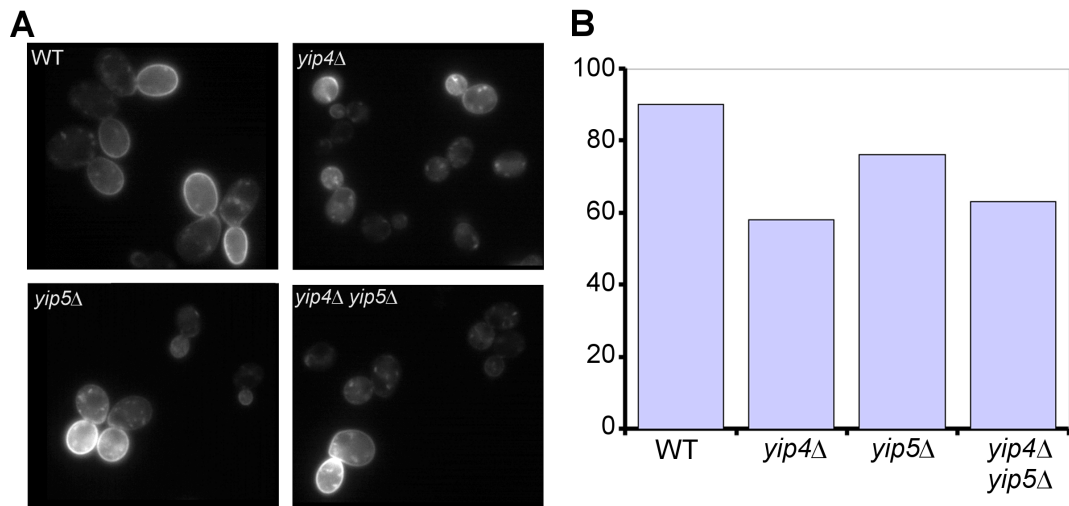


Fig. 4.42: **YIP4 deletion caused a mislocalization of GFP-Snc1p.** WT (BY4742), *yip4Δ*, *yip5Δ* and *yip4Δyip5Δ* (CPY2) strains were transformed with GFP-Snc1p plasmid (pGS416) grown into early logarithmic phase and viewed under a fluorescence microscope. **A:** Representative microscopy fields of WT, single and double mutants. **B:** Quantification of one representative experiment. Cells with and without a plasma membrane staining were counted and the percentage of cells with PM staining was determined. 90% of the WT cells and 76% of the *yip5Δ* cells showed a PM localization of GFP-Snc1p. For *yip4Δ* cells 58% cells with PM staining and for *yip4Δyip5Δ* 63% PM stained cells were counted. For each strain 150-200 cells were counted.

In the *yip4Δ* strain the amount of cells with PM localized GFP-Snc1p was reduced from 90% in the WT to 58% in the mutant (fig. 4.42). Compared to other GFP-Snc1p experiments a difference of more than 30% gives a good evidence for a significant defect. Like in the CPY assay the role of Yip4p seems to be more important than the role of Yip5p. In the *yip5Δ* strain 76% of the cells had a PM staining which is not in a significant range since the evaluation was obtained from one microscopy experiment. There is also no additional defect in the *yip4Δyip5Δ* double mutant (63% PM stained cells).

5 Discussion

In this work the structural and functional interaction of the ENTH domain protein Ent3p and the SNARE proteins Vti1p, Pep12p and Syn8p was characterized. The SNARE complex consisting of Vti1p, Pep12p and Syn8p as Q SNAREs and Ykt6p as R-SNARE functions in fusion events at the late endosome (Chidambaram *et al.*, 2004).

5.1 Characterization of the Ent3p-SNARE interaction

Ent3p (but not Ent5p) interacts directly with all three endosomal Q-SNAREs (Chidambaram *et al.* 2004). Ent3p and Ent5p belong to the family of cargo specific adaptor proteins and function as cargo adaptors for Pep12p, Vti1p and Syn8p (Chidambaram *et al.*, 2008). Ent3p is a more specific cargo adaptor as APs or Ggas and a sorting of SNAREs by this molecule prevents a competition of the SNAREs with the various cargo molecules of the classical adaptors. The cargo adaptor function of Ent3p for the SNAREs was also shown for the mammalian system where the Ent3p homologue epsinR functions as cargo adaptor for the SNARE vti1b (Vti1p in yeast) (Hirst *et al.*, 2004). To understand the mechanism of cargo sorting by Ent3p and Ent5p my task was to structurally characterize the interaction between Ent3p and the SNAREs.

For the yeast system no crystal structures of the single proteins of either the SNAREs nor Ent3p or Ent5p were available. At the starting point of my PhD thesis also the structure of the mammalian complex of epsinR and vti1b was not yet solved, so there was no information about the structural details of this interaction. Other adaptor proteins like APs and Ggas have conserved motifs for their interactions with cargo molecules. For example the mammalian VAMP4 contains a dileucine motif (LL) which was shown to be necessary for AP-1 interaction *in vitro* and for the (steady state) localization of the SNARE *in vivo*. An efficient interaction between VAMP4 and AP-1 was also dependent on PACS-1 and AP-1 phosphorylation (Hinnens *et al.*, 2003). But a lot of the SNAREs including the yeast

endosomal Q-SNAREs lack such a motif or a characterized interaction platform. The R-SNARE of the endosomal complex Ykt6p contains a longin domain and a prenyl-anchor which together are used for a correct membrane association of the SNARE (Meiringer *et al.*, 2008).

5.1.1 Pep12p interacts with Ent3p via its FSD motif

For Pep12p a role of Gga2p for its proper localization was described before (Black and Pelham, 2002). The Gga2p sorting function for Pep12p was dependent of a motif containing the amino acids FSDSPEF, called FSD motif. Black and Pelham described the importance of the FSD motif for the Pep12p localization in a sucrose density gradient. Also they showed a similar mislocalization for Pep12p in *gga1Δgga2Δ* cells as seen in the FSD mutants, but they could not prove that this effects were due to a direct physical interaction (Black and Pelham, 2002). Via an yeast two-hybrid approach and proven by a β-galactodidase assay and an *in vitro* pull down assay (fig. 4.1 and 4.2) I could show that Ent3p is the missing link between Pep12p and Gga2p. In the yeast two-hybrid assay the interaction of the F20L and the ΔFSD mutants was completely abolished, in the β-galactosidase assay this was proven for Pep12p F20L. The ΔFSD mutant showed some very weak residual binding capacity to Ent3p. In the pull down assay the binding of Ent3p to the F20L mutant was reduced to 10% and the binding of the ΔFSD mutant 30% of binding to WT Pep12p.

So Ent3p binds Pep12p directly via the FSD motif and also can directly bind to Gga2p through a cluster of acidic amino acids (Duncan *et al.*, 2003).

If Ent3p interaction is necessary for Pep12p localization a mislocalization of Pep12p F20L should be detectable. In *ent3Δent5Δ* cells Pep12p was indeed mislocalized in immunofluorescence microscopy and in a sucrose density gradient (Chidambaram *et al.*, 2008). The defect in the immunofluorescence microscopy was even stronger in *syn8Δent3Δent5Δ* triple mutants which points to a role of Ent5p and Syn8p in the transport of Pep12p. For the Pep12p FSD mutants this expectation could not be proven in the fluorescence microscopy approach (fig. 4.3). So either there is some residual sorting ability for Ent3p, Pep12p may get

sorted via a different mechanism or the non-specificity of the Pep12p antibody averts the detection of a small defect. A mislocalization in the more sensitive sucrose density gradient as also shown by Black and Pelham was detectable so the last option is the most plausible (fig. 4.4).

A further proof which supports the sucrose gradient data is that Pep12p F20L is more stable (checked by radioactive pulse-chase experiment; fig. 4.5). This defect also occurred in a comparable range for Pep12p in *ent3Δ* mutants. Possibly *ENT3* deletion and the lack of Ent3p interaction interferes with the transport of Pep12p to the vacuole where it is degraded.

If the transport of Pep12p fails the cells should be defect in Pep12p dependent transport routes. Pep12p is involved in fusion events at the late endosome (Gerrard *et al.*, 2000). The CPY transport (from TGN over late endosomes to the vacuole) which was shown to be completely blocked in a *pep12Δ* deletion strain (Becherer *et al.*, 1996) was not affected in the FSD mutants as shown by a pulse chase approach (fig. 4.6). The assay was difficult to evaluate since there was a high background binding of the CPY antibody. Neither the usage of a fresh antibody aliquot nor a new batch of Pansorbin could solve this problem. So a slight defect of the mutants may be veiled in this assay. However even if there is a slight defect in CPY transport which may be detectable in an overlay assay the defect is much less than in the *pep12Δ* strain. Although the Pep12p mutants can not efficiently interact with Ent3p there was enough functionality of the protein to sustain its function in the CPY transport.

One explanation could be that Pep12p is sorted together with other SNAREs (Vti1p, Syn8p or Ykt6p) and an efficient sorting of the other SNARE(s) may be enough to get Pep12p to the right place for mediating vesicle fusion. Such a model is postulated by Gordon *et al.*. They analyzed the sorting of mammalian R-SNAREs and found that VAMP3 and VAMP8 localization and internalization depends mainly on coiled coil interactions with Q-SNAREs (Gordon *et al.*, 2009). So not all SNAREs need an own sorting motif if they can possibly be transported in complex with other SNAREs. The observation that there is no visible mislocalization of the Pep12p F20L and Δ FSD mutants in WT cells and the functionality of the CPY transport fit to this hypothesis. If just the interaction of

Pep12p with Ent3p is disturbed, Pep12p may get sorted all the same to its destination by coiled-coil interactions with other SNAREs. The aspect of SNARE sorting as complex will be discussed in chapter 5.1.4.

Pep12p gets sorted via its interaction of the FSD motif with Ent3p which on its part directly binds membranes and Gga2p. Loss of one of these adaptors Gga2p or Ent3p caused localization defects of Pep12p. The Ent3p localization depends on Gga2p but not vice versa (Costaguta *et al.*, 2006) which accounts for an more upstream effect of Gga2p. Gga2p is important for the localization of Ent3p and Ent3p at its part sorts Pep12p into vesicles. The indirect sorting via other SNAREs like Vti1p or Syn8p maybe especially important if the sorting by cargo adaptors fails.

5.1.2 Structural characterization of the Ent3p interaction surface

5.1.2.1 Both halves of the ENTH domain are specifically involved in the SNARE binding

Before the crystal structure of the mammalian epsinR/vti1b was solved (Miller *et al.*, 2007) I already started an approach to compare the homology and binding specificity of Ent3p and epsinR ENTH domains to SNAREs. The human epsinR crystal structure was solved 2005 by Lunin *et al.* and the structure of epsin1 by Koshiba *et al.* 2001. Both structures were very homologous. The ENTH domains contain eight α -helices and after phosphatidylinositol binding with the first about 30 amino acids the formation of an additional helix is induced. This so called 0-helix inserts into to membrane leaflet (Ford *et al.*, 2002) and induces membrane curvature in the vesicle budding process. The other eight helices were arranged in a more globular formation.

In my approach parts of the Ent3p ENTH domain were exchanged to parts of the partially functional redundant Ent5p ANTH domain (ChimA and ChimB; fig. 4.7). Therefore constructs were made which contain each the first five (0-helix not counted) or the last three helices of the ENTH domain of Ent3p or the corresponding half of the Ent5p ANTH domain. The Ent5p ANTH domain was not able to bind any of the endosomal SNAREs (Chidambaram *et al.*, 2008). There are

crystal structures solved for the ANTH domains of human CALM (clathrin assembly lymphoid myeloid leukemia protein; Ford *et al.*, 2002) and the drosophila AP180 (Mao *et al.*, 2001). The ANTH domains of these proteins consist of ten α -helices organized in 5 double layers of helices. However, there is only a low sequence similarity between Ent5p and CALM (ClustalW score: 10) or AP180 (score: 11). For the alignments the first 180 amino acids of the proteins were used. By comparison, the sequence homology between Ent3p and Ent5p came to a score of 18 and between AP180 and CALM to 62. The score of the alignment between Ent3p and epsinR was 37. Besides the low homologies of Ent5p to the other ANTH domain proteins there are no homologous proteins in higher organisms as mouse or human.

The E/ANTH constructs were cloned into yeast two-hybrid vectors and transformed in L40 cells for interaction analysis. For all three SNAREs (Vti1p, Pep12p and Syn8p) the parts of the ENTH domain were not interchangeable with the corresponding parts of the ANTH domain (fig. 4.8.A). So both halves of the ENTH domain were involved in SNARE binding and can not be replaced by the ANTH domain. This indicates that the interacting part of Ent3p is not a single amino acid stretch like a Yxx Φ motif by APs (Ohno *et al.*, 1995). To prove that no potential interacting motif was located in the region where the E/ANTH parts were fused two further chimera were constructed (ChimE = Ent3p helix 1-6 fused to Ent5p helix 7-8 and ChimF = Ent5p helix 1-3 fused to Ent3p helix 4-8). This chimera could not interact with the SNAREs, either (fig. 4.8.B). So indeed at least two parts of Ent3p were involved in the interaction which is consistent with the crystal structure of the mammalian vti1b/epsinR complex where the interaction is mediated by a conformational motif (Miller *et al.*, 2007).

To test how high the homology between yeast and mammals for this interaction is Ent3p ENTH parts were exchanged with epsinR ENTH parts and the specificity between the species was checked by a yeast two-hybrid assay. It was already known that Ent3p can not bind to vti1b and epsinR not to Vti1p (Chidambaram *et al.*, 2004; personal communication with G. Fischer von Mollard). The chimera ChimC was built of Ent3 helix 1-5 and epsinR helix 6-8 and ChimD of epsinR helix 1-5 and Ent3 helix 6-8 (fig. 4.7). Interestingly ChimD still interacted strongly with vti1b and ChimC slightly with Vti1p and Syn8p (fig. 4.8.A). The interactions of

ChimC with Syn8p were hard to reproduce. The weaker interactions for the yeast system may be due to a lower expression or functionality of the yeast two-hybrid construct or to a difference in the way of interaction between Ent3p and epsinR. The expression of the chimera could not be checked by western blotting since the Ent3p antibody supposedly does not recognize the constructs. A further prove of the interactions may be achieved by changing the yeast two-hybrid vectors. Syn8p and Pep12p may produce a less background expression of the reporter gene in the pVP16-3 vector.

Taken the results from the chimera experiments together, the second half of the ENTH domain seems to be more conserved between the species and the first five helices determine the specificity.

5.1.2.2 Vti1p, Pep12p and Syn8p bind to the same surface on Ent3p but to different amino acids

When the data from Miller *et al.* was available we aligned the protein sequences of epsinR and Ent3p and constructed amino acid mutants at positions which were shown to be involved in the interaction with vti1b in mammals. The interaction of epsinR with vti1b is based on a conformational motif. On epsinR especially the loops between helix 2 and 3 and helix 4 and 5 and the complete helix 8 were involved in the binding of vti1b. In GST pulldown assays the amino acid mutants Ent3p F52D (Y60 in yeast), M53D/Y54D (Y54 = F62 in yeast) and R146E (R154) were defective for the interaction. The mutations G41S, E46W, E95W (E103 in yeast), K154D and Y159S had no effect on the binding (Miller *et al.*, 2007). The constructed yeast mutant proteins Ent3p with Y60D, F62D, E103W and R154E were tested in an yeast two-hybrid assay for the interaction with Vti1p, Pep12p and Syn8p. Like in the mammalian system Vti1p could not interact with Ent3p Y60D, F62D and R154E but still with E103W (fig. 4.10). So the interaction surface was conserved from yeast to mammals. For the interaction of Pep12p and Syn8p with Ent3p there was much less known since there was no appropriate crystal structure solved. Interactions with the mammalian homologues syntaxin7 (Pep12p) and syntaxin8 (Syn8p) with vti1b could be shown by yeast two-hybrid assays and in *in vitro* pulldown assays (Chidambaram *et al.*, 2008). Also Pep12p and Syn8p

interacted in yeast two-hybrid assays with Ent3p and for Pep12p (but not for Syn8p) this interaction was proven by a pulldown assay. In my work I could show that Pep12p and Syn8p bind to the same surface of Ent3p as Vti1p but to different amino acids. In all four Ent3p mutants the interaction with Pep12p was abolished. For the interaction with Syn8p the amino acids E103 and R154 were necessary but not F62 and Y60. The fact that Ent3p binds three SNAREs with the same surface raises the question how the interaction may work *in vivo*. The SNARE proteins are too large to bind to Ent3p at the same time. One plausible explanation is that on the budding vesicle is a whole network of adaptor proteins present. So Ent3p sorts the SNARE which is presently available and other SNAREs were sorted by other Ent3p molecules. This provides a flexible and dynamic system for the SNARE sorting process which is crucial for vesicle transport and fusion. During the cloning procedure the bachelor student Andrea Nolting obtained the additional mutant Ent3p F62D G58R. The F62D single mutant could only interact with Syn8p. The interaction with Pep12p and Vti1p was abolished. Interestingly the F62D G58R mutant interacted not only with Syn8p but also with Pep12p. From the structure alignment the amino acid G58 is the last C-terminal amino acid of the helix 2. But it seems not to interfere directly with the SNARE interaction. Supposedly the exchange from the small unpolar glycine to the larger basic arginine causes some structural changes which restore the interaction to Pep12p but not to Vti1p.

5.1.3 Proof of interacting amino acids by charge-swap experiments

To identify the interacting amino acids for Ent3p R154 on the SNARE side potential Pep12p and Vti1p acidic amino acids were mutated to a basic arginine. The SNARE charge-swap mutation should restore the interaction of the Ent3p R154E mutant in a yeast two-hybrid assay.

5.1.3.1 Interacting amino acids on Vti1p

Miller *et al.* described such a working charge-swap mutagenesis for vti1b E23R and epsinR R146E. In their alignment the corresponding yeast amino acid was E17 which was conserved in the alignment so a yeast E17R and additionally an E9R mutant were generated.

From the yeast two-hybrid result the Vti1p E9 and E17 amino acids were not involved in the Ent3p interaction since the E9R and E17R exchanges did not abolish the interaction with Ent3p (fig. 4.11). Additionally no interaction could be restored with the R154E mutant. So a charge-swap effect could not be observed. If the sequences of just the N-termini of vti1b and Vti1p were compared with ClustalW a different alignment as described from Miller *et al.* was obtained (fig. 5.1).

```

vti1b      MASSAASSEH-10FEKLHEI20FRGLHEDLQGV30PERLLGTAGTEEK40KKLIRDFDEK50QQEANETL
Vti1p (Miller) -----M10SSL-LISY10ESD10F10KTTLE10QAKASLAEAP-S30QPLSQRNTTLKHVE40QQQ40DEL50FDL50LI50
Vti1p new  MSSLLISY10ESD10F10KTTLE10QAKASLAEAPS30QPLSQRNTTLKHVE40QQQ40DEL50FDLLD50QMDVE60EVN60

```

Fig. 5.1: **The different alignments of Vti1p with human vti1b.** Shown are the first above sixty amino acids of vti1b and Vti1p. The first alignment (Vti1p Miller) was analogous to the alignment of Miller *et al.*, the second was performed with ClustalW and the first 120 amino acids of both proteins (Vti1p new). Conserved amino acids are boxed in red, homologous amino acids in grey. The in the Miller paper successful mutated charge swap amino acid E23 and the amino acids mutated during this work (E9 and E17) were marked with black arrow heads. Another potential charge swap mutation (E25) is marked with a grey arrow head.

In the alternative alignment *vti1b* E23 would be an alanin (A24) in *Vti1p*. Next to A24 is a glutamate E25 which may be the homologous amino acid for E23 in *vti1b*. E9 and E17 are in this alignment variant also conserved (E9 and E16 on *vti1b*) but this amino acid exchanges were not tested by Miller *et al.*. The crystal structure indicates that E9 may interact with R96 (R104 in *Vti1p*) and E16 may interact with K150 which is also conserved in *Ent3p* (K157). However, both mutations did not abolish the interaction with *Ent3p*. Even if E9 and E17 would interact with *Ent3p* this interaction is not crucial for the interaction of the whole protein. The *epsinR* mutant R96S was not able to bind *vti1b*. The possible interaction partners were *vti1b* E9 or S8 where a S8W mutation showed no longer an interaction with *epsinR* (E9 was not tested) (Miller *et al.*, 2007). Also in *Vti1p* there is a serine (S7) in the neighborhood of E9 which may be the homologue interacting partner for *Ent3p* R104. So the result that *Vti1p* E9 and E17 do not interfere with the *Ent3p* interaction does not contradict the model of *Vti1p* being highly homologue in ENTH binding.

A new yeast two-hybrid approach with a *Vti1p* E25R construct could potentially yield the desired charge-swap interaction and clarify which alignment between *Vti1p* and *vti1b* is valid.

5.1.3.2 Interacting amino acids on *Pep12p*

Vti1p, *Pep12p* and *Syn8p* are supposed to contain a three helix bundle at their N-terminus which was shown to interact with *Ent3p*. For the homologous mammalian complex such a three helical conformation could be shown for *vti1b* and *syntaxin7* (*Pep12p* homologue) (Antonin *et al.*, 2002, Miller *et al.*, 2007). Additionally secondary structure predictions and a high alpha-helical content of *Pep12p* and *Vti1p* confirm this assumption (Tishgarten *et al.*, 1999).

The mammalian homologue of *Pep12p* is *syntaxin7*. But *Pep12p* showed only poor sequence homologies to *syntaxin7*. *Pep12p* showed the highest sequence similarity to mammalian *syntaxin12* (*stx12* or *stx13*). For *stx12* a crystal structure for the N-terminus is available and shows also a three helix bundle structure (Abe *et al.*, 2006). But in structure modeling attempts for *Pep12p* (in Swiss-model and 3D-Jigsaw) the first helix (Ha) of the N-terminus started at E25 and the FSD motif

was not included in the modeled structure. As we know that the FSD motif is involved in Ent3p binding another alignment with the N-terminus of rat syntaxin6 was done with Swiss-model which yielded a model including also the amino acids 4-25. From the structure model of Pep12p the glutamate E12 seemed to be a potential candidate for a charge-swap mutation to restore the interaction with Ent3p R154. But the E12R mutation failed to restore the abolished interaction of the Ent3p R154E mutant and still interacted with WT Ent3p (fig. 4.11). Interestingly the interaction of the F62D and in a lower intensity the Y60D mutant interaction was restored. This are no real charge swap interactions since the native F62 and Y60 were no acidic amino acids but the result shows that the glutamate Pep12p E12 has to be located in direct proximity to the Ent3p amino acid F62 and Y60. With this information Pep12p can be adjusted to the Ent3p interaction site and new potential charge-swap partners for Ent3p R154E can be identified. Two candidates which can be checked by new yeast two-hybrid assays are D22 and E25 on Pep12p.

5.1.4 Vti1p, Pep12p and Syn8p were sorted as complex

The R154E mutant interrupted the interaction with all three SNAREs while the other mutants still interacted with one SNARE. With the four mutants as tools I studied the sorting of the SNAREs into the vesicles. If the SNAREs were sorted as complex one interacting SNARE should be enough to sort the whole complex. If each SNARE is sorted separately all four Ent3p point mutants should show an abnormal localization in the appropriate mutant strain. The mutant constructs were subcloned into yeast expression vectors under endogenous promotor and transformed into *ent3Δent5Δ* cells. Pep12p and Vti1p were mislocalized in a sucrose density gradient in *ent3Δent5Δ* double mutants and Pep12p showed a more dispersed distribution in a fluorescence microscopy approach. (Chidambaram *et al.*, 2008). For Vti1p no significant mislocalization under the fluorescence microscope was visible (fig. 4.13) which may due to the localization and function of Vti1p at various organelles. The Syn8p localization in this mutant was not tested yet. I could show that also the Syn8p localization depends on

Ent3p and Ent5p presence (fig. 4.15).

By analyzing the Ent3 mutants in the sucrose density gradient I found that Vti1p and Pep12p were mislocalized in the R154E mutant which was defect in the interaction with all three SNAREs (fig. 4.12 and 4.14). If only one SNARE partner was able to interact with Ent3p like in the Y60D mutant (Syn8p still interacted) or the E103W mutant (Vti1p) no shift in localization of the other two SNAREs occurred.

Therefore it can be concluded that Vti1p, Pep12p and Syn8p were sorted together in a complex. The interaction of one of these SNAREs is enough to transport also the others to their target membrane. The mode of interaction for SNARE complex sorting via a large conformational motif is unique up to now. There is one other example for the sorting of three SNAREs as complex in the anterograde ER to Golgi transport. The compounds of the COPII coat Sec23 and Sec24 sort the SNAREs Bet1p, Sed5p and Sec22p selectively into vesicles (Mossessova *et al.*, 2003). Bet1p is the v-SNARE of the fusion complex, Sed5p and Sec22p are together with Bos1p the t-SNAREs during fusion at the *cis*-Golgi. This sorting works mechanistically different from the sorting of the endosomal SNAREs since all three SNAREs interact to short amino acid sequences of the COPII subunits.

5.1.5 Vti1p and Pep12p are t-SNAREs and Syn8p is a v-SNARE

The sorting of Syn8p depends also on Ent3p and Ent5p as shown in the gradient with the double mutant. However, the the disruption of the direct interaction of all three SNAREs with Ent3p (in the R154E) does not lead to a significant mislocalization of Syn8p (fig. 4.15). There have to be always SNAREs located on the vesicle and on the target membrane. Ykt6p, the R-SNARE of the endosomal SNARE complex, does not contain a transmembrane domain which is supposed to be essential to mediate fusion (Jun *et al.*, 2007). So a composition of Ykt6p on one side of the fusion and Vti1p, Syn8p and Pep12p on the other side is unlikely. For Pep12p a localization at the late endosome is described. Pep12p is also involved in other fusion events with the late endosome as e.g. the retrograde transport from the vacuole to the LE (Gerrard *et al.*, 2000). It seems probable that Pep12p

remains at the LE and is a t-SNARE. The gradient experiments showed that an interaction of Ent3p with Vti1p is sufficient to correctly localize Pep12p as well. Since they were sorted together it seems likely that Vti1p is also a t-SNARE. This would mean that Syn8p has to be the v-SNARE of this complex what also fits to the observation from the gradient that Syn8p is sorted in a different manner. To prove this hypothesis an assay utilizing a *tlg2Δ* strain was constructed. Tlg2p is a SNARE involved in retrograde transport from endosomes to the TGN and endocytosis (Abeliovich *et al.*, 1998). For the mammalian homologue syntaxin16 functions in retrograde EE to TGN transport were known and also for the LE to TGN transport there was some evidence that syntaxin16 has a function (Amessou *et al.*, 2007; Medigeshi and Schu, 2003).

SNAREs which localization depends on correct recycling from the endosomes back to the TGN should show an altered distribution in a sucrose density gradient in *tlg2Δ* cells. SNAREs which remain on the LE and have not to be recycled should be unaffected in the *tlg2Δ* background.

Indeed the localization of Syn8p was changed in the *tlg2Δ* background and the Vti1p and Pep12p localization was the same as in the WT control (fig. 4.16 and 4.17). The R-SNARE Ykt6p could be immunoprecipitated with Syn8p (Lewis *et al.*, 2002) and it would be interesting to know if the sorting of Ykt6p and Syn8p is in tandem. Ykt6p has a longin domain which is proposed to be involved in sorting. The interaction with Ykt6p could provide an additional sorting capacity for Syn8p. Additionally, Syn8p is palmitoylated (Valdez-Taubas and Pelham, 2005) and may bind ubiquitin (Peng *et al.*, 2003; high throughput proteomics approach). This could provide an extra sorting motif which makes a SNARE-SNARE interaction for correct localization unnecessary. However the Syn8p sorting seems to be still dependent on Ent3p and Ent5p since it was mislocalized in the *ent3Δent5Δ* double mutant. This sorting defect may be of indirect nature.

The problem of this assay is that the functions of Tlg2p and the various defects of its deletion are not completely understood. So an assay which is independent from *TLG2* deletion should be done to prove the initial experiment. One possible approach might be to check the localization and kinetics of Pep12p and Syn8p in vivo by fluorescence microscopy. If Syn8p shows a more dynamic cycling behavior than Pep12p, which should be more static if the hypothesis is true, this would be a

further prove of Syn8p being localized on the vesicle and Pep12p on the late endosome. An analysis of Vti1p in this context may be difficult since it is located on various organelles including endosomes, the vacuole and all Golgi compartments.

5.1.6 *In vivo* functions of the Ent3p point mutants

In several tests the rescuing abilities of the Ent3p point mutants for the *ent3Δent5Δ* defects were checked to test their *in vivo* functionality.

5.1.6.1 *The Y60D mutant has a severe growth defect*

The strain containing the Y60D mutant had an even stronger growth defect than the double mutant (fig. 4.21). It showed a significant growth defect at 30°C where a defect for the double mutant was marginal. This strong possibly dominant negative effect of the Y60D mutant was not due to a reduced or higher expression of the protein (fig. 4.28). If this effect is really dominant negative can be checked by overexpressing the Y60D mutant in a wild type strain and analyzing the growth of this cells. Another Y60 (Y60H or *ent3-2*) mutant was already characterized by Friant *et al.* (2003). This mutant was defective in transport into the internal multivesicular body vesicles at 24°C but they described no severe growth defects. Additionally they saw a reduced membrane localization (in the 100.000 g fraction after subcellular fractionation) for this mutant. It would be interesting to see if the Y60D mutant is also defective in membrane binding and if it has a similar defect in MVB sorting. To further analyze the Y60D mutant another approach could be to test whether the growth defect is due to a defect in cell cycle progression or cell wall integrity. In first experiments with calcofluor stained *ent3Δent5Δ* cells containing the Ent3p mutant plasmid no severe defects were visible. There were not obviously more cells without bud scars and also no severe defects in chitin organization. So it could be tested if the overall kinetic of the cell cycle progression may be slowed down (e.g. with life cell imaging of cell cycle synchronized cells).

5.1.6.2 Rescuing abilities of the *Ent3p F62D*, *E103W* and *R154E* mutants

The growth defect of the Y60D mutant made conclusions for this mutant in the CPY and growth test assays with cell wall disturbing agents impossible, so the further discussion will be limited to the other three point mutants.

CPY transport

The absence of rescuing ability for the CPY transport in the overlay assay (fig. 4.18) indicates that even if Pep12p is sorted correctly as seen in the sucrose gradient this sorting may not be as efficient as with a direct interaction with Ent3p. In a less sensitive but more quantitative pulse chase approach no enhanced CPY secretion could be detected (fig. 4.19). Since there was such a high unspecific binding of the CPY antibody in the internal fraction and even in the double mutant only a little amount of secreted CPY was visible this assay may not be sensitive enough to see the lack of complementation with the point mutants. So at least some functionality of Ent3p must be maintained in the point mutants even in the R154E mutant. This is supported by the result that the point mutants complement the NaCl (and SDS) defect of the double mutant. The *pep12Δ* deletion strain was shown to be salt sensitive (Logg *et al.*, 2008) and the sensitivity was proposed to be due to a sorting defect of the plasma membrane ion pump Ena1p. That I could not observe a NaCl sensitivity for the three point mutants leads to the conclusion that the salt tolerance mechanisms of the cell, including the Ena1p transport, were intact in these mutants. So either there is some residual binding of Pep12p to Ent3p which allows enough correct sorting of Pep12p or the SNARE may be sorted on another route to the late endosome so that it can at least partially fulfill its functions.

Chs3p transport

On agar plates containing 50 µg/mL calcofluor, the point mutants could not complement the growth defect of *ent3Δent5Δ* (fig. 4.21). With 25 µg/mL calcofluor there was some rescuing ability for the mutants but still weaker than the WT Ent3p

plasmid. Also in the sedimentation assay (fig. 4.20) especially the R154E mutant was not functional. This indicates that the efficient SNARE binding and transport is involved in generating and maintaining an intact cell wall. The chitin synthase Chs3p was mislocalized in *ent3Δent5Δ* cells to the plasma membrane (Copic *et al.*, 2007) which explains the calcofluor sensitivity of the double mutant (Chidambaram, 2005). The Chs3p synthesizes the initial chitin ring at the bud neck of a budding yeast cell and the chitin dispersed in the cell wall. Chs3p is a transmembrane protein and sorted dependent on Chs6p and Chs5p to the plasma membrane where it fulfills its function (Valdivia *et al.*, 2002). Then it gets endocytosed and recycles over recycling endosomes and early endosomes back to the TGN. This recycling can be blocked by deletion of AP-1 subunits. *chs6Δ* cells show a calcofluor white resistance since the transport of Chs3p to the PM is blocked. The PM localization can be restored by an additional deletion of an AP-1 subunit. Similar to AP-1 deficient cells also for *ent3Δent5Δ* cells such a rescuing of calcofluor sensitivity in *chs6Δ* cells was shown (Copic *et al.*, 2007). Copic *et al.*, suggested a function of Ent3p and Ent5p in retention of Chs3p at the TGN.

My results show that the chitin dependent cell wall defects can not be rescued by Ent3p point mutants which lack the amino acids necessary for SNARE binding. Since extensive conformational changes within the point mutants were unlikely the sorting function for Vti1p, Pep12p and Syn8p for transport to the LE may be the cause for the Chs3p trafficking defect. Since the transport of Chs3p is not dependent on TGN to late endosomal transport this effect may be of indirect nature. Chs3p is shown to bind Ent5p directly and this interaction depends not on Ent3p or AP-1 presence (Copic *et al.*, 2007). Additionally the *ent5Δchs6Δ* mutant showed an enhanced calcofluor sensitivity (compared to *chs6Δ*) but the single *ent5Δ* mutant had no defects on calcofluor agar plates. This indicates some redundancy of Ent3p and Ent5p in this transport. The assay with the Ent3p point mutants was performed in an *ent3Δent5Δ* deletion background. So another explanation for the observed defect of the point mutants may be the lack of redundancy of the mutant Ent3p constructs with Ent5p.

SDS sensitivity

Another assay for cell wall integrity is the addition of SDS to the agar plates (fig. 4.21). In cells with a defect in cell wall integrity the plasma membrane is more accessible to the detergent SDS. SDS interferes with the PM lipids which results in pores and cell lysis. The SDS sensitivity of *ent3Δent5Δ* was complemented by the mutants which could be explained either by function of Ent3p independent of SNARE sorting in cell wall assembly or a Ent3p independent sorting of the SNAREs which was efficient enough to sustain the cell wall stability for SDS tolerance but not the Chs3p transport.

The F62D, E103W and R154E mutants could not rescue the defects of *ent3Δent5Δ* cells in the CPY overlay assay (fig. 4.18), chitin assembly (fig. 4.21) and sedimentation assay (fig. 4.20). The growth defects on agar plates containing SDS, sorbitol and NaCl could be completely rescued (fig. 4.21).

This leads to the hypothesis that Ent3p functions in at least two independent pathways. In one it has a function in CPY and possibly Chs3p transport which is dependent on efficient SNARE binding. Although Pep12p and Vti1p were sorted correctly in the F62D and E103W mutants in the sucrose gradient this is not sufficient to rescue the CPY and calcofluor sensitivity defect of the double mutant.

The other pathway seems independent from binding of the endosomal SNAREs since the point mutations had no impact on the function in salt/osmotic stress resistance and cell wall integrity.

5.1.7 Ent3p and Ent5p have a function in retrograde transport to the TGN independently from SNARE binding.

A role for Ent3p and Ent5p in the retention of Chs3p at the TGN was described by Copic *et al.* (2007). A function in SNARE sorting into vesicles destined for late endosomes was shown by Chidambaram *et al.* 2004 and 2008. To test whether Ent3p and Ent5p may have additional functions in recycling processes back to the TGN I analyzed the recycling of A-ALP, GFP-Snc1p and GFP-Yck2p in *ent3Δent5Δ* cells.

5.1.7.1 A-ALP transport from LE to the TGN

The retrograde transport from the late endosome to the TGN was analyzed with the A-ALP construct as marker protein. A-ALP consist of the luminal part of the alkaline phosphatase and the cytosolic DPAP A recycling signal. This constructs cycles between the late endosome and the TGN and the transport to the vacuole were the ALP part is cleaved to an active shorter form (mA-ALP) is very slow. *ent3Δ* and *ent5Δ* single mutants had no A-ALP defect (Chidambaram *et al.*, 2008). Here I showed that the *ent3Δent5Δ* double mutant has a slight transport defect of the A-ALP construct in a radioactive pulse chase approach (fig. 4.22). After 120 min 46% pA-ALP was still detectable in the WT (SD 25%) cells and 23% in the double mutant (SD 8%). Although the standard deviations were very high the tendencies of the values in the three experiments were the same. Since the defect was that small it would be interesting to see if there are some further genetic interactions which may enhance the defect. For example the Retromer subunit Vps35p or parts of the GARP tethering complex (involved in vesicle tethering at the TGN from late and early endosomes) may be potential candidates.

5.1.7.2 GFP-Snc1p

The GFP-Snc1p construct is an established model to analyze the retrograde transport from early endosomes to the TGN (Lewis *et al.*, 2000). The R-SNARE Snc1p is transported directly from the TGN to the plasma membrane, is then endocytosed and recycles from early endosomes back to the TGN. Its steady state localization is mainly on the plasma membrane. The *ent3Δent5Δ* mutants showed an almost complete loss of PM localized GFP-Snc1p (fig. 4.23). Only 4% of the *ent3Δent5Δ* cells showed PM staining (SD 3%) in contrast to 83% in WT cells (SD 5%). Also the *ent3Δ* and *ent5Δ* single mutants showed a significant defect. In the *ent3Δ* strain 64% of the cells had PM staining (SD 9%), in *ent5Δ* 68% (SD 6%). This is the first description of a defect in this transport step dependent on Ent3p and Ent5p. The GFP-Snc1p construct was partially mislocalized to the vacuole membrane, which could be proven by a co-localization with FM4-64 after 30 min incubation at 30°C (fig. 4.24). The protein seems to be further transported from the EE possibly over LE to the vacuole. The Ent3p point mutants showed no defects in the GFP-Snc1p recycling which points to a SNARE sorting independent function of Ent3p and Ent5p.

Because no functions of Ent3p or Ent5p in exocytosis from TGN to the plasma membrane were detected in the past the defect is very likely due to a blocked EE to TGN transport.

A role for Ent3/5 in exocytosis would be unlikely since it is no clathrin mediated transport and also the APs and Ggas do not play a role in this trafficking route.

A further proof that there is no defect in exocytosis could be obtained by analyzing the GFP-Snc1p transport in *ent3Δent5Δ* cells while blocking the endocytosis by latrunculin A (depolymerizes actin) or using a temperature sensitive mutant of *END3* (*END3* deleted cells are endocytosis deficient, Benedetti *et al.*, 1994). The double mutant cells should then accumulate GFP-Snc1p at the plasma membrane at non-permissive temperature. If there is a secretion defect in direct TGN to PM transport GFP-Snc1p would not reach the PM and accumulate intracellular.

5.1.7.3 GFP-Yck2p

The yeast casein kinase I isoform Yck2p is associated with the plasma membrane via a palmitoyl residue and is together with Yck1p essential for cell growth, cell morphology, endocytosis and budding processes (Robinson *et al.*, 1993; Babu *et al.*, 2004). Furthermore Yck2p is involved in septin assembly at the bud neck (Robinson *et al.*, 1999) and its trafficking depends on the SNARE Tlg2p (Panek *et al.*, 2000) and Rgp1p. Tlg2p is involved in the retrograde transport from endosomes to the TGN and Rgp1p is a GEF for Ypt6p (Rab GTPase for retrograde fusion at the TGN). So it is likely that the Yck2p localization depends on recycling to the TGN.

I could show that in *ent3Δent5Δ* GFP-Yck2p was partially mislocalized to the vacuolar membrane (fig 4.25). This proves that Yck2p recycles via the early endosomes. A defect in Yck2p is especially interesting since the *ent3Δent5Δ* mutants show, similar to Yck2p mutants (Robinson *et al.*, 1993), defects in maintaining the budding polarity of haploid and diploid cells (Zimmermann, 2006). Also for the Yck2p trafficking the direct SNARE interaction was not involved because the Ent3p point mutants had no defects. Both, Snc1p and Yck2p were not found as direct interaction partners for Ent3p by genomic assays. Ent5p was found as phosphorylation substrate for Yck2p in a high throughput approach but this is not proven yet (Ptacek *et al.*, 2005). So Ent5p may link Yck2p to Ent3p. Since the Snc1p N-terminus consists of only a few amino acids an interaction with Ent3p similar to Vti1p or Pep12p is unlikely. There are still some questions left, e.g. If the interaction is direct or if the Ent3p C-terminus has a sorting or a more general function in the EE to TGN transport. The first question could be checked by interaction studies like a yeast two-hybrid assay. The second question is more difficult to address since the anterograde transport where *ent3Δent5Δ* cells show also defects influences the retrograde transport, too. One approach to differentiate the functions of Ent3p in the two pathways is to analyze parts of Ent3p separately.

5.2 Functions of the Ent3p domains

In the GFP-Snc1p assay I could show that Ent3p has a function in the retrograde EE to TGN transport which is independent from SNARE binding. So I wondered if the Ent3p C-terminus, the SNARE binding ENTH domain or both domains arrange this function. Therefore yeast expression vectors (*CEN* vectors, overexpressing through TPI promotor) were constructed which contain either the ENTH domain or the C-terminus. Additionally a full length Ent3p just lacking the PI binding first 28 amino acids was tested. The constructs were transformed into *ent3Δent5Δ* double mutants and their rescuing abilities of the double mutant defects were analyzed by several approaches.

5.2.1 The Ent3p C-terminus is sufficient for GFP-Snc1p and GFP-Yck2p recycling

In the GFP-Snc1p and GFP-Yck2p assays the ENTH domain alone was not able to rescue the defects of the *ent3Δent5Δ* double mutant (fig. 4.26). The C-term. alone and the -PI mutants rescued the mislocalization of Snc1p and Yck2p. This indicates a function for the C-terminus but not for the ENTH domain in the retrograde early endosome to TGN transport. The defect of the ENTH construct was not due to a changed expression level (fig. 4.28). Since the endosomal SNAREs bind to the ENTH domain their efficient sorting or recycling seems to be unnecessary for this transport. Interestingly a WT like membrane binding seems also not to be crucial for the Ent3p function in this transport. The membrane binding of the C-terminus was reduced in the membrane association assay from 42% (SD 11%) membrane bound Ent3p in WT cells to 20% (SD 13%) in *ent3Δent5Δ* cells containing the overexpressed Ent3p C-terminus (fig. 4.29). This residual membrane binding can be explained by the binding of Ent3p to other vesicle associated proteins like Gga2p or clathrin. The membrane binding of the C-term may be enough to sustain the function in the retrograde transport or Ent3p has some functions where membrane binding is not needed. In the first case the

Ent3p C-terminus alone already may have stabilizing functions for the vesicle coat network. It contains binding moieties for Gga2p, AP-1 and clathrin and a tight linkage of this coat proteins could be necessary for efficient vesicle budding.

To distinguish between this two possibilities is experimentally difficult since we could not completely block the membrane binding with our constructs. But deleting the binding motifs for the other adaptor proteins and clathrin may yield an Ent3p mutant which is completely deficient in membrane binding. With this mutant a discrimination between functions of the membrane bound and unbound Ent3p may be possible. Additionally the role of the interacting proteins for the Ent3p functions can be analyzed. In an immunofluorescence approach no localization difference could be seen for the ENTH and the -PI mutants (fig. 4.30). Ent3p was localized dispersed throughout the cell. The antibody reaction was to some extent unspecific and a small defect would have been hard to detect. The HA-tagged C-terminus could not be analyzed by immunofluorescence microscopy since the HA antibody was highly unspecific in IF and no specific staining could be obtained even with preabsorption and several dilutions of the antibody.

The rescuing effects of the Ent3p C-terminus were the first description of epsin functions which are independent from its ENTH domain. In *Dictyostelium discoideum* both domains were necessary for a correct localization of the Dictyostelium epsin but for the function the ENTH domain was the crucial part of the protein (Brady *et al.*, 2008). The ENTH domain alone was able to rescue the abnormal spore phenotype but the C-terminus alone could not. From their membrane association experiments Brady *et al.* proposed that the C-terminus has an inhibiting function for membrane binding. The ENTH domain alone bound stronger to membranes than the whole protein. I could not prove this observation for the yeast Ent3p. The membrane binding was not significantly lower in the full length Ent3p (42%; SD 11%), compared to the ENTH domain (49%; SD 12%). Another function for the C-terminus was analyzed in *Drosophila melanogaster*. Overstreet *et al.* divided the Drosophila epsin Liquid facets (Lqf) and showed that either part, the ENTH domain and the C-terminus, could rescue the DI (DI= Delta trans membrane ligand of the Drosophila eye) endocytosis defect. They hypothesized that each part of the epsin has another redundant protein (Overstreet *et al.*, 2003).

Both, the Dictyostelium epsin and Lqf are more homologous to the yeast Ent1p and Ent2p than to Ent3p. Lqf ENTH could even rescue the lethality of the *ent1Δent2Δ* yeast cells (Overstreet *et al.*, 2003). For Ent1p and Ent2p it was shown that at least one of the Ent1/2p ENTH domains has to be present to sustain the yeast viability (Wendland *et al.*, 1999). The C-terminus instead was not required. Overexpression of the Ent2p ENTH domain induced defects in cell separation and septum formation which were due to a ENTH dependent misregulation of the septin interactor Bem3p (Mukherjee *et al.*, 2009) but a function of the C-terminus was not analyzed.

One approach to get a better insight into the domain functions could be to overexpress the Ent3p domains in WT cells and to see if there are some effects for example in the Snc1p or the Yck2p transport or if the cell wall assembly may be disturbed.

5.2.1.1 Vacuole morphology of the Ent3p/Ent5p mutants

Another ENTH independent effect was the vacuolar morphology defect of the mutants. *ent3Δent5Δ* cells have numerous small vacuoles (fig. 4.24) and this defect could be rescued by the Ent3p C-terminus and the -PI mutant (fig. 4.26). The observation of the vacuole morphology in the domain mutants was done indirectly over the GFP-Yck2p staining and should be proven by a FM4-64 staining. Fragmented vacuoles can occur when the vacuole fusion process is disturbed like in the retromer subunit deletion *vps5Δ* or in the deletion mutant of the scaffold protein Bem1p (Xu and Wickner, 2006). The retromer functions in the retrograde endosome to TGN transport so the *vps5Δ* defect has to be of indirect nature. An example for a direct defect of vacuolar morphology was found in the deletion mutant of the HOPS subunit Vps39p (Raymond *et al.*, 1992). The HOPS complex is necessary for homotypic vacuole fusion and other vesicle fusion events at the vacuole and possibly also at the endosomes (Peterson and Emr, 2001). Bem1p is involved in maintaining the cell polarity and cell morphogenesis and cofractionates with Vti1p and Ykt6p (Xu and Wickner, 2006). Additionally it is a potential phosphorylation substrate for Yck2p (Fiedler *et al.*, 2009). A direct interaction with Ent3p or Ent5p was not found but a slight genetic interaction with

ENT1 (Aguiliar *et al.*, 2006; Bem1p rescued growth defects of the Ent1 ENTH Y100R mutant to some extent). An analysis of the genetic interactions between Ent3p/Ent5p and Bem1p may give further insights into the functions of Ent3p.

5.2.2 Both Ent3p domains were necessary for CPY sorting

The deletion of just the *ENT3* gene caused no severe defects besides a weak CPY missorting to the extracellular space. The *ent3 Δ ent5 Δ* double mutant in contrast shows much stronger defects in the CPY sorting and also in sorting of the Carboxypeptidase S (CPS) and the chitin synthase 3 (Chs3p) (Duncan *et al.*, 2003, Copic *et al.*, 2007). To see which of the Ent3p domains is necessary for a correct CPY transport a CPY overlay assay was done with the Ent3p domain mutant proteins in *ent3 Δ ent5 Δ* cells (fig. 4.27). It turned out that both, the C-terminus and the ENTH domain, were necessary for a proper CPY sorting. I already showed that the SNARE binding was important for CPY sorting. This corresponds with the result that the C-terminus alone was not able to rescue the CPY defect. The ENTH domain alone was also insufficient for CPY transport. The CPY transport defect is due to a partial block in the anterograde transport since the cycling CPY receptor Vps10p is not missorted in *ent3 Δ ent5 Δ* cells (Chidambaram *et al.*, 2008). So both domains have to cooperate in this anterograde CPY transport step which was not true for the retrograde GFP-Snc1p and GFP-Yck2p trafficking. There the C-terminus was enough to maintain the transport from endosomes to TGN. A radioactive pulse chase approach was not done for the domain mutants because also for the point mutants it was not possible to detect a significant difference in this assay and the CPY secretion in the overlay assay was comparable in the point mutants and in the domain mutants.

The mutant which lacks the phosphatidylinositol binding (-PI) domain had only a partial defect in CPY sorting. Ent3p binds to PI-3,5-bisphosphate (PI(3,5)P₂; Friant *et al.*, 2003; Chidambaram *et al.*, 2004) which is generated of PI(3)P from the kinase Fab1p. There was also some indication for a binding capacity of Ent3p for the more abundant PI(4,5)P₂ (Narayan and Lemmon, 2006; Michell *et al.*, 2006). PI(3,5)P₂ has functions in the MVB sorting process and is important for retrograde

transport from the vacuole and the late endosome (Dove *et al.*, 2002; Michell *et al.*, 2006). The main PI on the Golgi apparatus where Ent3p and Ent5p are thought to have a function as cargo adaptor is PI(4)P. So if the PI(3,5)P₂ binding is only necessary for Ent3p/Ent5p function at the MVB or for retrograde transport and not at the TGN this may explain the lack of a strong CPY defect in the -PI mutant. In the retrograde GFP-Snc1p and GFP-Yck2p transport no defect for the -PI mutant was detectable. According to this the -PI mutant is either functional enough for the retrograde transport or the PI(3,5)P₂ binding is just necessary for the MVB sorting function of Ent3p/Ent5p.

To prove this the functionality of the MVB sorting for the -PI mutant could be checked by e.g. following the transport of Carboxypeptidase S (Cps1p) or a GFP-Phm5p construct. Both proteins are sorted via the internal MVB vesicles to the vacuole. The -PI mutant had a reduced membrane binding ability (fig. 4.29). In WT cells 42% (SD 11%) was bound to membranes in the *ent3Δent5Δ* strain containing the Ent3p -PI construct just 32% (SD 12%). So reduced membrane binding could also play a role for the slight CPY defect of the -PI mutant.

5.2.3 Cell wall defects

From the PhD thesis of S. Chidambaram and my own diploma thesis we got some indications that Ent3p and Ent5p have functions in the cell wall assembly, cell polarity and cell septation. These defects may partially be caused by the Chs3p trafficking defect. This enzyme is involved in the chitin synthesis of the bud neck chitin ring and the chitin dispersed in the cell wall. However, the phenotype was in *ent3Δent5Δ* cells much stronger especially in combination with SNARE mutations like *SYN8* deletion or insertion of the *vti1-2* mutation as described for *CHS3* deficient cells in the literature (Shaw *et al.*, 1991).

Yeast cells build their buds in a specific pattern dependent on the site of the last bud emerge. Haploid cells build the second and every next bud in their life cycle directly adjacent to the last one (axial budding pattern). Diploids should build the second bud at the opposite pole of the first one and emerge then further buds from both poles of the oval shaped cells (bipolar budding pattern). The budding pattern

and cell separation behavior in haploid *ent3Δent5Δ* cells transformed with overexpressing domain mutants was analyzed by calcofluor staining of the cell wall chitin (fig. 4.32 and 4.33). No significant differences to the WT could be observed for all three mutants (see also tab. 3) although the mutant constructs were not able to rescue the growth defect of the double mutant on calcofluor containing agar plates (fig. 4.35) and the decreased half-life sedimentation time (fig. 4.31). The mutant lacking the C-terminus showed the least ability for rescuing the budding patterns and cell separation abnormalities and the calcofluor accumulations of the double mutant. But since the double mutant had only partial defects and the results were very variable the defect of the ENTH mutant (without C-Term) was not within a significant range.

Diploid *ent3Δent5Δ* cells had a more severe defect in budding and cell wall assembly (Chidambaram, 2005; Zimmermann, 2006). The diploid *ent3Δent5Δ* cells were generated by mating. Therefore the mating type of the BY *ent3Δent5Δ* mutant (BKY13) was switched by a pHO plasmid encoding a endonuclease which cuts in the primary mating locus. If the primary mating locus is destroyed the cells express the opposite *MAT* gene products of the optional *MAT* locus. The HO-endonuclease is expressed under a *GAL*-promotor which is repressed by addition of glucose as present in the YEPD and SD media. To transform the diploid cells with the domain constructs the pHO plasmid had to be removed because it had an *URA* marker for selection like the Ent3p mutant plasmids. The removal was done by plasmid shuffling and the cells were stained with Calcofluor and viewed under the fluorescence microscope. For a control the diploid and haploid cells with pHO plasmid were also analyzed. From the results the pHO plasmid had some influence on the cell morphology and separation behavior of the cells (fig. 4.34). The diploid cells without pHO plasmid looked like haploid cells with an axial budding pattern. The severe defects of the strain with plasmid were lost. Also in the haploid *ent3Δent5Δ* cells with and without pHO plasmid strong differences were visible. The mating type switched mutants with plasmid had more calcofluor accumulations and more morphological defects, even though in normal haploid mutants no strong defect could be detected. The reason for the effects of the pHO plasmid are elusive. Since the cells were grown in glucose containing media no expression from the plasmid should occur. Maybe the plasmid had some toxic

effects on the cells especially in combination with the *ent3Δent5Δ* deletions. So this initial experiment shows that the domain constructs can not be analyzed in diploid cells which are generated by mating type switch. They should be checked in diploid cells generated exclusively by gene deletion (in a pure SEY/BY or a mixed background).

The result that all three domain mutants could not complement the calcofluor growth defects (25 μg/mL calcofluor) indicates that all three domains (ENTH, C-terminus and PI binding domain) were necessary for a correct chitin assembly. Since trafficking defects for Chs3p in *ent3Δent5Δ* mutants were already described it is likely that a disturbed trafficking of this enzyme is the reason for the calcofluor sensitivity. The retention of Chs3p at the TGN was not dependent on recycling from the LE but on the AP-1 dependent recycling from EE (Valdivia *et al.*, 2002). Ent3p and Ent5p have a function in this retrograde transport and may therefore induce the calcofluor sensitivity by blocking the Chs3p recycling. Contradictory to the results from the calcofluor growth test the ENTH domain and the PI binding domain were not necessary for GFP-Snc1p and GFP-Yck2p transport which were also routed via the EE to the TGN. So either the Chs3p transport works on a different mechanism or the -PI and C-term mutants had still enough functionality to sustain Snc1p and Yck2p transport but not the Chs3p trafficking. Chs3p was shown to bind directly to Ent5p (Copic *et al.*, 2007), but *ent5Δ* cells had no defect on Calcofluor plates. The trafficking assays were made with *ent3Δent5Δ* double mutants so maybe for the Chs3p transport both adaptors, Ent5p and Ent3p, have to be present for an efficient Chs3p recycling.

5.2.4 Interactions of the ENTH domain with ANTH and itself

The ENTH domain of Ent3p binds to the SNAREs and the C-terminus acts as contact surface for example for Gga2p and AP-1. I showed that the function of Ent3p in the anterograde TGN to late endosome transport depends on both domains but the retrograde EE to TGN transport only on the C-terminus. To understand how Ent3p functions it is necessary to know how it is regulated. Possible mechanisms for regulating of Ent3p are for example an autoinhibitory function by interaction with itself, a regulation by phosphorylation or both. To see if the Ent3p ENTH domain interacts with its own C-terminus the appropriate constructs were cloned into yeast two-hybrid vectors and the interaction was checked on THULL agar plates containing 3-aminotriazole. In this assay I could not detect any interaction of the ENTH domain with the C-terminus (fig. 4.36). There was a very weak auto-interaction between the ENTH domains in both vectors, but this was hard to reproduce since the ENTH domain in pLexN gave a high background signal. A stronger interaction could interestingly be observed for the ENTH domain and the ANTH domain of Ent5p. The ANTH domain interacted even stronger than the full length Ent5p and this interaction was reproducible in three experiments. This supports the data from Eugster *et al.* (2004). They could immunoprecipitate an GFP-Ent5p construct with Ent3p but since this is an *in vivo* assay they could not exclude that this interaction is indirect. My data points to a direct interaction between Ent3p and Ent5p but for a final proof the interaction should be checked by a pull down assay. Ent3p-GFP and Ent5p-RFP colocalize in fluorescence microscopy to about 30-40% (Costaguta *et al.*, 2006) and cofractionate in a gel filtration approach (Eugster *et al.*, 2004). In *vps27Δ* cells both Ent3p and Ent5p were mislocalized in the gel filtration but while the GFP-Ent5p construct was found in higher fractions (lower molecular weight complexes) Ent3p localization was shifted to even larger complexes. Costaguta *et al.*, also found some differences in Ent3p and Ent5p functions. From their interaction and localization profile with AP-1 and the Gga adaptors they propose that Ent3p acts in a more Gga2p dependent pathway and Ent5p in a AP-1 dependent transport route (Costaguta *et al.*, 2006).

Additionally Ent3p but not Ent5p showed genetic interactions with Gga2p in calcofluor sensitivity (Copic *et al.*, 2007). So it may be conceivable that Ent3p and Ent5p interact in just one pathway directly and in the other pathway(s) their interaction is genetic (by redundancy) or indirect. *ent3Δ* cells have a slight CPY defect but not *ent5Δ* cells. To rescue this defect both Ent3p domains were necessary. Also for the Chs3p transport both Ent3p domains were necessary. For the GFP-Snc1p both deletion strains have a small defect but the Ent3p C-terminus seems to be the crucial domain for this function. For GFP-Yck2p recycling and the sorbitol resistance again the C-terminus is important. There is the forward, CPY transport where both domains were needed and the retrograde transport where just the C-term. is necessary. Without ENTH domain Ent3p can not bind SNAREs and possibly also not Ent5p. Ent3p and Ent5p may function together in the forward transport and in parallel in the retrograde transport, but this hypothesis should be proven by more experiments. Additionally the membrane binding of the C-term is strongly reduced and seems therefore not to be crucial for the Ent3p function in the retrograde transport.

The SDS and NaCl sensitivity defects of the double mutant could be complemented by both Ent3p domains. Furthermore the ENTH domain alone had also some rescuing ability for the GFP-Snc1p transport and there was also some weak rescuing ability for the calcofluor sensitivity. This points to cellular mechanisms which can complement the loss of one half of Ent3p. This may be due to redundancies as suggested by Overstreet *et al.* for the *Drosophila* epsin Lqf.

5.2.5 Ent3p phosphorylation

A further or additional regulation mechanism is the phosphorylation of Ent3p. I could show via isoelectric focusing that Ent3p is phosphorylated (fig. 4.37). The assay was hard to reproduce because the inhibition of phosphatases with NaN₃ and vanadate as a crucial step to inhibit dephosphorylation was not optimal. But finally the phosphorylation could be reproduced three times by this assay. In large scale phosphorylation screens several amino acids at the Ent3p C-terminus were identified which were potentially phosphorylated. The serines S203, S294, S320, S365 and S407 were obtained in this assays but only the S203 was found in two

independent screens (Li *et al.*, 2007, Albuquerque *et al.*, 2008). Additionally the *ent3-1* mutant containing the amino acid exchanges Y60H and D202G showed defects in growth at 37°C and was deficient for sorting CPS and Phm5p into the MVB vesicles (Friant *et al.*, 2003). The MVB defects were also visible in a point mutant containing only the Y60H mutation (*ent3-2*) so that for the MVB sorting both amino acids or just the Y60 was necessary. However the D202G mutation which is directly adjacent to the potential phosphorylation site S203 seems to have an influence on the cell growth which may be another hint that this region has an important role for the Ent3p function.

A repetition of the IEF experiment with a Ent3p S203A mutant as phosphorylation insufficient and a S203D mutant which mimics constitutive phosphorylation may further support my data. In a screen for substrates of yeast kinases Ent3p was found as substrate for the two kinases Hrr25p and Mek1p (Ptacek *et al.*, 2005). The protein kinase Hrr25p is involved in various events including also protein trafficking. Mek1p is a meiosis-specific kinase and is not involved in protein transport, so it is no promising candidate for phosphorylating Ent3p. Another candidate kinase is Scy1p. The mammalian homologue of the potential kinase Scy1p is CVAK104. This kinase was shown to interact with epsinR and knock down of CVAK104 causes loss in syntaxin8 and vti1b from clathrin coated vesicles (Borner *et al.*, 2007). Interactions of Ent3p with Hrr5p or Scy1p could yield further information about the regulation of Ent3p by phosphorylation.

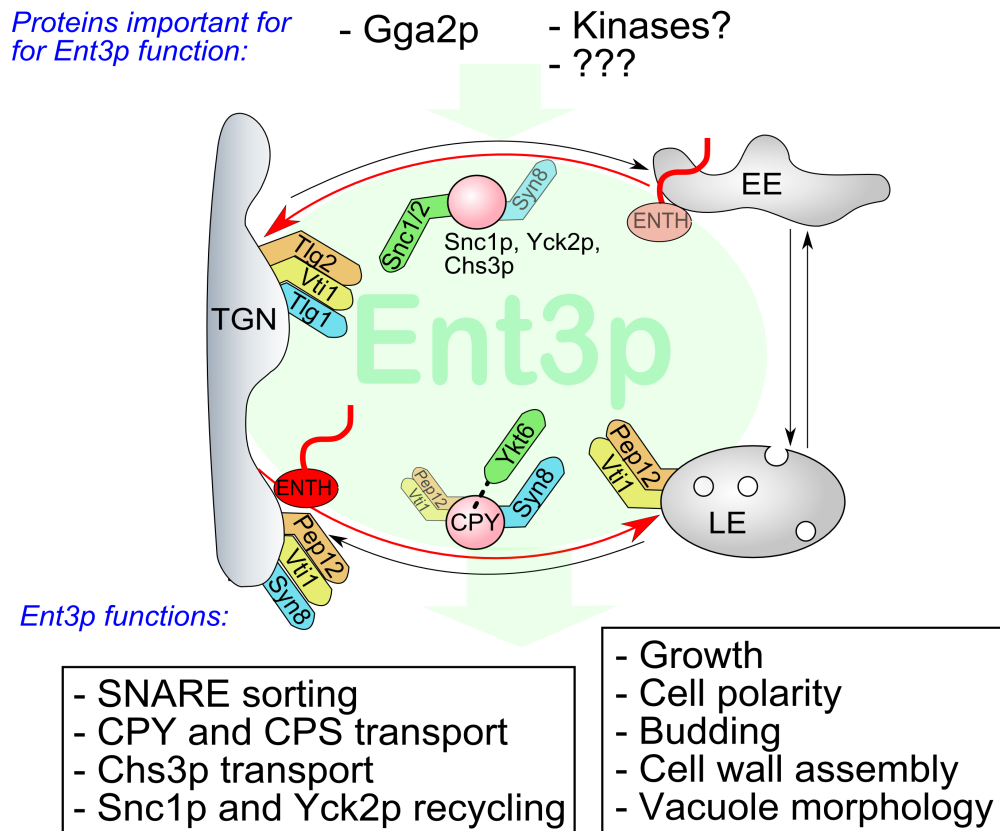


Fig. 5.2: **Functions of Ent3p in endosomal transport.** Ent3p functions in anterograde (CPY) transport from TGN to LE and retrograde EE to TGN trafficking (Snc1p, Yck2p, Chs3p recycling). The functions which are defect in *ent3Δ* or *ent3Δent5Δ* cells were written below the scheme. Proteins necessary for Ent3p function are written above. For the forward transport both Ent3p parts and in the retrograde transport just the C-terminus were necessary. Ent3p sorts Pep12p, Vti1p and Syn8p together to the late endosome. The Syn8p is a v-SNARE and cycles Ent3/5p dependent back to the TGN. The other two Q-SNAREs remain at the LE after an initial transport to this organelle.

5.3 Tvp23p and Yip4p have a function in the retrograde EE to TGN transport

5.3.1 Vti1p and Tvp23p show genetic interactions in retrograde transport.

In previous studies Tvp23p (Tlg2p compartment vesicle protein of 23 kDa) was found as suppressor of the temperature sensitive growth defect of *vti1-2* (Dilcher, 2002; Stein, 2007). Tvp23p colocalizes with Tlg2p at the late Golgi and *tvp23Δ* cells had no severe phenotype defects (including CPY and ALP trafficking). A genetic interaction with the Ras-like GTPase Ypt6p (Inadome *et al.*, 2005) and a yeast two-hybrid interaction with Ypt35p (Uetz *et al.*, 2000) were found which implicated a role in endosomal transport for Tvp23p. The interaction of Tvp23p with Yip4p and Yip5p could be proven by two independent yeast two-hybrid approaches (Uetz *et al.*, 2000, Ito *et al.* 2001) and by immunoprecipitation (Inadome *et al.*, 2007). The yeast SNARE Vti1p is involved in fusion processes at the *trans*- and *cis*-Golgi, the endosomes and the vacuole. The three temperature sensitive Vti1p mutants have each two amino exchanges in or directly before their SNARE motif. The different amino acids exchanges cause diverse defects in the different Vti1p dependent pathways (Fischer von Mollard and Stevens, 1999). Therefore it can be concluded that the mutations interfere with different Vti1p interactors. The *vti1-2* mutant has two amino acid exchanges in the SNARE motif (S130P shortly before the -7 layer of the SNARE motif and I51T in the -2 layer) and Tvp23p expressed from a 2μ plasmid suppressed the growth defect of *vti1-2* at 37°C (but not the *vti1-11* growth defect) (Stein *et al.*, 2009). No genetic interaction of *TVP23* with *VTI1-2* could be detected in CPY or ALP transport but in the growth at 37°C. Since no interaction in the forward transport was found (Stein, 2007) I analyzed the retrograde transport from early endosomes via the GFP-Snc1p recycling and from the late endosomes via A-ALP transport. Preliminary experiments were done by Anna Gottfried during her diploma thesis (Gottfried, 2007). I could reproduce her initial experiments which showed that Tvp23p and

Vti1p act together in the retrograde EE to TGN (Snc1p) transport but not in the LE to TGN (A-ALP) transport (fig. 4.38 and 4.39). I then analyzed the recycling of the GFP-Snc1p quantitatively. *vti1-2* mutants showed a reduction of GFP-Snc1p plasma membrane cells from 74% in WT to 46% in *vti1-2* mutant. This phenotype was even stronger with an additional *TVP23* deletion (35% PM stained cells). Just the *tvp23Δ* deletion caused a minor but significant defect of 68% PM stained cells ($P = 0.0043$ in Student's t-test). The less pronounced phenotype of *tvp23Δ* may be a result of a redundant protein which substitutes for Tvp23p or the protein may have regulatory functions on the EE to TGN transport.

In the retrograde late endosome to TGN transport (A-ALP transport, fig. 4.40) no defect was detectable for the *tvp23Δ* strain. So either its function is specific for the retrograde transport from the early endosomes or the defect is too small for detection with a radioactive pulse chase approach.

A direct interaction between Vti1p and Tvp23p was not tested yet. High throughput yeast two-hybrid screens did not yield such an interaction but since both proteins are transmembrane proteins a detection in such an assay would be difficult. Even specific yeast two-hybrid assays may cause severe difficulties since Tvp23p has three transmembrane domains and each cytoplasmic domain has to be tested separately. And even then this would just work if only a single loop is needed for the interaction. An alternative approach may be the split-ubiquitin yeast two-hybrid system where the interaction is tested in the cytosol (Thaminy *et al.*, 2004). In this system the N- and C-terminal parts of ubiquitin were fused to the interacting proteins and a transcription factor is additionally linked to the C-terminal ubiquitin part. When the ubiquitin parts come close together the transcription factor gets removed by ubiquitin binding proteins (UBP), is transported to the nucleus and activates the reporter genes similar to the classical yeast two-hybrid system. A co-immunoprecipitation or a co-purification (e.g. with the TAP-tag) approach could also solve the problem but if the interaction is very weak or dynamic an possible interaction may not be detectable with this method. The Tvp23p protein is conserved throughout various species from different yeasts as *S. pombe* and *K. lactis* to zebrafish, mouse and human (FAM18b) which indicates that it has a fundamental function in the cell. But non of this proteins is further characterized or a function could be proposed. Proteins with a sequence homology in yeast cells

could not be found. At least some further interaction data was obtained for Tvp23p (fig. 5.3). One interactor is the Phox homology (PX) domain containing Ypt35p. The PX domain binds phosphatidylinositides and in the case of Ypt35p a strong binding to PI(3)P could be detected (Vollert and Uetz, 2004). Ypt35p binds to several other proteins involved in endosomal or ER to Golgi transport but its concrete function is not solved yet. Among the known Ypt35p interactors were the ER to Golgi SNARE proteins Bos1p (reproducible Y2H interaction), Bet1p and Pep12p (not consistently reproducible) and members of the Yip1p family proteins Yip1p, Yip4p and Yip5p. Additionally Yif1p was found which is involved together with Yip1p in the fusion of ER-derived COPII vesicles (Barrowman *et al.*, 2003). The interactions with Yip1p, Yip4p and Yif1p were also proven by GST-pulldown assays (Vollert and Uetz, 2004). Yip4p (and Yip5p) also directly interact with Tvp23p (Inadome *et al.* 2007). There are some speculations that the Yip1p family members may act as GDI (GDP dissociation inhibitor) displacement factors for Rab GTPases as shown for the mammalian Yip3p which had a GDI displacement factor function for Rab9 (Sivars *et al.*, 2003).

Since Rabs were involved in vesicle fusion a loss of GDI displacement factor function would result in a failure in Rab activation and therefore cause a defect in vesicle fusion.

The result that the growth defect of *vti1-2* was suppressed by *TVP23* overexpression and aggravated by *TVP23* as well as the genetic interaction in the GFP-Snc1p recycling can be interpreted in two different ways. Either Vti1p and Tvp23p act in the same pathway e.g. when Tvp23p directly regulates Vti1p activity or function or they may act in different trafficking events. This would be the case if the Tvp23p would influence for example the activity of the Rab protein Ypt6p which is involved in the fusion of early endosome derived vesicles with the Golgi and was also found as interactor of Yip4p (Calero *et al.*, 2002). A better insight into this complicated protein network of the TGN fusion machinery may be obtained by investigating the function of the Yip1 family proteins Yip4p and Yip5p.

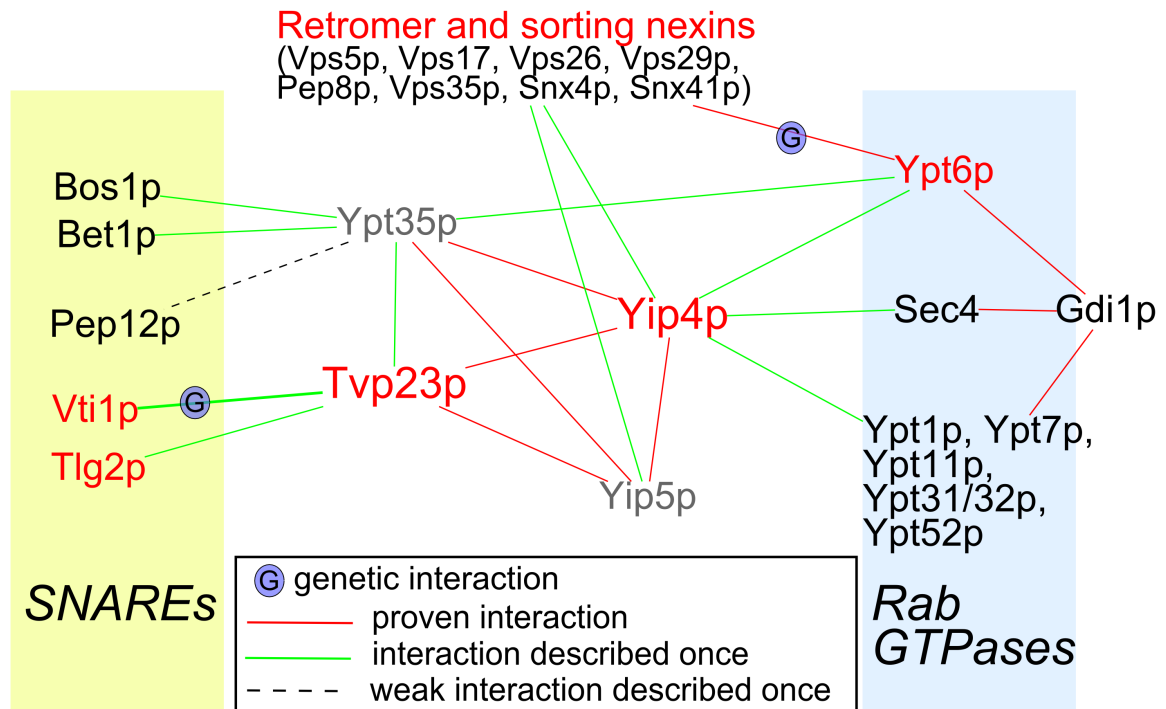


Fig. 5.3: **Interaction network of Tvp23p, Yip4p and Yip5p.** The interactions are direct physical interactions if not marked with a “G”. Proteins involved in retrograde transport where written in red letters and proteins with unknown function in grey.

5.3.2 Yip4p has a function in retrograde EE to TGN and CPY transport

The Yip1 (Ypt interacting protein) family proteins were known as interactors of various Rab GTPases. Yip3p and another family member Yif1p were selectively packed into COPII vesicles and may function as Rab regulators at the vesicle (Otte et al., 2001). As described previously there is some evidence that Yip1 family members may act as GDI (GDP dissociation inhibitor) displacement factors or at least compete with the GDIs for Rab binding. For Yip4p and Yip5p no function was characterized up to now. In my studies I showed that Yip4p but not Yip5p is involved in retrograde early endosome to TGN transport and in trafficking of CPY (fig. 4.41 and 4.42). The amount of cells with GFP-Snc1p staining was reduced from 80% in the WT and 78% in the *yip5Δ* cells to 58% in the *yip4Δ* cells. The experiment was conducted just once and should be reproduced. The light defect observed in the CPY overlay assay was comparable in strength with the defect of

ent3Δ and was reproducible in three experiments. This first experiments indicate that Yip4p may function in two pathways, the EE to TGN and TGN to LE transport. To prove that Yip4p has indeed a direct function in CPY transport from TGN to the LE the recycling of the CPY transporter Vps10p should be checked.

It would be interesting to know if there are further genetic interactions for example of *TVP23* or *VTI1* with *YIP4*. Also the interaction with the Rab GTPases could be further analyzed to prove a role in the Rab-GDI communication. Gdi1p regulates the Ypt6p function (and of several other Rabs). Ypt6p is involved in vesicle fusion events at the TGN so it is an interesting candidate for an functional interaction with Yip4p. To test if Yip4p may interfere with this Ypt6p-Gdi1p interaction the membrane association of Ypt6p could be analyzed in an *in vitro* approach.

5.4 Outlook

The loading of vesicles with functional important cargo like SNAREs is a crucial process in maintaining the cell vitality. However the research in this field is still at the beginning. I analyzed the functions of Ent3p in forward and retrograde transport. To fully understand all Ent3p functions it is necessary to understand how it is regulated. I showed that Ent3p is phosphorylated and the next step would be to find the responsible kinase(s) and to analyze how the phosphorylation influences the Ent3p functions. The role of the functional redundant Ent5p which plays also a role in endosomal transport should be further characterized since Ent3p and Ent5p seem to cooperate in at least one transport step. Investigating the functions of Ent3p in full length and its separated domains in diploid *ent3Δent5Δ* cells, which had more severe defects in budding and cell wall assembly, may clarify the functions of Ent3p in this cell division and cell wall maintaining processes.

Crystal structures of yeast Vti1p, Pep12p and Syn8p alone or in complex with Ent3p may give further hints how the interaction and therewith the sorting of this SNARE complex works.

In my work I described a first function for Tvp23p and Yip4p in retrograde endosomal transport. Still the function of Tvp23p is completely unknown and for Yip4p a function as GDI displacement factor is not analyzed. Investigating this proteins may help to understand the complicated network of proteins which are involved in anterograde and retrograde transport processes.

6 Summary

Based on the results of my diploma thesis I further investigated the interaction between the ENTH domain protein and cargo adaptor Ent3p and the endosomal SNAREs in *Saccharomyces cerevisiae*.

In a first project I identified a stretch of amino acids on the late endosomal SNARE Pep12p called the FSD motif to be necessary for the interaction with Ent3p. I identified Ent3p as the missing link between the SNARE and the Gga2p adaptor protein which plays also an important role in cargo sorting (Chidambaram *et al.*, 2008). Further I could prove that the interaction of the yeast Ent3p/Vti1p complex works on the same principles as in the mammalian epsinR/vti1b complex and was highly conserved. I characterized the interaction surface with the two other SNAREs (Pep12p and Syn8p) of the complex which was not analyzed before in the homologous mammalian complex. With mutant constructs which were deficient for the binding of 2 (of the three) SNARE partners for Ent3p I could show that these SNAREs were sorted as complex and furthermore that Syn8p is recycled as v-SNARE while Pep12p and Vti1p are t-SNAREs at the late endosome.

In another approach I analyzed the functions of Ent3p and its separated domains in the retrograde early endosome (EE) to *trans*-Golgi network (TGN) trafficking. A functional EE to TGN transport is necessary for Snc1p and Yck2p recycling. In the *ent3Δent5Δ* mutants the GFP-Snc1p recycling was almost completely and the GFP-Yck2p recycling partially blocked. The Ent3p ENTH domain binds to membranes and SNAREs. The C-terminus binds other adaptor proteins like Gga2p and clathrin but less was known about the *in vivo* function of these interactions. I showed that the C-terminus but not the ENTH domain is involved in retrograde EE to TGN transport. The Ent3p dependent transport from EE to TGN was important for cell wall assembly, cell polarity and cell separation.

In a side project I investigated the suppressor of a Vti1p mutant phenotype (*vti1-2*) Tvp23p and its interactors Yip4p and Yip5p. All three proteins were not well characterized and I proved a first function for Tvp23p (Stein *et al.*, 2009) and Yip4p but not Yip5p in the retrograde EE to TGN transport. Additionally I found that Yip4p plays a role in the transport of the carboxypeptidase Y.

Zusammenfassung

Basierend auf den Ergebnissen meiner Diplomarbeit habe ich die Interaktion zwischen dem ENTH Protein Ent3p und den endosomalen SNAREs Vti1p, Pep12p und Vti1p, weiter untersucht.

In meinem ersten Projekt habe ich ein Interaktionsmotiv, das sogenannte FSD Motiv, auf Pep12p als für die Interaktion mit Ent3p notwendig identifiziert. Damit konnte ich Ent3p als fehlendes Bindeglied zwischen Pep12p und Gga2p (einem weiteren Adaptorprotein) herausstellen (Chidambaram *et al.*, 2008). Des Weiteren konnte ich nachweisen, dass die Interaktion des Hefe Vti1p/Ent3p Komplexes nach den gleichen Prinzipien funktioniert wie die Interaktion des homologen Säugerklomplexes aus vti1b und epsinR. Ich habe die Interaktionsoberfläche auf Ent3p mit zwei weiteren SNAREs (Pep12p und Syn8p) analysiert. Über diese Interaktionen sowohl im Hefe- als auch im homologen Säugersystem war bislang nur sehr wenig bekannt. Mit Hilfe von Ent3p Mutationskonstrukten, die die Interaktion zu zwei (der drei untersuchten) endosomalen SNAREs verloren haben, konnte ich zeigen, dass diese SNAREs als Komplex sortiert werden. Zusätzlich konnte ich Syn8p als v-SNARE identifizieren, welches vom Endosom zurück zum *trans*-Golgi Netzwerk (TGN) transportiert wird sowie Pep12p und Vti1p als t-SNAREs, welche nach einmaligem anterogradem Transport am späten Endosom verbleiben.

In einem weiteren Ansatz habe ich die Funktionen von Ent3p und dessen verschiedenen Domänen im retrograden frühen Endosom (EE) zum TGN Transport untersucht. Dieser Transportweg wird für das Recycling von Snc1p und Yck2p benötigt. In der *ent3Δent5Δ* Deletionsmutante war das Recycling von GFP-Snc1p fast vollständig und das Recycling von GFP-Yck2p teilweise blockiert. Die ENTH Domäne bindet Membranen und SNAREs, der C-Terminus interagiert mit anderen Adaptorproteinen wie APs und Ggas und bindet Clathrin. Über die *in vivo* Funktionen dieser Interaktionen war bislang jedoch wenig bekannt. Ich konnte zeigen, dass der Ent3p C-Terminus, aber nicht die ENTH Domäne, für den Transportweg vom EE zurück zum TGN notwendig ist. Dieser Ent3p abhängige Transport ist notwendig für den Zellwandaufbau, Zellpolarität und Zellseparation.

In einem Nebenprojekt habe ich das Protein Tvp23p und seine Interaktionspartner Yip4p und Yip5p untersucht. Tvp23p ist ein Suppressor der temperatursensitiven Vti1p Mutante *vti1-2*. Weitere Funktionen für Tvp23p, Yip4p oder Yip5p waren bisher nicht bekannt. In dieser Arbeit konnte ich Tvp23p (Stein *et al.*, 2009) und Yip4p (nicht aber Yip5p) eine Funktion im retrograden EE zu TGN Transport zuweisen. Zusätzlich habe ich gezeigt, dass Yip4p auch eine Rolle bei dem Transport der Carboxypeptidase Y spielt.

7 Bibliography

Abeliovich, H.; Grote, E.; Novick, P.; Ferro-Novick, S. (1998). "*Tlg2p*, a yeast syntaxin homolog that resides on the Golgi and endocytic structures." J Biol Chem **19**: 11719–11727.

Aguilar, R. C.; Longhi, S. A.; Shaw, J. D.; Yeh, L.-Y.; Kim, S.; Schön, A.; Freire, E.; Hsu, A.; McCormick, W. K.; Watson, H. A.; Wendland, B. (2006). "Epsin N-terminal homology domains perform an essential function regulating Cdc42 through binding Cdc42 GTPase-activating proteins." Proc Natl Acad Sci U S A **11**: 4116–4121.

Aguilar, R. C.; Watson, H. A.; Wendland, B. (2003). "The yeast Epsin Ent1 is recruited to membranes through multiple independent interactions." J Biol Chem **12**: 10737–10743.

Albuquerque, C. P.; Smolka, M. B.; Payne, S. H.; Bafna, V.; Eng, J.; Zhou, H. (2008). "A multidimensional chromatography technology for in-depth phosphoproteome analysis" Mol. Cell Proteomics **7**: 1389–1396.

Amessou, M.; Fradagrada, A.; Falguières, T.; Lord, J. M.; Smith, D. C.; Roberts, L. M.; Lamaze, C.; Johannes, L. (2007). "Syntaxin 16 and syntaxin 5 are required for efficient retrograde transport of several exogenous and endogenous cargo proteins" J. Cell. Sci. **Pt 8**: 1457–1468.

Antonin, W.; Holroyd, C.; Fasshauer, D.; Pabst, S.; von Mollard, G. F.; Jahn, R. (2000). "A SNARE complex mediating fusion of late endosomes defines conserved properties of SNARE structure and function." EMBO J **23**: 6453–6464.

Antonin, W.; Dulubova, I.; Arac, D.; Pabst, S.; Plitzner, J.; Rizo, J.; Jahn, R. (2002). "The N-terminal domains of syntaxin 7 and *vti1b* form three-helix bundles that differ in their ability to regulate SNARE complex assembly." J Biol Chem **39**: 36449–36456.

Antonin, W.; Fasshauer, D.; Becker, S.; Jahn, R.; Schneider, T. R. (2002). "Crystal structure of the endosomal SNARE complex reveals common structural principles of all SNAREs." Nat Struct Biol **2**: 107–111.

Babu, P.; Deschenes, R. J.; Robinson, L. C. (2004). "Akr1p-dependent palmitoylation of Yck2p yeast casein kinase 1 is necessary and sufficient for plasma membrane targeting" J. Biol. Chem. **26**: 27138–27147.

Barrowman, J.; Wang, W.; Zhang, Y.; Ferro-Novick, S. (2003). "The Yip1p.Yif1p complex is required for the fusion competence of endoplasmic reticulum-derived vesicles" J. Biol. Chem. **22**: 19878–19884.

Becherer, K. A.; Rieder, S. E.; Emr, S. D.; Jones, E. W. (1996). "Novel syntaxin homologue, *Pep12p*, required for the sorting of luminal hydrolases to the lysosome-like vacuole in yeast." Mol Biol Cell **4**: 579–594.

Behnia, R.; Munro, S. (2005). "Organelle identity and the signposts for membrane traffic" Nature **7068**: 597–604.

Bénédicti, H.; Raths, S.; Crausaz, F.; Riezman, H. (1994). "The *END3* gene encodes a protein that is required for the internalization step of endocytosis and for actin cytoskeleton organization in yeast" Mol. Biol. Cell **9**: 1023–1037.

Black, M. W.; Pelham, H. R. (2000). "A selective transport route from Golgi to late endosomes that requires the yeast GGA proteins." J Cell Biol **3**: 587–600.

- Bonifacino, J. S.; Glick, B. S. (2004).** "The mechanisms of vesicle budding and fusion" *Cell* **2**: 153–166.
- Borner, G. H.H.; Rana, A. A.; Forster, R.; Harbour, M.; Smith, J. C.; Robinson, M. S. (2007).** "CVAK104 is a novel regulator of clathrin-mediated SNARE sorting" *Traffic* **7**: 893–903.
- Bowers, K.; Stevens, T. H. (2005).** "Protein transport from the late Golgi to the vacuole in the yeast *Saccharomyces cerevisiae*" *Biochim. Biophys. Acta* **3**: 438–454.
- Brady, R. J.; Wen, Y.; O'Halloran, T. J. (2008).** "The ENTH and C-terminal domains of *Dictyostelium* epsin cooperate to regulate the dynamic interaction with clathrin-coated pits" *J. Cell. Sci.* **Pt 20**: 3433–3444.
- Brandhorst, D.; Zwilling, D.; Rizzoli, S. O.; Lippert, U.; Lang, T.; Jahn, R. (2006).** "Homotypic fusion of early endosomes: SNAREs do not determine fusion specificity" *Proc. Natl. Acad. Sci. U.S.A.* **8**: 2701–2706.
- Brent, R.; Ptashne, M. (1985).** "A eukaryotic transcriptional activator bearing the DNA specificity of a prokaryotic repressor" *Cell* **3 Pt 2**: 729–736.
- Brickner, J. H.; Blanchette, J. M.; Sipos, G.; Fuller, R. S. (2001).** "The Tlg SNARE complex is required for TGN homotypic fusion" *J. Cell Biol.* **6**: 969–978.
- Burston, H. E.; Maldonado-Báez, L.; Davey, M.; Montpetit, B.; Schluter, C.; Wendland, B.; Conibear, E. (2009).** "Regulators of yeast endocytosis identified by systematic quantitative analysis" *J. Cell Biol.* **6**: 1097–1110.
- Cabib, E.; Silverman, S. J.; Shaw, J. A. (1992).** "Chitinase and chitin synthase 1: counterbalancing activities in cell separation of *Saccharomyces cerevisiae*" *J. Gen. Microbiol.* **1**: 97–102.
- Calero, M.; Winand, N. J.; Collins, R. N. (2002).** "Identification of the novel proteins Yip4p and Yip5p as Rab GTPase interacting factors." *FEBS Lett* **1-3**: 89–98.
- Chant, J.; Pringle, J. R. (1991).** "Budding and cell polarity in *Saccharomyces cerevisiae*" *Curr. Opin. Genet. Dev.* **3**: 342–350.
- Cheever, M. L.; Sato, T. K.; Beer, T. de; Kutateladze, T. G.; Emr, S. D.; Overduin, M. (2001).** "Phox domain interaction with PtdIns(3)P targets the Vam7 t-SNARE to vacuole membranes" *Nat. Cell Biol.* **7**: 613–618.
- Chidambaram, S. (2005).** "Characterization of ENTH domain proteins and their interaction with SNAREs in *S. cerevisiae*" *Dissertation*.
- Chidambaram, S.; Müllers, N.; Wiederhold, K.; Haucke, V.; von Mollard, G. F. (2004).** "Specific interaction between SNAREs and epsin N-terminal homology (ENTH) domains of epsin-related proteins in trans-Golgi network to endosome transport." *J Biol Chem* **6**: 4175–4179.
- Chidambaram, S.; Zimmermann, J.; von Mollard, G. F. (2008).** "ENTH domain proteins are cargo adaptors for multiple SNARE proteins at the TGN endosome" *J. Cell. Sci.* **Pt 3**: 329–338.
- Cooper, A. A.; Stevens, T. H. (1996).** "Vps10p cycles between the late-Golgi and prevacuolar compartments in its function as the sorting receptor for multiple yeast vacuolar hydrolases" *J. Cell Biol.* **3**: 529–541.
- Copic, A.; Starr, T. L.; Schekman, R. (2007).** "Ent3p and Ent5p exhibit cargo-specific functions in trafficking proteins between the trans-Golgi network and the endosomes in yeast." *Mol Biol Cell* **5**: 1803–1815.

- Costaguta, G.; Duncan, M. C.; Fernández, G. E.; Huang, G. H.; Payne, G. S. (2006). "Distinct roles for TGN/endosome epsin-like adaptors *Ent3p* and *Ent5p*." *Mol Biol Cell* **9**: 3907–3920.
- Deng, Y.; Guo, Y.; Watson, H.; Au, W.-C.; Shakoury-Elizeh, M.; Basrai, M. A.; Bonifacino, J. S.; Philpott, C. C. (2009). "Gga2 mediates sequential ubiquitin-independent and ubiquitin-dependent steps in the trafficking of ARN1 from the trans-Golgi network to the vacuole" *J. Biol. Chem.* **35**: 23830–23841.
- Dilcher, M.; Köhler, B.; von Mollard, G. F. (2001). "Genetic interactions with the yeast Q-SNARE *Vti1* reveal novel functions for the R-SNARE *Ykt6*." *J Biol Chem* **37**: 34537–34544.
- Dilcher, M. (2002). "Charakterisierung von SNARE-Proteinen in der Hefe *Saccharomyces cerevisiae*" *Dissertation*.
- Dove, S. K.; McEwen, R. K.; Mayes, A.; Hughes, D. C.; Beggs, J. D.; Michell, R. H. (2002). "Vac14 controls *PtdIns(3,5)P(2)* synthesis and *Fab1*-dependent protein trafficking to the multivesicular body" *Curr. Biol.* **11**: 885–893.
- Dulubova, I.; Sugita, S.; Hill, S.; Hosaka, M.; Fernandez, I.; Südhof, T. C.; Rizo, J. (1999). "A conformational switch in syntaxin during exocytosis: role of *munc18*" *EMBO J.* **16**: 4372–4382.
- Duncan, M. C.; Costaguta, G.; Payne, G. S. (2003). "Yeast epsin-related proteins required for Golgi-endosome traffic define a gamma-adaptin ear-binding motif." *Nat Cell Biol* **1**: 77–81.
- Duncan, M. C.; Payne, G. S. (2003). "ENTH/ANTH domains expand to the Golgi." *Trends Cell Biol* **5**: 211–215.
- Escamilla, M.; Lee, B. D.; Ontiveros, A.; Raventos, H.; Nicolini, H.; Mendoza, R.; Jerez, A.; Munoz, R.; Medina, R.; Figueroa, A.; Walss-Bass, C.; Armas, R.; Contreras, S.; Ramirez, M. E.; Dassori, A. (2008). "The epsin 4 gene is associated with psychotic disorders in families of Latin American origin" *Schizophr. Res.* **2-3**: 253–257.
- Eugster, A.; Pécheur, E.-I.; Michel, F.; Winsor, B.; Letourneur, F.; Friant, S. (2004). "*Ent5p* is required with *Ent3p* and *Vps27p* for ubiquitin-dependent protein sorting into the multivesicular body." *Mol Biol Cell* **7**: 3031–3041.
- Fiedler, D.; Braberg, H.; Mehta, M.; Chechik, G.; Cagney, G.; Mukherjee, P.; Silva, A. C.; Shales, M.; Collins, S. R.; van Wageningen, S.; Kemmeren, P.; Holstege, F. C.P.; Weissman, J. S.; Keogh, M.-C.; Koller, D.; Shokat, K. M.; Krogan, N. J. (2009). "Functional organization of the *S. cerevisiae* phosphorylation network" *Cell* **5**: 952–963.
- Filippini, F.; Rossi, V.; Galli, T.; Budillon, A.; D'Urso, M.; D'Esposito, M. (2001). "Longins: a new evolutionary conserved VAMP family sharing a novel SNARE domain" *Trends Biochem. Sci.* **7**: 407–409.
- Fischer von Mollard, G.; Nothwehr, S. F.; Stevens, T. H. (1997). "The yeast v-SNARE *Vti1p* mediates two vesicle transport pathways through interactions with the t-SNAREs *Sed5p* and *Pep12p*." *J Cell Biol* **7**: 1511–1524.
- Fischer von Mollard, G.; Stevens, T. H. (1999). "The *Saccharomyces cerevisiae* v-SNARE *Vti1p* is required for multiple membrane transport pathways to the vacuole." *Mol Biol Cell* **6**: 1719–1732.
- Foote, C.; Nothwehr, S. F. (2006). "The clathrin adaptor complex 1 directly binds to a sorting signal in *Ste13p* to reduce the rate of its trafficking to the late endosome of yeast" *J. Cell Biol.* **4**: 615–626.

- Ford, M. G.; Pearse, B. M.; Higgins, M. K.; Vallis, Y.; Owen, D. J.; Gibson, A.; Hopkins, C. R.; Evans, P. R.; McMahon, H. T. (2001). "Simultaneous binding of PtdIns(4,5)P₂ and clathrin by AP180 in the nucleation of clathrin lattices on membranes" *Science* **5506**: 1051–1055.
- Ford, M. G.J.; Mills, I. G.; Peter, B. J.; Vallis, Y.; Praefcke, G. J. K.; Evans, P. R.; McMahon, H. T. (2002). "Curvature of clathrin-coated pits driven by epsin" *Nature* **6905**: 361–366.
- Friant, S.; Pécheur, E. I.; Eugster, A.; Michel, F.; Lefkir, Y.; Nourrisson, D.; Letourneur, F. (2003). "Ent3p Is a PtdIns(3,5)P₂ effector required for protein sorting to the multivesicular body." *Dev Cell* **3**: 499–511.
- Gerrard, S. R.; Levi, B. P.; Stevens, T. H. (2000). "Pep12p is a multifunctional yeast syntaxin that controls entry of biosynthetic, endocytic and retrograde traffic into the prevacuolar compartment" *Traffic* **3**: 259–269.
- Gordon, D. E.; Mirza, M.; Sahlender, D. A.; Jakovleska, J.; Peden, A. A. (2009). "Coiled-coil interactions are required for post-Golgi R-SNARE trafficking" *EMBO Rep.* **8**: 851–856.
- Gottfried, A. (2007). "Untersuchung des endosomalen Transports in Hefe zur Analyse der Funktion von Tvp23p" *Diploma thesis*.
- Halic, M.; Beckmann, R. (2005). "The signal recognition particle and its interactions during protein targeting" *Curr. Opin. Struct. Biol.* **1**: 116–125.
- Hasilik, A.; Tanner, W. (1978). "Biosynthesis of the vacuolar yeast glycoprotein carboxypeptidase Y. Conversion of precursor into the enzyme" *Eur. J. Biochem.* **2**: 599–608.
- Hayashi, R. (1976). "Carboxypeptidase Y" *Meth. Enzymol.*: 568–587.
- Hess, D. T.; Slater, T. M.; Wilson, M. C.; Skene, J. H. (1992). "The 25 kDa synaptosomal-associated protein SNAP-25 is the major methionine-rich polypeptide in rapid axonal transport and a major substrate for palmitoylation in adult CNS" *J. Neurosci.* **12**: 4634–4641.
- Hettema, E. H.; Lewis, M. J.; Black, M. W.; Pelham, H. R. B. (2003). "Retromer and the sorting nexins Snx4/41/42 mediate distinct retrieval pathways from yeast endosomes." *EMBO J* **3**: 548–557.
- Hinners, I.; Wendler, F.; Fei, H.; Thomas, L.; Thomas, G.; Tooze, S. A. (2003). "AP-1 recruitment to VAMP4 is modulated by phosphorylation-dependent binding of PACS-1" *EMBO Rep.* **12**: 1182–1189.
- Hirst, J.; Miller, S. E.; Taylor, M. J.; von Mollard, G. F.; Robinson, M. S. (2004). "EpsinR is an adaptor for the SNARE protein Vti1b." *Mol Biol Cell* **12**: 5593–5602.
- Hirst, J.; Motley, A.; Harasaki, K.; Peak Chew, S. Y.; Robinson, M. S. (2003). "EpsinR: an ENTH domain-containing protein that interacts with AP-1." *Mol Biol Cell* **2**: 625–641.
- Inadome, H.; Noda, Y.; Adachi, H.; Yoda, K. (2005). "Immunoisolation of the yeast Golgi subcompartments and characterization of a novel membrane protein, Svp26, discovered in the Sed5-containing compartments." *Mol Cell Biol* **17**: 7696–7710.
- Inadome, H.; Noda, Y.; Kamimura, Y.; Adachi, H.; Yoda, K. (2007). "Tvp38, Tvp23, Tvp18 and Tvp15: novel membrane proteins in the Tlg2-containing Golgi/endosome compartments of *Saccharomyces cerevisiae*." *Exp Cell Res* **4**: 688–697.
- Itoh, T.; Koshiba, S.; Kigawa, T.; Kikuchi, A.; Yokoyama, S.; Takenawa, T. (2001). "Role of the ENTH domain in phosphatidylinositol-4,5-bisphosphate binding and endocytosis." *Science* **5506**: 1047–1051.

- Jahn, R.; Scheller, R. H. (2006). "SNAREs—engines for membrane fusion." *Nat Rev Mol Cell Biol* **9**: 631–643.
- Jun, Y.; Xu, H.; Thorngren, N.; Wickner, W. (2007). "Sec18p and Vam7p remodel trans-SNARE complexes to permit a lipid-anchored R-SNARE to support yeast vacuole fusion" *EMBO J.* **24**: 4935–4945.
- Kalthoff, C.; Groos, S.; Kohl, R.; Mahrhold, S.; Ungewickell, E. J. (2002). "Clint: a novel clathrin-binding ENTH-domain protein at the Golgi." *Mol Biol Cell* **11**: 4060–4073.
- Klionsky, D. J.; Emr, S. D. (1989). "Membrane protein sorting: biosynthesis, transport and processing of yeast vacuolar alkaline phosphatase" *EMBO J.* **8**: 2241–2250.
- Koshiba, S.; Kigawa, T.; Kikuchi, A.; Yokoyama, S. (2003). "Solution structure of the epsin N-terminal homology (ENTH) domain of human epsin." *J Struct Funct Genomics* **1**: 1–8.
- Kweon, D.-H.; Shin, Y.-K.; Shin, J. Y.; Lee, J.-H.; Lee, J.-B.; Seo, J.-H.; Kim, Y. S. (2006). "Membrane topology of helix 0 of the Epsin N-terminal homology domain." *Mol Cells* **3**: 428–435.
- Kweon, Y.; Rothe, A.; Conibear, E.; Stevens, T. H. (2003). "Ykt6p is a multifunctional yeast R-SNARE that is required for multiple membrane transport pathways to the vacuole" *Mol. Biol. Cell* **5**: 1868–1881.
- Legendre-Guillemain, V.; Wasiak, S.; Hussain, N. K.; Angers, A.; McPherson, P. S. (2003). "ENTH/ANTH proteins and clathrin-mediated membrane budding." *J Cell Sci Pt* **1**: 9–18.
- Lewis, M. J.; Nichols, B. J.; Prescianotto-Baschong, C.; Riezman, H.; Pelham, H. R. (2000). "Specific retrieval of the exocytic SNARE Snc1p from early yeast endosomes" *Mol. Biol. Cell* **1**: 23–38.
- Lewis, M. J.; Pelham, H. R. B. (2002). "A new yeast endosomal SNARE related to mammalian syntaxin 8." *Traffic* **12**: 922–929.
- Li, X.; Gerber, S. A.; Rudner, A. D.; Beausoleil, S. A.; Haas, W.; Villén, J.; Elias, J. E.; Gygi, S. P. (2007). "Large-scale phosphorylation analysis of alpha-factor-arrested *Saccharomyces cerevisiae*" *J. Proteome Res.* **3**: 1190–1197.
- Lipke, P. N.; Ovalle, R. (1998). "Cell wall architecture in yeast: new structure and new challenges" *J. Bacteriol.* **15**: 3735–3740.
- Logg, K.; Warringer, J.; Hashemi, S. H.; Käll, M.; Blomberg, A. (2008). "The sodium pump *Ena1p* provides mechanistic insight into the salt sensitivity of vacuolar protein sorting mutants" *Biochim. Biophys. Acta* **6**: 974–984.
- Lupashin, V. V.; Pokrovskaya, I. D.; McNew, J. A.; Waters, M. G. (1997). "Characterization of a novel yeast SNARE protein implicated in Golgi retrograde traffic" *Mol. Biol. Cell* **12**: 2659–2676.
- Mao, Y.; Chen, J.; Maynard, J. A.; Zhang, B.; Quioco, F. A. (2001). "A novel all helix fold of the AP180 amino-terminal domain for phosphoinositide binding and clathrin assembly in synaptic vesicle endocytosis" *Cell* **3**: 433–440.
- Mayer, A.; Wickner, W.; Haas, A. (1996). "Sec18p (NSF)-driven release of Sec17p (alpha-SNAP) can precede docking and fusion of yeast vacuoles" *Cell* **1**: 83–94.
- Medigeschi, G. R.; Schu, P. (2003). "Characterization of the *in vitro* retrograde transport of MPR46" *Traffic* **11**: 802–811.
- Meiringer, C. T.A.; Auffarth, K.; Hou, H.; Ungermann, C. (2008). "Depalmitoylation of Ykt6 prevents its entry into the multivesicular body pathway" *Traffic* **9**: 1510–1521.

- Michell, R. H.; Heath, V. L.; Lemmon, M. A.; Dove, S. K. (2006). "Phosphatidylinositol 3,5-bisphosphate: metabolism and cellular functions" *Trends Biochem. Sci.* **1**: 52–63.
- Miller, S. E.; Collins, B. M.; McCoy, A. J.; Robinson, M. S.; Owen, D. J. (2007). "A SNARE-adaptor interaction is a new mode of cargo recognition in clathrin-coated vesicles." *Nature* **7169**: 570–574.
- Mills, I. G.; Praefcke, G. J. K.; Vallis, Y.; Peter, B. J.; Olesen, L. E.; Gallop, J. L.; Butler, P. J. G.; Evans, P. R.; McMahon, H. T. (2003). "EpsinR: an AP1/clathrin interacting protein involved in vesicle trafficking." *J Cell Biol* **2**: 213–222.
- Mossessova, E.; Bickford, L. C.; Goldberg, J. (2003). "SNARE selectivity of the COPII coat" *Cell* **4**: 483–495.
- Mukherjee, D.; Coon, B. G.; Edwards, D. F.; Hanna, C. B.; Longhi, S. A.; McCaffery, J. M.; Wendland, B.; Retegui, L. A.; Bi, E.; Aguilar, R. C. (2009). "The yeast endocytic protein Epsin 2 functions in a cell-division signaling pathway" *J. Cell. Sci. Pt* **14**: 2453–2463.
- Nakamura, N.; Yamamoto, A.; Wada, Y.; Futai, M. (2000). "Syntaxin 7 mediates endocytic trafficking to late endosomes." *J Biol Chem* **9**: 6523–6529.
- Narayan, K.; Lemmon, M. A. (2006). "Determining selectivity of phosphoinositide-binding domains" *Methods* **2**: 122–133.
- Nasmyth, K. A. (1982). "The regulation of yeast mating-type chromatin structure by SIR: an action at a distance affecting both transcription and transposition" *Cell* **2**: 567–578.
- Ni, L.; Snyder, M. (2001). "A genomic study of the bipolar bud site selection pattern in *Saccharomyces cerevisiae*" *Mol. Biol. Cell* **7**: 2147–2170.
- Nothwehr, S. F.; Hines, A. E. (1997). "The yeast VPS5/GRD2 gene encodes a sorting nexin-1-like protein required for localizing membrane proteins to the late Golgi" *J. Cell. Sci.*: 1063–1072.
- Nothwehr, S. F.; Roberts, C. J.; Stevens, T. H. (1993). "Membrane protein retention in the yeast Golgi apparatus: dipeptidyl aminopeptidase A is retained by a cytoplasmic signal containing aromatic residues" *J. Cell Biol.* **6**: 1197–1209.
- Ohno, H.; Stewart, J.; Fournier, M. C.; Bosshart, H.; Rhee, I.; Miyatake, S.; Saito, T.; Gallusser, A.; Kirchhausen, T.; Bonifacino, J. S. (1995). "Interaction of tyrosine-based sorting signals with clathrin-associated proteins" *Science* **5232**: 1872–1875.
- Ohya, T.; Miaczynska, M.; Coskun, U.; Lommer, B.; Runge, A.; Drechsel, D.; Kalaidzidis, Y.; Zerial, M. (2009). "Reconstitution of Rab- and SNARE-dependent membrane fusion by synthetic endosomes" *Nature* **7250**: 1091–1097.
- Otte, S.; Belden, W. J.; Heidtman, M.; Liu, J.; Jensen, O. N.; Barlowe, C. (2001). "Erv41p and Erv46p: new components of COPII vesicles involved in transport between the ER and Golgi complex" *J. Cell Biol.* **3**: 503–518.
- Overstreet, E.; Chen, X.; Wendland, B.; Fischer, J. A. (2003). "Either part of a *Drosophila* epsin protein, divided after the ENTH domain, functions in endocytosis of delta in the developing eye" *Curr. Biol.* **10**: 854–860.
- Panek, H. R.; Conibear, E.; Bryan, J. D.; Colvin, R. T.; Goshorn, C. D.; Robinson, L. C. (2000). "Identification of Rgp1p, a novel Golgi recycling factor, as a protein required for efficient localization of yeast casein kinase 1 to the plasma membrane" *J. Cell. Sci.*: 4545–4555.
- Peterson, M. R.; Emr, S. D. (2001). "The class C Vps complex functions at multiple stages of the vacuolar transport pathway" *Traffic* **7**: 476–486.

- Pimm, J.; McQuillin, A.; Thirumalai, S.; Lawrence, J.; Queded, D.; Bass, N.; Lamb, G.; Moorey, H.; Datta, S. R.; Kalsi, G.; Badacsonyi, A.; Kelly, K.; Morgan, J.; Punukollu, B.; Curtis, D.; Gurling, H. (2005). "The Epsin 4 gene on chromosome 5q, which encodes the clathrin-associated protein enthoprotin, is involved in the genetic susceptibility to schizophrenia" *Am. J. Hum. Genet.* **5**: 902–907.
- Piper, R. C.; Bryant, N. J.; Stevens, T. H. (1997). "The membrane protein alkaline phosphatase is delivered to the vacuole by a route that is distinct from the VPS-dependent pathway" *J. Cell Biol.* **3**: 531–545.
- Pringle, J. R. (1991). "Staining of bud scars and other cell wall chitin with calcofluor" *Meth. Enzymol.* **732**–735.
- Pruyne, D.; Bretscher, A. (2000). "Polarization of cell growth in yeast" *J. Cell. Sci.* **571**–585.
- Pryor, P. R.; Jackson, L.; Gray, S. R.; Edeling, M. A.; Thompson, A.; Sanderson, C. M.; Evans, P. R.; Owen, D. J.; Luzio, J. P. (2008). "Molecular basis for the sorting of the SNARE VAMP7 into endocytic clathrin-coated vesicles by the ArfGAP Hrb" *Cell* **5**: 817–827.
- Ptacek, J.; Devgan, G.; Michaud, G.; Zhu, H.; Zhu, X.; Fasolo, J.; Guo, H.; Jona, G.; Breitskreutz, A.; Sopko, R.; McCartney, R. R.; Schmidt, M. C.; Rachidi, N.; Lee, S.-J.; Mah, A. S.; Meng, L.; Stark, M. J.R.; Stern, D. F.; Virgilio, C. de; Tyers, M.; Andrews, B.; Gerstein, M.; Schweitzer, B.; Predki, P. F.; Snyder, M. (2005). "Global analysis of protein phosphorylation in yeast" *Nature* **7068**: 679–684.
- Pylypenko, O.; Schönichen, A.; Ludwig, D.; Ungermann, C.; Goody, R. S.; Rak, A.; Geyer, M. (2008). "Farnesylation of the SNARE protein Ykt6 increases its stability and helical folding" *J. Mol. Biol.* **5**: 1334–1345.
- Raymond, C. K.; Howald-Stevenson, I.; Vater, C. A.; Stevens, T. H. (1992). "Morphological classification of the yeast vacuolar protein sorting mutants: evidence for a prevacuolar compartment in class E vps mutants" *Mol. Biol. Cell* **12**: 1389–1402.
- Ritter, B.; McPherson, P. S. (2006). "There's a GAP in the ENTH domain." *Proc Natl Acad Sci U S A* **11**: 3953–3954.
- Robinson, J. S.; Klionsky, D. J.; Banta, L. M.; Emr, S. D. (1988). "Protein sorting in *Saccharomyces cerevisiae*: isolation of mutants defective in the delivery and processing of multiple vacuolar hydrolases" *Mol. Cell. Biol.* **11**: 4936–4948.
- Robinson, L. C.; Bradley, C.; Bryan, J. D.; Jerome, A.; Kweon, Y.; Panek, H. R. (1999). "The Yck2 yeast casein kinase 1 isoform shows cell cycle-specific localization to sites of polarized growth and is required for proper septin organization" *Mol. Biol. Cell* **4**: 1077–1092.
- Robinson, L. C.; Bradley, C.; Bryan, J. D.; Jerome, A.; Kweon, Y.; Panek, H. R. (1999). "The Yck2 yeast casein kinase 1 isoform shows cell cycle-specific localization to sites of polarized growth and is required for proper septin organization" *Mol. Biol. Cell* **4**: 1077–1092.
- Rosenthal, J. A.; Chen, H.; Slepnev, V. I.; Pellegrini, L.; Salcini, A. E.; Di Fiore, P. P.; De Camilli, P. (1999). "The epsins define a family of proteins that interact with components of the clathrin coat and contain a new protein module." *J Biol Chem* **48**: 33959–33965.
- Rossi, V.; Banfield, D. K.; Vacca, M.; Dietrich, L. E.P.; Ungermann, C.; D'Esposito, M.; Galli, T.; Filippini, F. (2004). "Longins and their longin domains: regulated SNAREs and multifunctional SNARE regulators" *Trends Biochem. Sci.* **12**: 682–688.

- Rothman, J. E.; Wieland, F. T. (1996). "Protein sorting by transport vesicles" *Science* **5259**: 227–234.
- Saint-Pol, A.; Yélamos, B.; Amessou, M.; Mills, I. G.; Dugast, M.; Tenza, D.; Schu, P.; Antony, C.; McMahon, H. T.; Lamaze, C.; Johannes, L. (2004). "Clathrin adaptor epsinR is required for retrograde sorting on early endosomal membranes." *Dev Cell* **4**: 525–538.
- Schwartz, S. L.; Cao, C.; Pylypenko, O.; Rak, A.; Wandinger-Ness, A. (2007). "Rab GTPases at a glance" *J. Cell. Sci.* Pt **22**: 3905–3910.
- Shakoori, A.; Fujii, G.; Yoshimura, S.-I.; Kitamura, M.; Nakayama, K.; Ito, T.; Ohno, H.; Nakamura, N. (2003). "Identification of a five-pass transmembrane protein family localizing in the Golgi apparatus and the ER" *Biochem. Biophys. Res. Commun.* **3**: 850–857.
- Shaw, J. A.; Mol, P. C.; Bowers, B.; Silverman, S. J.; Valdivieso, M. H.; Durán, A.; Cabib, E. (1991). "The function of chitin synthases 2 and 3 in the *Saccharomyces cerevisiae* cell cycle" *J. Cell Biol.* **1**: 111–123.
- Sheu, Y. J.; Santos, B.; Fortin, N.; Costigan, C.; Snyder, M. (1998). "Spa2p interacts with cell polarity proteins and signaling components involved in yeast cell morphogenesis" *Mol. Cell. Biol.* **7**: 4053–4069.
- Sivars, U.; Aivazian, D.; Pfeffer, S. R. (2003). "Yip3 catalyses the dissociation of endosomal Rab-GDI complexes" *Nature* **6960**: 856–859.
- Stahelin, R. V.; Long, F.; Peter, B. J.; Murray, D.; De Camilli, P.; McMahon, H. T.; Cho, W. (2003). "Contrasting membrane interaction mechanisms of AP180 N-terminal homology (ANTH) and epsin N-terminal homology (ENTH) domains." *J Biol Chem* **31**: 28993–28999.
- Stein, I. S. (2007). "Identifikation von Interaktionspartnern des Hefe SNAREs Vti1p mittels Suppressor-Screening und Funktionsanalyse durch Herstellung und Charakterisierung von Mutanten" *Diploma thesis*.
- Stein, I. S.; Gottfried, A.; Zimmermann, J.; Fischer Mollard, G. von (2009). "TVP23 interacts genetically with the yeast SNARE VT11 and functions in retrograde transport from the early endosome to the late Golgi" *Biochem. J.* **1**: 229–236.
- Sutton, R. B.; Fasshauer, D.; Jahn, R.; Brunger, A. T. (1998). "Crystal structure of a SNARE complex involved in synaptic exocytosis at 2.4 Å resolution." *Nature* **6700**: 347–353.
- Thaminy, S.; Miller, J.; Stagljar, I. (2004). "The split-ubiquitin membrane-based yeast two-hybrid system" *Methods Mol. Biol.*: 297–312.
- Tishgarten, T.; Yin, F. F.; Faucher, K. M.; Dluhy, R. A.; Grant, T. R.; Fischer von Mollard, G.; Stevens, T. H.; Lipscomb, L. A. (1999). "Structures of yeast vesicle trafficking proteins." *Protein Sci* **11**: 2465–2473.
- Toret, C. P.; Lee, L.; Sekiya-Kawasaki, M.; Drubin, D. G. (2008). "Multiple pathways regulate endocytic coat disassembly in *Saccharomyces cerevisiae* for optimal downstream trafficking" *Traffic* **5**: 848–859.
- Valdez-Taubas, J.; Pelham, H. (2005). "Swf1-dependent palmitoylation of the SNARE Tlg1 prevents its ubiquitination and degradation" *EMBO J.* **14**: 2524–2532.
- Valdivia, R. H.; Schekman, R. (2003). "The yeasts *Rho1p* and *Pkc1p* regulate the transport of chitin synthase III (*Chs3p*) from internal stores to the plasma membrane" *Proc. Natl. Acad. Sci. U.S.A.* **18**: 10287–10292.

- Valdivieso, M. H.; Mol, P. C.; Shaw, J. A.; Cabib, E.; Durán, A. (1991).** "CAL1, a gene required for activity of chitin synthase 3 in *Saccharomyces cerevisiae*" *J. Cell Biol.* **1**: 101–109.
- Vollert, C. S.; Uetz, P. (2004).** "The phox homology (PX) domain protein interaction network in yeast" *Mol. Cell Proteomics* **11**: 1053–1064.
- Watson, H. A.; Cope, M. J.; Groen, A. C.; Drubin, D. G.; Wendland, B. (2001).** "In vivo role for actin-regulating kinases in endocytosis and yeast epsin phosphorylation." *Mol Biol Cell* **11**: 3668–3679.
- Wendland, B.; Steece, K. E.; Emr, S. D. (1999).** "Yeast epsins contain an essential N-terminal ENTH domain, bind clathrin and are required for endocytosis." *EMBO J* **16**: 4383–4393.
- Xu, H.; Wickner, W. (2006).** "Bem1p is a positive regulator of the homotypic fusion of yeast vacuoles" *J. Biol. Chem.* **37**: 27158–27166.
- Xu, Y.; Seet, L. F.; Hanson, B.; Hong, W. (2001).** "The Phox homology (PX) domain, a new player in phosphoinositide signalling." *Biochem J Pt 3*: 513–530.
- Yang, S.; Ayscough, K. R.; Drubin, D. G. (1997).** "A role for the actin cytoskeleton of *Saccharomyces cerevisiae* in bipolar bud-site selection" *J. Cell Biol.* **1**: 111–123.
- Yoshida, Y.; Suzuki, K.; Yamamoto, A.; Sakai, N.; Bando, M.; Tanimoto, K.; Yamaguchi, Y.; Sakaguchi, T.; Akhter, H.; Fujii, G.; Yoshimura, S.-I.; Ogata, S.; Sohda, M.; Misumi, Y.; Nakamura, N. (2008).** "YIPF5 and YIF1A recycle between the ER and the Golgi apparatus and are involved in the maintenance of the Golgi structure" *Exp. Cell Res.* **19**: 3427–3443.
- Zimmermann, J. (2006).** "Interaktionen von Ent3p und Ent5p mit endosomalen SNAREs und deren Funktion bei der Zellwandsynthese in *S. cerevisiae*" *Diploma thesis*.

Appendix

I Oligonucleotides

Tab. 4: Oligonucleotides

Theme	Oligo	Sequence	T m	Experiment	Dig. site
1	SH103	GCAGAGCTTCACCATTGA	45	forward Sequencing primer for pLexN	
1	SH88	CTTTAAGYGGGCTTAA	45	reverse Sequencing primer for pLexN	
1	SP6m	CGCCAAGCTATTTAGGTGACAC		Rev. sequencing primer for pGEM T-easy	
1	T7	GTAATACGACTCACTATAGGGC		fw. sequencing primer for pGEM T-easy	
1	T7e	TAATACGACTCACTATAGGG		forward sequencing primer for pET28b	
1	T3e	ATTAACCTCACTAAAGGGA	56	reverse sequencing primer for pET28b	
2	Ent3 172 Bam	CGGGATCCTTATCCAGCAACGCCCTTGAC	55	Cloning Ent3p ENTH domain (binds at 516)	<i>BamHI</i>
2	Ent3 250 f	AGTGGAGGCAAATTTATAAAGC	55	Internal <i>ENT3</i> primer for sequencing, starts at 250bp	
2	Ent3 28	GCCATGGGTAATTATACTGAGATGGAGGGGA AAGTTCG	57	Cloning of ENT3 N28-408	<i>NcoI</i>
2	Ent3 Aux3	TTATAAAACATTTACATATTGTGTAAACCAA TAATATCACGGTATTTACACCCGATA	53	Deletion of <i>ENT3</i>	<i>BamHI</i>
2	Ent3 Aux5	CGTCGATAGGAGATCACATCGTTAATTAGTG TTAGGAAGATTGTAAGTGCACCAT	53	Deletion of <i>ENT3</i>	<i>EcoRI</i>
2	Ent3 D60f	CAAGGAACTGACAATTTCAAGGAAAG	54	Site directed mutagenesis: Ent3 Y60D	
2	Ent3 D60r	CCCTGAAATTGTCAGTTCCTTGAGAAATC	54	Site directed mutagenesis: Ent3 Y60D	
2	Ent3 D62f	GGAACCTACAATGACAGGAAAGAGAAGAAA TTTTG	55	Site directed mutagenesis: Ent3 F62D	
2	Ent3 D62r	TCCCTGTCATTGTAAGTTCCTTGAGAAATC	55	Site directed mutagenesis: Ent3 F62D	
2	Ent3 del3	TGAAGGGCACTTCAACTCTCGA	59	Deletion of 'ENT3	
2	Ent3 del5	CCATTTTGCTAAGCCAATTCAGC	59	Deletion of 'ENT3	
2	Ent3 E154f	CGATAATAAGATAGAAGCAGAAAGAAAAAG G	54	Site directed mutagenesis: Ent3 R154E	
2	Ent3 E154r	TTTCTTTCTGCTTCTATCTTATTATCGTCGC	54	Site directed mutagenesis: Ent3 R154E	
2	Ent3 Eco-6	GCGAATTCAGGAAGAATGAGTTTAGAGGATA C	61	Cloning of ENT3 constructs from -6	<i>EcoRI</i>
2	Ent3 stop	GGTCGACTCAAAGGAAAGTAAATCGATTC T	59	Cloning of ENT3 constructs till Stop (aa 408)	<i>Sall</i>
2	Ent3 UT3	GCTCTAGAAGGGCACTTCAACTCTC	58	Cloning of ENT3 (+277 downstream stop)	<i>XbaI</i>

Theme	Oligo	Sequence	T m	Experiment	Dig. site
2	Ent3 UT5	CGGGATCCATTTTGCTAAGCCAATTC	56	Cloning of ENT3 (-226 upstream ATG)	<i>BamHI</i>
2	Ent3 W103f	GGTTCTTGGAGGTTTATCGATGATACAAGG	55	Site directed mutagenesis: Ent3 E103W	
2	Ent3 W103r	CGATAAACCTCCAAGAACCGTGTGGATAAG GT	55	Site directed mutagenesis: Ent3 E103W	
2	Ent3-3	CGGAATTCATCCAGCAACGCCCTTGATC	55	Cloning of ENT3 ENTH domain (aa 1-172)	<i>EcoRI</i>
2	Ent3 158f	CGGAATTCAAAAAGGCAAGAGAAACGGC	55	Subcloning of Ent3-C-Term into pLexN wrong Digestion site	<i>EcoRI</i>
2	Ent3 157f	GGATCCGAAAAAGGCAAGAGAAACGGC	59	Subcloning of Ent3-C-Term into pLexN	<i>BamHI</i>
2	Ent3-5	CGGGATCCGAATGAGTTTAGAGGATACATT	53	Cloning of ENT3 ENTH domain (aa 1-172)	<i>BamHI</i>
3	Chim Af	CAAGGAATAGCATTGAATTCCTATTATTGAA CG	55	Construction of Ent-Chimera: Ent3 1-S112 + Ent5 I113-172	<i>EcoRI</i>
3	Chim Ar	GGAATTC AATGCTATTCCTTGTATCATCG	55	Construction of Ent-Chimera: Ent3 1-S112 + Ent5 I113-172	<i>EcoRI</i>
3	Chim Bf	GTCTAGTAGTCATTA ACTTAATTAGGATTTT AG	51	Construction of Ent-Chimera: Ent5 1-V111 + Ent3 I113-172	
3	Chim Br	CTAATTAAGTTAATGACTACTAGACATTTTA AGAC	57	Construction of Ent-Chimera: Ent5 1-V111 + Ent3 I113-172	
3	Chim Cf	CAAGGAATAGCATT TATGATTTGCGATCCCT G	57	Construction of Ent-Chimera: Ent3 1-S112 + EpsinR I105-162	
3	Chim Cr	CAAATCATAAATGCTATTCCTTGTATCATCG CAGAGAACACATTA ACTTAATTAGGATTTTA G	53	Construction of Ent-Chimera: Ent3 1-S112 + EpsinR I105-162	
3	Chim Df		51	Construction of Ent-Chimera: epsinR 1- H104 + Ent3 I113-172	
3	Chim Dr	CTAATTAAGTTAATGTGTTCTCTGGCGCTTG	55	Construction of Ent-Chimera: epsinR 1- H104 + Ent3 I113-172	
3	Chim Ef	CACTATATTGATTCATGTTTGCTCACTCATA AGC	59	Construction of Ent-Chimera: Ent3 1-D126 + Ent5 S130-172	
3	Chim Er	GAGCAAACATGAATCAATATAGTGAAAAGTT TCTAAAATC	59	Construction of Ent-Chimera: Ent3 1-D126 + Ent5 S130-172	
3	Chim Ff	CATATCGCTACCGAGTGGAGGCAAAATTTATA AAGC	59	Construction of Ent-Chimera:Ent5 1-T82 + Ent3 E83-172	
3	Chim Fr	CTCCACTCGGTAGCGATATGGTCGACTAATC	63	Construction of Ent-Chimera:Ent5 1-T82 + Ent3 E83-172	
4	Delta fo	GGAACGGTTCCCAAACGTTGAAAGAAGAGGT TG	62	Oligo for site directed mutagenesis: Pep12 DR19-F26	
4	Delta re	CAACGTTTGGGAACCGTTCCAAACGGCTTC	66	Oligo for site directed mutagenesis: Pep12 DR19-F26	
4	F20L fo	GTTCCAGATTAAGTGATTCACCTGAGTTCCA AAC	66	Oligo for site directed mutagenesis: Pep12 F20L	
4	F20L re	GGTGAATCACTTAATCTGGAACCGTTCCAAA CG	62	Oligo for site directed mutagenesis: Pep12 F20L	
4	Pep12 200	CGGGATCCTATTGCTCGATAAGATTTTGCTG	58	Cloning of Pep12	<i>BamHI</i>
4	Pep12 ATG	GGAATTCATGTCGGAAGACGAATTTTTTGG	64	Cloning of Pep12 constructs (binds ATG)	<i>EcoRI</i>

Theme	Oligo	Sequence	T m	Experiment	Dig. site
4	Pep12 Nde	GCATATGTCGGAAGACGAATTTTTTGG	57	primer for His-tagging Pep12 in pET28b	<i>NdeI</i>
4	Pep12 SOL	CCGGCTCGAGCTACCTCCATCTGCTCGTACG	57	primer for His-tagging Pep12 in pET28b	<i>XhoI</i>
4	Pep12f	CGGGATCCTCTCACACAGTGGCATCGTG	57	Cloning of PEP12 (-258 bp upstream ATG)	<i>BamHI</i>
4	Pep12r	GCGAATTCACCTTTCATTAGGGTATGATG	57	Cloning of PEP12 (240 bp downst. stop)	<i>EcoRI</i>
4	Pep12 E12R r	CCAAACGGCTCGATTATCACCACCAAAAAAT TCGTC	59	Pep12 E12R mutagenesis primer	
4	Pep12 E12R f	GGTGATAATCGAGCCGTTTGGACGGTTCC AG	59	Pep12 E12R mutagenesis primer	
5	Vti1 ATG	CATGCCATGGCTATGAGTTCCTATTAATAT C	58	Amplification of Vti1p from ATG	<i>NcoI</i>
5	Vti #10	TGAGTTCCTATTAATATCATA C	55	Amplif. of Vti1p upstream seq. from ATG	
5	Vti115- Bam	CGGGATCCTAATCGTCAATATTAGATGCG	57	Insertion of BamHI site and Stop at aa 115	<i>BamHI</i>
5	Vti1 ATG-Nde	CCATATGAGTTCCTATTAATATCATA C	57	Cloning of Vti1p into His-tag vector pET28b	<i>NdeI</i>
5	Vti1- Bam f	CTATGGGATCCAGTTCCTATTAATATCATA CG	53	Insertion of BamHI site after ATG for GFP tagging	<i>BamHI</i>
5	Vti1- Bam r	GGGAAC TGGATCCCATAGTAAGCCATGCAGC	53	Insertion of BamHI site after ATG for GFP tagging	<i>BamHI</i>
5	Vti1 E17R f	ACAACCTTACGACAAGCCAAAGCGAGCTTA GC	57	Vti1p E17R mutagenesis primer	
5	Vti1 E17R r	GCTTTGGCTTGTCGTAAGGTTGTTTGAAGT CAGATTC	57	Vti1p E17R mutagenesis primer	
	Vti1 E9R f	CTATTAATATCATAACCGTTCTGACTTCAAAA CAACCTTAG	55	Vti1p E9R mutagenesis primer	
	Vti1 E9R r	GAAGTCAGAACGGTATGATATTAATAGGGAA CTC	54	Vti1p E9R mutagenesis primer	
	Vti1 E25R f	GCGAGCTTAGCAGAGGCCCTCACAACCGT TATC	59	Vti1p E17R mutagenesis primer	
	Vti1 E25R r	GGGGCCCTCTGCTAAGCTCGCTTTGGCTTG	59	Vti1p E17R mutagenesis primer	
5	yEGFP f	CGCGGATCCAAAGGTGAAGAATTACTACTG	53	Amplification of GFP cassette from pUG34	<i>BamHI</i>
5	yEGFP r	CGCGGATCCTTTGTACAATTCATCCATACC	53	Amplification of GFP cassette from pUG34	<i>BamHI</i>
6	Yip4 -250f	TTGCAGTTTCACCAAGTATAGC	57	deletion control primer, binds 250bp upstream ATG	
6	Yip4 +200r	TTTGCCAGACTCTGCGCTACC	57	deletion control primer, binds 200bp downstream stop	
6	Yip4 Aux3	AATTCTATGTCCATGATATTGGGTTTTATAC ATATGTAAGTACTAGTGGGTATTTACACCGCAT A	47	Yip4 deletion primer	
6	Yip4 Aux5	TTTAGCAATATTTGTAGAAAGATATGTCACA AGAGGGCAGGCAAATTTGACTGAGAGTGCAC CAT	47	Yip4 deletion primer	

Theme	Oligo	Sequence	T m	Experiment	Dig. site
6	Yip5 Aux3	ATACTAGTCATAAAAAGTATTGTGTATAG ACGTGCGCATATTTTCGGTATTTACACCGCA TA	51	Yip5 deletion primer	
6	Yip5 Aux5	CGATTGTATACTAGCAAATAGGATTGACTCG ACAAAAGCAGAAAATTGTTACTGAGAGTGCAC CAT	51	Yip5 deletion primer	
6	Yip5 -240 f	TACATAACGTAACAGTATATCGG	54	Yip5 deletion control primer, binds 240bp upstream ATG	
6	Yip5 +200 r	CATAAACATTTTCATCCAAAATCTC	54	Yip5 deletion control primer, binds 200bp downstream stop	
7	Ent5-3	TGCTCTAGACTATTGCAAGATAAGTTCTCCC	53	Cloning of ENT5 ANTH constructs (binds at 516)	<i>XbaI</i>
7	Ent5-5	CGGGATCCAAATGGACTCATTATCAAAAAAG	63	Cloning of ENT5 ANTH constructs (binds at ATG)	<i>BamHI</i>
7	Ent5- delF	CAATCTAGATTTTAGTTTTTCGG	54	Deletion of ENT5	
7	Ent5- delR	TTTCTTCTGCATGGATAATGAC	54	Deletion of ENT5	

Tab. 5: Oligo categories

Theme	Oligos
1	sequencing
2	Ent3 oligos
3	ENTH chimera
4	Pep12 oligos
5	Vti1
6	Yip4
7	Ent5

II Plasmids

Tab. 6: **Plasmids.** Plasmids which were generated during this study by bachelor students or technical staff were marked with an asterisk in the reference line

Plasmid	Selection marker	Construction	Reference
pAN1	<i>AmpR</i>	PCR amplified Ent3 (aa1-172, ent3-3/5 and D62f/r primer) with F62D Mutation cloned into pGEM T-easy	Andrea Nolting*
pAN2	<i>AmpR</i>	PCR amplified Ent3 (aa1-172, ent3-3/5 and W103f/r primer) with E103W Mutation cloned into pGEM T-easy	Andrea Nolting*
pAN3	<i>AmpR</i>	PCR amplified Ent3 (aa1-172, ent3-3/5 and D62f/r primer) with F62D and G58R Mutation cloned into pGEM T-easy	Andrea Nolting*
pAN4	<i>AmpR</i> , <i>LEU2</i>	Ent3 F62D subcloned from pAN1 into pVP16-3 via <i>BamHI EcoRI</i>	Andrea Nolting*
pAN5	<i>AmpR</i> , <i>LEU2</i>	Ent3 E103W subcloned from pAN2 into pVP16-3 via <i>BamHI EcoRI</i>	Andrea Nolting*
pAN6	<i>AmpR</i> , <i>LEU2</i>	Ent3 F62D G58R subcloned from pAN3 into pVP16-3 via <i>BamHI EcoRI</i>	Andrea Nolting*
pASK-IBA3	<i>AmpR</i>	bacterial expression vector for adding C-terminal Strep-tag	IBA
pBK111	<i>AmpR</i> , <i>TRP1</i>	PCR-amplified mVti1b AA1-128 in <i>EcoRI-BamHI</i> pLexN from <i>EcoRI-BamHI</i> pAP7	Beate Köhler
pBK118	<i>AmpR</i> , <i>TRP1</i>	Vti1p AA1-115 in pLexN via <i>EcoRI-BamHI</i> with oligos: Vti-ATG RI (<i>EcoRI</i>) Vti 1-115 (<i>BamHI</i>)	Beate Köhler
pBK130	<i>AmpR</i> , <i>LEU2</i>	ENTH-domain (AA1-162) of EpsinR in <i>BamHI-EcoRI</i> pVP16-3 (Oligos: Z0 (ATG, <i>BamHI</i>) Z2 (stop, <i>EcoRI</i>))	Beate Köhler

Plasmid	Selection marker	Construction	Reference
pBK160	<i>AmpR, LEU2</i>	PCR amplified (Oligos: Ent5 5 (<i>BamHI</i>), Ent5 3 (<i>XbaI</i>)) Ent5 ENTH domain (AA 1-172) via <i>BamHI-XbaI</i> into pVP16	Beate Köhler
pBK165	<i>AmpR, TRP1</i>	N-term Syn8 (AA1-169) from <i>EcoRI-BamHI</i> pNK1 into <i>EcoRI-BamHI</i> pLexN	Beate Köhler
pBK171	<i>AmpR, TRP1</i>	PCR-amplified Pep12 N-term (AA1-200) via <i>EcoRI-BamHI</i> into pLexN	Beate Köhler
pBK172	<i>AmpR, TRP1</i>	PCR-amplified Tlg1 N-term (AA1-137) via <i>EcoRI-BamHI</i> into pLexN	Beate Köhler
pCP10	<i>AmpR</i>	PCR amplified -336 Ent3 +277 (UT3/5 and D62f/r primer) with F62D Mutation cloned into pGEM T-easy	Claudia Prange*
pCP11	<i>AmpR, URA3</i>	Ent3 F62D from pGEMTeasy into pRS316 via <i>BamHI-XbaI</i>	Claudia Prange*
pCP11	<i>AmpR, URA3</i>	Ent3 F62D from pGEMTeasy into pRS316 via <i>BamHI-XbaI</i>	Claudia Prange*
pCP12	<i>AmpR</i>	PCR amplified -336 Ent3 +277 (UT3/5 and W103f/r primer) with E103W Mutation cloned into pGEM T-easy	Claudia Prange*
pCP13	<i>AmpR, URA3</i>	Ent3 E103W from pGEMTeasy into pRS316 via <i>BamHI-XbaI</i>	Claudia Prange*
pCP13	<i>AmpR, URA3</i>	Ent3 E103W from pGEMTeasy into pRS316 via <i>BamHI-XbaI</i>	Claudia Prange*
pCP2	<i>KanaR</i>	Ent5strep subcloned into pET28b via <i>HindIII/XbaI</i>	Claudia Prange*
pCP22	<i>AmpR, TRP1</i>	Ent3 aa157-408 cloned from pGEMTeasy into plexN via <i>Sall/BamHI</i>	Claudia Prange*
pCP25	<i>AmpR, HIS3</i>	GFP-Snc1p cloned from pGS416 via <i>XhoI SacI</i> into pRS313	Claudia Prange*
pCP25	<i>AmpR, HIS3</i>	GFP-Snc1p cloned from pGS416 via <i>XhoI SacI</i> into pRS313	Claudia Prange*
pCP26	<i>AmpR, LEU2</i>	Ent3-C-Terminus from pGEMT-easy via <i>BamHI-NotI</i> into pVP16-3	Claudia Prange*
pCP27	<i>AmpR, TRP1</i>	Ent3-ENTH from pVP16-3 cloned via <i>BamHI-Sall</i> into plexN	Claudia Prange*
pCP28	<i>AmpR, HIS3</i>	GFP-Yck2ts from pRC2 cloned via <i>XbaI/SacI</i> into pRS313	Claudia Prange*
pCP29	<i>AmpR, HIS3</i>	GFP-Yck2 from pL2.992 cloned via <i>XbaI/SacI</i> into pRS313	Claudia Prange*

Plasmid	Selection marker	Construction	Reference
pCP3	<i>AmpR, HIS3</i>	Pep12 F20L subcloned from pJZ11 into pRS313 via <i>EcoRI</i>	Claudia Prange*
pCP32	<i>AmpR</i>	PCR amplified Vti1pE9R with T3/Vti1E9Rrev and Vti1E9Rfw/T7 primer from pJAL1 (2.PCR with T3/T7 primer)	Claudia Prange*
pCP33	<i>AmpR, TRP1</i>	Vti1p E9R 1-115 subcloned from pCP32 via <i>HindIII</i> into pLexN.	Claudia Prange*
pCP34	<i>AmpR, TRP1</i>	Pep12p E12R 1-200 subcloned from pJZ24 via <i>HindIII</i> into pLexN.	Claudia Prange*
pCP4	<i>AmpR, TRP1</i>	-260 Pep12 deltaFSD +240 cloned from pGEM-T easy into pRS314 via <i>EcoRI</i>	Claudia Prange*
pCP5	<i>AmpR</i>	PCR amplified Ent3 ENTH (from pKW3) with Ent3 Eco-6 and Ent3 172Bam primer in pGEMT-easy	Claudia Prange*
pCP6	<i>AmpR</i>	PCR amplified Ent3 N28-408 (from pSC4) with Ent3-28 and Ent3-stop primer in pGEMT-easy	Claudia Prange*
pCP7	<i>AmpR, URA3</i>	Ent3 ENTH from pGEMTeasy into pYX112 via <i>EcoRI-BamHI</i>	Claudia Prange*
pCP8	<i>AmpR, URA3</i>	Ent3 N28-408 from pGEMTeasy into pYX112 via <i>NcoI-Sall</i>	Claudia Prange*
pCP9	<i>AmpR, URA3</i>	Ent3 N158-408 from pSC2 into pYX112 via <i>BamHI/HindIII</i>	Claudia Prange*
pCW1	<i>AmpR</i>	ENTH Chim A ent3 aa1-S112 + Ent5 aa I111-172; Overlapping PCRs with primers including <i>BamHI XbaI</i>	Christiane Wiegand*
pCW10	<i>AmpR</i>	ENTH Chim F ent5 aa1-T82 + Ent3 aa 83-172; Overlapping PCRs with primers including <i>BamHI EcoRI</i>	Christiane Wiegand*
pCW11	<i>AmpR, LEU2</i>	ChimE subcloned from pCW9 via <i>BamHI XbaI</i> into Y2H vector pVP16	Christiane Wiegand*
pCW12	<i>AmpR, LEU2</i>	ChimF subcloned from pCW10 via <i>BamHI EcoRI</i> into Y2H vector pVP16	Christiane Wiegand*
pCW2	<i>AmpR</i>	ENTH Chim B ent5 aa1-V110 + ent3 aa I113-172; Overlapping PCRs with primers including <i>BamHI EcoRI</i>	Christiane Wiegand*

Plasmid	Selection marker	Construction	Reference
pCW3	<i>AmpR</i>	ENTH Chim C ent3 aa1-S112 + epsinR aa 105-162; Overlapping PCRs with primers including <i>BamHI EcoRI</i>	Christiane Wiegand*
pCW4	<i>AmpR</i>	ENTH Chim D epsinR aa 1-H104 + ent3 aa 113-172; Overlapping PCRs with primers including <i>BamHI EcoRI</i>	Christiane Wiegand*
pCW5	<i>AmpR, LEU2</i>	ChimA subcloned from pCW1 via <i>BamHI XbaI</i> into Y2H vector pVP16	Christiane Wiegand*
pCW6	<i>AmpR, LEU2</i>	ChimB subcloned from pCW2 via <i>BamHI EcoRI</i> into Y2H vector pVP16	Christiane Wiegand*
pCW7	<i>AmpR, LEU2</i>	ChimB subcloned from pCW3 via <i>BamHI EcoRI</i> into Y2H vector pVP16	Christiane Wiegand*
pCW8	<i>AmpR, LEU2</i>	ChimB subcloned from pCW4 via <i>BamHI EcoRI</i> into Y2H vector pVP16	Christiane Wiegand*
pCW9	<i>AmpR</i>	ENTH Chim E ent3 aa1-D126 + Ent5 aa 130-172; Overlapping PCRs with primers including <i>BamHI XbaI</i>	Christiane Wiegand*
pET28b	<i>KanR</i>	bacterial expression vector for adding C-or N-terminal 6xHis-tag	Novagen
pFvM135	<i>KanR</i>	6His-Pep12 soluble (aa 1-268) from <i>NdeI-XhoI</i> pFvM132 into pET28-b	G. Fischer von Mollard
pFvM28	<i>AmpR, TRP1</i>	<i>XhoI-XbaI</i> of pFvM23 + <i>XbaI-SacI</i> of pFvM26 into <i>XhoI-SacI</i> pRS314 (vti1 WT)	G. Fischer von Mollard
pFvM29	<i>AmpR, URA3</i>	<i>XhoI-XbaI</i> of pFvM23 + <i>XbaI-SacI</i> of pFvM26 into <i>XhoI-SacI</i> pRS316 (vti1 WT)	G. Fischer von Mollard
pFW3	<i>KanR</i>	6His Tlg1 N-term (AA1-137) into pET28 via <i>NdeI-BamHI</i>	Friederike Wolk
pFW5	<i>AmpR LEU2</i>	full length Ent5 via <i>BamHI - Xba I</i> into pVP16-3	Friederike Wolk
pGS416	<i>AmpR, URA3</i>	GFP-Snc1 in pRS316	Mike Lewis
pJAL1	<i>AmpR</i>	<i>HindIII</i> fragment from Vti1p pLexN subcloned into pBluescript SK+	J. Alonso Lunar*
pJAL2	<i>AmpR</i>	<i>HindIII</i> fragment from Pep12 pLexN subcloned into pBluescript SK+	J. Alonso Lunar*
pJAL3	<i>AmpR</i>	PCR amplified Pep12 E12R -258-+240 with Pep12r/f and E12Rfw/rev primer from pBK19	J. Alonso Lunar*

Plasmid	Selection marker	Construction	Reference
pJAL4	<i>AmpR</i>	PCR amplified Vti1p E17R <i>Xho/Xba</i> fragment from pFvM29 with T3, Vti1-115Bam, E17Rfw/rev primer	J. Alonso Lunar*
pJAL5	<i>AmpR</i>	PCR amplified Vti1p E17R/pLexN fragment from pJAL1 with T3,Vti115Bam, E17Rfw/rev primer	J. Alonso Lunar*
pJAL6	<i>AmpR, HIS3</i>	Pep12 E12R -258-+240 subcloned from pJAL3 into pRS314 with <i>EcoRI BamHI</i>	J. Alonso Lunar*
pJAL7	<i>AmpR, TRP1</i>	Vti1p E17R 1-115 subcloned from pJAL5 into pLexN via <i>EcoRI BamHI</i>	J. Alonso Lunar*
pJAL8	<i>AmpR</i>	Vti1p E17R fragment from pFvM29 ampl. with T3, Vti1-115Bam in pGemTeasy subcloned into pFvM28 via <i>XhoI, BglII</i>	J. Alonso Lunar*
pJAL8	<i>AmpR</i>	Vti1p E17R fragment from pFvM29 ampl. with T3, Vti1-115Bam in pGemTeasy subcloned into pFvM28 via <i>XhoI, BglII</i>	J. Alonso Lunar*
pJZ10	<i>AmpR</i>	Pep12 DFSD AA1-200 cloned via <i>EcoRI BamHI</i> into pLexN	This study
pJZ11	<i>AmpR, TRP1</i>	-260 Pep12 F20L +240 cloned from pGEM-T easy into pRS314 via <i>EcoRI</i>	This study
pJZ12	<i>AmpR</i>	-260 Pep12 +240bp deltaFSD overlapping PCRs cloned into pGEM T-easy	This study
pJZ13	<i>AmpR</i>	PCR amplified -336 Ent3 +277 (UT3/5 and D60f/r primer) with Y60D Mutation cloned into pGEM T-easy	This study
pJZ14	<i>AmpR</i>	PCR amplified -336 Ent3 +277 (UT3/5 and E154f/r primer) with R154E Mutation cloned into pGEM T-easy	This study
pJZ15	<i>AmpR</i>	PCR amplified Ent3 (aa1-172, ent3-3/5 and D60f/r primer) with Y60D Mutation cloned into pGEM T-easy	This study
pJZ16	<i>AmpR</i>	PCR amplified Ent3 (aa1-172, ent3-3/5 and E154f/r primer) with R154E Mutation cloned into pGEM T-easy	This study

Plasmid	Selection marker	Construction	Reference
pJZ17	<i>AmpR</i> , <i>URA3</i>	Ent3 Y60D subcloned from pJZ13 into pRS316 via <i>BamHI XbaI</i>	This study
pJZ18	<i>AmpR</i> , <i>URA3</i>	Ent3 R154E subcloned from pJZ14 into pRS316 via <i>BamHI XbaI</i>	This study
pJZ19	<i>AmpR</i> , <i>LEU2</i>	Ent3 Y60D subcloned from pJZ15 into pVP16-3 via <i>BamHI EcoRI</i>	This study
pJZ20	<i>AmpR</i> , <i>LEU2</i>	Ent3 R154E subcloned from pJZ16 into pVP16-3 via <i>BamHI EcoRI</i>	This study
pJZ21	<i>AmpR</i> , <i>HIS3</i>	3x-HA-Syn8 (Syn8 1.15kb Fragment with UTRs) subcloned via <i>XbaI</i> , <i>XhoI</i> into pRS313	This study
pJZ22	<i>AmpR</i>	PCR amplified Ent3 aa158-408 (Ent3 158f Eco/Ent3-stop primer) cloned into pGEM T-easy	This study
pJZ23	<i>AmpR</i>	PCR amplified Ent3 aa157-408 (Ent3 157f Bam/Ent3-stop primer) cloned into pGEM T-easy	This study
pJZ24	<i>AmpR</i>	PCR amplified Pep12p E12R from pJAL2 with mutagenesis and T3/T7 primer cloned into pGEM-T easy	This study
pJZ9	<i>AmpR</i>	Pep12 F->L AA1-200 cloned via <i>EcoRI BamHI</i> into pLexN	This study
pKW3	<i>AmpR</i> , <i>LEU2</i>	PCR amplified (Oligos: Ent3 5 (<i>BamHI</i>), Ent3 3 (<i>EcoRI</i>)) Ent3 ENTH domain (AA1-172) via <i>BamHI-EcoRI</i> into pVP16	Katrin Wiederhold
pL2.992	<i>AmpR</i> , <i>LEU2</i>	GFP-Yck2	Robinson LC
pLexN	<i>AmpR</i> , <i>TRP1</i>	yeast two hybrid bait vector with LexA DNA binding domain	Stan Hollenberg
pLS1	<i>AmpR</i> , <i>URA3</i>	N-terminal 3xHA-tag cloned via <i>BglII</i> into <i>BamHI</i> digested Ent3-C-Terminus in pYX112	Lasse Schindler*
pMB285	<i>AmpR</i> , <i>URA3</i>	F20L mutation in FSD motif of Pep12p with <i>TPI</i> promoter for GFP.	Pelham
pMB286	<i>AmpR</i> , <i>URA3</i>	FSD motif deletion (19-26 a.a) of Pep12p with <i>TPI</i> promoter for GFP.	Pelham
pPB1	<i>AmpR</i> , <i>URA3</i>	GFP-Yck2ts	Robinson LC
pPB2	<i>AmpR</i> , <i>URA3</i>	GFP-Yck2	Robinson LC

Plasmid	Selection marker	Construction	Reference
pRC2	<i>AmpR</i> , <i>LEU2</i>	GFP-Yck2ts	Robinson LC
pRS313	<i>AmpR</i> , <i>HIS3</i>	Yeast expression vector with <i>HIS3</i> , <i>CEN6</i> , <i>ARSH4</i>	Sikorski and Hieter
pRS314	<i>AmpR</i> , <i>TRP1</i>	Yeast expression vector with <i>TRP1</i> , <i>CEN6</i> , <i>ARSH4</i>	Sikorski and Hieter
pRS315	<i>AmpR</i> , <i>LEU2</i>	Yeast expression vector with <i>LEU2</i> , <i>CEN6</i> , <i>ARSH4</i>	Sikorski and Hieter
pRS316	<i>AmpR</i> , <i>URA3</i>	Yeast expression vector with <i>URA3</i> , <i>CEN6</i> , <i>ARSH4</i>	Sikorski and Hieter
pSC2	<i>AmpR</i> , <i>LEU2</i>	C-terminus of Ent3 (AA158-408 end, PCR) overexpressed under TPI promotor 2 μ into pXYX242 via <i>BamHI-HindIII</i>	S. Chidambaram
pSC4	<i>AmpR</i> , <i>LEU2</i>	1,7 kb PCR-amplified ENT3 into <i>XbaI-BamHI</i> YEp351	S. Chidambaram
pSK Bluescript	<i>AmpR</i>	bacterial 3kb cloning vector with <i>AmpR</i>	Stratagene
pSK1	<i>AmpR</i>	Pep12 F20L amplified with Pep12SOL and Pep12Nde primers from pMB285 cloned into pGEM T-easy	Sabine Kossmann*
pSK2	<i>AmpR</i>	Pep12 DFSD amplified with Pep12SOL and Pep12Nde primers from pMB286 cloned into pGEM T-easy	Sabine Kossmann*
pSK3	<i>KanaR</i>	Pep12 F20L via <i>NdeI XhoI</i> into His6 Expression vector pET28b	Sabine Kossmann*
pSK4	<i>KanaR</i>	Pep12 deltaFSD via <i>NdeI XhoI</i> into His6 Expression vector pET28b	Sabine Kossmann*
pSK5	<i>AmpR</i>	-260 Pep12 +240bp F20L overlapping PCRs cloned into pGEM T-easy	Sabine Kossmann*
pSM492	<i>AmpR</i>	3xHA-tag via <i>BglII</i> ends in pBluescript II SK+	Morrie Mannolson
pTW1	<i>KanaR</i>	Syntaxin8 into pET28b with Clontech InFusion Kit	Torsten Wundenberg*
pTW2	<i>KanaR</i>	Syntaxin7 into pET28b with Clontech InFusion Kit	Torsten Wundenberg*

Plasmid	Selection marker	Construction	Reference
pTW3	<i>AmpR</i>	PCR amplified Ent5 (from pBK160) with Ent5-ST3/5 primer via <i>BsaI</i> into Strep-expression vector pASK-IBA3	Torsten Wundenberg*
pVP16-3	<i>AmpR</i> , <i>LEU2</i>	yeast two hybrid prey vector with VP16 transcription activating domain	Stan Hollenberg
pYX112	<i>AmpR</i> , <i>URA3</i>	vector backbone with <i>CEN</i> and <i>TPI</i> promotor	R&D systems
pYX242	<i>AmpR</i> , <i>LEU2</i>	2μ vector backbone with <i>TPI</i> promotor	R&D systems

III Yeast Strains

Tab. 7: Yeast strains

Strain	Genotype	Back-ground	Reference
AGY4	<i>MATa leu2-3,112 ura3-52 his3-Δ200 ade2-101 trp1-Δ901 suc2-Δ9 mel- pho8Δ::ADE2 tvp23Δ::kanMX4</i>	SEY6211	Stein <i>et al.</i> , 2009
AHY41	<i>MATa leu2-3,112 ura3-52 his3-Δ200 trp1-Δ901 lys2-801 suc2-Δ9 mel- vps5Δ::HIS3 pho8Δ::LEU2</i>	SEY6210	S. Nothwehr
BKY13	<i>MATa his3Δ1 leu2Δ0 lys2Δ0 ura3Δ0 ent5Δ::kanMX4 ent3Δ::LEU2</i>	BY4742	Chidambaram <i>et al.</i> , 2004
BY4741	<i>MATa his3Δ1 leu2Δ0 met15Δ0 ura3Δ0</i>	BY4741	Euroscarf
BY4742	<i>MATa his3Δ1 leu2Δ0 lys2Δ0 ura3Δ0</i>	BY4742	Euroscarf
CPY1	<i>MATa leu2-3,112 ura3-52 his3-Δ200 ade2-101 trp1-Δ901 suc2-Δ9 mel- ent3Δ::kanMX4 ent5Δ::URA3 pho8Δ::ADE2</i>	SEY6211	C. Prange
CPY2	<i>MATa his3Δ1 leu2Δ0 lys2Δ0 ura3Δ0 yip4Δ::kanMX5 yip5Δ::LEU2</i>	BY4742	C. Prange
<i>ent3Δ</i>	<i>MATa his3Δ1 leu2Δ0 lys2Δ0 ura3Δ0 ent3Δ::kanMX4</i>	BY4742	Euroscarf
<i>ent5Δ</i>	<i>MATa his3Δ1 leu2Δ0 lys2Δ0 ura3Δ0 ent5Δ::kanMX4</i>	BY4742	Euroscarf
FvMY24	<i>MATa leu2-3,112 ura3-52 his3-Δ200 ade2-101 trp1-Δ901 suc2-Δ9 mel- vti1-2</i>	SEY6211	F. v. Mollard and Stevens, 1999
ISY5	<i>MATa leu2-3,112 ura3-52 his3-Δ200 trp1-Δ901 lys2-801 suc2-Δ9 mel- tvp23Δ::kanMX4</i>	SEY6210	Stein <i>et al.</i> , 2009
ISY6	<i>MATa leu2-3,112 ura3-52 his3-Δ200 ade2-101 trp1-Δ901 suc2-Δ9 mel- vti1-2 tvp23Δ::kanMX4</i>	SEY6211	Stein <i>et al.</i> , 2009
JZY9	<i>MATa/α his3Δ1/ his3Δ1 leu2Δ0/leu2Δ0 lys2Δ0/LYS2 ura3Δ0/ ura3Δ0 MET15/met15Δ0</i>	BY4741x BY4742	This study
L40	<i>MATa leu2-3,112 his3-Δ200 ade2-101 trp1-Δ901 LYS2::(lexAop)4-HIS3 URA3::(lexAop)4-lacZ gal80</i>	L40	Vojtek and Hollenberg, 1995
SCY2	<i>MATa leu2-3,112 ura3-52 his3-Δ200 trp1-Δ901 lys2-801 suc2-Δ9 mel- ent3Δ::kanMX4</i>	SEY6210	Chidambaram <i>et al.</i> , 2008
SCY25	<i>MATa leu2-3,112 ura3-52 his3-Δ200 trp1-Δ901 lys2-801 ent5Δ::kanMX4</i>	SEY6210	Chidambaram <i>et al.</i> , 2008
SCY26	<i>MATa leu2-3,112 ura3-52 his3-Δ200 ade2-101 trp1-Δ901 suc2-Δ9 mel- ent3Δ::LEU2 ent5Δ::kanMX4</i>	SEY6211	Chidambaram <i>et al.</i> , 2008

Strain	Genotype	Back-ground	Reference
SCY27	<i>MATα leu2-3,112 ura3-52 his3-Δ200 trp1-Δ901 lys2-801 suc2-Δ9 mel- pep12Δ::URA3</i>	SEY6210	Chidambaram <i>et al.</i> , 2008
SCY34	<i>MATα his3Δ1 leu2Δ0 lys2Δ0 ura3Δ0 ent5Δ::kanMX4 ent3Δ::LEU2</i>	BY4742	S. Chidambaram
SCY35	<i>MATα/α his3Δ1/ his3Δ1 leu2Δ0/ leu2Δ0 lys2Δ0/ lys2Δ0 ura3Δ0/ ura3Δ0 ent5Δ::kanMX4 ent3Δ::LEU2</i>	BY4741x BY4742	S. Chidambaram
SEY6210	<i>MATα leu2-3,112 ura3-52 his3-Δ200 trp1-Δ901 lys2-801 suc2-Δ9 mel-</i>	SEY6210	Robinson <i>et al.</i> , 1988
SEY6211	<i>MATα leu2-3,112 ura3-52 his3-Δ200 ade2-101 trp1-Δ901 suc2-Δ9 mel-</i>	SEY6211	Robinson <i>et al.</i> , 1988
SNY18	<i>MATα leu2-3,112 ura3-52 his3-Δ200 ade2-101 trp1-Δ901 suc2-Δ9 mel- pho8Δ::ADE2</i>	SEY6211	Nothwehr <i>et al.</i> , 1995
<i>yip4Δ</i>	<i>MATα his3Δ1 leu2Δ0 lys2Δ0 ura3Δ0 yip4Δ::kanMX5</i>	BY4742	Euroscarf
<i>yip5Δ</i>	<i>MATα his3Δ1 leu2Δ0 lys2Δ0 ura3Δ0 yip5Δ::kanMX6</i>	BY4742	Euroscarf
<i>ent3Δ</i>	<i>MATα/α his3Δ1/ his3Δ1 leu2Δ0/leu2Δ0 lys2Δ0/LYS2 ura3Δ0/ ura3Δ0 MET15/met15Δ0 ent3Δ::kanMX4/ ent3Δ::kanMX4</i>	BY4743	Euroscarf
<i>ent5Δ</i>	<i>MATα/α his3Δ1/ his3Δ1 leu2Δ0/leu2Δ0 lys2Δ0/LYS2 ura3Δ0/ ura3Δ0 MET15/met15Δ0 en5Δ::kanMX4/ ent5Δ::kanMX4</i>	BY4743	Euroscarf

IV Curriculum Vitae

- Born at the 14.06.1982 in Siegen (NRW, Germany)

- **Abitur** at Gymnasium Wilnsdorf (Kreis Siegen, NRW, Germany) in 2001

- **10/2001-10/2005 Studies of biochemistry**, University Bielefeld (Germany). I acquired the Diploma degree in biochemistry.

- **10/2005-08/2006 Diploma work** in biochemistry at the University Bielefeld. My diploma work with the topic "Interactions between Ent3p and Ent5p with endosomal SNAREs at cell wall synthesis in *Saccharomyces cerevisiae*" was carried out in the lab of Prof. Gabriele Fischer von Mollard. My work was supervised by Dr. Subbulakshmi Chidambaram.

- **10/2006-12/2006** Three month **practical training** in Prof. Mark Marsh's lab (University College London, MRC LMCB) from Oct. till Dec. 2006. Field: "Interaction between the *simian immunodeficiency virus* (SIV) and the ESCRT-machinery". In a second project I also investigated the trafficking of CD63 and its interactions with the ESCRT complex.

- **From 01/2007 PhD (Dr. rer. nat.)** work in Prof. G. Fischer von Mollard's lab at the University of Bielefeld from February 2007 to presumably March/April 2010 with the title: "Characterization of the yeast adaptor protein Ent3p and its interaction with the endosomal SNAREs Vti1p, Pep12p and Syn8p."

V Publications

Subbulakshmi Chidambaram, **Jana Zimmermann**, Gabriele Fischer von Mollard (2008). “*Characterization of ENT3 and ENT5 mutants and their interaction with endosomal SNAREs.*” J. Cell Sci. 121(3), 329-338.

Sebastian I. Stein, Anna Gottfried, **Jana Zimmermann**, Gabriele Fischer von Mollard (2009). “*TVP23 interacts genetically with the yeast SNARE VTI1 and functions in retrograde transport from the early endosome to the late Golgi.*” Biochem. J. 419, 229-236.

Jana Zimmermann, Subbulakshmi Chidambaram, Gabriele Fischer von Mollard. “*Ent3p functions in retrograde traffic from the early endosome to the TGN and binds three SNAREs via distinct amino acid residues.*” Manuscript submitted to J. Biol. Chem.

Danksagung

An erster Stelle möchte ich mich bei Prof. Gabriele Fischer von Mollard für die ausgezeichnete Betreuung und die vielen interessanten Projekte bedanken. Danke Gabi, dass du immer ein Ohr für mich offen hattest und mir beim Schreiben dieser Arbeit hilfreich zur Seite gestanden hast.

Vielen lieben Dank auch an Prof. Thomas Dierks für die Übernahme des Korreferats dieser Arbeit.

Mein weiterer Dank geht insbesondere an Claudia Prange, die durch ihr glückliches Händchen bei Klonierungen so manches Projekt vorm Untergang bewahrt hat und mir durch meine gesamte Promotionszeit eine sehr große Hilfe war.

Bedankt sei auch Christiane Wiegand für die Ent3p Chimären und die vielen IEFs die sie immer gut gelaunt für mich erledigt hat.

Einen recht herzlichen Dank möchte ich auch an meine Bachelor- und Masterstudenten loswerden, die sich sehr tapfer sechs Wochen lang unter meiner Anleitung durch die Wirren und Tücken der Molekularbiologie gekämpft haben. Danke an Torsten Wundenberg, Alexander Brock, Sabine Kossmann, Lasse Schindler, Andrea Nolting und Jaqueline Alonso Lunar, für eure Hilfe bei meinen Projekten und die nette Zeit mit euch.

Special thanks natürlich auch an meine beiden Lektoren Sascha Browski und Michael Gossing. But however without you so for proof this work would have been an heavy grammatically disaster ;).

Natürlich möchte ich mich bei allen aktuellen und ehemaligen Kollegen der BC3, für das tolle und humorvolle Arbeitsklima und für die mal mehr, mal weniger fachlichen Diskussionen bedanken. Ich werde euch bestimmt sehr vermissen.

Die BCI soll auch nicht unbedankt bleiben, auch an euch einen lieben Dank vor allem auch wegen der schönen Zeit bei Betriebsfeiern/Ausflügen Grillabenden und dem Finnbahnlauf.

Außerdem möchte ich auch noch ganz besonders Eva Westendorf und meinen Jonglierkollegen danken, die dafür gesorgt haben, dass ich neben Hefen auch noch andere spannende Dinge zu sehen bekomme ;).

Meine vorletzte Danksagung geht an meinen großartigen Freund Christoph Niehaus, der in den vergangenen drei Jahren keine Mühe und Kilometer gescheut hat um mich so oft es ging zu besuchen. Vielen Dank für Deine seelische und moralische Unterstützung, danke auch für Deine Geduld und dafür das du immer für mich da warst.

Und zu guter Letzt möchte ich mich bei meiner Familie bedanken. Danke Mama und Papa, dass ihr an mich geglaubt habt und ich immer auf eure Unterstützung zählen konnte. Danke auch an Lars, Sabrina, Philip, Anna, Ralph und Carolin dass ihr dafür gesorgt habt, dass ich mich im Siegerland immer sofort wieder heimisch gefühlt habe.

Erklärung

Ich erkläre hiermit, dass ich die vorliegende Doktorarbeit selbst verfasst und mich dabei keiner anderen als der von mir ausdrücklich bezeichneten Quellen und Hilfen bedient habe.

Jana Zimmermann